Characterization of the indicator of amyloid clearance activity: Aβ34 production, degradation, and its role as a novel biomarker in Alzheimer disease

Irem Ulku

Integrated Program in Neuroscience
Faculty of Medicine and Health Sciences
McGill University, Montréal, Québec

October 2022

A thesis submitted to McGill University in partial fulfillment
of the requirements of the degree of

Doctor of Philosophy

`

DEDICATION

Her zaman yanımda olup beni destekleyen canım aileme,

`

ABSTRACT

Alzheimer disease (AD) is a neurodegenerative disorder that is clinically characterized by a progressive cognitive decline and neuropathologically defined by extracellular plaques, mainly consisting of amyloid-β (Aβ) peptide aggregates, and intraneuronal misfolded phosphorylated tau forming neurofibrillary tangles. However, molecular causes of the disease and biomarkers for the detection of the disease prior to formation of plaques are still subjects of ongoing research.

Aβ peptides are produced by sequential cleavage of the amyloid precursor protein (APP), firstly by the β-secretase (BACE1) then followed by the γ-secretase. This *amyloidogenic* pathway generates Aβ peptides of varying lengths that are subject to proteolytic degradation. BACE1 exerts the first step in amyloid production (amyloidogenic processing of APP) and unexpectedly, BACE1 is also a major enzyme to degrade Aβ peptides into a short form with 34 amino acid residues, i.e., Aβ34. The cleavage of longer Aβ peptides into Aβ34 is called *amyloidolytic* processing.

My thesis focuses on the investigation of the life cycle of Aβ34: (i) analysis of the dual role of BACE1 in AD (amyloidogenic vs. amyloidolytic processing), (ii) characterization of the enzymes that are involved in the Aβ34 metabolism and (iii) investigation of the cellular localization of Aβ34 generation. Besides being non-toxic and non-aggregating, Aβ34 also serves as an indicator of Aβ clearance. To further establish Aβ34 as a biomarker, it's important to reveal molecular details of Aβ34 metabolism by studying its production and degradation.

Manuscript I: We hypothesized that amyloidolytic activity of BACE1 could explain the inverse relationship between BACE1 and Aβ levels in AD model systems which was described as a paradox in the literature. The biochemical and pharmacological analyses of human AD brain

`

tissue, wild-type mice and AD mouse models showed an association between the levels of BACE1 and Aβ34. We showed that the majority of Aβ34 is produced in the endo-lysosomal system by BACE1 and that BACE1 recognizes Aβ peptides as substrates produced by Presenilin 2-γ-secretase complexes. Furthermore, BACE1 inhibitor effects depended on the enzyme to substrate (BACE1:APP) ratio, suggesting that the ratio is the critical factor that determines the balance between amyloidogenic (Aβ production) and amyloidolytic activities (Aβ clearance) of BACE1.

Manuscript II: We determined the role of Aβ-degrading enzymes (ADEs) in Aβ34 degradation. Our cellular analysis revealed that BACE1 produces Aβ34 in the endo-lysosomal system. Therefore, we hypothesized that ADEs, that are primarily active in endosomes/lysosomes, may also be capable of degrading Aβ34. Knockdown or pharmacological inhibition of proteases revealed the highest increase of Aβ34 upon either knockdown or inhibition of Endothelin Converting Enzyme 1 (ECE1). Under the conditions of ECE1 overexpression, Aβ34 levels were significantly reduced. Thus, our results suggest that ECE1 is the major Aβ34 degrading protease compared to other proteases tested.

Overall, we have identified and characterized the main enzymes involved in Aβ34 production and clearance. Our data show that (i) BACE1 is the critical enzyme to produce Aβ34, (ii) that the ratio of BACE1:APP determines the level of the amyloidolytic activity, and (iii) ECE1 is the main protease to degrade Aβ34. Such findings are important to establish Aβ34 as a biomarker of clearance in AD since Aβ34 is a stable intermediate product in body fluids. Further, the identification of downstream pathways will guide the development of novel preventive approaches and biomarker discovery with the aim to enhance amyloid clearance before potentially toxic peptides aggregate into oligomers and fibrils.

`

RÉSUMÉ

La maladie d'Alzheimer (MA) est une maladie neurodégénérative caractérisée cliniquement par un déclin cognitif progressif. Cette maladie est neuropathologiquement défini par des plaques extracellulaires, principalement constituées d'agrégats de peptides amyloïdes-β (Aβ), et de protéine tau hyper et anormalement phosphorylée qui s'agrège dans les neurones formant les dégénérescences neurofibrillaires. Cependant, les causes moléculaires ainsi que les biomarqueurs pour la détection de la maladie avant la formation de plaques font toujours l'objet de recherches en cours. Une approche établie pour la prévention ou un traitement efficace reste manquant.

Les peptides Aβ sont produit par le clivage séquentiel de la protéine précurseur amyloïde (APP), d'abord par la β-sécrétase (BACE1) puis suivie par la γ-sécrétase. Cette cascade de clivage génère des peptides Aβ de longueurs variables qui sont normalement dégradés par plusieurs protéases. Étonnamment, BACE1 qui exerce la première étape de la production d'amyloïde (clivage amyloïdogénique d'APP) est également une enzyme importante dans la dégradation des peptides Aβ en peptides plus courtes (clivage amyloïdolytique), c'est-à-dire la peptide Aβ non-amyloïdogène de 34 acides aminés de longueur.

Ma thèse se concentre sur l'investigation du cycle de vie de l'Aβ34 : (i) analyse du double rôle de BACE1 dans la MA (clivage amyloïdogénique vs amyloïdolytique). (ii) caractérisation des enzymes impliquées dans le métabolisme de l'Aβ34 et (iii) étude de la localisation cellulaire de la génération d'Aβ34. En plus d'être non toxique et non agrégant, Aβ34 sert également de

`

biomarqueur potentiel pour la dégradation d'Aβ ; par conséquent, il est important de révéler les détails moléculaires du métabolisme de l'Aβ34, y compris sa production et sa dégradation.

Manuscrit I – Nous avons postulé que le clivage amyloïdolytique de BACE1 pourrait expliquer la relation inverse « paradoxale » entre les niveaux de BACE1 et Aβ dans les cerveaux MA, c'est-à-dire la réduction des espèces Aβ avec inhibition de BACE1. Ainsi, nous avons étudié les aspects cellulaires et moléculaires du clivage amyloïdogénique et amyloïdoytique de BACE1 en utilisant divers approches biochimique et pharmacologique. Les expériences avec du tissue cérébral humain atteint de MA, et des souris de type naturel ainsi que de modèle MA ont démontrées une association entre les niveaux de BACE1 et Aβ34. Différents inhibiteurs de BACE1 ont eu des effets différents sur les espèces d'Aβ dépendant du rapport entre BACE1 et APP indiquant que ce rapport affecte directement la balance entre les deux activités enzymatiques de BACE1. De plus, nous avons obtenu de l'évidence indiquant que (i) la majorité d'Aβ34 est produit dans le système endo-lysosome par BACE1, (ii) BACE1 reconnait les peptides Aβ, produit par γ-sécrétase contenant le subunité catalytique Presenilin-2, en tant que substrats. En tout, nous avons d'une part analysé le clivage amyloïdolytique de BACE1 au niveau moléculaire et cellulaire, et de l'autre part montré que le rapport substrat:enzyme est un facteur très important déterminant la balance entre le clivage amyloïdogénique (production d'Aβ) et le clivage amyloïdolytique (dégradation d'Aβ) de BACE1.

Manuscrit II: Nous avons analysé le rôle des enzymes dégradant Aβ (EDAs) ainsi que leur contribution à la dégradation d'Aβ34. Notre analyse cellulaire a relevé que BACE1 produit Aβ34 dans le système endo-lysosome. Par conséquent, nous avons postulé que les EDAs comme enzyme de conversion de l'endothéline 1 (ECE1), Cathepsin B et Cathepsin D, qui sont principalement actives dans les endosomes/lysosomes, pourraient dégrader Aβ34. Lorsque nous avons testé

`

différentes conditions incluant le knockdown des gènes ainsi que l'inhibition pharmacologique des protéases, la plus grande augmentation d'Aβ34 était associée avec à la fois le knockdown et l'inhibition d'ECE1. Dans les conditions où l'expression d'ECE1 était augmenté, les niveaux d'Aβ34 ont été significativement réduits. Collectivement, nos résultats suggèrent qu'ECE1 est la protéase principale impliquée dans la dégradation d'Aβ34 parmi les protéases testées.

Dans l'ensemble, nous avons identifié et caractérisé les enzymes principales impliquées dans la production et dégradation d'Aβ34. Notre data indique que (i) BACE1 est la plus importante enzyme pour produire Aβ34, (ii) le rapport moléculaire BACE1:APP détermine l'équilibre entre le clivage amyloïdogénique et le clivage amyloïdolytique de BACE1, et (iii) ECE1 est l'enzyme principale qui dégrade Aβ34. Ces résultats sont importants pour le développement d'Aβ34 comme biomarqueur étant donné que ce peptide est un produit intermédiaire dans la cascade de dégradation d'amyloïde de même qu'un indicateur de l'activité de dégradation d'amyloïde. Nos trouvailles vont non seulement influencer l'identification de nouveaux biomarqueurs mais également le développement de nouveaux traitements préventives ; par exemple, en améliorant la dégradation d'amyloïde avant que les peptides toxiques ne s'agrègent en oligomères ou fibrilles.

`

TABLE of CONTENTS

`

`

`

ACKNOWLEDGEMENTS

This Ph.D. thesis could not have been possible without the help and support of some amazing people.

First of all, I would like to thank my supervisor, Dr. Gerhard Multhaup, for letting me explore projects that excite me, for supporting me to guide my projects independently and for being there and providing guidance when I need help. I appreciate the scientific freedom and collaborative environment.

I would like to thank my advisory committee members, Dr. Dusica Maysinger and Dr. Jean- François Trempe, for their guidance and input that led to fruitful discussions and motivated me to take further steps throughout the years. I appreciate the friendly scientific environment that they created.

I would like to thank all past and current members of Multhaup laboratory. I would like to thank Dr. Filip Liebsch for introducing me to the lab techniques and for being supportive to initiate my project. I would like to thank Dr. Adeola Shobo and Dr. Mark Hancock for scientific discussions, Jean-Robert Kwizera for his help with orders and administrative issues, Phoebe, Christelle, Hedi and Isabel for their support and friendship, and all members of Bellini first floor for both scientific conversations and non-scientific extracurricular activities.

In particular, I would like to emphasize the friendship and continued support I have received from Can and James, my lifelong friends! This journey could not have been this fun

`

without you. I enjoyed every second of our time together, including the coffee breaks, laughter, success, and troubles we went through.

I would like to thank all our collaborators including Dr. Paul Saftig, Dr. Luka Kulic, Dr. Christoph Hock, Dr. Claus Pietrzik, Dr. Gopal Thinakaran, and Roche Pharmaceutical Research Unit for providing samples that are valuable to our studies.

I would like to thank Integrated Program in Neuroscience (IPN), Centre de Recherche en Biologie Structurale (CRBS), Faculty of Medicine, the VELUX Foundation, Natural Sciences and Engineering Research Council of Canada (NSERC) and Canadian Institutes of Health Research (CIHR) for financial support they provided to me and the research projects I was involved in.

I would also like to thank all my friends for amazing times we spend together, all the conversations that make us grow, all the food and fun we share. “Sharing is caring” came to life with you and your amazing presence in my life!

Finally, I would like to thank my family – canım annem Firdevs, canım babam Altan, diger yarim canım kardeşim Mine – and my extended family including my grandparents, my cousins, my aunts and my uncles. You have always been there for me, supportive, loving and encouraging at every step I take. Without you, I would not have been the person I am today. Sizi çok ama çok seviyorum en değerlilerim.

Last but not least, I would like to thank my best friend, Andreas. Thank you for always being there, being supportive and motivating. Having you by my side and sharing every moment together for better or worse are priceless. Σ'αγαπώ πάρα πολύ.

`

AUTHOR CONTRIBUTIONS

As outlined in the McGill Thesis Guidelines, this thesis is presented in a manuscript-based format and is composed of a literature review, one article that is currently in revision (Manuscript I), one manuscript (Manuscript II) that is in preparation for publication and that will be submitted in an altered form for publication, and a general discussion. I am the first author of the two manuscripts. A detailed description of contribution of authors are listed below:

Manuscript I: The Beta-site Amyloid Precursor Protein (APP) Cleaving Enzyme (BACE1) Has a Critical Role in Amyloid Homeostasis Which Primarily Affects Amyloid-β Clearance

In revision.

Irem Ulku, Filip Liebsch, S. Can Akerman, Jana F. Schulz, Luka Kulic, Christoph Hock, Claus Pietrzik, Alessandro Di Spiezio, Gopal Thinakaran, Paul Saftig, Gerhard Multhaup

IU and FL contributed equally to this work. IU, FL and GM designed research; IU, FL, SCA, JFS, and ADS performed research; IU, FL, LK, CH, CP, GT, PS, and GM analyzed data; IU, FL, and GM wrote the paper. All authors mentioned in the manuscript have agreed for authorship, read and approved the final version of the manuscript.

Manuscript II: The Endothelin Converting Enzyme 1 Regulates the Levels of the Amyloid Clearance Indicator, Aβ34, and is the Predominant Protease in Aβ34 Degradation

The Invention Disclosure D2023-0074 based on findings reported in Manuscript II has been approved by McGill (status: under review; October 13th, 2022).

Irem Ulku, S. Can Akerman, Gerhard Multhaup

`

I designed and performed all the experiments, analyzed data, prepared the figures, and wrote the manuscript. G.M. conceived the study, designed experiments, analyzed data, and wrote the manuscript. SCA prepared plasmids and revised the manuscript for intellectual content. All authors have read and approved the version of the manuscript presented in this thesis.

In addition to these manuscripts, I have included one publication, to which I have contributed experimental results during my Ph.D., in the appendix of this thesis (Appendix A), and another publication, to which I have contributed experimental results during my Ph.D., that is currently under review (published in December 2022) (Appendix B).

Aβ34 is a BACE1-derived Degradation Intermediate Associated with Amyloid Clearance and Alzheimer's Disease Progression

Nat Commun., 10, 2240 (2019). https://doi.org/10.1038/s41467-019-10152-w

Filip Liebsch, Luka Kulic, Charlotte Teunissen, Adeola Shobo, Irem Ulku, Vivienne Engelschalt, Mark A. Hancock, Wiesje M. van der Flier, Peter Kunach, Pedro Rosa-Neto, Philip Scheltens, Judes Poirier, Paul Saftig, Randall J. Bateman, John Breitner, Christoph Hock & Gerhard Multhaup

Cathepsin D: Analysis of Its Potential Role as an Amyloid Beta Degrading Protease

Neurobiol Dis., 175, 105919 (2022). https://doi.org/10.1016/j.nbd.2022.105919

Lisa Gallwitz, Alessandro Di Spiezio, Lina Schmidt, André R. A. Marques, Florian Bleibaum, Andreas Tholey, Liam Cassidy, Irem Ulku, Gerhard Multhaup and Paul Saftig

`

CONTRIBUTION to ORIGINAL KNOWLEDGE

Manuscript I: The Beta-site Amyloid Precursor Protein (APP) Cleaving Enzyme (BACE1) Has a Critical Role in Amyloid Homeostasis Which Primarily Affects Amyloid-β Clearance

This study investigates the dual role of BACE1 in Aβ production and Aβ clearance, cellular localization of Aβ34 production and enzymes involved in Aβ34 production.

We found that

i. there is an association between BACE1 protein levels and Aβ34 levels in human AD brain tissues, wild-type and transgenic mouse models and cellular assays,

ii. BACE1 but not APP overexpression increases Aβ34 levels in cell lines,

iii. under the surplus of the 99 amino acid long carboxy terminus of APP, Aβ34 levels increase and Aβ40 and Aβ42 levels decrease dose-dependently with BACE1,

iv. amyloidolytic activity of BACE1 (Aβ34 production) takes place in endo-lysosomal system,

v. PS2-γ-secretase that is present in endo-lysosomal system rather than PS1-γ-secretase that is mainly on the plasma membrane provides Aβ species, such as Aβ40 and Aβ42, as substrates for BACE1's amyloidolytic activity,

vi. substrate to enzyme (APP:BACE1) ratio modulates the balance between BACE1-mediated Aβ production (amyloidogenic activity) and Aβ clearance (amyloidolytic activity).

    a. under APP surplus, BACE1 inhibition decreases Aβ40 and Aβ42 levels,

`

b. under APP-C99 surplus (which bypasses the initial BACE1 cleavage step), BACE1 inhibition decreases Aβ34 levels,

c. under BACE1 surplus, BACE1 inhibition increases Aβ40 and Aβ42 levels.

`

Manuscript II: The Endothelin Converting Enzyme 1 Regulates the Levels of the Amyloid Clearance Indicator, Aβ34, and is the Predominant Protease in Aβ34 Degradation

Aβ34 is a metastable intermediate and is a potential biomarker for AD progression and monitoring amyloid clearance, e.g., upon drug treatment; therefore, it is important to investigate its clearance and stability. This study investigates the potential roles of Aβ-degrading enzymes in Aβ34 degradation.

We found that

i. Endothelin Converting Enzyme 1 (ECE1) knockdown increases primarily Aβ34 levels under both endogenous and surplus of BACE1,
ii. Aβ34 levels increase dose-dependently with ECE1 knockdown,
iii. Aβ34 levels decrease dose-dependently with ECE1 overexpression,
iv. Aβ34 levels are significantly reduced prior to other Aβ species upon ECE1 overexpression,
v. effect of ECE1 on Aβ34 dominates over other proteases tested upon combinatorial knockdowns of different proteases,
vi. pharmacological inhibition of Neprilysin, ECE1 and Angiotensin Converting Enzyme by Phosphoramidon increases Aβ34 and Aβ40 levels with a greater effect on Aβ34,
vii. pharmacological inhibition of ECE1 by an ECE1 specific inhibitor increases Aβ34 but not Aβ40 or Aβ42 levels, and
viii. pharmacological inhibition by the ECE1 specific inhibitor yields a greater increase in Aβ34 levels and increases Aβ34 levels at a lower concentration of the inhibitor treatment compared to pharmacological inhibition by Phosphoramidon.

`

LIST of FIGURES

`

LIST of SUPPLEMENTARY FIGURES

`

LIST of TABLES

LIST of SUPPLEMENTARY TABLES

`

Chapter I :

GENERAL INTRODUCTION

`

1. ALZHEIMER DISEASE

The first case of Alzheimer Disease (AD) had been formally identified by Dr. Alois Alzheimer more than 100 years ago. Auguste Deter presented worsening symptoms of memory loss and behavioral changes. Dr. Alzheimer's post-mortem analysis discovered shrinking of certain brain areas and abnormal deposits throughout her brain (Alzheimer, 1907, Alzheimer, 1911). These cerebral deposits have been described as hallmarks of AD pathology, which are now commonly referred to as plaques. For more than fifty years following its discovery, AD was believed to be a rare form of dementia and was not studied in detail. AD research gained more interest and attention when it was scientifically acknowledged that Alzheimer is the most common form of dementia and that it is the fourth leading cause of death in the United States (Katzman, 1976). Unfortunately, our understanding of the complex nature of AD is still incomplete and requires more research to better comprehend the causes and the driving forces of the disease progression in order to design strategies for the prevention and treatment of AD.

1.1. Pathological Hallmarks of Alzheimer Disease

Alzheimer Disease is a chronic neurodegenerative disorder that is clinically characterized by a progressive decline in cognitive functioning. Neuropathologically, the hallmarks include brain atrophy, senile plaques consisting of amyloid-β (Aβ) peptides and neurofibrillary tangles (NFT) consisting of phosphorylated tau (Dickson, 1997a, Holtzman et al., 2011, Jellinger, 1998).

1.1.1. Extracellular Amyloid Plaques

The first studies in Alzheimer research revealed that risk of dementia increases with the number of amyloid plaques in the patients' brains (Blessed et al., 1968, Graeber et al., 1997, Maurer et al., 1997, Möller and Graeber, 1998). These extracellular plaques are heterogenous

`

lesions composed of protein deposits, mainly Aβ peptides (Masters et al., 1985, Glenner and Wong, 1984). Among various Aβ peptides found in plaques, 42-amino acid long Aβ peptide (Aβ42) is the most predominant component (Rozemuller et al., 1989) and widely thought to be the most neurotoxic of the Aβ species.

The two main categories of plaques are called neuritic (dense-core) plaques and diffuse plaques. Neuritic plaques have a dense core of Aβ and in the periphery, they have damaged tubulin-associated unit (tau) containing axons and dendrites (i.e., neurites), microglia and astrogliosis associated with synaptic loss and inflammation (Itagaki et al., 1989, Knowles et al., 1999, Pike et al., 1995, Serrano-Pozo et al., 2011, Vehmas et al., 2003, Yasuhara et al., 1994). On the other hand, diffuse plaques have filamentous Aβ and have less diagnostic specificity (Dickson, 1997b, Thal et al., 2006). Due to their nature, neuritic plaques but not diffuse plaques can be stained by β-pleated sheet structure binding dyes, such as Congo red or thioflavin S (Davies and Mann, 1993, Thal et al., 2006).

1.1.2. Intracellular Neurofibrillary Tangles

The other pathological hallmark of AD, NFTs, reside in neurons and are mainly composed of the hyperphosphorylated form of the tau protein (Alonso et al., 1996, Alonso et al., 2001, Brion et al., 1985, Grundke-Iqbal et al., 1986a, Grundke-Iqbal et al., 1986b, Kidd, 1963). NFTs were also reported in other neurodegenerative disorders, such as frontotemporal dementia, Huntington Disease and Pick's disease (Lee et al., 2001). Although hyperphosphorylation of tau is the commonality of these tauopathies, the phosphorylation patterns and tau isoforms involved are different (Barthélemy et al., 2016, Connell et al., 2005, Duka et al., 2013, Samimi et al., 2021).

In the first stages of AD, NFTs are observed in temporal lobe, then spreading to limbic areas and ultimately to the large areas of neocortex (Arnold et al., 1991, Braak and Braak, 1991,

`

Hyman et al., 1984). NFT formation correlates with cognitive decline and synaptic loss in patients (Bierer et al., 1995, Gómez-Isla et al., 1997, Haroutunian et al., 2007). A recent study suggested that aggregation patterns of tau within the brain network is distinct for each tested clinical AD phenotype (Therriault et al., 2022).

1.2.Amyloidogenic Pathway

The amyloidogenic pathway is a linked series of enzymatic reactions to produce Aβ peptides from the amyloid precursor protein (APP). Two secretases convert APP to Aβ, namely β-secretase (BACE1) and γ-secretase complex, the latter of which then cleaves its substrate multiple times starting at the carboxy terminal end to produce a series of C-terminally truncated Aβ peptides, intermediate forms of which are toxic and prone to aggregate to form amyloid plaques.

1.2.1. The Amyloid Precursor Protein and its Processing

APP is a type I single-pass transmembrane protein that is part of a family of related proteins which also includes amyloid precursor-like proteins (APLP1 and APLP2) in mammals (Kang et al., 1987, Slunt et al., 1994, Wasco et al., 1992). All three proteins have a highly conserved amino acid sequence in the cytoplasmic region and the ectodomain; however, only APP contains the Aβ sequence. Although the exact physiological function of APP remains elusive, it has been shown to be important for proper synaptic function and plasticity, cell growth, cell survival, motility, neurite outgrowth and metal homeostasis (Allinquant et al., 1995, Ciccotosto et al., 2014, Dawson et al., 1999, Hérard et al., 2006, Maynard et al., 2002, Müller et al., 1994, Perez et al., 1997, Phinney et al., 1999, Phinney et al., 2003, Ring et al., 2007, Seabrook et al., 1999, Young-Pearse et al., 2008, Zheng et al., 1995).

APP is highly expressed in neurons (Kim et al., 1995, Rodrigues et al., 2014). Once being co-translationally inserted into the endoplasmic reticulum (ER) membrane, APP is first trafficked

`

to the plasma membrane along secretory pathways via the trans-Golgi network (TGN) (Choy et al., 2012, Koo et al., 1990). When APP is inserted into the plasma membrane, it undergoes ectodomain cleavage by α-secretase that is located on cell surface, to initiate non-amyloidogenic (non Aβ-generating) pathway (Figure 1) (Haass and Selkoe, 1993). This cleavage generates a soluble sAPPα fragment and membrane bound C-terminus of APP (α-CTF), which consecutively undergoes γ-secretase-mediated proteolysis to generate p3 peptide and APP intracellular domain (AICD) fragment. Alternatively, plasma membrane APP can be internalized and recycled back into the cell through endo-lysosomal compartments (Haass et al., 2012) as a result of the interaction of adaptor proteins with the YENPTY motif of the cytoplasmic domain of APP (Chen et al., 1990).

APP in endo-lysosomal system undergoes β-secretase ectodomain shedding, which is the first step of the amyloidogenic (Aβ-generating) pathway (Figure 1). β-site cleavage produces a soluble sAPPβ fragment and a membrane bound 99-amino acid long C-terminus of APP (β-CTF or APP-C99) (O'brien and Wong, 2011) that consecutively undergoes γ-secretase-mediated proteolysis to generate AICD and Aβ peptides of varying lengths with different biophysical and biochemical properties (De Strooper et al., 2010, Olsson et al., 2014, Yan and Vassar, 2014). Among these peptides, Aβ40 is the most abundant in the brain and relatively non-toxic and Aβ42 is most prone to form toxic oligomers, accumulate and aggregate into amyloid plaques (Cleary et al., 2005, Kayed et al., 2003, Lambert et al., 1998, Zhao et al., 2012). A shorter peptide, "protective" Aβ38, has recently been shown to interact with Aβ42 thereby impeding aggregate formation (Quartey et al., 2021). Alternative to β-site cleavage, β-secretase can cleave APP at the β'-site resulting in the generation of N-terminally truncated Aβ peptides of varying lengths (Aβ11-X) (Figure 1) (Gouras et al., 1998, Lee et al., 2003, Vetrivel et al., 2011). In addition to its role in

`

amyloid pathology, some reports suggested beneficial effects of Aβ peptides with respect to synaptic plasticity and potentiation (Puzzo et al., 2008, Zhou et al., 2022).

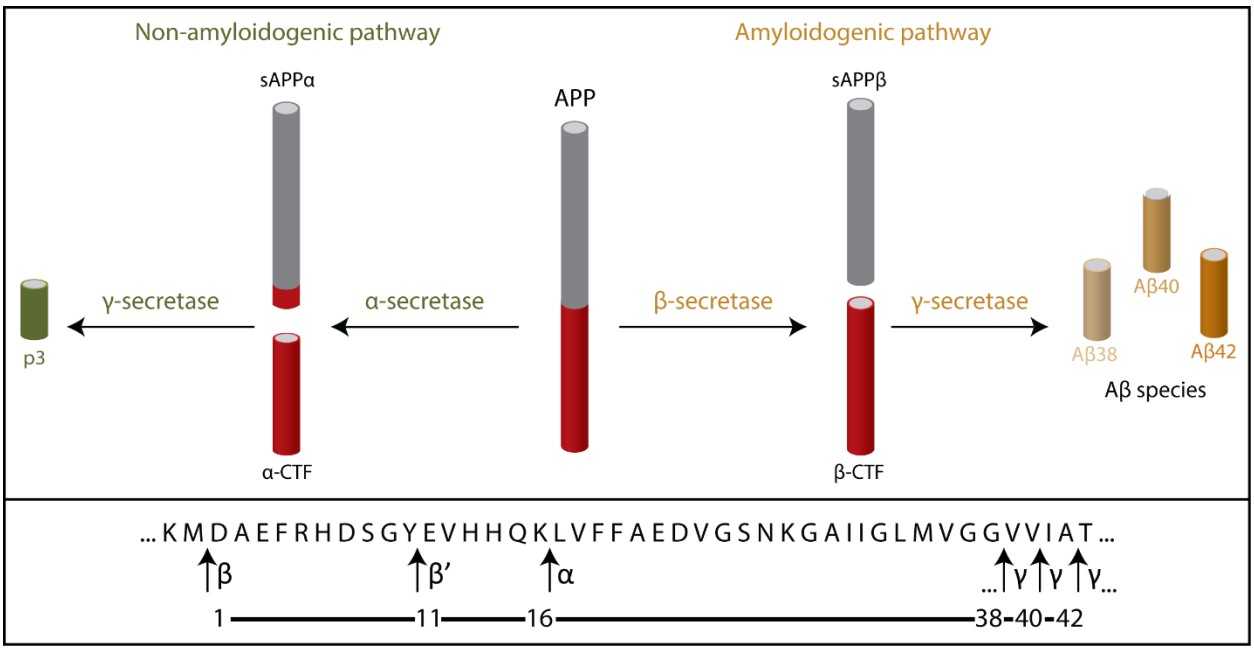

Figure 1: Processing of APP by α-, β- and γ-secretases

In the amyloidogenic pathway, APP is first cleaved by β-secretase to generate sAPPβ and β-CTF which sequentially undergoes γ-secretase cleavage to produce Aβ peptides of varying lengths. In the non-amyloidogenic pathway, APP is first cleaved by α-secretase to generate sAPPα and α-CTF which sequentially undergoes γ-secretase cleavage to produce p3 peptide. As an alternative cleavage, BACE1 can also cleave APP or β-CTF at β'-site to generate Aβ11-X.

APP proteolysis is not exclusive to α-, β- and γ-secretases; it can be cleaved by other proteases at various cleavage sites (Andrew et al., 2016, Paschkowsky et al., 2016, Willem et al., 2015, Zhang et al., 2015), such as η-secretase that cleaves far from β-site leading to generation of Aη peptides (Ahmad et al., 2006, Higashi and Miyazaki, 2003). Another example of alternative APP cleaving metalloproteases is Meprin β (Becker-Pauly and Pietrzik, 2017) that cleaves APP at the β-site leading to generation of Aβ species such as Aβ40 and Aβ42 and their N-terminally truncated variants (Bien et al., 2012, Jefferson et al., 2011). It has also been shown that APP can

`

be cleaved within its transmembrane domain upstream of Aβ40 and Aβ42 cleavage sites, i.e., ϵ- and ζ-cleavage sites, in a presenilin-dependent manner (Weidemann et al., 2002, Zhao et al., 2004).

1.2.2. Amyloid Hypothesis

The amyloid hypothesis states that Aβ production initiates the disease pathology due to a failure in Aβ clearance followed by oligomerization, accumulation and deposition of Aβ peptides into plaques (Selkoe and Hardy, 2016). Deposition into plaques alters neuronal homeostasis and eventually leads to neuronal dysfunction and dementia. According to this hypothesis, Aβ deposition and plaque formation are disease processes that trigger the further pathology characteristic of AD, including neurofibrillary tangle formation, cell loss, vascular damage and dementia (Hardy and Higgins, 1992).

1.3. Early- and Late-onset AD and Stages of AD

About 5% of the AD cases the pathology starts before the age of 65 and are therefore classified as early-onset Alzheimer Disease (Bekris et al., 2010). Approximately 10-15% of these cases have a genetic cause linked to mutations in three different genes, *APP*, *Presenilin 1* or *Presenilin 2* (Campion et al., 1999, Di Fede et al., 2009). To date, about 50 mutations in *APP* (https://www.alzforum.org/mutations/app), approximately 300 mutations in *PSEN1* (https://www.alzforum.org/mutations/psen-1) and about 90 mutations in *PSEN2* (https://www.alzforum.org/mutations/psen-2) have been reported. Late-onset AD starts after the age of 65 that is caused by a combination of environmental and genetic risk factors, such as *APOE4* (Bertram and Tanzi, 2004, Borenstein et al., 2006, Corder et al., 1993, Saunders et al., 1993). A recent GWAS meta-analysis combining multiple European datasets identified 42 new risk loci for AD (75 loci in total) that are related to amyloid and tau pathways, endocytosis and microglia (Bellenguez et al., 2022).

`

Preclinical AD is considered as the stage of the disease before clinical diagnosis where molecular changes have started but symptoms are not noticeable. As the disease progresses, the symptoms of brain dysfunction become apparent, which is called prodromal AD (also referred to as mild cognitive impairment (MCI)) (Albert et al., 2011). The dementia stage occurs when an individual is not able to function independently due to the impairments in social, occupational and cognitive functioning (McKhann et al., 2011). Clinical studies suggest that disease-modifying agents would be more effective if they are applied at early stages. It is very important to identify molecular changes in the preclinical stage to take preventative measures. Therefore, search for AD biomarkers is currently the focus of AD research (Jack Jr et al., 2010).

1.4.Biomarkers of AD

Cerebrospinal fluid (CSF) analysis helps diagnose conditions affecting the brain and can accurately distinguish between a wide range of CNS diseases, including AD, that can otherwise be difficult to diagnose (Blennow et al., 2015, Rasmussen et al., 2018). Extracellular Aβ species present in the CSF can be quantified and give an indication of the amyloid burden within the brain. Stable isotope labeling kinetics (SILK) analysis of Aβ in the CSF and studies with different cohorts carrying familial AD (FAD) mutations, i.e., *APP*, Presenilin 1 (*PSEN1*) and Presenilin 2 (*PSEN2*), suggested that CSF Aβ42 levels start to decrease as early as 25 years before the diagnosis prior to appearance of amyloid deposits, elevation of tau levels in CSF and cognitive impairment (Bateman et al., 2012, Selkoe and Hardy, 2016). Although three core biomarkers ((i) Aβ peptides, (ii) total tau (t-tau) and phosphorylated tau (p-tau), and (iii) positron emission tomography (PET) imaging of amyloid burden) are established in the diagnosis of AD, search for less invasive accurate biomarker detection and quantification is still ongoing (Olsson et al., 2016). Recent studies focus on biomarker detection in blood/plasma, which is important for understanding

`

the pathogenic sequence of AD progression that cannot be identified by brain imaging (Hampel et al., 2014) as well as for longitudinal tracking, early detection, and treatment of the disease (Baldacci et al., 2018, Hampel et al., 2018, Olsson et al., 2016, Selkoe and Hardy, 2016, Kaeser et al., 2022, Barthélemy et al., 2020a, Barthélemy et al., 2020b).

First reports showed a reduction in CSF-Aβ42 in AD patients (Motter et al., 1995), followed by several studies suggesting an inverse relationship between CSF-Aβ42 levels and plaque load in the brain observed with PET (Fagan et al., 2006, Grimmer et al., 2009, Jagust et al., 2009, Strozyk et al., 2003, Tapiola et al., 2009). Under normal conditions, after generation in the brain, soluble Aβ peptides could be irreversibly lost from the brain by several mechanisms including transport to CSF (Wang et al., 2006). As Aβ42 deposits into plaques, there is less soluble Aβ42 in CSF (Rasmussen et al., 2018). Although CSF-Aβ40 is not recognized as a core biomarker alone, CSF-Aβ42/Aβ40 ratio compared to CSF-Aβ42 *per se* correlates better with PET imaging (Hansson et al., 2019, Janelidze et al., 2016b, Leuzy et al., 2016, Lewczuk et al., 2017, Pannee et al., 2016). CSF-Aβ42/Aβ40 ratio is also strongly associated with CSF t-tau and p-tau (Delaby et al., 2022), and is better at distinguishing AD from non-AD dementias (Dorey et al., 2015, Janelidze et al., 2016b). Both CSF-t-tau and p-tau are found to be increased in AD cases (Dubois et al., 2014, Maia et al., 2013, McKhann et al., 2011). Nevertheless, combination of both CSF-tau and CSF-Aβ42 increases the diagnostic accuracy of AD (Fagan et al., 2011, Hulstaert et al., 1999, Rivero-Santana et al., 2017, Seeburger et al., 2015, Shaw et al., 2009).

Due to the invasiveness of lumbar puncture that is used to collect CSF and limited access to resources, current studies focus on the detection of biomarkers in plasma/blood (Hansson et al., 2022, Lista et al., 2013a, Lista et al., 2013b). Plasma Aβ42/Aβ40 ratio is shown to decrease in patients with Aβ-positive PET and to correlate with CSF-Aβ42/Aβ40 ratio and plaque load

`

(Janelidze et al., 2016a, Keshavan et al., 2021, Nakamura et al., 2018, Verberk et al., 2018). The reduction in blood Aβ42/Aβ40 (8-15%) is rather small in comparison to CSF levels (40-60%) (Hansson, 2021, Janelidze et al., 2021) likely because Aβ levels in the extracerebral tissues are not greatly affected by the changes in brain Aβ metabolism and pathology (Hansson et al., 2022). Plasma p-tau levels are reported to be elevated in AD cases and show a similar diagnostic accuracy as CSF-p-tau levels (Palmqvist et al., 2020, Thijssen et al., 2021). However, biomarker detection in blood provides several challenges, namely, detection of low levels of Aβ, and differentiation between distinct phosphorylated tau forms, both of which are areas of ongoing innovation.

`

2. PROTEASES INVOLVED in Aβ CLEARANCE

Recent studies show that Aβ clearance is as important as Aβ production to develop pathology and in disease progression. It has been determined that under physiological conditions, Aβ clearance rate in human CSF is ~8% per hour (Bateman et al., 2006). The clearance from central nervous system (CNS) slows down with age and is impaired by ~30% in sporadic AD (Mawuenyega et al., 2010, Patterson et al., 2015). Aβ can be cleared from CNS by several mechanisms including cellular uptake, passive elimination, transport to CSF and proteolysis (Deane et al., 2008, Iliff et al., 2012, Sagare et al., 2007, Wildsmith et al., 2013). A variety of proteases with distinct characteristics, including Aβ specificity, optimal pH, and subcellular localization are involved in Aβ degradation (Saido and Leissring, 2012).

2.1.β-secretase (BACE1)

β-site APP-cleaving Enzyme 1 (BACE1) is a type I transmembrane aspartyl protease with two catalytically active aspartic acids (D_{93} and D_{289}) in the extracellular domain (Acquati et al., 2000, Vassar et al., 1999). BACE1 expression is high in the brain, particularly in neuronal cells (Haniu et al., 2000, Vassar et al., 1999, Zhao et al., 2007). BACE1 has also been detected in healthy pre-synaptic terminals and in dystrophic neurites in the vicinity of the Aβ plaques (Kandalepas et al., 2013, Sadleir et al., 2016, Zhao et al., 2007).

Pro-BACE1 is synthesized in the ER before it is transported to the trans-Golgi network to undergo maturation and is trafficked to the plasma membrane (Haniu et al., 2000, Vassar et al., 1999). From cell surface, it is internalized to the endosomal compartments (Huse et al., 2000, Walter et al., 2001) where the acidic environment is optimal for BACE1's proteolytic activity (pH = ~ 4.5) (Vassar et al., 1999).

`

2.1.1. BACE1 in AD

BACE1 is extensively studied and implicated in brain amyloidogenesis because of its role in the amyloidogenic pathway. Since BACE1 knockout mouse models showed diminished Aβ production (Cai et al., 2001, Cai et al., 2012, Dominguez et al., 2005, Harrison et al., 2003, Luo et al., 2001, Roberds et al., 2001), BACE1 cleavage of APP is considered as the rate-limiting step for Aβ production.

Vast majority of mutations associated with familial AD are found in *APP*, *PSEN1* or *PSEN2* genes (Bekris et al., 2010, Bird et al., 1988, Campion et al., 1999, Cruts and Van Broeckhoven, 1998, Finckh et al., 2000, Goate et al., 1991, Sherrington et al., 1995). Although there is no *BACE1* mutation associated with AD to date, mutations in *APP* affecting β-site cleavage by BACE1 have a strong effect on Aβ production. Some of these mutations increase the processing of APP by BACE1, such as the Swedish mutation KM670/671NL (Citron et al., 1992, Mullan et al., 1992) and an Italian variant A673V (Di Fede et al., 2009) while others inhibit the processing of APP by BACE1, such as the Icelandic variant A673T (Jonsson et al., 2012, Peacock et al., 1993).

BACE1 protein levels and enzymatic activity are higher in human AD brain extracts compared to healthy controls (Fukumoto et al., 2002, Holsinger et al., 2002, Li et al., 2004, Tyler et al., 2002, Yang et al., 2003) (Manuscript 1). CSF BACE1 levels and activity are also elevated in MCI and used in discriminating MCI from AD and healthy controls as it also associates with other CSF and neuroimaging biomarkers of AD (Ewers et al., 2011, Ewers et al., 2008, Molinuevo et al., 2018, Wu et al., 2012, Zetterberg et al., 2008, Zhong et al., 2007).

Due to its role in Aβ production, BACE1 has been a drug target for AD. Among BACE1 inhibitors, LY2811376 and LY2886721 caused auto-fluorescent deposits in retina (May et al.,

`

2011) and liver toxicity (May et al., 2015), respectively, and their phase II trials were terminated (Kumar et al., 2018). Verubecestat (MK-8931) had promising results, and in phase I clinical trial, it mitigated CSF levels of Aβ40, Aβ42 and sAPPβ without any dose-dependent side effects (Kennedy et al., 2016). Although reduction in Aβ levels was only observed in short-term treatment trials, phase III studies were conducted with prodromal AD patients and showed a decrease in amyloid plaques without any improvement to cognitive function (Forman et al., 2013, Forman et al., 2012, Kennedy et al., 2016, Kumar et al., 2018). All other BACE1 inhibitors that were in randomized clinical trials were halted for safety or futility reasons which could be a consequence of (1) the side-effects from multiple substrates of BACE1, (2) the off-target effects of BACE1 inhibitors, such as its homolog BACE2, or (3) timing of BACE1 inhibition over the course of AD.

2.1.2. Role of BACE1 in Aβ Clearance: Amyloidolytic Processing

Besides its role in Aβ production, i.e., β-site cleavage of APP in amyloidogenic pathway resulting in the production of Aβ species, BACE1 is also involved in Aβ clearance. After being generated by BACE1 and γ-secretase (amyloidogenic pathway), Aβ peptides (e.g., Aβ38, Aβ40, and Aβ42) can undergo amyloidolytic processing, leading to their degradation. Amyloidolytic processing takes place when soluble Aβ peptides are further cleaved by BACE1 at β^{34}-site into a non-amyloidogenic 34-amino acid long Aβ fragment (Aβ34) (Fluhrer et al., 2003, Hernandez-Guillamon et al., 2015, Liebsch et al., 2019, Shi et al., 2003) (Figure 2). This implies that BACE1 has a dual role in amyloid metabolism. Firstly, it has a key role in amyloid production by cleaving APP (amyloidogenic activity). Secondly, BACE1 recognizes Aβ42 and Aβ40 as substrates (amyloidolytic activity) and is involved in amyloid clearance.

`

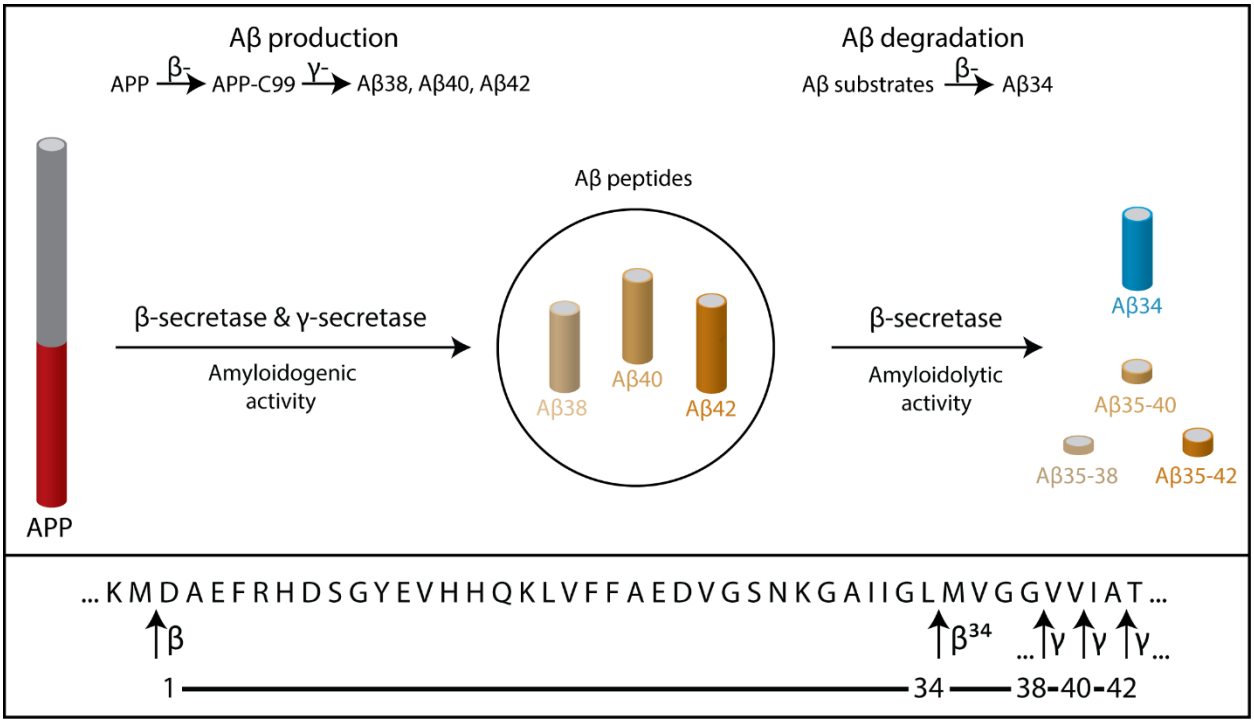

Figure 2: Dual role of BACE1 in Aβ production (amyloidogenic) and Aβ clearance (amyloidolytic)

BACE1 has a dual role in Aβ metabolism. Amyloidogenic activity of BACE1 is cleavage of APP at the β-site that leads to production of Aβ peptides, such as Aβ38, Aβ40 and Aβ42. Amyloidolytic activity of BACE1 is cleavage of Aβ species at the β^{34}-site to produce the non-amyloidogenic Aβ34 peptide.

2.2.γ-secretase Complex

The γ-secretase complex has four subunits: nicastrin, anterior pharynx-defective 1, presenilin enhancer 2, and either Presenilin 1 (PS1) or its homolog Presenilin 2 (PS2) (Kimberly et al., 2003, Zhang et al., 2014). Presenilin, an aspartyl protease, is the proteolytic subunit of the γ-secretase complex (Wolfe et al., 1999) and requires the assembly of other subunits to become stable and proteolytically active (Edbauer et al., 2003, Takasugi et al., 2003). Although both PS1- and PS2-γ-secretases possess overlapping enzymatic properties, PS1-γ-secretase and PS2-γ-secretase have distinct influence on Aβ abundance and differ in their susceptibility to γ-secretase inhibitors (Lai et al., 2003).

`

PS1 is more broadly distributed in the cell and mainly located on the plasma membrane. Contrastingly, the presence of a C-terminal motif including a hydrophobic methionine and a serine in PS2 allows a phosphorylation-dependent interaction with Adaptor Protein 1 (AP-1), which restricts PS2 localization to late endosomes and lysosomes (Sannerud et al., 2016, Meckler and Checler, 2016). This distinct localization of PS1- and PS2-γ-secretase complexes leads to different access to substrates. PS1 selectively cleaves substrates on the cell surface, whereas PS2 selectively cleaves substrates in late endosomes/lysosomes. PS1-γ-secretase-derived Aβs are released from the cell surface into the extracellular space, whereas PS2-γ-secretase-derived Aβs are generated intracellularly (Sannerud et al., 2016).

2.2.1. Role of γ-secretase in Aβ Clearance: Sequential Cleavage of APP-C99

The stepwise cleavage of APP-C99 by γ-secretase is part of Aβ degradation as it leads to production of non-amyloidogenic peptides. APP cleavage by γ-secretase occurs in a stepwise manner, indicating that γ-secretase can trim a substrate by processing it several times (Kakuda et al., 2006, Olsson et al., 2014, Takami et al., 2009). For example, the first γ-secretase cleavage can generate either Aβ49 or Aβ51. The subsequent cleavage sites are separated approximately by three or four amino acids leading to production of Aβ40 and Aβ42 from Aβ49 and Aβ51, respectively. Further processing of Aβ40 and Aβ42 by γ-secretase leads to the convergence of these distinct pathways in the production of the common non-amyloidogenic metastable Aβ34 intermediate (Olsson et al., 2014, Takami et al., 2009).

2.3.Aβ Degrading Enzymes

Different types of proteases involved in Aβ clearance from the CNS are collectively referred as Aβ-degrading enzymes (ADEs), including metallo-, serine-, aspartyl-, cysteine- and threonine-proteases (Saido and Leissring, 2012, Wildsmith et al., 2013). With regards to Aβ

`

degradation, the most important difference among these proteases is their subcellular localization. These proteases determine the lifetime of Aβ species, which in turn restricts trafficking of Aβ peptides away from the compartment in which they are generated. Aβ species can be processed by ADEs either proximal or distal to the sites where they are generated, and Aβ pools are defined according to subcellular localization; interstitial (extracellular), ER/golgi, endosomal, lysosomal, and cytosolic (Reviewed in (Saido and Leissring, 2012)).

Studying ADEs is important to better understand the molecular basis of the disease as well as to guide the search for AD biomarkers (Portelius et al., 2012, Saido and Leissring, 2012). A selected list of proteases and some of their properties are listed in Table 1.

Table 1: A selection of proteases implicated in AD

Protease	Type	Membrane bound?	Optimal pH	Aβ pools
Endothelin Converting Enzyme 1 (ECE1)	Zinc metalloprotease	Type II	5.0 – 7.0	Endosomal
Insulin Degrading Enzyme (IDE)	Zinc metalloprotease	Cytosolic, membrane bound and secreted	6.0 – 8.5	Extracellular, Cytosolic
Cathepsin B (Cat B)	Cysteine protease	Secreted	4.5 – 5.5	Extracellular, Lysosomal, Cytosolic
Cathepsin D (Cat D)	Aspartyl protease	Secreted	4.5 – 5.0	Lysosomal
Matrix Metalloproteinase 2 (MMP2)	Calcium dependent Zinc metalloprotease	Secreted	4.5 – 9.5	Extracellular
Matrix Metalloproteinase 9 (MMP9)	Calcium dependent Zinc metalloprotease	Secreted	4.5 – 9.5	Extracellular
Angiotensin Converting Enzyme (ACE)	Zinc metalloprotease	Type I	7.4	NA
Neprilysin (NEP or MME)	Zinc metalloprotease	Type II	7 – 9	Extracellular

`

2.3.1. Endothelin Converting Enzyme 1 (ECE1)

ECE1 is a membrane bound endopeptidase with a catalytic site that either resides in the extracellular space or in the lumen of organelles and vesicles (Johnson et al., 1999, Xu et al., 1994). Although not exclusive, ECE1 is present throughout the CNS and heavily expressed in the vascular endothelial cells (Korth et al., 1999, Xu et al., 1994), mainly hydrolyzing inactive big endothelin-1 into active endothelin-1 (Turner and Murphy, 1996). ECE1 can be found in the plasma membrane or in intracellular components, such as TGN or endosomes, depending on the isoform (Kuruppu and Smith, 2012, Schweizer et al., 1997, Valdenaire et al., 1999).

ECE1 is highly active at acidic pH (Fahnoe et al., 2000, Johnson et al., 1999) and cleaves Aβ40 most efficiently at pH 5.6 (Eckman et al., 2001). It has been shown to have no effect on Aβ degradation when cells were treated with exogenous Aβ40 peptides (Pacheco-Quinto and Eckman, 2013), indicating that ECE1 is involved in intracellular Aβ clearance. Pharmacological inhibition of endogenous ECE activity in APP-overexpressing cells leads to extracellular as well as intracellular Aβ accumulation in endo-lysosomal compartments (Eckman and Eckman, 2013). Moreover, heterozygous ECE1 knockout mice have significantly elevated levels of both Aβ40 and Aβ42 in the brain (Eckman et al., 2003) further supporting its role in Aβ clearance.

2.3.2. Insulin Degrading Enzyme (IDE)

IDE is a metalloprotease that is mainly localized in the cytosol, primarily degrading insulin (Duckworth et al., 1998a, Falkevall et al., 2006). The optimal pH for its enzymatic activity ranges between 6.0 – 8.5 (Duckworth et al., 1998b). *In vitro* studies suggest that IDE is involved in Aβ degradation; more effective in degrading monomers than oligomers and fibrils (Sudoh et al., 2002, Vekrellis et al., 2000, Qiu et al., 1997). Although primarily cytosolic, IDE can be secreted and found in the extracellular space and at the cell surface (Zhao et al., 2009). In IDE knockout rats

`

and mice, increased levels of Aβ species are reported (Farris et al., 2003, Farris et al., 2004). Gene expression analysis of total brain samples reveals that AD patients have decreased IDE expression (da Costa et al., 2017). Further meta-analysis suggests a reduction in IDE protein levels in AD cases with no change in IDE mRNA and enzyme activity (Zhang et al., 2018). With subgroup analysis, reduced IDE protein levels are found to be in cortex and hippocampus whereas IDE mRNA is higher in the cortex but not in the hippocampus (Zhang et al., 2018). Changes in IDE protein level and activity in AD remains controversial.

2.3.3. Cathepsins (Cat B and Cat D)

Cat B is a lysosomal cysteine protease and is one of the most abundantly expressed cathepsins in the brain (Hsu et al., 2018). The optimal pH for its enzymatic activity ranges between 4.5 – 5.5 (Linebaugh et al., 1999). It has been proposed as an alternative β-secretase with different substrate selectivity (APP with Swedish mutation is preferred by BACE1 over wild type APP and vice versa for Cat B) (Hook et al., 2008, Kindy et al., 2012). However, it has also been proposed as an Aβ degrading protease. *In vivo* studies have conflicting results. Cat B ablation in transgenic mice overexpressing human APP (hAPP) elevates Aβ levels and does not affect hAPP levels (Wang et al., 2012). A similar study in the same transgenic mouse model shows a reduction in Aβ levels and β-CTF (Hook et al., 2009). Several studies suggested an increase in Cat B protein levels in plasma, serum, and CSF in AD patients (Morena et al., 2017, Sun et al., 2015, Sundelöf et al., 2010). Furthermore, high protein levels and activity of Cat B are detected in amyloid plaques (Cataldo and Nixon, 1990, Mueller-Steiner et al., 2006).

Cat D is an aspartyl protease that is active only at acidic pHs (4.5 – 5.0) (lysosomes) (Briozzo et al., 1988, Westley and May, 1999). The substrate affinity of Cat D for Aβ42 and Aβ40 is reported to be in the nanomolar and micromolar range, respectively (Saido and Leissring, 2012,

`

Suire et al., 2020). Genetic deletion of Cat D results in an increase in both soluble and insoluble Aβ levels, ~30% increase in cerebral Aβ42/Aβ40 ratio (Leissring et al., 2009, Suire et al., 2020) and accumulation of Aβ in lysosomes (Suire and Leissring, 2021). Lysosomal Cat D is found to be elevated in the neocortex of AD patients (Chai et al., 2019), and reduced plasma levels of Cat D were detected in AD patients (Kim et al., 2021). Recently, our collaboration with Paul Saftig group showed that pro-Cat D treatment did not change Aβ pathology *in vivo* and did not affect Aβ degradation *in vitro* and *in vivo* (Gallwitz et al., 2022).

2.3.4. Matrix Metalloproteinases (MMP2 and MMP9)

MMPs are secreted calcium dependent zinc metalloproteases. The optimal pH for MMPs' enzymatic activity varies between 4.5 – 9.5 (Johnson et al., 2000, Stack and Gray, 1990). Among those, MMP2 and MMP9 have been shown to cleave Aβ with a high processing efficiency at the carboxy terminus as well as α-secretase cleavage site with less efficiency (Hernandez-Guillamon et al., 2015, Yan et al., 2006). MMP9 can cleave preformed Aβ fibrils and amyloid plaques, which makes it distinct from other ADEs (Yan et al., 2006). Both MMP2 and MMP9 knockout mice have elevated Aβ levels in the brain (Yin et al., 2006). MMP2 and MMP9 are produced by reactive astrocytes and their levels are increased in astrocytes surrounding Aβ plaques both in transgenic mouse model and in hippocampal neurons of post-mortem AD brains (Backstrom et al., 1996, Girard et al., 2014, Yin et al., 2006). MMP9 is lower in the CSF of AD brain (Mroczko et al., 2014). Studies with plasma have contradicting results: one study reports reduced levels of MMP9 and MMP2 (Horstmann et al., 2010) whereas two other studies report elevated levels of MMP9 in plasma of AD patients (Lorenzl et al., 2003, Lorenzl et al., 2008). In addition to its involvement in Aβ degradation, increased levels of MMP2 are detected in association with phosphorylated tau in

`

NFTs and dystrophic neurites in early stages of AD suggesting that MMP2 might be involved in the elimination of toxic tau species (Terni and Ferrer, 2015).

2.3.5. Angiotensin Converting Enzyme (ACE)

ACE is a type I metalloprotease that is active at neutral pH (Aydin et al., 2021). It has a carboxypeptidase activity that converts Aβ42 to Aβ40 (Zou et al., 2007). Although it has been shown to degrade monomeric Aβ and inhibit Aβ aggregation *in vitro* (Zou et al., 2007, Hu et al., 2001), neither gene inactivation nor pharmacological inhibition of ACE have an effect on Aβ levels in the brain *in vivo* (Eckman et al., 2006, Hemming et al., 2007, Saito et al., 2003) except in one study where ACE inhibition enhanced Aβ deposition in the brain (Zou et al., 2007). Despite the lack of direct evidence for ACE involvement in Aβ clearance, due to the genetic evidence that ACE polymorphisms could be associated with the risk of AD (Farrer et al., 2000, Hu et al., 1999, Nacmias et al., 2007), it is still considered as an ADE.

2.3.6. Neprilysin / Membrane Metallo-endopeptidase (NEP or MME)

NEP, is a type II transmembrane protein mainly localized to the plasma membrane (Landry et al., 1993) with an optimal pH ranging between 7 – 9 (Tsan and Jiang, 1985). NEP was first identified by treating rats, that received radiolabeled Aβ42 injection, with NEP inhibitors (Iwata et al., 2000). Following the NEP inhibition, the degradation of the infused Aβ is reduced. Both *in vitro* and *in vivo* studies show that NEP hydrolyzes Aβ40 and Aβ42 and its absence or inhibition leads to enhanced Aβ levels in the brain (Fukami et al., 2002, Iwata et al., 2001, Yasojima et al., 2001b). Further studies combine NEP and ECE1 knockout in mice which show enhanced Aβ levels in the brain compared to single knockouts (De Strooper, 2010, Eckman et al., 2006). NEP activity is also shown to be lowered by γ-secretase inhibition or PS deficiency in mouse brain that is mediated by AICD, suggesting that NEP is part of a feedback loop with PSs (Pardossi-Piquard et

`

al., 2005). Some studies suggest that in aged mice and sporadic AD patients, NEP levels are reduced in the brain (Iwata et al., 2002, Yasojima et al., 2001a). More recently, treatment of cynomolgus monkey with NEP inhibitor reduced Aβ clearance and increased CSF Aβ levels on day 1 but not after day 15 with no effect on brain Aβ levels (Schoenfeld et al., 2017).

`

3. IMPORTANCE of Aβ34

Through various pathways, including amyloidolytic processing by β-secretase, sequential cleavage by γ-secretase and proteolytic degradation by proteases, Aβ34 can be generated from Aβ40 and Aβ42. Unlike Aβ40 and Aβ42, Aβ34 was shown to be non-toxic and non-aggregating (Hernandez-Guillamon et al., 2015). Besides being classified as a non-amyloidogenic Aβ species, Aβ34 shows strong potential as a biomarker of AD progression. Recent studies have shown a positive correlation between CSF-Aβ34 levels and overall Aβ clearance rates in amyloid plaque positive individuals, a significant elevation of CSF-Aβ34 levels in patients with MCI who later develop AD, and a correlation between CSF-Aβ34/Aβ42 ratio and current pre-clinical AD biomarkers, including p-tau and t-tau levels (Liebsch et al., 2019). The elevated CSF-Aβ34/Aβ42 ratio is a sign of a decrease in soluble CSF-Aβ42 as it becomes deposited in the plaques, and this ratio has a better diagnostic accuracy for prodromal AD compared to the traditional Aβ40/Aβ42 ratio. Therefore, CSF-Aβ34/Aβ42 ratio, Aβ42 being a marker of amyloid deposition and Aβ34 being a marker of amyloid clearance, could serve as a possible biomarker for earlier detection of prodromal and pre-symptomatic AD. Furthermore, Aβ34 is an important intermediate in the amyloidogenic degradation cascade that can be utilized to develop novel drugs for preventative approaches, such as modulation of BACE1 dual activity. One of the potential therapeutic strategies is to favor amyloidolytic activity of BACE1 rather than inhibiting BACE1 activity entirely. Enhancing amyloidolytic activity results in the degradation of amyloidogenic peptides into Aβ34 before they aggregate into toxic oligomers and fibrils. If successful, this approach can also explain the reason behind the failure of BACE1 inhibitors in clinical trials.

`

4. RATIONALE of THIS THESIS

As outlined in the previous sections, Aβ clearance is as important as Aβ production in AD progression as the disease state starts with an imbalance between Aβ production and clearance. The traditional Aβ42/Aβ40 ratio has been used as a diagnostic biomarker together with PET imaging and tau. This ratio includes levels of two Aβ peptides both of which are markers of Aβ production. Recent studies showed that Aβ34/Aβ42 ratio has a potential to serve as a biomarker with better diagnostic accuracy. This ratio includes markers for both Aβ production, Aβ42, and Aβ clearance, Aβ34, which further underlines the need for a better understanding of Aβ clearance and Aβ34 in AD field. Although molecular details of Aβ42 and Aβ40 production pathway, i.e., amyloidogenic pathway, and some of their degradation pathways, e.g., ADEs, are heavily studied, little is known about amyloidolytic activity of BACE1 to produce Aβ34, and where and how Aβ34 is generated and further degraded in the cell.

To better understand molecular and cellular aspects of BACE1 as a potential drug target (by inhibiting amyloidogenic and promoting amyloidolytic activity), we performed biochemical and pharmacological tests with post-mortem human brain tissue, animal models and cell culture systems. We aimed to assess (i) relationship between BACE1 protein levels and absolute Aβ34 levels in AD patients and mouse models, (ii) how BACE1:APP ratio affects the balance between BACE1-mediated Aβ production and degradation, (iii) cellular localization of amyloidolytic activity, (iv) involvement of PS1- and PS2-γ-secretase complexes in Aβ34 generation, and (v) effect of BACE1 inhibitors on amyloidogenic vs. amyloidolytic activities. We hypothesized that reported "paradoxical" BACE1 overexpression in AD cases in the literature could be due to its Aβ

`

degrading activity, and that BACE1 produces Aβ34 in the intracellular compartments through cleavage of longer Aβ species, e.g., Aβ40 and Aβ42, generated by PS2-γ-secretase (Manuscript I).

Most ADEs are mainly studied in the context of Aβ40 and Aβ42 and proteases involved in Aβ34 clearance haven't been identified. We aimed to test different ADEs that are implicated in Aβ clearance for their potential role in Aβ34 degradation. We performed genetic, including small-interfering RNA (siRNA) knockdowns and transient overexpression, and pharmacological approaches to dissect the involvement of different proteases in Aβ34 metabolism. Based on the results we obtained from Manuscript I, Aβ34 is produced by BACE1 from PS2-γ-secretase-derived Aβ species in the endo-lysosomal system. Therefore, we hypothesized that ADEs that are localized to endo-lysosomal system, namely ECE1, Cat B, and Cat D have higher access to Aβ34 and are involved in Aβ34 degradation (Manuscript II).

Overall, this thesis revealed molecular details of the Aβ34 life cycle with a focus on its production and clearance. The findings not only provide new insights in Aβ metabolism but also will pave the way to develop new methods for biomarker development in CSF and blood/plasma. Understanding the dual role of BACE1 in both Aβ production and Aβ clearance enables screening for compounds to regulate each activity of BACE1 separately and to design more effective BACE1 inhibitors to treat AD. The identification of proteases responsible for Aβ34 degradation helps to better understand the role of Aβ34 as an indicator for clearance and to facilitate approaches to manipulate the levels of Aβ34 in body fluids that will be beneficial to biomarker research.

`

Chapter II :

EXPERIMENTAL SECTION

`

MANUSCRIPT I

The Beta-site Amyloid Precursor Protein (APP) Cleaving Enzyme (BACE1) Has a Critical Role in Amyloid Homeostasis Which Primarily Affects Amyloid-β Clearance

Irem Ulku[1], Filip Liebsch[1,2], S. Can Akerman[3], Jana F. Schulz[4], Luka Kulic[5], Christoph Hock[6], Claus Pietrzik[7], Alessandro Di Spiezio[8], Gopal Thinakaran[9], Paul Saftig[8], Gerhard Multhaup[1,3]

1. Integrated Program in Neuroscience, McGill University, Montreal, QC, Canada, H3G 0B1
2. Department of Chemistry University of Cologne, Institute of Biochemistry, 50674 Cologne, Germany
3. Department of Pharmacology & Therapeutics, McGill University, Montreal, QC, Canada, H3G 1Y6
4. Institut für Chemie und Biochemie, Freie Universität Berlin, 14195 Berlin; Current address: Cardiovascular and Metabolic Sciences, Max Delbrück Center for Molecular Medicine in the Helmholtz Association (MDC), 13125 Berlin, Germany
5. F.Hoffmann-La Roche Ltd., Roche Pharma Research & Early Development, 4070 Basel, Switzerland
6. Institute for Regenerative Medicine, University of Zurich, 8952 Schlieren, Switzerland; Neurimmune, 8952 Schlieren, Switzerland
7. University Medical Center of the Johannes Gutenberg-University of Mainz, Institute of Pathobiochemistry, Department Molecular Neurodegeneration, Duesbergweg 6, 55099 Mainz, Germany
8. Biochemisches Institut, CAU Kiel, Olshausenstr. 40, D-24098 Kiel, Germany
9. Department of Molecular Medicine and Byrd Alzheimer's Institute, University of South Florida, Tampa, FL 33613, USA

`

1.1.Abstract

The beta-site amyloid precursor protein (APP) cleaving enzyme (BACE1) was discovered due to its “amyloidogenic” activity which contributes to the production of amyloid-beta (Aβ) peptides. However, BACE1 also possesses an “amyloidolytic” activity, whereby it degrades longer Aβ peptides into a non-toxic Aβ34 intermediate. Here, we examine conditions that shift the equilibrium between BACE1 amyloidogenic and amyloidolytic activities by altering BACE1/APP ratios. In Alzheimer disease brain tissue, we found an association between elevated levels of BACE1 and Aβ34. In mice, the deletion of one BACE1 gene copy reduced BACE1 amyloidolytic activity by ~50%. In cells, a stepwise increase of BACE1 expression promoted amyloidolytic cleavage. An enzyme surplus in combination with inhibition of BACE1 activity elevated Aβ40 and Aβ42 levels while a substrate surplus lowered Aβ34 levels. Thus, our findings suggest that the BACE1/APP ratio primarily affects the balance between BACE1-mediated Aβ production and clearance assigning a critical role to BACE1 in amyloid clearance.

`

1.2.Introduction

Alzheimer disease (AD) is a progressive neurological disease characterized by intracellular neurofibrillary tangles and extracellular amyloid plaques, which are mainly composed of amyloid beta (Aβ) peptides (Holtzman et al., 2011, Iwatsubo et al., 1994). Traditionally, AD research has focused on Aβ production and the role of secretases in Aβ generation. In general, the process is initiated when β-secretase (BACE1) cleaves the amyloid precursor protein (APP) to generate sAPPβ and APP-C99 and involves a second protease, namely γ-secretase processing APP-C99 (Chow et al., 2010, Hussain et al., 1999, Sinha et al., 1999, Yan et al., 1999, Luo et al., 2001). BACE1 is a type-I transmembrane aspartic acid protease (Vassar et al., 1999) whose optimal activity requires an acidic environment in endosomes and lysosomes (Saric et al., 2013, Vassar et al., 2009). The γ-secretase, which further cleaves APP-C99 into Aβ peptides of varying lengths (e.g., Aβ40 and Aβ42), exists as a complex with four subunits, including the catalytic subunit Presenilin-1 or 2 (PS1 or PS2) (Rogaev et al., 1995, Sato et al., 2008, Shirotani et al., 2004, Zhang et al., 2014). Although both PS1- and PS2-γ-secretases possess overlapping enzymatic properties, due to their distinct localization, they have different access to substrates and differently influence Aβ abundance. PS1 selectively recognizes substrates on the cell surface, whereas PS2 preferentially cleaves substrates in late endosomes and lysosomes (Sannerud et al., 2016).

BACE1 has a relatively loose sequence specificity, and regions outside of its main cleavage site are less important for substrate selection (Hemming et al., 2009). This finding may explain why, in addition to its role in Aβ production (i.e., BACE1 amyloidogenic activity), BACE1 was found to cleave longer Aβ isoforms (e.g., Aβ40 and Aβ42) at position 34, i.e., the β34-site, which is a third BACE1 cleavage site in addition to the two canonical β- and the β'-sites (Fluhrer et al., 2003, Shi et al., 2003). However, the cut at the β34-site occurs only with longer Aβ peptides (such

`

as Aβ40 and Aβ42) as substrates previously released from γ-secretase complexes (Shi et al., 2003). Unlike other Aβ species, Aβ34 has been described as non-toxic and non-aggregating (Hernandez-Guillamon et al., 2015); therefore, the β34-cleavage is due to an amyloidolytic BACE1 activity as opposed to an amyloidogenic activity, which initiates production of aggregation prone Aβ peptides.

More recently, Aβ34 has been discovered by us as an early biomarker of amyloid clearance activity in prodromal AD (Liebsch et al., 2019). The Aβ34/Aβ42 ratio showed a better diagnostic accuracy for prodromal AD than the traditional Aβ40/Aβ42 ratio. CSF Aβ34 levels were elevated in early clinical stages of AD and correlated with Aβ clearance rates in subjects with evidence of cerebral amyloid deposition (Liebsch et al., 2019). Analyses with cultured human primary pericytes that normally regulate the blood-brain barrier function revealed a time and dose dependent production of Aβ34 upon treatment with recombinant Aβ40 peptides (Kirabali et al., 2019).

Numerous studies tried to correlate BACE1 activity with amyloid peptide production that resulted in conflicting findings both *in vivo* and *in vitro*. In transgenic mice overexpressing human BACE1, high BACE1 overexpression inhibited amyloid formation despite increased β-cleavage of APP (Lee et al., 2005) which is in sharp contrast to the expectation that increased BACE1 activity is causing increased amyloid production. The same apparently paradoxical behavior was observed in several pharmacological studies (Mattsson et al., 2012, Scholz et al., 2018). Post-mitotic human neurons treated with low concentrations of BACE1 inhibitors resulted in the expected decreased cellular BACE1 activity but unexpectedly higher levels of longer Aβ forms (Scholz et al., 2018). These findings have shifted our interest to the amyloidolytic activity of

`

BACE1 as a possible explanation which is a fairly neglected enzymatic function in the equation of production and elimination of Aβ peptides.

Here, we investigated molecular and cellular aspects of amyloidogenic and amyloidolytic activities of BACE1 by biochemical and pharmacological means. We provide *in vivo* and *in vitro* evidence that the BACE1/APP ratio primarily determines BACE1-mediated Aβ clearance: In AD brain tissue, we found levels of both BACE1 and Aβ34 approximately two-fold elevated. Analysis of brain cortices from wild-type mice and mouse lines with reduced expression levels of BACE1 revealed an association between BACE1 and Aβ34. Notably, a pharmacological inhibition of cellular BACE1 enzymatic activity caused a robust increase in Aβ40 and Aβ42 levels, most likely through the inhibition of its amyloidolytic activity. A decrease in Aβ34 levels observed upon downregulation of PS2, while Aβ40 and Aβ42 levels remained unaltered, implies a role for PS2 in Aβ34 generation in the endo-lysosomal system in conjunction with BACE1. In summary, we provide molecular explanations for the previously reported and paradoxical inverse relationship for BACE1 expression and Aβ levels by addressing the questions (i) why high BACE1 overexpression inhibits amyloid formation despite increased amyloidogenic processing of APP and (ii) why a reduction of BACE1 activity does not necessarily lower Aβ levels or plaque load.

`

1.3.Results

1.3.1. BACE1's amyloidogenic and amyloidolytic in vivo activities are determined by the enzyme to substrate ratio

To test whether there is a dichotomy between the amyloidogenic and amyloidolytic roles of BACE1 (Figure 3) *in vivo*, we measured Aβ levels in human brain tissue, in wild-type, BACE1 knock-out (BACE1 -/-), heterozygous mice with half of the normal amount of active BACE1 (BACE1 +/-), and in APP transgenic mice expressing the human APP gene with the London mutation V717I. First, we examined BACE1 and APP levels in post-mortem human temporal cortical samples from 20 AD patients and 5 controls (Figure 4a-c; supplemental Table 1). Western blot analysis revealed that cerebral BACE1 levels were ~2.1-fold elevated in AD patients compared to non-AD (Figure 4c), which is in agreement with previous studies where BACE1 protein and activity levels were found to be increased in the brain regions affected by amyloid deposition (Fukumoto et al., 2002, Holsinger et al., 2002, Li et al., 2004, Yang et al., 2003). Cerebral APP levels did not differ between AD patients and non-demented controls (Figure 4b). We did not perform a correlation test due to our small sample size. In order to have more statistical power and conclusive results, a larger data set would be required.

We hypothesized that a surplus of BACE1 would lead to increased Aβ34, given that BACE1 levels are significantly elevated in AD, while APP levels and Aβ40 and Aβ42 production rates do not change (Mawuenyega et al., 2010). Therefore, levels of Aβ34 and the longer Aβ species, i.e., Aβ40 and Aβ42 resulting from the classical amyloidogenic processing of APP, were measured in human brain extracts using our previously developed 4-plex assay (MSD - Meso Scale Discovery) (Liebsch et al., 2019). Aβ34 levels were elevated ~1.8 fold, which is very similar to the ~2.1-fold elevated BACE1 level in AD brain tissue. Thus, both cerebral BACE1 and Aβ34

`

levels increased approximately ~2-fold (Figure 4d), suggesting that excess BACE1 may generate more Aβ34 in AD brain tissue. Notably, Aβ40 and Aβ42 species were significantly elevated in the AD group by ~44- and ~23-fold, respectively (Figure 4e and f), possibly due to aggregated amyloid as previously reported (Hardy and Allsop, 1991).

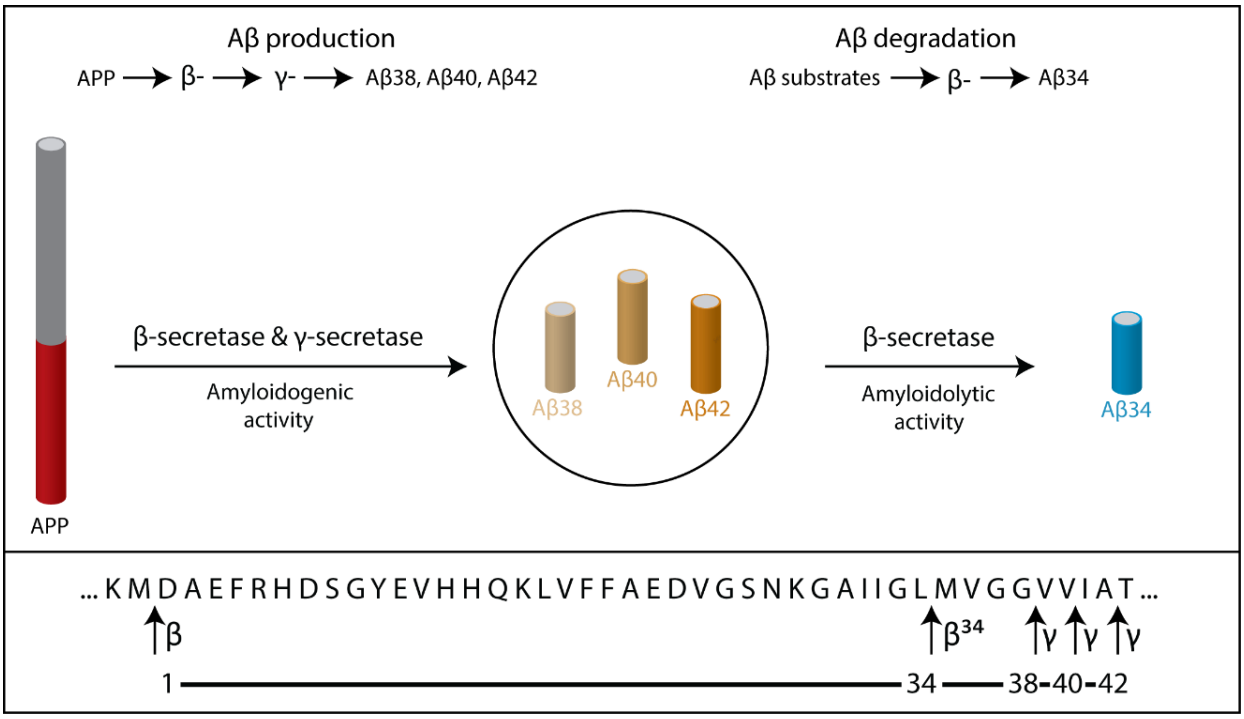

Figure 3: APP processing by β- and γ-secretases and amyloid degradation into Aβ34 and smaller fragments

In the amyloidogenic pathway, sequential cleavage of APP by β-secretase and γ-secretase generates Aβ species of varying lengths including Aβ38, Aβ40 and Aβ42. In the Aβ amyloidolytic pathway, Aβ peptides resulting from the production pathway can be cleaved by β-secretase at the β34 site as part of the degradation pathway yielding the C-terminally truncated Aβ species, Aβ34.

To test whether the absence of aggregated amyloid yields a similar relationship between BACE1 and the different Aβ species, we measured Aβ34, Aβ40 and Aβ42 levels in the cortices of 6 months-old wild-type (+/+), heterozygous (+/-) and homozygous BACE1 knockout (-/-) mice (3 females and 3 males for each genotype) expressing endogenous levels of APP. We observed that Aβ34 levels were significantly reduced in BACE1 +/- animals but not the Aβ40 and Aβ42 levels.

`

The loss of one BACE1 allele led to a significant decrease in Aβ34 levels (compare BACE1 +/+ and BACE1 +/-) (Figure 4g), while no significant effects were observed for Aβ40 and Aβ42 (Figure 4h and i). Unaltered levels of Aβ40 and Aβ42 were also observed by others under the condition of lowered endogenous BACE1 activity (Georgievska et al., 2015, Liebsch et al., 2019, Nishitomi et al., 2006, Weber et al., 2017). Thus, Aβ34 levels positively correlate with BACE1 levels, which is not the case for Aβ40 and Aβ42 levels that remain unaltered with the loss of one BACE1 allele.

Then, we utilized transgenic mice expressing human APP, i.e., *in vivo* overexpressing conditions, to analyze the effect of substrate overexpression. Cortical Aβ levels of wild-type animals (7 females and 3 males) were compared to cortical Aβ levels of 6 months-old (pre-plaque) mice with the London mutation driven by the Thy1 promoter (4 females and 3 males). Aβ34 levels were increased ~2.5 fold and Aβ40 and Aβ42 were found elevated ~4- and ~5-fold, respectively (Figure 4j-l). Western blot analysis revealed that APP transgenic mice had ~2.2 fold more APP in their cortex (data not shown). Altogether, the results show that amyloidogenic activity was maintained with a single copy of the endogenous BACE1 gene (Figure 4h and i), while amyloidolytic activity was reduced upon the loss of one BACE1 gene copy (Figure 4g).

`

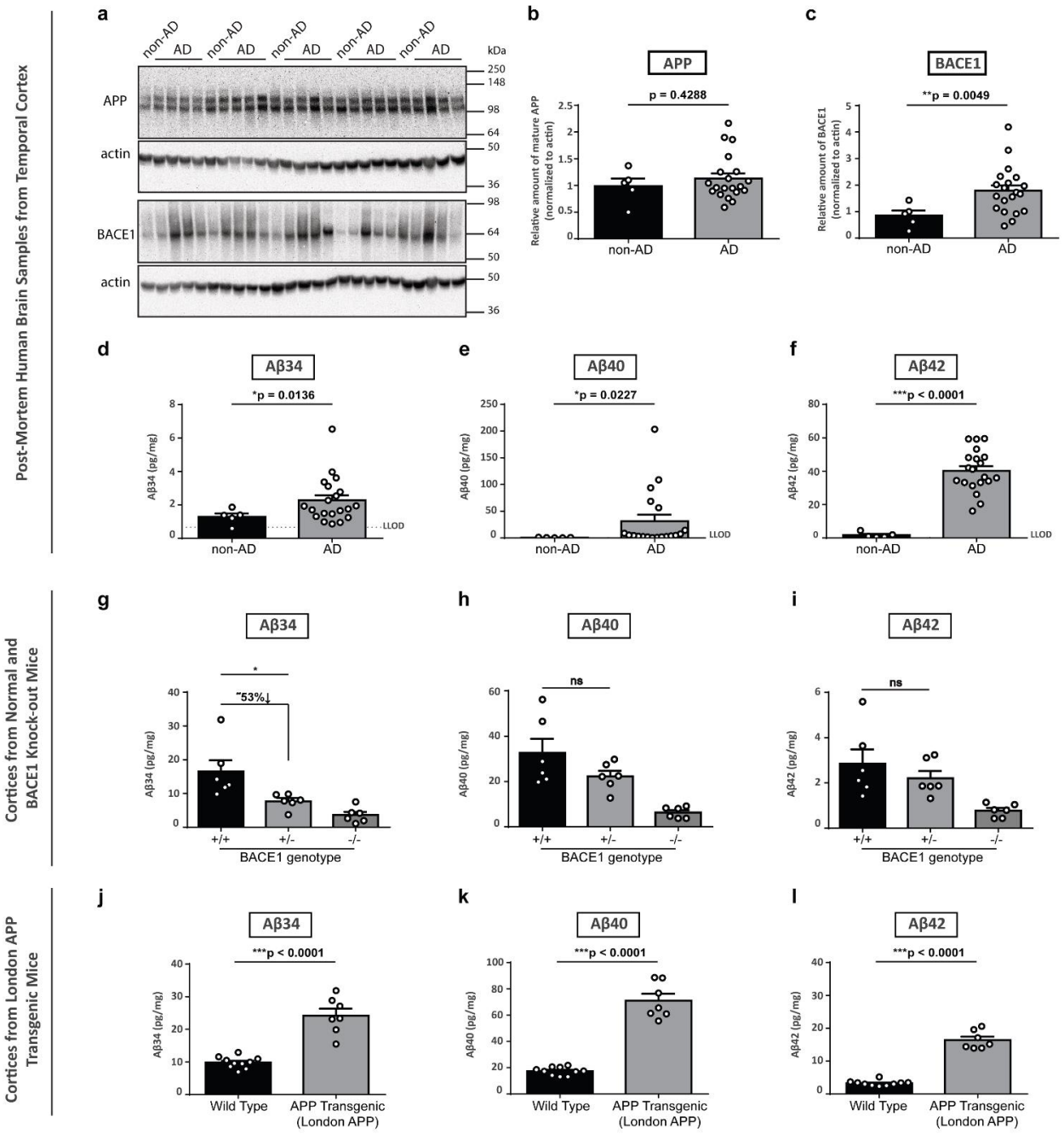

Figure 4: Aβ34 levels in AD post-mortem brain and in mouse brain tissue correlated with altered BACE1 expression and enhanced Aβ40 and Aβ42 levels

Expression of APP and BACE1, and Aβ34, Aβ40 and Aβ42 levels from post-mortem temporal brain and mouse cortices homogenates were analyzed by Western blot and MSD assays, respectively. Western blot for the examination of APP and BACE1 expression levels (a). Quantification of relative protein amounts of APP (b) and BACE1 (c) of AD and non-AD. Absolute amounts of Aβ34 (d, g, and j), Aβ40 (e, h, and k) and Aβ42 (f, i, and l) determined with MSD 4-plex assays. For BACE1 knockout mice, cortices of 6 months-old 3 females and 3 males (g-i) and for London APP Transgenic mice, cortices of 6 months-old 7 females

`

and 3 males (for WT) and 4 females and 3 males (for transgenic) (j-l) were analyzed. Data (b-f) were analyzed using unpaired Welch's t-tests (due to violations of the normality assumption). Bars and error bars indicate mean ± s.e.m. (b) $t(7)=0.84$, (c) $t(13)=3.34$, (d) $t(20)=2.71$, (e) $t(18)=2.54$, (f) $t(21)=13.42$. Data (d-f and j-l) were analyzed by unpaired t-test. Data (g-i) were analyzed by 1-WAY ANOVA and Tukey's post-hoc tests were performed for pairwise comparisons; selected comparisons are highlighted ***$p < 0.001$, **$p < 0.01$, *$p < 0.05$. (g) Aβ34, 1-WAY ANOVA, $F(2,15)=10.33$, $p = 0.0015$, (h) Aβ40, 1-WAY ANOVA, $F(2,15)=11.75$, $p = 0.0009$, (i) Aβ42, 1-WAY ANOVA, $F(2,15)=6.637$, $p = 0.0086$.

1.3.2. BACE1 expression promotes Aβ34 generation from APP and APP-C99 in vitro

To further determine how increased APP or BACE1 expression is influencing the balance between amyloidogenic and amyloidolytic cleavages, we tested cells transfected with increasing amounts of cDNA of either BACE1 or APP.

When corresponding Western blots were quantified, increases in sAPPβ and $sAPP_{total}$ were observed under both APP695 and BACE1 overexpression conditions. However, the increase in APP processing by β-secretase, indicated by sAPPβ levels, was more pronounced under BACE1 overexpression compared to APP695 overexpression (Supplementary Figure 1a-d). Upon dose-dependently increased BACE1 levels (Figure 5a), Aβ34 levels started to rise above Lower Limit of Detection (LLOD) with the lowest amount of BACE1 transfected and in a linear manner ($y = 0.3225x + 103.0$, $p< 0.0001$) over the entire range (Figure 5c). APP overexpression in HEK293T cells resulted in increased levels of APP but left Aβ34 levels unaltered (Figure 5b and c). These results demonstrate that a surplus of BACE1, but not of APP, promotes amyloidolytic cleavage yielding higher Aβ34 levels in non-neuronal cells where endogenous BACE1 expression is naturally low (Colombo et al., 2013).

To study Aβ34 formation independently from prior β-secretase cleavage of APP by BACE1 (cleavage at the Asp^1 residue), we used a construct that encodes for the immediate γ-secretase substrate β-CTF, termed as APP-C99 (Cole and Vassar, 2007, Lichtenthaler et al., 1999) (Figure 5d). HEK293T cells were co-transfected with both increasing concentrations of BACE1

`

and a constant amount of APP-C99 and expression was verified by Western blot (Figure 5d and e). Aβ34 levels were below LLOD under mock condition. A steady rise of Aβ34 levels was observed in BACE1 and APP-C99 co-transfected cells. Additionally, Aβ40 and Aβ42 levels were dose-dependently reduced in these co-transfected cells (Supplementary Figure 1e and f). To prove that Aβ34 generation depended on the cleavage at the β34 site, we used an engineered mutant construct, where amino acid residue 35 (M35) of APP-C99 was mutated to Ile encoding for APP-C99 M35I (Figure 5e). Under these conditions amyloidolytic cleavage at the β34 site was abolished (Figure 5f).

The quantitative analysis of the conditioned media from APP-C99 and BACE1 co-transfected HEK293T cells showed that BACE1 overexpression increased Aβ34 levels (Figure 5g) while Aβ40 and Aβ42 levels were diminished (Figure 5h and i). Surprisingly, Aβ34 peptides were the predominating species under BACE1 and APP-C99 co-expressing conditions, as verified in immunoprecipitates by Matrix-Assisted Laser Desorption/Ionization Mass Spectrometry (MALDI-MS) (Figure 5j and k). Quantitative and qualitative results confirm that longer and shorter Aβ species are released by cells only overexpressing APP-C99 (Figure 5k) but increased BACE1 levels correspond with increased detection of Aβ34 species.

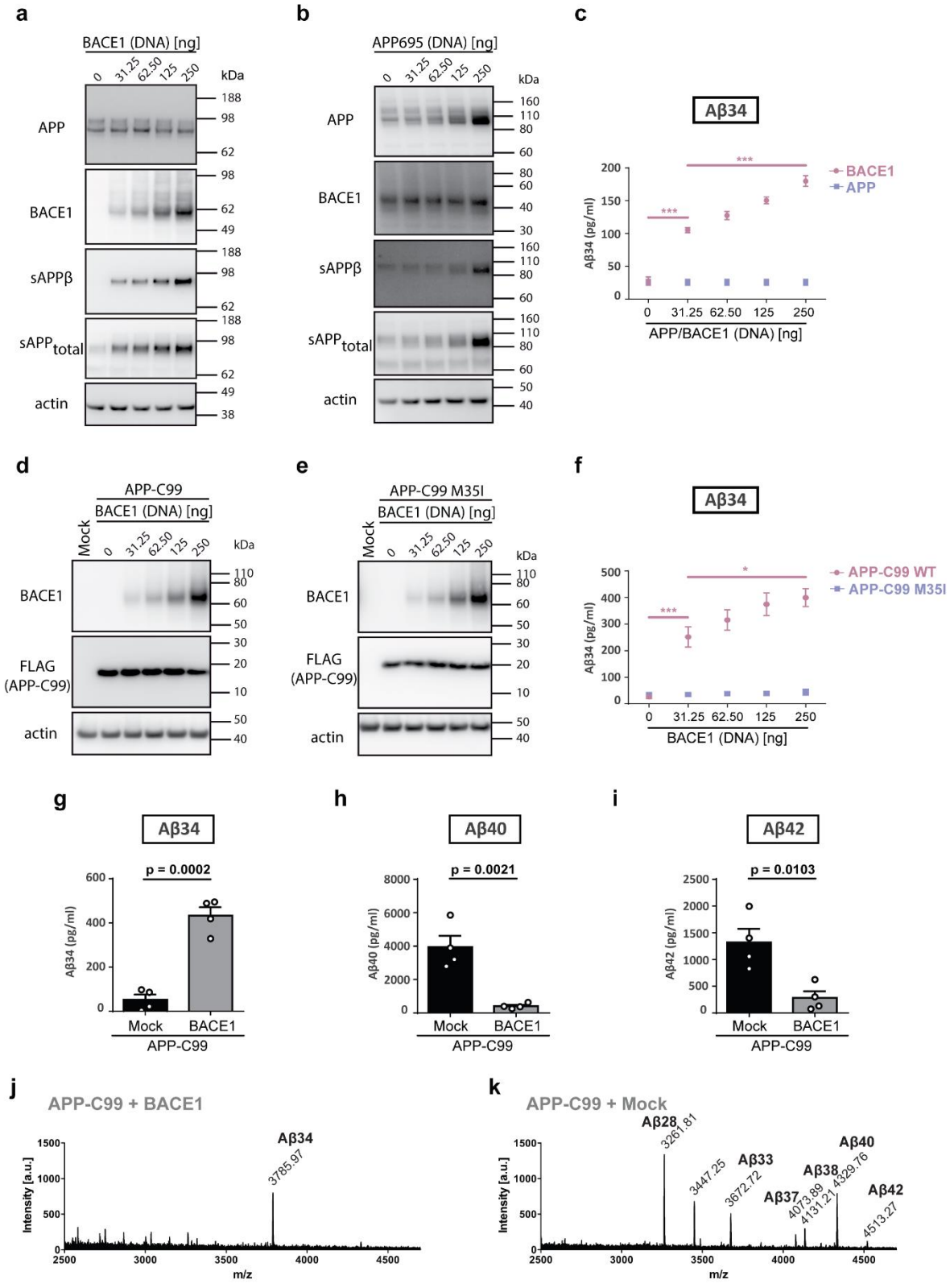

Figure 5: BACE1 overexpression and co-expression with APP-C99 enhanced Aβ34 production from Aβ40 and Aβ42

`

Expression of APP, APP-C99, and BACE1 and Aβ34 generated from endogenous levels of APP and under APP and APP-C99 overexpression conditions (wild-type APP-C99 and APP-C99 M35I mutant) were analyzed by Western blot and ELISA, respectively. HEK293T cells were transfected with indicated increasing amounts of cDNA coding for BACE1 (a) or APP695 (b) or APP-C99 and BACE1 (d) or APP-C99 M35I and BACE1 (e). Representative Western blots from 5 independent experiments for the examination of APP, BACE1, sAPPβ and $sAPP_{total}$ expression (a, b, d and e). Quantification of absolute amounts of Aβ34 by ELISA (c and f). Aβ generation from BACE1 and/or APP-C99 overexpressing HEK293T cells was analyzed by ELISA, and immunoprecipitation (IP) Matrix Assisted Laser Desorption/Ionization (MALDI) mass spectrometry (MS). Cells were transfected with APP-C99, BACE1, and/or empty vector (Mock). Quantification of absolute amounts of Aβ34 (g), Aβ40 (h), and Aβ42 (i) with specific ELISAs. Aβ species were immunoprecipitated with monoclonal W02 and analyzed by MALDI-MS. Representative spectra from 3 independent experiments (j and k). Bars and error bars indicate mean ± s.e.m. Tukey's post-hoc tests were performed for pairwise comparisons; selected comparisons are highlighted ***$p < 0.001$, *$p < 0.05$. (c) Aβ34, 1-WAY ANOVA, $F(4,20)=89.90$, $p < 0.0001$, (f) Aβ34, 1-WAY ANOVA, $F(5,24)=28.28$, $p < 0.0001$, (g) t-test, $t(6)=8.44$, (h) t-test, $t(6)=5.16$, (i) t-test, $t(6)=3.68$. Linear regression was performed for the linearity test between BACE1 overexpression and Aβ34 levels (between 31.25 ng and 250 ng BACE1 DNA treatment). $F(4,20) = 72.21$, $p < 0.0001$ with the equation $y = 0.3225x + 103.0$.

1.3.3. Cellular localization of BACE1 modulates its amyloidolytic activity

Next, we verified whether Aβ34 is generated in the endo–lysosomal system. We tested BACE1 mutants with amino acid substitutions in the acidic cluster motif, DDISLL (residues 495–500 of BACE1 contained within its cytosolic C-terminal domain) that are well-known for altering intracellular localization and trafficking of BACE1. Notably, substitutions of D495 or L499-L500 in the [DE]XXXL[LI] signal (Kinoshita et al., 2003) were described to decrease endosomal localization and increase plasma membrane localization of BACE1 (Bonifacino and Traub, 2003, Prabhu et al., 2012).

We explored the amyloidolytic activity under the condition of impaired endosomal localization and trafficking using two different BACE1 constructs (LL/AA [DDIS*AA*] and D495R [*R*DISLL]) in cells either stably overexpressing full-length APP or APP-C99. Unlike Aβ40 and Aβ42 levels, which were approximately 7-and 5-fold higher in APP-C99-overexpressing cells, respectively, compared to APP-overexpressing cells, Aβ34 levels were relatively similar in both cell types, which supports the results from APP-C99 and BACE1 co-transfected cells shown above

`

(Figure 5f) implying that BACE1 most likely is the limiting factor for amyloidolytic activity. At similar expression levels of wild-type BACE1 and of the mutant constructs (Figure 6a and f), relative levels of Aβ40 and Aβ42 remained unaltered when compared to the control ("Mock") (Figure 6c, d, h and i). In contrast, Aβ34 levels were reduced by ~55% (compared to wt) for both BACE1 trafficking mutants in APP overexpressing cells (Figure 6b) and by ~25% (LL/AA) and ~10% (D495R) in APP-C99 overexpressing cells (Figure 6g). The observed effect was attenuated in APP-C99 overexpressing cells, likely due to an excessive supply of substrate, i.e., 10- (compare Figure 6c and h) and 6-fold higher levels (compare Figure 6d and i) of Aβ40 and Aβ42, respectively.

We verified the cellular localization of BACE1 mutants that impair endosomal trafficking (Bonifacino and Traub, 2003) by immunocytochemistry (ICC). Briefly, wild-type BACE1 showed a punctate like staining (Figure 6e and j) which overlapped with both the early-endosome marker EEA1 (early-endosome associated protein 1) and the lysosome marker LAMP1 (lysosome-associated membrane protein 1) in both cell types (Chia et al., 2013, Sannerud et al., 2011) (Supplementary Figure 2). Quantitative colocalization analyses showed a significantly reduced colocalization with early endosomal marker EEA1 and lysosomal marker LAMP1 for both BACE1 variants, LL/AA and D495R (Supplementary Figure 2g and h), which is in agreement with previous reports(Andrew et al., 2017, Kang et al., 2012, Prabhu et al., 2012).

Altogether, quantification and colocalization results suggest that Aβ34 is mainly produced within the endo-lysosomal compartments, and mutations altering BACE1 localization impair Aβ34 production due to mislocalization or a delayed transport of the mutant enzyme.

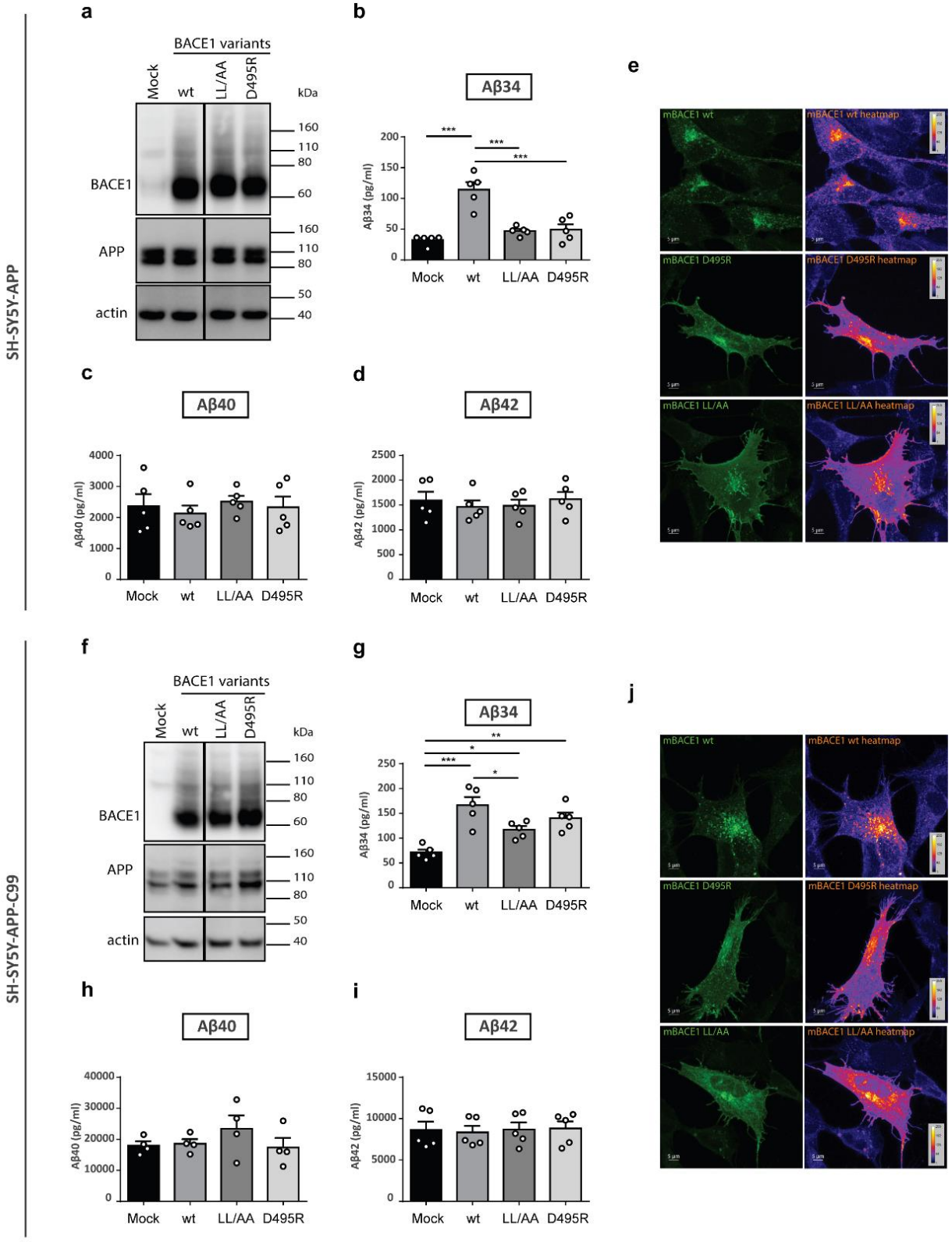

Figure 6: Altered localization of BACE1 to the endo-lysosomal system affected Aβ34 production

`

Expression of BACE1 mutants and Aβ34, Aβ40 and Aβ42 levels were analyzed by Western blot and ELISA assays, respectively. Localization of BACE1 encoded by mutant constructs was analyzed by ICC. Representative Western blots of BACE1 and APP expression from 5 independent experiments with SH-SY5Y-APP (a) and SH-SY5Y-APP-C99 cells (f) transfected with different variants affecting BACE1 trafficking or mock. Absolute amounts of Aβ34 (b and g), Aβ40 (c and h), and Aβ42 (d and i). Representative ICC heatmaps of BACE1 wild-type, D495R and LL/AA in SH-SY5Y-APP (e) and SH-SY5Y-APP-C99 (j) cells from 3 independent experiments. Bars and error bars indicate mean ± s.e.m. Tukey's post-hoc tests were performed for pairwise comparisons; selected comparisons are highlighted ***$p < 0.001$, **$p < 0.01$, *$p < 0.05$. (c) Aβ34, 1-WAY ANOVA, $F(3,16)=21.41$, $p < 0.0001$, (d) Aβ40, 1-WAY ANOVA, $F(3,16)=0.2724$, $p = 0.8444$, (e) Aβ42, 1-WAY ANOVA, $F(3,16)=0.2775$, $p = 0.8408$, (g) Aβ34, 1-WAY ANOVA, $F(3,16)=13.20$, $p < 0.0001$, (h) Aβ40, 1-WAY ANOVA, $F(3,16)=0.9514$, $p = 0.4468$, (i) Aβ42, 1-WAY ANOVA, $F(3,16)=0.05190$, $p = 0.9838$.

1.3.4. PS2 γ-secretase but not PS1 complexes contribute to Aβ34 production

Literature indicates that numerous C-terminally truncated Aβ species are generated by the γ-secretase complex in a PS1/2-dependent manner (Beher et al., 2002, Olsson et al., 2014, Vandermeeren et al., 2001) and that γ-secretase activity is required first to produce secreted Aβ species (Fluhrer et al., 2003, Olsson et al., 2014) which are then cleaved again by BACE1 to generate Aβ34.

To dissect the roles of PS1- and PS2-containing γ-secretase complexes in Aβ34 generation, we performed titration experiments with small interfering RNAs (siRNAs) to silence *PSEN1* or *PSEN2* expression. In a double knockdown titration experiment with either decreasing or increasing amounts of PS1 or PS2 siRNA and *vice versa* (Figure 7), the total siRNA amount was equivalent to 15 pmol. The gradual downregulation of *PSEN1* or *PSEN2* was verified by Western blot analysis (Figure 7a-c). Aβ34, Aβ40 and Aβ42 levels were quantified by ELISA in cell media (Figure 7d-f) and by MSD in cell lysates (Figure 7g-i). A significant gradual decrease in Aβ34 levels was uniquely observed with decreasing PS2 while Aβ40 and Aβ42 levels remained unchanged in cell media (Figure 7d-f). The highest PS2 knockdown resulted in a significant reduction of Aβ34 by ~20% (Figure 7d). In contrast, Aβ34, Aβ40 or Aβ42 levels remained constant in cell lysates (Figure 7g-i). In cell media, Aβ40/Aβ42 ratio did not change at any given

`

knockdown; however, in cell lysates Aβ40/Aβ42 ratio significantly decreased with the highest PS1 knockdown (data not shown), which has been previously reported in the literature (Sannerud et al., 2016). Notably, PS1 protein levels increased 1.5-fold above the levels yielded by controls upon gradual PS2 knockdown, likely as a compensatory reaction (Figure 7b). This effect was specific for PS1 and not observed for PS2 since upon PS1 siRNA treatment, PS2 protein levels remained constant (Figure 7c). Aβ34 levels were not affected by the compensatory increase of PS1 but surprisingly decreased with PS2 reduction. This result suggests that PS2-γ-secretase complexes possess a unique role in Aβ34 generation while PS1 is not involved.

We verified the results of the combinatorial knockdown experiment with single knockdowns of either *PSEN1* or *PSEN2* (Supplementary Figure 3). The gradual downregulation of *PSEN1* or *PSEN2* was analyzed by Western blot (Supplementary Figure 3a-c and e-g) and Aβ34, Aβ40 and Aβ42 levels in cell media were quantified by ELISA (Supplementary Figure 3d and i). Downregulation of *PSEN1* left Aβ34, Aβ40 and Aβ42 levels unaltered (Supplementary Figure 3d) and PS2 levels did not change upon gradual PS1 knockdown as described above (Supplementary Figure 3c). In agreement with data shown in Figure 7b, PS1 levels showed an unexpected compensatory increasing trend upon gradual PS2 knockdown (Supplementary Figure 3g). Similar to the combinatorial knockdown experiments (Figure 7), a significant gradual decrease in Aβ34 levels was observed with decreasing PS2 while Aβ40 and Aβ42 levels remained unchanged (Supplementary Figure 3i) and the highest PS2 knockdown resulted in an approximately 20% reduction of Aβ34 levels, confirming the result above that PS2-γ-secretase but not PS1 contributes to Aβ34 generation.

`

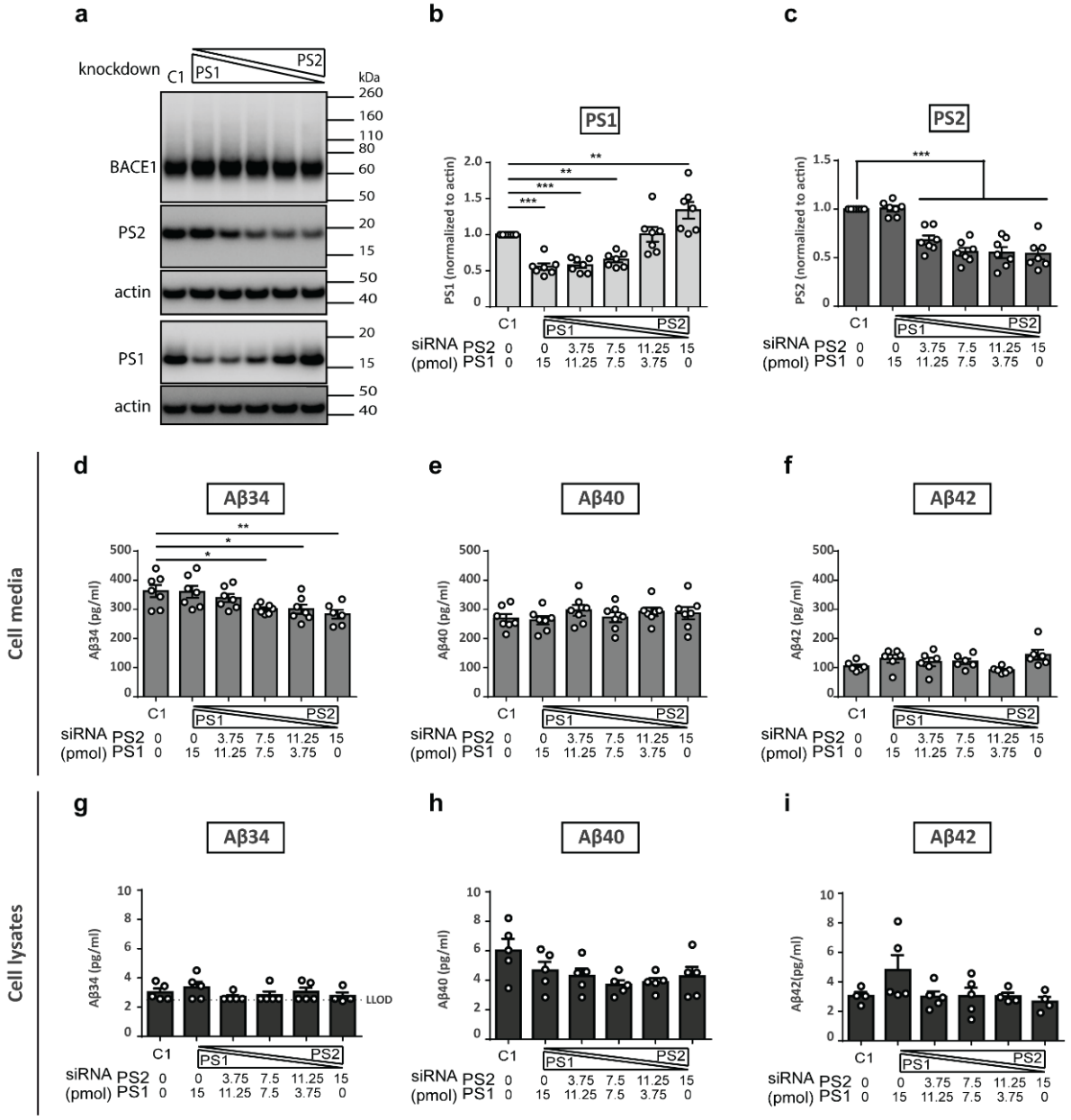

Figure 7: PS2 but not PS1 knockdown reduced Aβ34 levels from BACE1 overexpressing cells

Expression of PS1 and PS2 and Aβ levels were analyzed by Western blot, ELISA and MSD assays, respectively. Representative Western blots from 7 independent experiments for combinatorial PS1 and PS2 knockdown in SH-SY5Y BACE1 overexpressing cells (a). Quantification of relative amounts of PS1 (b) and of PS2 (c), and absolute amounts of Aβ34 (d), Aβ40 (e), and Aβ42 (f) in cell media by ELISA and Aβ34 (g), Aβ40 (h), and Aβ42 (i) in cell lysates by MSD. Bars and error bars indicate mean ± s.e.m. Dunnett's post-hoc tests were performed for pairwise comparisons; selected comparisons are highlighted ***$p < 0.001$, **$p < 0.01$, *$p < 0.05$. (b) PS1, 1-WAY ANOVA, $F(5,36)=20.06$, $p < 0.0001$, (c) PS2, 1-WAY ANOVA, $F(5,36)=26.37$, $p < 0.0001$, (d) Aβ34, 1-WAY ANOVA, $F(5,35)=4.268$, $p < 0.005$, (e) Aβ40, 1-WAY ANOVA, $F(5,36)=0.6677$, $p = 0.6504$, (f) Aβ42, 1-WAY ANOVA, $F(5,36)=2.502$, $p = 0.0523$, (g) Aβ34, 1-WAY ANOVA, $F(5,23)=0.8428$, $p = 0.5334$, (h) Aβ40, 1-WAY ANOVA, $F(5,24)=2.276$, $p = 0.0791$, (i) Aβ42, 1-WAY ANOVA, $F(5,21)=1.869$, $p = 0.1429$.

`

1.3.5. Pharmacological inhibition of BACE1 differentially affects amyloidogenic and amyloidolytic activities

To investigate how BACE1 inhibition can affect Aβ34 generation under the conditions of APP, APP-C99 or BACE1 overexpression in SH-SY5Y cells we tested the BACE1-specific inhibitor LY2811376 (10^{-7} M) (May et al., 2011).

We verified protein levels and overexpression by Western blot (Figure 8a). When supernatants of wild-type cells (control) were analyzed, all Aβ forms were below LLOD of ELISA (Figure 8b). Note that, stably BACE1 overexpressing cells have higher Aβ34 levels compared to stably APP or APP-C99 overexpressing cells, since more BACE1 leads to more Aβ34 production. APP-C99 overexpressing cells showed significantly decreased levels of Aβ34 upon LY2811376 treatment but Aβ40 and Aβ42 levels remained constant at a high level (Figure 8c). Aβ40 and Aβ42 substrate levels are ~100 fold higher than Aβ34 levels in these cells; therefore, it would be nearly impossible to see a slight increase in Aβ40 and Aβ42 levels which is expected to result from a decreased amyloidolytic activity indicated by altered Aβ34 levels. In BACE1 overexpressing cells, Aβ34 levels remained unaltered at a very high level whereas Aβ40 and Aβ42 levels were significantly elevated when BACE1 was inhibited (Figure 8d). In contrast to BACE1 overexpressing cells, APP overexpressing cells showed significantly decreased levels of Aβ40 and Aβ42 upon endogenous BACE1 inhibition, most likely due to decreased amyloidogenic activity of BACE1. Aβ34 levels were below LLOD (Figure 8e). Taken together, these findings indicate that changes in the levels of either APP, APP-C99 or BACE1 primarily affect the balance between BACE1-mediated Aβ production and clearance.

`

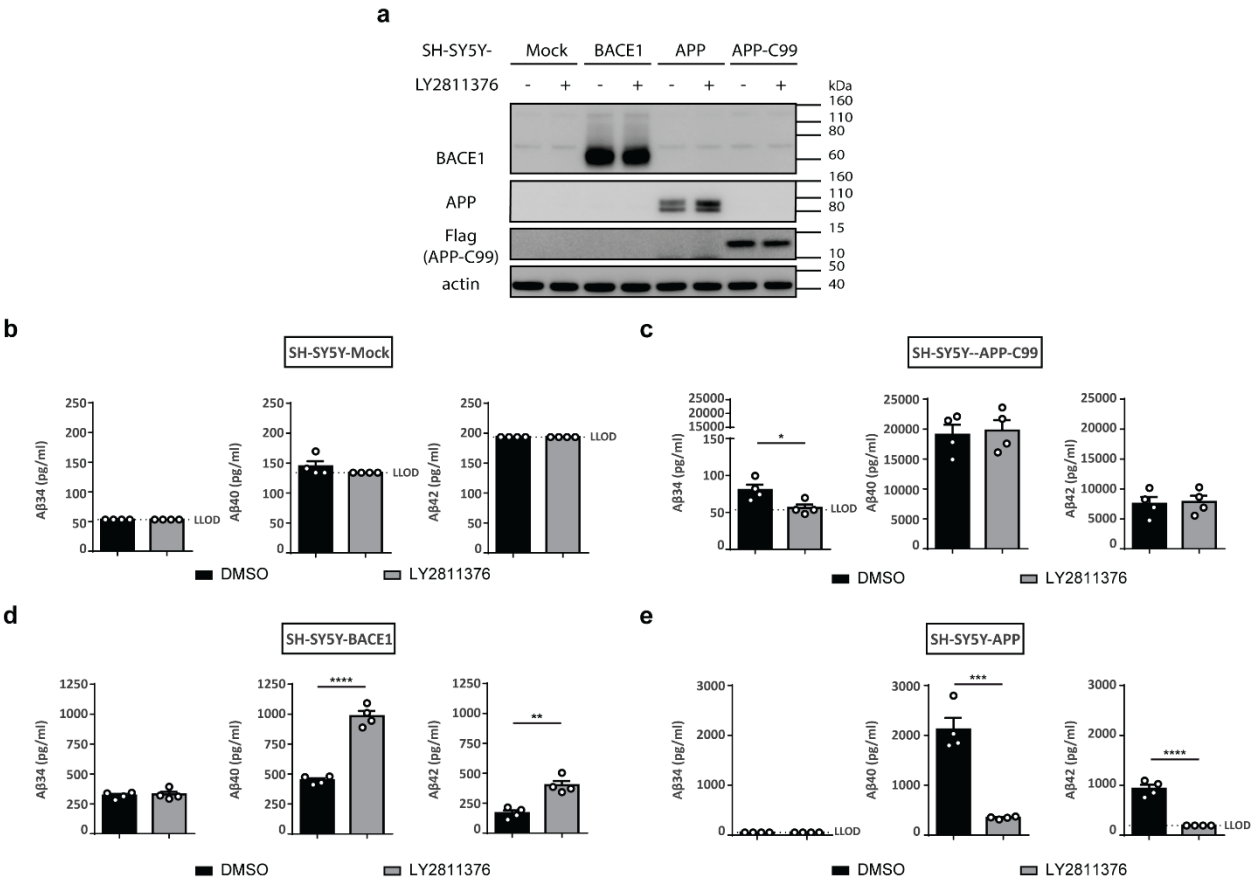

Figure 8: Pharmacological inhibition of BACE1 reduced Aβ34 levels in APP-C99 overexpressing cells and increased Aβ40 and Aβ42 levels in BACE1 overexpressing cells

Expression of APP, BACE1 and APP-C99 was analyzed by Western blot and Aβ34, Aβ40 and Aβ42 levels were measured by ELISA. Representative Western blots from 4 independent experiments for BACE1 inhibition by 10^{-7} M LY2811376 in SH-SY5Y-Mock, -APP, -APP-C99 and -BACE1 overexpressing cells (a). Quantification absolute amounts of Aβ34, Aβ40, and Aβ42 in SH-SY5Y-Mock (b), SH-SY5Y-APP-C99 (c), SH-SY5Y-BACE1 (d) and SH-SY5Y-APP (d) cell media. Bars and error bars indicate mean ± s.e.m. Data were analyzed by unpaired t-test and selected comparisons are highlighted ****$p < 0.0001$, ***$p < 0.001$, **$p < 0.01$, *$p < 0.05$. (c) Aβ34, $t(6) = 2.881$, (d) Aβ40, $t(6) = 11.43$, Aβ42, $t(6) = 5.524$, (e) Aβ40, $t(6) = 7.642$, Aβ42, $t(6) = 9.447$.

`

1.4.Discussion

An imbalance between the formation and elimination of Aβ peptides has been suggested as the trigger in the pathogenesis of AD (Bateman et al., 2006, Neumann et al., 2015). However, the knowledge about proteolytic degradation of Aβ discovered to date is rather limited to the family of amyloid-degrading enzymes (ADEs) with both membrane-bound and soluble members including extracellular matrix metalloproteinases (MMP2 and MMP9), IDE, NEP and ECE (Hernandez-Guillamon et al., 2015, Saido and Leissring, 2012, Grimm et al., 2013, Nalivaeva et al., 2014, Pacheco-Quinto and Eckman, 2013).

Previous reports showed that a cleavage between L34 and M35 of the Aβ sequence exerted by BACE1 produced the non-amyloidogenic Aβ34 peptide, a soluble and non-toxic C-terminally truncated degradation product of longer Aβ peptides (Fluhrer et al., 2003, Shi et al., 2003, Caillava et al., 2014). Aβ34 thus differs from aggregation prone Aβ species deposited in AD brain tissue. We identified Aβ34 as an indicator of amyloid clearance since Aβ34 was elevated in individuals with mild cognitive impairment (Liebsch et al., 2019). Moreover, a significantly decreased Aβ34/Aβ40 ratio was observed in microvessels from AD patients due to a reduced proteolytic degradation of amyloid peptides in AD (Kirabali et al., 2019).

Here, we provide mechanistic evidence *in vitro* and *in vivo* supporting a prominent role of BACE1 in Aβ clearance. Under conditions of either elevated levels of APP or of BACE1, Aβ34 production was only enhanced under a surplus of BACE1. Increasing amounts of BACE1 resulted in a dose-dependent increase in Aβ34 levels in all our experimental test systems. Specifically, the levels of Aβ34 depends directly on increased BACE1 levels in AD brain, i.e., Aβ34 levels were approximately 2-fold elevated in the brains of individuals with AD compared to non-demented controls and levels coincided with roughly 2-fold higher BACE1 levels *in vivo*. While increased

`

BACE1 levels and its amyloidogenic activity in AD have been reported before (Fukumoto et al., 2002, Holsinger et al., 2002, Li et al., 2004, Yang et al., 2003), the biological significance of BACE1 for amyloid clearance had remained enigmatic. We successfully confirmed an association between BACE1 expression and Aβ34 levels indicating amyloid clearance (i) in genetically modified mice where a single copy of the BACE1 gene (BACE1 +/-) halved Aβ34 levels and (ii) in cell culture systems where the linearity between BACE1 and Aβ34 levels remained stable even at high BACE1/APP ratios. Thus, our findings provide an explanation for the previously reported and paradoxical inverse relationship for BACE1 expression and Aβ levels measured in *in vitro* and *in vivo* test systems under conditions of genetic and pharmacological manipulation of BACE1 expression (Bodendorf et al., 2002, Chiocco et al., 2004, Egan et al., 2018, Lee et al., 2003, Lee et al., 2005, Rockenstein et al., 2005, Scholz et al., 2018).

Further, we identified the endo-lysosomal system as the critical compartment for amyloidolytic cleavage of longer Aβ species into Aβ34 product. The finding that two BACE1 trafficking mutants known to impair endosomal trafficking (Bonifacino and Traub, 2003) reduced Aβ34 levels while Aβ40 and Aβ42 levels remained unchanged is in agreement with reports that BACE1 activity is optimal at acidic pH in early endosomes and lysosomes (Shimizu et al., 2008, Toh et al., 2018, Bonifacino and Traub, 2003). Further, knockdowns of either the PS1 or the PS2 subunit showed that Aβ34 levels were specifically reduced upon PS2 knockdown. Thus, PS2-γ-secretase, rather than PS1, is involved in Aβ34 generation which is in full alignment with their reported cellular activities, as PS2 selectively cleaves late endosomal/lysosomal localized substrates and generates the prominent pool of intracellular Aβ peptides (Sannerud et al., 2016). This assumption implies that Aβ peptide substrates are originating from PS2-γ-secretase complexes for BACE1 amyloidolytic cleavage. Thus, we propose that BACE1 amyloidolytic

`

activity in the endo-lysosomal system might provide specificity and a spatial and temporal control of amyloid clearance through the BACE1-amyloidolytic-activity pathway. In agreement with this view, longer Aβ forms are more prone to aggregation in acidic compartments (Esbjörner et al., 2014, Hu et al., 2009) requiring that clearance of Aβ40 and Aβ42 in acidic compartments is essential and must be highly effective.

Studies in rats, monkeys and dogs reported a decrease in Aβ40 and Aβ42 levels in CSF upon BACE1 inhibition (Kennedy et al., 2016, Mattsson et al., 2012) together with a slight decrease of Aβ34 levels (Mattsson et al., 2012). This decreased trend in Aβ40 and Aβ42 levels resemble those we observed with APP-overexpressing cells in which BACE1 is the limiting factor for amyloidogenic pathway. When BACE1 is inhibited, there is less processing of APP and reduced production of Aβ species. On the other hand, we also analyzed APP-C99 overexpressing cells, in which the initial BACE1-mediated β-site cleavage of APP, as a factor that directly influences Aβ34 production, is bypassed. Under such conditions, Aβ34 levels were primarily decreased upon BACE1 inhibition, indicating that the inhibitor treatment first and foremost affected amyloidolytic activity of BACE1. However, in BACE1 overexpressing cells, where APP is the limiting factor for the amyloidogenic pathway, both Aβ40 and Aβ42 levels were increased upon BACE1 inhibition with no effect on Aβ34 levels. This observation could result from either an increased amyloidogenic activity, a possibility which we did not investigate, or more likely, a reduced amyloidolytic activity of BACE1. The differential effect of the BACE1 inhibitor on Aβ levels suggests that the substrate to enzyme ratio is the major factor to affect the balance between amyloidogenic and amyloidolytic activity of BACE1. Under pathological conditions, i.e., elevated BACE1 levels in AD, especially in specific brain regions and in dystrophic neurites surrounding amyloid plaques (Sadleir et al., 2016, Peters et al., 2018), could potentially create an environment

`

in which an incomplete BACE1 inhibition may lead to increased levels of amyloidogenic and potentially toxic Aβ.

`

1.5.Materials and Methods

1.5.1. Plasmids and siRNAs

A human BACE1 construct (full length BACE1, isoform A; pcDNA3.1+/Zeo; Invitrogen), APP695 (with an N-terminal Myc-tag; pcDNA3.1+/Zeo; Invitrogen) and APP-C99 (with a C-terminal FLAG-tag; pcDNA3.1+/Zeo; Invitrogen) were used for transient overexpression in HEK293T cells. Point mutations were introduced by site-directed mutagenesis, using PfuUltra II Fusion HS (Stratagene/Agilent) followed by DpnI (NEB) digestion. All constructs were verified by DNA sequencing. For creating stably expressing SH-SY5Y cells, full-length human BACE1 (isoform A) and full-length human APP (isoform APP695, with an N-terminal Myc tag), in the mammalian expression vector pCEP4, Hygro (Invitrogen) were used. Mouse wild type BACE1 construct with an N-terminal FLAG tag immediately following the propeptide cleavage was generated by overlap extension PCR and cloned in pSport6. LL/AA or D495R variants were then generated by PCR using reverse primers with the mutant sequence. Mock controls for corresponding plasmid backbones were used. For knockdown, siGENOME non-Targeting siRNA Pool #1 (D-001206-13-05), SMARTpool siGENOME Presenilin 1 (M-004998), and Presenilin 2 (M-006018) were used.

1.5.2. Human Brain Samples

The brain samples were obtained from The Netherlands Brain Bank (NBB), Netherlands Institute for Neuroscience, Amsterdam (open access: www.brainbank.nl). All material has been collected from donors having provided written informed consent for a brain autopsy and the use of the material and for whom clinical information for research purposes had been obtained by the NBB. Frozen samples from the temporal cortex from non-demented controls (n=5) and confirmed Alzheimer disease Braak 4 to Braak 6 (n=20) were prepared as previously described (Kulic et al.,

`

2012). In brief, brain samples were thawed on ice, weighed and homogenized in buffer A (100 mM Tris-HCl, 150 mM NaCl, 2x complete protease inhibitor cocktail (Roche)) using gentleMACS™ M Tubes/Dissociator at 4°C (Miltenyi Biotech). TritonX-100, final concentration 1%, was added and samples were incubated for 1 h with agitation at 4°C. Lysates were centrifuged at 10,621 rcf in a microfuge (Eppendorf) at 4°C for 15 minutes to remove the nuclear fraction. Samples were measured with bicinchoninic acid assay (BCA assay, Thermo Fisher Scientific Inc., Pierce) and MSD assays.

1.5.3. Mouse Brain Lysates

Cortices of transgenic mice expressing London APP and their wild-type littermates were provided by Dr. Claus Pietrzik's laboratory at the University of Mainz, Germany. Cortices of BACE1 +/+, BACE +/- and BACE1 -/- mice were provided by Dr. Paul Saftig's laboratory in University of Kiel, Germany. All mice were on C57BL/6 strain genetic background and were 6-months of age when sacrificed. Frozen mouse brains were thawed on ice, weighed, and homogenized in the homogenization buffer (100 mM Tris-HCl pH: 7.5, 150 mM NaCl and 2x complete protease inhibitor cocktail (Roche)) using Dounce homogenizer. 10% Triton-X was added to the homogenates (final concentration: 1%). Brain homogenates were lysed at 4°C for 1 hour on a rotator. Lysates were centrifuged at 10,621 rcf in a microfuge (Eppendorf) at 4°C for an hour to remove the debris. Supernatants were collected and diluted in the appropriate buffers for BCA, Western blot and MSD assays.

1.5.4. Cell Culture and Transfection

Human Embryonic Kidney (HEK293T) cells (DSMZ No. ACC305; DSMZ, Braunschweig, Germany) cells were grown in DMEM (High glucose (4.5g/l), 10% fetal bovine serum (FBS), 2mM glutamine, 1 mM pyruvate) in a humidified incubator at 37°C 5% CO_2. For

`

transient transfection experiments, cells were seeded on 6-well plates (Fisher) coated with poly-D-lysine (Sigma) and transiently transfected (with the plasmids indicated for each experiment) 20-24 hours later by using TransFectin according to the protocol provided by the manufacturer (Biorad). 24 hours after transfection, media of the cells were changed, and cells were conditioned for 16 hours before sample collection.

Human neuroblastoma (SH-SY5Y) cells (DSMZ No. ACC209; DSMZ, Braunschweig, Germany) stably overexpressing BACE1, APP or APP-C99 were cultured in DMEM/F12 (10% fetal bovine serum (FBS), 2 mM L-glutamine, 1 mM sodium pyruvate) in a humidified incubator at 37°C 5% CO_2. Stable cell lines were selected with 250 µg/ml Hygromycin B (Milipore). For the experiment involving LY2811376, cells were seeded in 6-well plates (Fisher). LY2811376 was dissolved in DMSO and compared to vehicle treatment (1:1000 = 0.1 %). 24 hours later, they were treated with the inhibitor. 72 hours after treatment, cells were harvested. For BACE1 localization, cells were seeded on 6-well plates (Fisher) and transfected with FuGENE HD (Promega) after 24 hours. 72 hours after the transfection, cells were harvested. For PS1 and/or PS2 knockdown experiments, cells were seeded on 6-well plates (Fisher) and treated with either control, PS1 or PS2 siRNA (concentration of the siRNA depended on the experiment) 24 hours later by using RNAiMax according to the protocol provided by the manufacturer (Invitrogen). 72 hours after the treatment, cells were harvested. For ICC experiments, cells were seeded on 24-well plates (Fisher) and the same protocols were applied.

1.5.5. Sample Preparation

For all experiments performed, cells were harvested on ice. Conditioned media were centrifuged at 2000 rpm at 4°C for 10 minutes and Aβ34, Aβ40 and Aβ42 levels were quantified by ELISA. Cells were washed with cold PBS and lysed with Whole Cell Extract Buffer (25 mM

`

HEPES (pH 7.7), 0.3 M NaCl, 1.5 mM $MgCl_2$, 0.2 mM ethylenediaminetetraacetic acid, 0.1% Triton-X-100, 0.5 mM dithiothreitol, 4 mM NaF, 0.1 mM Na_3VO_4, 1 mM PMSF, Complete Protease Inhibitor Cocktail (Roche)) at 4°C for 60 mins. Cell lysates were cleared from nuclear material by centrifugation at 10000 rpm at 4°C for 15 minutes and protein levels were detected by Western Blot.

1.5.6. Western Blot Analysis

Samples were prepared by adding LDS loading buffer and 2-Mercaptoethanol to the cell lysates according to the protocol provided by the manufacturer (Invitrogen). The proteins were solubilized and denatured by heating the samples to 70°C for 10 mins. Proteins were separated on 4-12% Bis-Tris gradient gels (Invitrogen) and were transferred to 0.45 µm nitrocellulose (Biorad) or polyvinylidene difluoride (PVDF) (Millipore) membranes at 400 mA at 4°C for 2.5 hours. Proteins were detected by the antibodies indicated in the antibodies section. The primary and secondary antibodies were used in phosphate-buffered saline. Signals were recorded on ImageQuant LAS 500 and LAS 600 (GE Healthcare Life Sciences).

The primary antibodies used for Western Blot analysis were the following: anti-BACE1 1:2,000 dilution (monoclonal D10E5, Cell Signaling), anti-BACE1 1:2,000 dilution (B0681, Sigma-Aldrich), anti-actin 1:5,000 dilution (monoclonal mab1501, Millipore), anti-sAPPβ 1:2,000 dilution (IBL), and anti-APP ectodomain 22C11 1:10,000 dilution (Millipore), anti-flag 1:1,000 dilution (M2, F1804, Sigma-Aldrich), anti-PS2 (ab51249, Abcam), and anti-PS1 1:10,000 dilution (ab76083, Abcam).

The secondary antibodies used for Western Blot analysis were the following: anti-mouse- and anti-rabbit-horseradish peroxidase 1:10,000 dilution (Promega).

`

Quantification of the Western Blots were performed with ImageJ and all protein levels were normalized to actin.

1.5.7. Meso Scale Discovery (MSD) Assay

Custom-printed 4-plex plates were used as described previously (Liebsch et al., 2019). Plates were blocked with 150 µl 5% MSD Blocker A solution for an hour at room temperature with gentle shaking and washed 3 times with 250 µl PBS-T (0.05% tween). Peptide calibrators were diluted in MSD Diluent 35. Plates were loaded with samples and calibrators together with SULFO-TAG^{TM} 4G8 or 6E10 detection antibody diluted in MSD Diluent 100 and incubated overnight at 4°C with gentle shaking. After three washes with 250 µl PBS-T, 150 µl 2x MSD read buffer was added to the wells. Plates were read by an MSD QuickPlex SQ 120 Imager and data were analyzed by MSD Workbench® software.

1.5.8. Sandwich-based Enzyme-Linked Immunosorbent Assay (ELISA)

5 µg/ml monoclonal anti-Aβ34 (226), anti-Aβ40 (G2-10) or anti-Aβ42 (G2-13) capture antibody in 100 mM sodium carbonate (pH 9.6) were used to coat the 96-well NuncTM plates (Thermo Fisher Scientific Inc.). The sealed plates were incubated overnight at 4°C with gentle shaking. Plates were washed 5 times 10 minutes with PBS-T washing buffer (1.1 mM NaH_2PO_4, 8.5 mM Na_2HPO_4, 13.7 mM NaCl, (pH 7.4), 0.1% Tween-20). 250 µl Stabil Coat®Immunoassay Stabilizer (SurModics Inc.) was used for blocking and plates were incubated for 2 hours at room temperature with gentle shaking. 50 µl of 0.075 µg/ml detection antibody, W02-biotin, in assay buffer (90% 11 mM NaH_2PO_4, 85 mM Na_2HPO_4, 137 mM NaCl, (pH 7.4), 0.5% Tween-20, 1.5% BSA, 0.01% Thimerosal, and 10% SeaBlock blocking buffer (Thermo Fisher Scientific Inc.) was loaded to the wells together with 50 µl sample (cell media) or calibrator (synthetic peptide standards diluted in DMEM or DMEM/F12). After overnight incubation at 4°C with gentle

`

shaking, plates were washed 5 times for 10 minutes with PBS-T washing buffer. For Aβ40 ELISA, 100 µl Mono-HRP-conjugated-streptavidin (Pierce) (0.1 µg/ml) in Mono-HRP buffer (11 mM NaH_2PO_4, 85 mM Na_2HPO_4, 137 mM NaCl, (pH 7.4), 0.05% Tween-20, 6% PEG) or for Aβ34 and Aβ42 ELISA (for higher sensitivity), 100 µl Poly-HRP-conjugated-streptavidin (Pierce) (1:20,000 dilution) in Poly-HRP buffer (1.1 mM NaH_2PO_4, 8.5 mM Na_2HPO_4, 13.7 mM NaCl, (pH 7.4), 0.1% Tween-20, 5% BSA) was added to the wells. Plates were incubated for 1 hour at room temperature with gentle shaking and washed 5 times for 10 minutes with PBS-T washing buffer. For the initiation of enzymatic reaction, 100 µl 1-StepTM Ultra TMB-ELISA Substrate (Thermo Fisher Scientific Inc.) solution was added to the wells and the plates were incubated at room temperature in the dark for up to 30 minutes. To stop the reaction, 50 µl 1 M H_2SO_4, per well, was added. Using Synergy H1, BioTek Instruments Inc. plate reader, absorbance at 450 nm and 630 nm as a reference was measured. The data analysis was performed with Gen5 BioTek®software. For the fitting of standard curves obtained from the absorbance of calibrators, a non-linear four-parameter logistic fit without weighting was used as follows

$$y = b_2 + \frac{b_1 - b_2}{1 + (\frac{x}{b_3})^{b_4}}$$

where y is signal, x is concentration, b2 is estimated response at the infinite concentration, b1 is estimated response at zero concentration, b3 is mid-range concentration and b4 is slope factor.

1.5.9. Immunocytochemistry

For all immunofluorescence experiments, 12 mm coverslips were used (Fisherbrand™ Catalog# 12CIR1602811G). SH-SY5Y cell lines were fixed with 4% formaldehyde in phosphate buffered saline. Cells were then permeabilized with 1% Triton X-100 for 10 minutes and blocked immediately for 30 minutes with 2% bovine serum albumin (BSA) in phosphate buffered saline

`

solution. After blocking, coverslips were incubated with the primary antibody overnight at 4 °C. The following day, the primary antibody was washed off, the coverslips were washed 3 times in 2% BSA buffer and were then incubated with secondary antibody for 30 minutes. After incubation, coverslips were washed in PBS and nuclei were stained with NucBlue (ThermoFisher catalog #R37606). In order to visualize the actin network some cells were stained with Phalloidin for 20 minutes according to the manufacturer's instructions (ThermoFisher catalog #A22287). Coverslips were then mounted onto microscope slides using the Aqua-Poly/Mount media (Polysciences Catalog #18606-20).

The primary antibodies used for immunofluorescence were the following: anti-EEA1 antibody 1:200 dilution (Cell Signaling #3288), anti-LAMP1 antibody 1:200 dilution (Cell Signaling #9091), and anti-BACE1 C-term antibody 1:100 dilution (Millipore MAB5308).

The secondary antibodies were acquired from Life Technologies: goat anti-rabbit IgG cross adsorbed Alexa Fluor 647 (ThermoFisher catalog #A-21245; diluted 1:10,000), goat anti-mouse IgG cross absorbed Alexa Fluor 568 (ThermoFisher catalog #A-11031) or goat anti-mouse IgG cross absorbed Alexa Fluor 488 (ThermoFisher catalog #A-11001).

1.5.10. Confocal Microscopy and Image Analysis

Single- or double-immunolabeled (Alexa Fluor-488, -568 or -647) samples were analyzed at the Imaging & Molecular Biology Platform (IMBP; McGill Life Sciences Complex) using a TCS SP8 multi-photon confocal microscope (Leica) with 63x/1.40 oil-immersion objectives (Leica,Wetzlar, Germany). Samples were excited with Coherent Chameleon Vision II multiphoton at 730 nm (2660mW) for DAPI imaging. For each sample, 12–30 z-stack images were acquired using the same laser intensity settings for quantification. Z-stack images were processed using Image-J (Rasband, W.S., ImageJ, U. S. National Institutes of Health, Bethesda, Maryland, USA,

`

https://imagej.nih.gov/ij/, 1997-2018) and total cell fluorescence was quantified with the analyze tool. To better visualize BACE1 localization, a heatmap was generated using Fire LUT in Image-J. The IMARIS Image Analysis Software (Bitplane (Oxford Instruments), MA, USA) software was used for cross-sectional analysis. BACE1 colocalization with EEA1 and LAMP1 were analyzed using ImageJ plugin JACoP (Bolte and Cordelières, 2006).

1.5.11. Matrix-Assisted Laser Absorption Ionization Mass Spectrometry (MALDI-MS)

Samples were first immunoprecipitated (IP). For each IP (4 °C, 18 h), 0.5 mL of conditioned cell culture supernatant was combined with 5 µg W02 (anti-Ab antibody) and 25 µL protein-G sepharose beads (GE Healthcare) in PBS (1 mL final volume). The samples were sequentially washed with PBS, followed by 10 mM Tris pH 7.5; 150 mM NaCl; 0.2% NP-40; 2 mM EDTA, followed by 10 mM Tris pH 7.5; 500 mM NaCl; 0.2% NP-40; 2 mM EDTA, followed by three-times PBS and finally three-times 100 mM ammonium acetate (pH 7.4). The IPs were eluted twice using 350 µl volumes of 50% acetic acid. The vacuum-dried samples were resuspended in 10 µl of TA30 (33% acetonitrile and ultrasonicated. Samples were mixed 1:1 with α-cyanocinnamic acid matrix (CCA, Bruker Daltonics; 20 mg/mL in TA30) and applied to ground steel MALDI targets using the dried droplet method. Mass spectra were recorded on an UltrafleXtreme MALDI-TOF/TOF system (Bruker Daltonics) using the reflector positive 900-4500 method (ion source 1 = 25 kV; ion source 2 = 22.30 kV; lens = 9.40 kV; reflector = 26.45 kV; reflector 2 = 13.40 kV; pulsed ion extraction = 150 ns) and flexControl v1.4 and flexAnalysis v1.4 software. Ion intensity was evaluated by averaging four measurements of 500 shots each (i.e., 2000 shots total per sample).

`

1.5.12. Statistical Analysis

For all experiments, different conditions were analyzed by one factor ANOVA (between subject design) or two factor ANOVA. Pairwise comparisons were performed either with Dunnet's or Tukey's post-hoc tests. The statistical analysis was run by GraphPad Prism 5. For human brain samples, Welch's t-tests were performed.

`

1.6.Ethics Approval and Consent to Participate

Prior to starting the study, ethical approvals have been obtained. The study was conducted in accordance with Helsinki Declaration as revised in 2013. Post-mortem samples were collected from donors with a written informed consent for a brain autopsy and the use of the material for research purposes was obtained by the Netherlands Brain Bank. We complied with all relevant ethical regulations for animal tissue testing and research. Details on ethics approvals for animal studies are available from the laboratories in Germany that provided the material.

`

1.7.Authors Contributions

All authors mentioned in the manuscript have agreed for authorship, read and approved the manuscript. IU and FL contributed equally to this work. IU, FL and GM designed research; IU, FL, SCA, JFS, and ADS performed research; IU, FL, LK, CH, CP, GT, PS, and GM analyzed data; IU, FL, and GM wrote the paper.

`

1.8.Acknowledgments

GM holds both a Canada Research Chair Tier 1 in Molecular Pharmacology and Canada Foundation for Innovation (CFI) funding. This study was funded by the Canadian Institute of Health Research (MOP-133411; PJT-173407); Australia National Health and Medical Research Council (NHMRC) APP1129627; Chair Allocation from Faculty of Medicine, McGill University; Brain@McGill; the Velux Stiftung, the Natural Sciences and Engineering Research Council of Canada and the Canadian Consortium on Neurodegeneration in Aging (CCNA) awarded to GM or CH and LK. GT was funded by the National Institutes of Health grant AG019070. Thanks to Jean-Robert Kwizera for technical support, Drs. Mark A. Hancock and Adeola Shobo for helpful discussions and Robert Vassar for providing materials and feedback on the manuscript.

`

1.9.Supplementary Figures and Tables

Disease state	*Braak stage*	*Sex*	*Age*	*Postmortem delay (hours)*
Non-demented control	0	M	62	09:35
Non-demented control	0	M	51	07:44
Non-demented control	0	M	51	07:45
Non-demented control	0	M	49	06:15
Non-demented control	0	M	76	06:45
Alzheimer disease	6	M	58	05:15
Alzheimer disease	6	F	54	06:25
Alzheimer disease	4	F	85	06:00
Alzheimer disease	4	M	88	05:00
Alzheimer disease	6	M	57	03:50
Alzheimer disease	6	M	74	05:35
Alzheimer disease	4	M	80	04:00
Alzheimer disease	4	M	85	08:35
Alzheimer disease	4	F	93	05:20
Alzheimer disease	6	F	61	05:10
Alzheimer disease with congophilic angiopathy	6	F	72	04:00
Alzheimer disease with congophilic angiopathy	6	F	78	04:30
Alzheimer disease with congophilic angiopathy	4	F	87	03:35
Alzheimer disease with congophilic angiopathy	4	F	83	04:10
Alzheimer disease with congophilic angiopathy	4	M	87	03:45
Alzheimer disease with congophilic angiopathy	4	F	80	05:10
Alzheimer disease with congophilic angiopathy	6	M	71	04:00
Alzheimer disease with congophilic angiopathy	6	M	71	04:00
Alzheimer disease with congophilic angiopathy	4	F	64	08:05
Alzheimer disease with congophilic angiopathy	6	M	66	07:00

Supplementary Table 1: Disease state, sex and age of the AD patients and controls

Disease state, Braak stage, sex, age, and postmortem delay of post-mortem brain temporal cortex tissues used for analysis shown in figure 4.

`

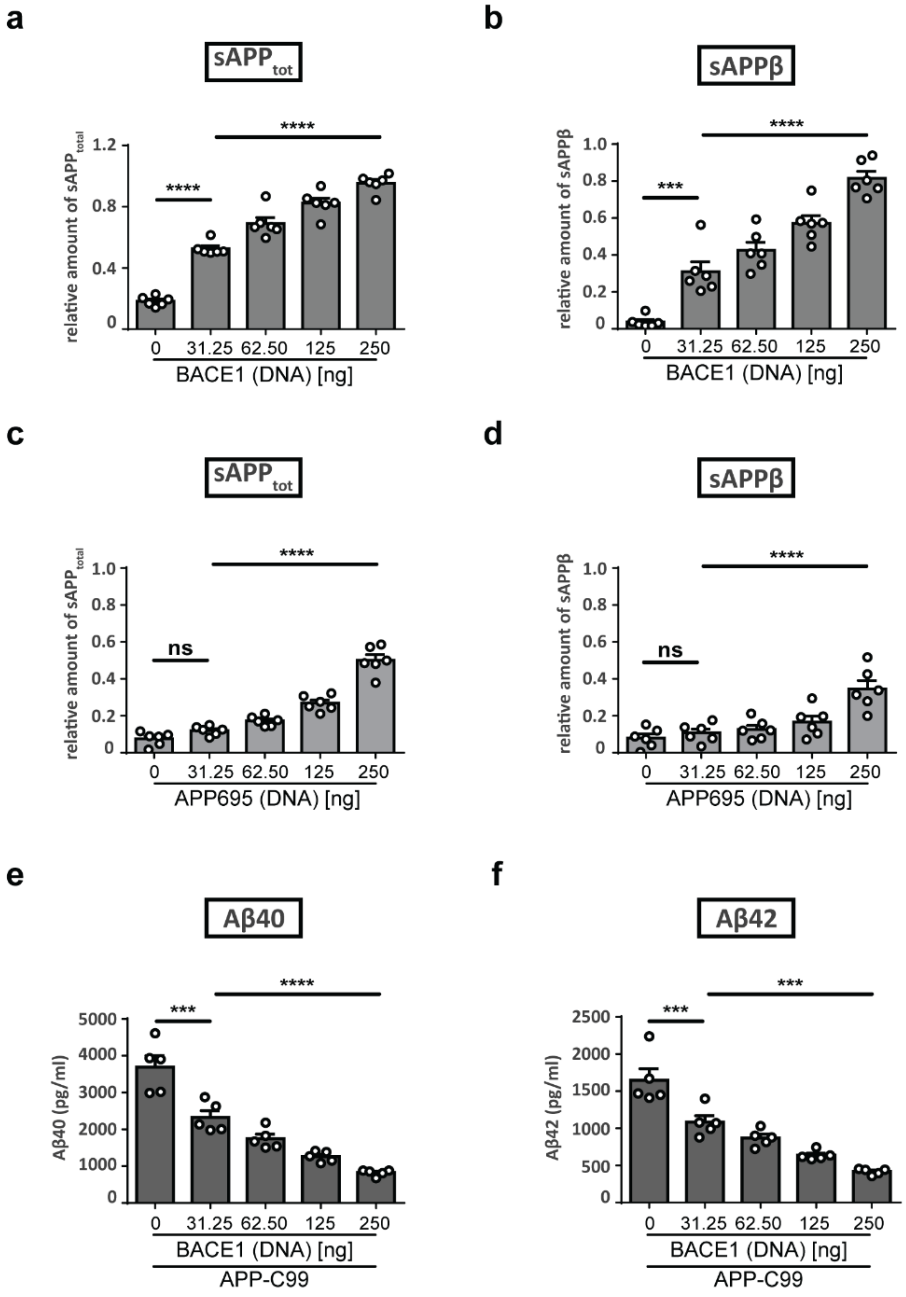

Supplementary Figure 1: APP processing under BACE1, APP695 or APP-C99 overexpression conditions

Western blot quantification of relative amounts of $sAPP_{total}$ and sAPPβ under BACE1 (a and b) or APP695 (c and d) overexpression conditions presented in Figure 5a and Figure 5b. ELISA quantification of absolute amounts of Aβ40 (e) and Aβ42 (f) under BACE1 and APP-C99 co-overexpression from the experiment presented in Figure 5d. Bars and error bars indicate mean ± s.e.m. Tukey's post-hoc tests were performed for pairwise comparisons; selected comparisons are highlighted ****$p < 0.0001$, ***$p < 0.001$, ns = not significant. (a) $sAPP_{total}$, 1-WAY ANOVA, $F(4,25)=124.1$, $p < 0.0001$, (b) sAPPβ, 1-WAY ANOVA, $F(4,25)=52.83$, $p < 0.0001$, (c) $sAPP_{total}$, 1-WAY ANOVA, $F(4,25)=85.79$, $p < 0.0001$, (d) sAPPβ, 1-WAY ANOVA, $F(4,25)=12.35$, $p < 0.0001$, (e) Aβ40, 1-WAY ANOVA, $F(4,20)=42.04$, $p = p < 0.0001$, (f) Aβ42, 1-WAY ANOVA, $F(4,20)=31.91$, $p < 0.0001$.

`

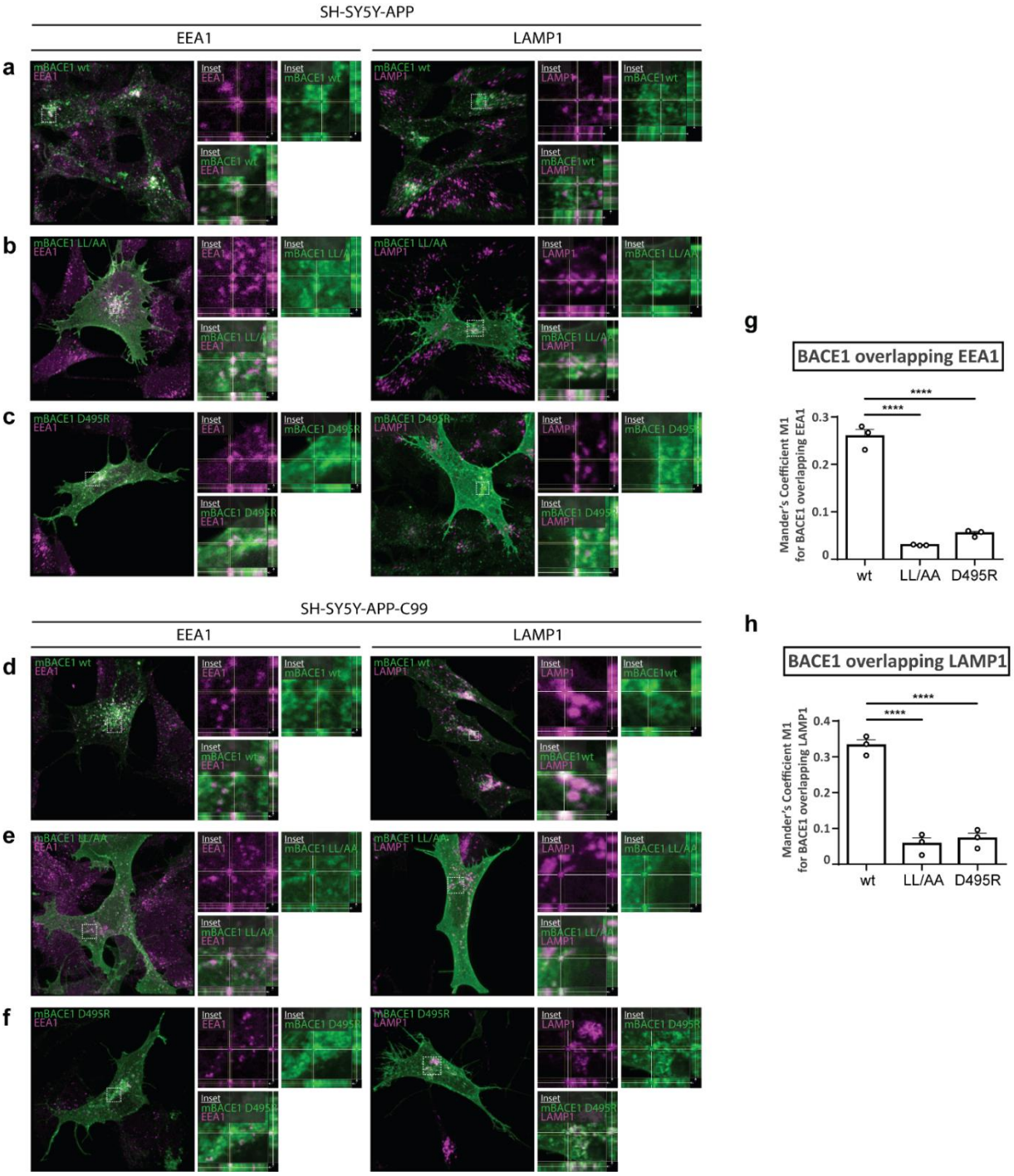

Supplementary Figure 2: Cellular localization of BACE1 mutants is altered

Cellular localization of BACE1 mutants was analyzed by ICC from 3 independent experiments with BACE1 transfected SH-SY5H-APP and SH-SY5H-APP-C99 cells. Cross-sectional analysis of co-staining of WT BACE1 (a) and localization mutants of BACE1, D495R (b) and LL/AA (c) with EEA1 and LAMP1 in SH-SY5Y-APP and co-staining of WT BACE1 (d) and localization mutants of BACE1, D495R (e) and LL/AA (f) with EEA1 and LAMP1 in SH-SY5Y-APP-C99 cells. BACE1 colocalization with EEA1 (g) and LAMP1 (h) were analyzed in SH-SY5Y-APP-C99 cells using ImageJ plugin JACoP from 3 independent experiments. Bars and error bars indicate mean ± s.e.m. Dunnett's post-hoc tests were performed for

`

pairwise comparisons; selected comparisons are highlighted ****p < 0.0001. (g) BACE1 overlapping EEA1, 1-WAY ANOVA, $F(2,6)=204.6$, $p < 0.0001$, (h) BACE1 overlapping LAMP1, $F(2,6)=96.29$, $p < 0.0001$.

`

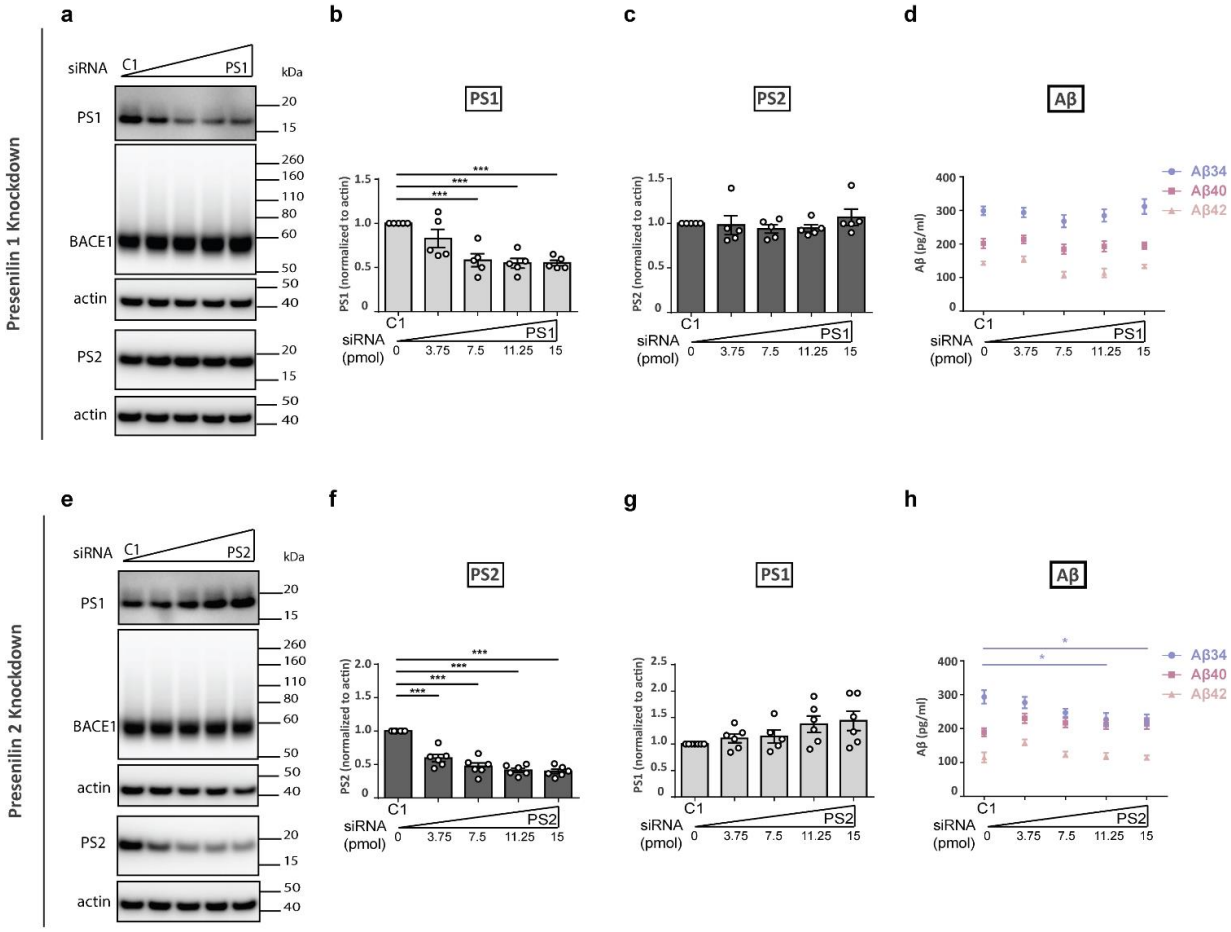

Supplementary Figure 3: Unlike PS1, PS2 knockdown leads to reduced Aβ34 levels in BACE1 overexpressing cells

Expression of PS1 and PS2 were analyzed by Western blot and Aβ levels determined by ELISA. Data in a-d represent PS1 knockdown and data in e-i represent PS2 knockdown in SH-SY5Y-BACE1 cells. Representative Western blots from 6 independent experiments for PS1 knockdown (a) and from 5 independent experiments for PS2 knockdown (e). Western Blot quantification of relative amounts of PS1 (b and g) and of PS2 (c and f), and absolute amounts of Aβ34, Aβ40, and Aβ42 (d and i). Bars and error bars indicate mean ± s.e.m. Dunnett's post-hoc tests were performed for pairwise comparisons; selected comparisons are highlighted ***$p < 0.001$, **$p < 0.01$, *$p < 0.05$. (b) PS1, 1-WAY ANOVA, $F(4,20)=10.33$, $p < 0.0001$, (c) PS2, 1-WAY ANOVA, $F(4,20)=0.5776$, $p = 0.5776$, (d) Aβ34, 1-WAY ANOVA, $F(4,20)=0.8744$, $p = 0.4966$, Aβ40, 1-WAY ANOVA, $F(4,20)=0.6853$, $p = 0.6104$, Aβ42, 1-WAY ANOVA, $F(4,20)=4.961$, $p = 0.0061$, (f) PS2, 1-WAY ANOVA, $F(4,25)=40.91$, $p < 0.0001$, (g) PS1, 1-WAY ANOVA, $F(4,25)=2.448$, $p = 0.0726$, (i) Aβ34, 1-WAY ANOVA, $F(4,24)=3.077$, $p < 0.05$, Aβ40, 1-WAY ANOVA, $F(4,25)=1.175$, $p = 0.3456$, Aβ42, 1-WAY ANOVA, $F(4,24)=3.177$, $p < 0.05$.

`

Bridging Statement to Manuscript II

In Manuscript I, we investigated the pathways and enzyme/substrate relationships that determine the levels of Aβ34 *in vivo* and *in vitro*. We showed that there is an association between elevated levels of BACE1 and Aβ34 both in human and mouse brain tissue and in different cell culture systems. We provided evidence that changing enzyme to substrate ratios (BACE1:APP) intimately affects the balance between amyloidogenic (Aβ producing) and amyloidolytic (Aβ degrading) activities of BACE1. Furthermore, we discovered that Aβ34 is produced by BACE1 in the endo-lysosomal system and that BACE1 uses Aβ species as substrates generated by Presenilin 2 containing γ-secretase for amyloidolytic processing.

Aβ34 is a metastable intermediate product and serves as an indicator of amyloid clearance; therefore, in the following manuscript, we investigated Aβ34 degradation by various Aβ degrading enzymes (ADEs) to further establish Aβ34 as a biomarker in early AD. We tested ADEs that are implicated in Alzheimer disease for their potential roles in Aβ34 degradation. With a combination of genetic manipulations of cells, including transient overexpression and siRNA knockdown of proteases, and by using pharmacological tools, we identified the predominant protease in comparison to other proteases having a major role in Aβ metabolism.

`

MANUSCRIPT II

The Endothelin Converting Enzyme 1 regulates the levels of the amyloid clearance indicator, Aβ34, and is the predominant protease in Aβ34 degradation

Irem Ulku[1], S. Can Akerman[2], Gerhard Multhaup[1,2]

The Invention Disclosure D2023-0074 based on findings reported in Manuscript II has been approved by McGill (status: under review; October 13th, 2022).

1. Integrated Program in Neuroscience, McGill University, Montreal, QC, Canada, H3G 0B1

2. Department of Pharmacology & Therapeutics, McGill University, Montreal, QC, Canada, H3G 1Y6

`

2.1.Abstract

The amyloid hypothesis suggests that the imbalance between amyloid-β (Aβ) production and clearance is the leading cause of Alzheimer Disease (AD). Proteases collectively referred as Aβ-degrading enzymes (ADEs) are involved in Aβ clearance; however, they are mainly studied in the degradation of Aβ40 and Aβ42. Here, we tested eight different ADEs for their potential roles in the clearance of Aβ34, a non-amyloidogenic peptide that could potentially serve as a biomarker for AD progression. We found that Aβ34 levels increased upon the knockdown of Endothelin Converting Enzyme 1 (ECE1) under both endogenous and β-secretase overexpressing conditions. Interestingly, among the proteases tested, only Cathepsin B knockdown resulted in a decrease in Aβ34 levels. When combined with the knockdown of other proteases, the effect of ECE1 on Aβ34 dominated over other proteases tested. Furthermore, ECE1 overexpression led to a reduction in Aβ34 levels. Pharmacological inhibition of ECE1 primarily increased Aβ34 levels. Thus, our findings suggest that ECE1 is the major enzyme involved in Aβ34 degradation.

`

2.2.Introduction

Alzheimer Disease (AD) is characterized by two pathological hallmarks: intracellular neurofibrillary tangles and extracellular amyloid plaques mainly consisting of amyloid beta (Aβ) species (Holtzman et al., 2011). Among those, 42-amino acid long Aβ peptide (Aβ42) is prone to aggregate ultimately forming larger fibrils and plaques in the brain that cause cognitive decline (Cleary et al., 2005, Hardy and Higgins, 1992, Rozemuller et al., 1989, Zhao et al., 2012); therefore, its elevated production is believed to be the main culprit of the disease. Although traditionally the production of Aβ peptides has been the focus of AD field, recent research has revealed that amyloid clearance is equally important as its production in influencing AD progression and dysregulation of protein metabolism, i.e., both/either increased production and/or decreased clearance of Aβ peptides, is the cause of the disease (Bateman et al., 2006, Skovronsky et al., 2006).

Amyloid production, i.e., amyloidogenic pathway, includes sequential processing of amyloid precursor protein (APP) by β-secretase (BACE1) (APP → APP-C99) and γ-secretase (APP-C99 → Aβ peptides) to generate varying lengths of Aβ species (Chow et al., 2010, O'brien and Wong, 2011, Olsson et al., 2014, Yan and Vassar, 2014). On the other hand, Aβ clearance and degradation are mediated by a number of proteases with distinct characteristics, including Aβ specificity, optimal pH and subcellular localization (Saido and Leissring, 2012).

The first mechanism of Aβ degradation is the stepwise cleavage of APP-C99 by γ-secretase. The first γ-secretase cleavage generates either Aβ49 or Aβ51 and further processing of these distinct pathways converge in the production of the common non-amyloidogenic metastable intermediate, i.e., Aβ34 (Olsson et al., 2014, Takami et al., 2009). The second mechanism occurs via the amyloidolytic processing of Aβ peptides by BACE1. After being generated by the

`

amyloidogenic pathway, Aβ peptides (e.g., Aβ38, Aβ40, and Aβ42) can undergo amyloidolytic processing, leading to their degradation into Aβ34 (Fluhrer et al., 2003, Hernandez-Guillamon et al., 2015, Liebsch et al., 2019, Shi et al., 2003). Our previous studies showed that BACE1 uses Aβ species produced by Presenilin 2-containing γ-secretase complex as substrates and produces Aβ34 in the endo-lysosomal system (Manuscript I).

The third mechanism involves different types of proteases collectively referred as Aβ-degrading enzymes (ADEs), including Endothelin Converting Enzyme 1 (ECE1), Insulin Degrading Enzyme (IDE), Cathepsin B (Cat B), Cathepsin D (Cat D), Matrix metallopeptidase 2 (MMP2), Matrix metallopeptidase 9 (MMP9), Angiotensin Converting Enzyme (ACE), Neprilysin (NEP; Membrane Metallo-Endopeptidase, MME) (Saido and Leissring, 2012, Wildsmith et al., 2013). In the context of Aβ degradation, the most important difference among these proteases is their subcellular localization. Each protease has different substrate selectivity and contributes to a specific Aβ pool which are defined as interstitial (extracellular), ER/Golgi, endosomal, lysosomal and cytosolic (Saido and Leissring, 2012). Although most of the proteases have been extensively studied for degradation of Aβ40 and Aβ42, none of them have been characterized in detail for Aβ34 degradation.

A recent study showed that changes in cerebrospinal fluid (CSF) Aβ34 levels correlate with overall Aβ clearance in amyloid positive individuals and that Aβ34/Aβ42 ratio which involves markers for Aβ clearance (Aβ34) and Aβ production (Aβ42) has a better diagnostic accuracy compared to Aβ40/Aβ42 which involves markers only for Aβ production for prodromal AD (Liebsch et al., 2019). As Aβ34 has a strong potential to serve as a biomarker for AD progression, it is important to study the pathways and identify the enzymes involved in Aβ34 production and Aβ34 degradation.

`

Here, we tested eight different ADEs implicated in AD for their ability to degrade Aβ34. We hypothesized that proteases localized to endo-lysosomal system, namely ECE1, Cat B and Cat D, have higher access to Aβ34 since it is the compartment where BACE1 generates Aβ34, and are therefore involved in Aβ34 degradation. We performed small interfering RNA (siRNA) knockdowns, transient overexpression and pharmacological inhibition of proteases in both wild-type and stably BACE1 overexpressing SH-SY5Y neuroblastoma cells. Compared to other proteases tested, including IDE, Cat B, Cat D, MMP2, MMP9, ACE and MME, ECE1 knockdown yielded the largest increase in Aβ34 levels and Aβ34 levels were decreased dose-dependently with ECE1 overexpression. Pharmacological inhibition of ECE1, MME and ACE by Phosphoramidon (PA) increased Aβ34 levels significantly higher than other Aβ species tested. Treatment with CGS35066, which is a potent ECE1 inhibitor, affected Aβ34 levels at a lower concentration of the inhibitor treatment and led to a larger increase in Aβ34 levels. Overall, our study suggests that ECE1 is the major enzyme involved in Aβ34 clearance.

`

2.3.Results

2.3.1. ECE1 knockdown significantly elevated Aβ34 levels under both elevated and endogenous levels of BACE1

Considering different Aβ pools in the cell, we hypothesized that ECE1, Cat B and Cat D could be directly involved in Aβ34 degradation because they are mainly localized to and active in endosomes (or lysosomes) (Saido and Leissring, 2012) where BACE1 is also active to produce Aβ34 (Manuscript I). We performed small interfering RNA (siRNA) knockdowns of each protease, namely, ECE1, Cat B, IDE, Cat D, MMP2, MMP9, ACE and MME, in SH-SY5Y cells that were stably overexpressing BACE1 (SH-SY5Y-BACE1) and measured Aβ34, Aβ40 and Aβ42 levels with ELISA (Figure 9a-c). Significant increase in Aβ34 levels was observed upon individual knockdowns of ECE1 (~303%), MMP2 (~74%) and MMP9 (~99%). The greatest increase in Aβ34 levels was observed with ECE1 knockdown which was ~303% compared to the control condition where endogenous levels of ECE1 were present in the cells (Figure 9a). Knockdowns of IDE, MMP9 and MME led to ~53%, ~63% and ~57% increase in Aβ40 levels, respectively, (Figure 9b) and knockdown of MMP9 led to ~67% increase in Aβ42 levels (Figure 9c).

We also tested the effect of each protease knockdown in wild-type SH-SY5Y cells that had endogenous BACE1 levels (Figure 9d-f). Although Aβ34 levels were below Lower Limit of Detection (LLOD) of ELISA in most of the experimental conditions including the control where endogenous levels of ECE1 are present, ECE1 knockdown yielded elevated levels of Aβ34 that were above LLOD which was at least 82% increase (Figure 9d). Significant increase in Aβ40 levels was observed with each protease knockdown except Cat B (percent increases are indicated

`

in Figure 9e). We didn't observe any significant changes in Aβ42 levels with any of the protease knockdowns in these cells (Figure 9f).

Altogether, these results suggested that ECE1 is involved in Aβ34 clearance under both elevated and endogenous levels of BACE1.

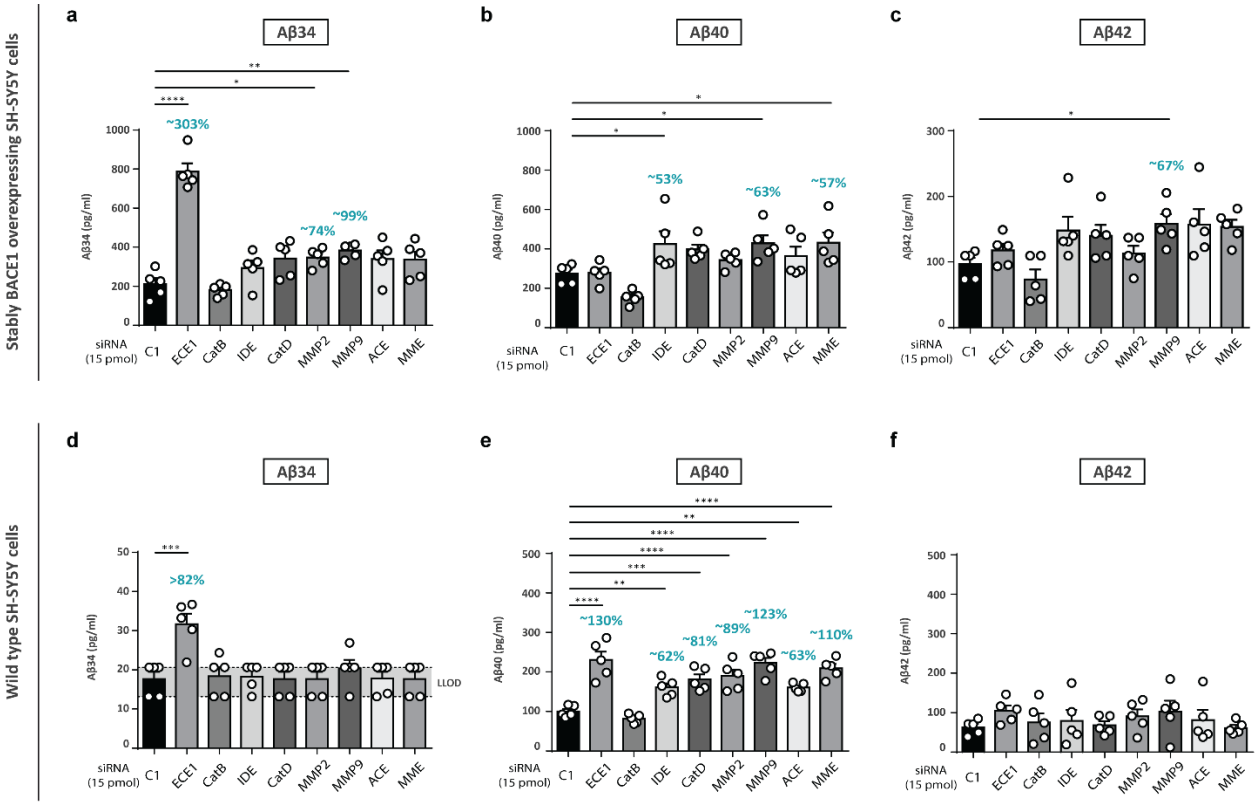

Figure 9: ECE1 knockdown elevated Aβ34 levels in both wild-type and BACE1-overexpressing SH-SY5Y cells

Aβ34, Aβ40 and Aβ42 levels were quantified by ELISA assays in stably BACE1 overexpressing (a, b and c) and wildtype (d, e and f) SH-SY5Y cells. Data were collected from 5 independent experiments for each cell line. Percent changes in Aβ levels compared to the endogenous levels are indicated above each bar. Bars and error bars indicate mean ± s.e.m. Dunnett's post-hoc tests were performed for pairwise comparisons; selected comparisons are highlighted ****p < 0.0001, ***p < 0.001, **p < 0.01, *p < 0.05. (a) Aβ34, 1-WAY ANOVA, $F(8,36)=26.27$, $p < 0.0001$, (b) Aβ40, 1-WAY ANOVA, $F(8,36)=6.060$, $p < 0.0001$, (c) Aβ42, 1-WAY ANOVA, $F(8,36)=3.746$, $p = 0.0028$, (d) Aβ34, 1-WAY ANOVA, $F(8,36)=5.317$, $p < 0.0002$, (e) Aβ40, 1-WAY ANOVA, $F(8,36)=17.94$, $p < 0.0001$, (f) Aβ42, 1-WAY ANOVA, $F(8,36)=0.6693$, $p = 0.7147$.

`

2.3.2. Changes in ECE1 levels gradually and primarily affected Aβ34 levels

In order to elaborate on the role of ECE1 in Aβ34 degradation, we performed a titration experiment where we gradually increased siRNA concentration against ECE1 (Figure 10). We verified the decrease in ECE1 protein levels and also checked changes in APP levels by Western blot (Figure 10a). Compared to the control, ECE1 protein levels were decreased in the knockdown conditions gradually from 55% to 60% (Figure 10a and b) and APP levels were not significantly different from each other (Figure 10a and c). ELISA quantification of Aβ levels showed that Aβ34 levels were gradually elevated (from ~87% to ~254%) with increasing concentration of siRNA against ECE1 (Figure 10d) and that Aβ40 and Aβ42 levels did not change with the knockdowns (Figure 10e and f). The titration experiment suggested that with decreasing levels of ECE1 in the cells, Aβ34 levels increase in a concentration-dependent manner.

We performed the same titration experiment for all proteases listed above (Figure 9) and quantified Aβ levels (Supplementary Figure 4, 5 & 6). Aβ34 levels were increased with the highest concentration of siRNA in each experimental setup except Cat B knockdown; however, the greatest increase was observed with ECE1 knockdown which was 254% increase (Table 2). Unlike other proteases, Cat B knockdown led to a decrease in all Aβ34, Aβ40 and Aβ42 levels (Supplementary Figure 6).

`

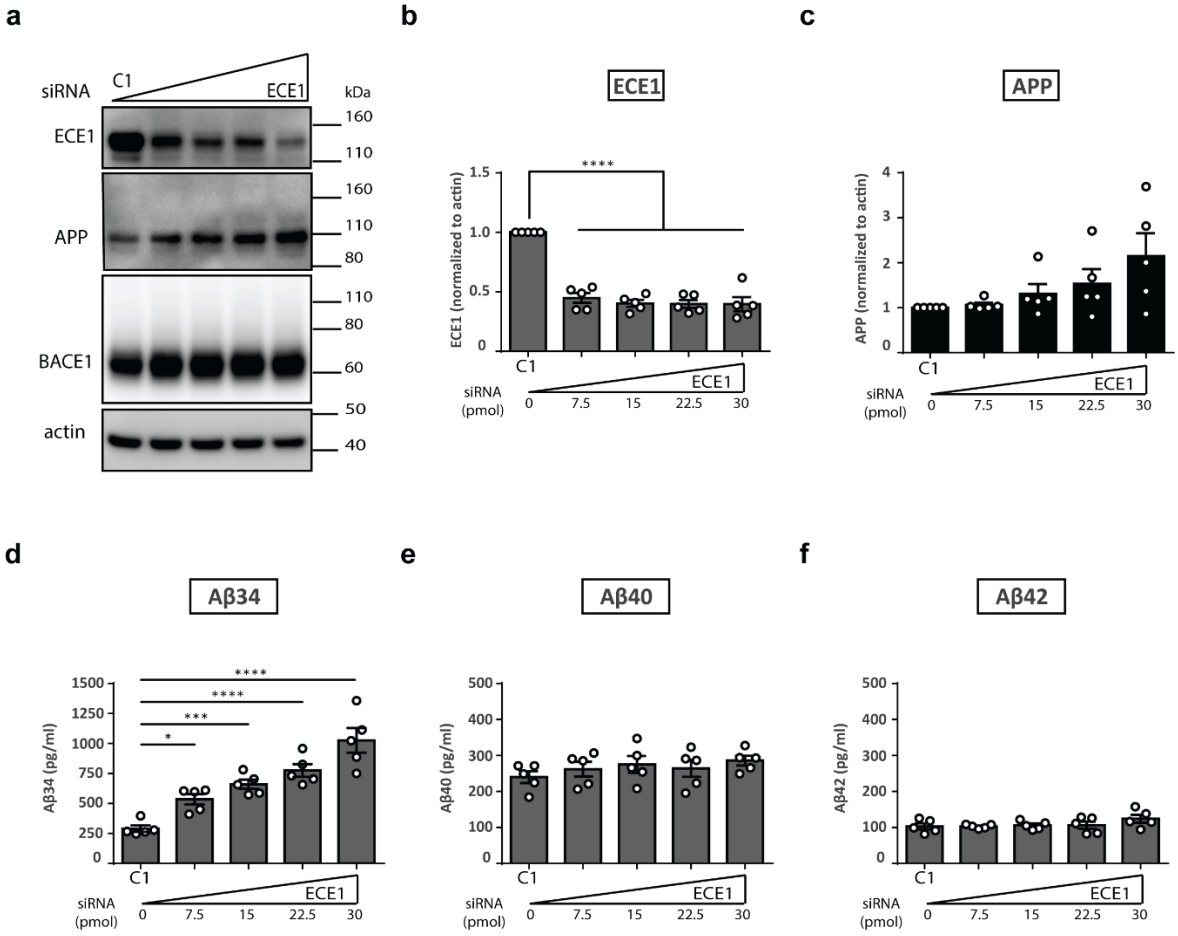

Figure 10: Aβ34 levels gradually increased with increasing ECE1 knockdown

Expression of ECE1 and APP and Aβ levels were analyzed by Western blot and ELISA, respectively. Representative Western blots from 5 independent experiments for ECE1 knockdown titration in SH-SY5Y-BACE1 cells (a). Quantification of relative amounts of ECE1 (b) and of APP (c), and absolute amounts of Aβ34 (d), Aβ40 (e), and Aβ42 (f) in cell media by ELISA. Bars and error bars indicate mean ± s.e.m. Dunnett's post-hoc tests were performed for pairwise comparisons; selected comparisons are highlighted ****$p < 0.0001$, ***$p < 0.001$, *$p < 0.05$. (b) ECE1, 1-WAY ANOVA, $F(4,20)=48.52$, $p < 0.0001$, (c) APP, 1-WAY ANOVA, $F(4,20)=2.628$, $p = 0.0651$, (d) Aβ34, 1-WAY ANOVA, $F(4,20)=0.7519$, $p = 0.5690$, (e) Aβ40, 1-WAY ANOVA, $F(4,20)=0.6677$, $p = 0.6504$, (f) Aβ42, 1-WAY ANOVA, $F(4,20)=1.259$, $p = 0.3189$.

`

Knockdown	*% decrease in protease levels*	Aβ34		Aβ40	Aβ42
ECE1	~60 %	↑ ****	254 %	ns	ns
CatB	~82 %	*** ↓	30 %	**** ↓	ns
IDE	~63 %	↑ *	24 %	↑ **	ns
CatD	~55 %	↑ ****	70 %	↑ *	↑ *
MMP2	~68 %	↑ **	71 %	↑ *	ns
MMP9	~35 %	↑ ***	90 %	↑ ****	ns
ACE	~48 %	↑ ***	63 %	ns	ns
MME	N/A	↑ ****	75 %	↑ *	ns

Table 2: Changes in Aβ levels with corresponding protease knockdowns

siRNA knockdown titration experiments against each protease in SH-SY5Y-BACE1 cells. Reported changes are the ones obtained with the highest concentration of the knockdowns. Percent decreases in protein levels were relative protein amounts normalized to actin (Western blot analysis). Arrows pointing upwards show an increase in the corresponding Aβ level and arrows pointing downwards show a decrease in the corresponding Aβ level. Selected comparisons are highlighted ****$p < 0.0001$, ***$p < 0.001$, **$p < 0.01$, *$p < 0.05$, ns = not significant.

Next, to complement the ECE1 knockdown experiment, we gradually overexpressed ECE1 in the same cell line (Figure 11). We verified increasing protein levels of ECE1 by Western blot (Figure 11a and b). APP levels did not change with the increasing ECE1 levels (Figure 11a and c). We observed a gradual decrease in Aβ34 levels (Figure 11d). The decrease was already significant (~27%) with the lowest concentration of the ECE1 cDNA introduced to the cells and reached ~61% decrease with the highest concentration of the ECE1 cDNA (Figure 11g). A gradual decrease was observed for Aβ40 levels as well (Figure 11e). However, the decrease was only significant (~31%) with the second lowest concentration of ECE1 cDNA and reached ~47% decrease with the highest concentration of the ECE1 cDNA (Figure 11h). Aβ42 levels were not significantly changed with ECE1 overexpression (Figure 11f and i).

`

Taken together, Aβ34 levels were elevated and reduced upon ECE1 knockdown and ECE1 overexpression, respectively. Furthermore, changes in ECE1 levels affected Aβ34 levels before the other Aβ species.

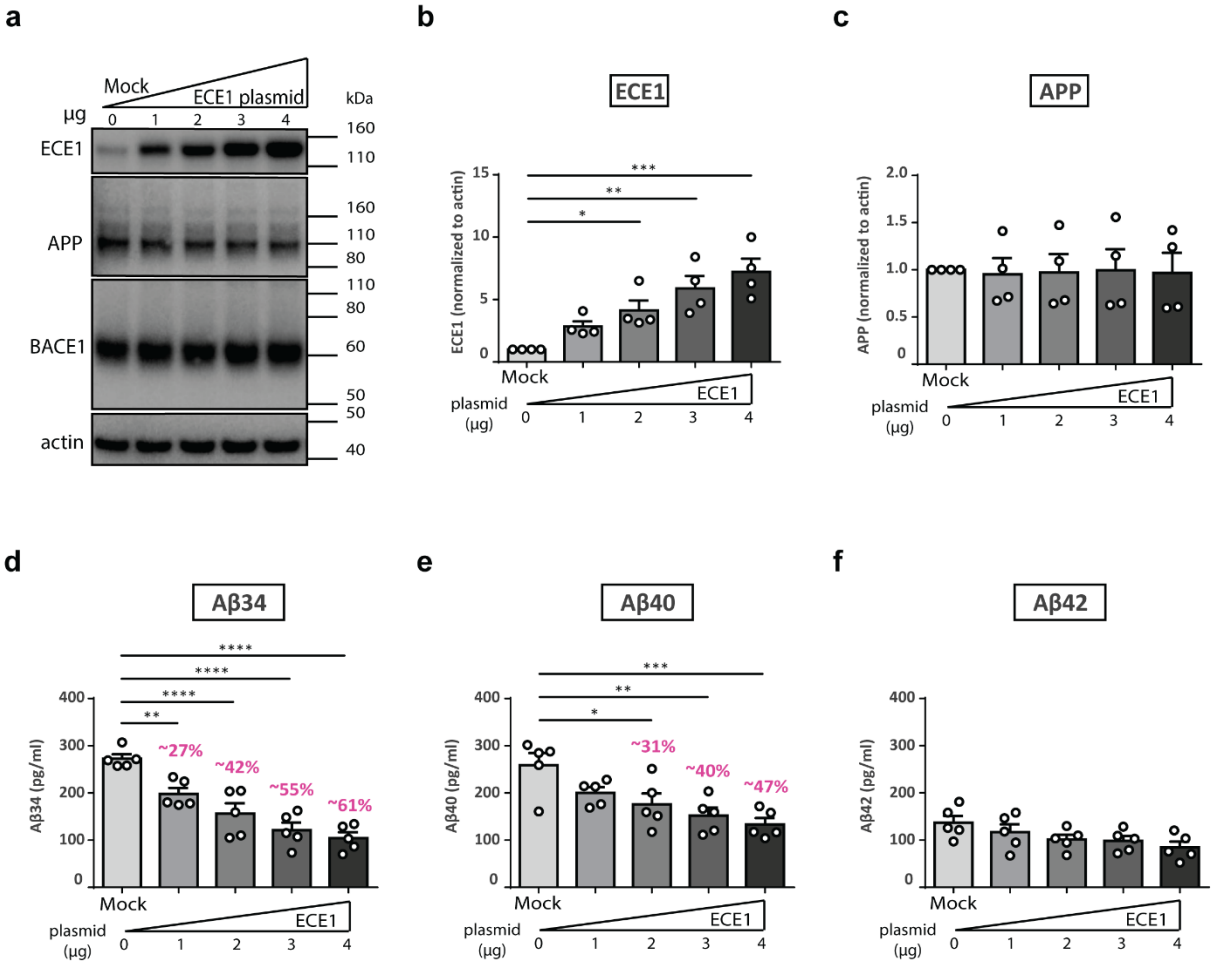

Figure 11: Aβ34 levels dose-dependently decreased with increasing ECE1 overexpression and were affected primarily by the overexpression

Expression of ECE1 and APP and Aβ levels were analyzed by Western blot and ELISA, respectively. Representative Western blots from 5 independent experiments for ECE1 overexpression in SH-SY5Y-BACE1 cells (a). Quantification of relative amounts of ECE1 (b) and of APP (c), and absolute amounts of Aβ34 (d), Aβ40 (e), and Aβ42 (f) in cell media by ELISA. Percent changes in Aβ levels compared to the endogenous levels are indicated above each bar. Bars and error bars indicate mean ± s.e.m. Dunnett's post-hoc tests were performed for pairwise comparisons; selected comparisons are highlighted ****$p < 0.0001$, ***$p < 0.001$, **$p < 0.01$, *$p < 0.05$. (b) ECE1, 1-WAY ANOVA, $F(4,15)=10.29$, $p = 0.0003$, (c) APP, 1-WAY ANOVA, $F(4,15)=0.01198$, $p = 0.9997$, (d) Aβ34, 1-WAY ANOVA, $F(4,20)=20.59$, $p < 0.0001$, (e) Aβ40, 1-WAY ANOVA, $F(4,20)=6.725$, $p = 0.0013$, (f) Aβ42, 1-WAY ANOVA, $F(4,20)=2.345$, $p = 0.0896$.

`

2.3.3. ECE1 had a greater effect on Aβ34 levels than other proteases tested

To evaluate the effect of combinatorial knockdowns, we knocked down pairs of proteases including ECE1, Cat B, IDE and Cat D (Figure 12). The setup included 7.5 pmol and 15 pmol siRNA against each protease as controls (Figure 12a, c and e) and 1:1 siRNA (protease X) : siRNA (protease Y) as experimental conditions (Figure 12b, d and f). Changes in protein levels of proteases upon knockdowns were verified by Western blot (Supplementary Figure 7). ELISA measurements showed that Aβ34 levels were increased in all conditions where ECE1 was knocked down either alone or in combination with other proteases. Even when combined with Cat B knockdown, which led to ~23% decrease in Aβ34 levels on its own, the levels of Aβ34 were significantly higher than the endogenous levels (~33%) (Figure 12a). Unlike Aβ34, Aβ40 and Aβ42 levels were elevated only when ECE1 knockdown was combined with Cat D knockdown (Figure 12b and c). These results suggest that ECE1 dominates over other proteases tested in Aβ34 clearance.

`

a

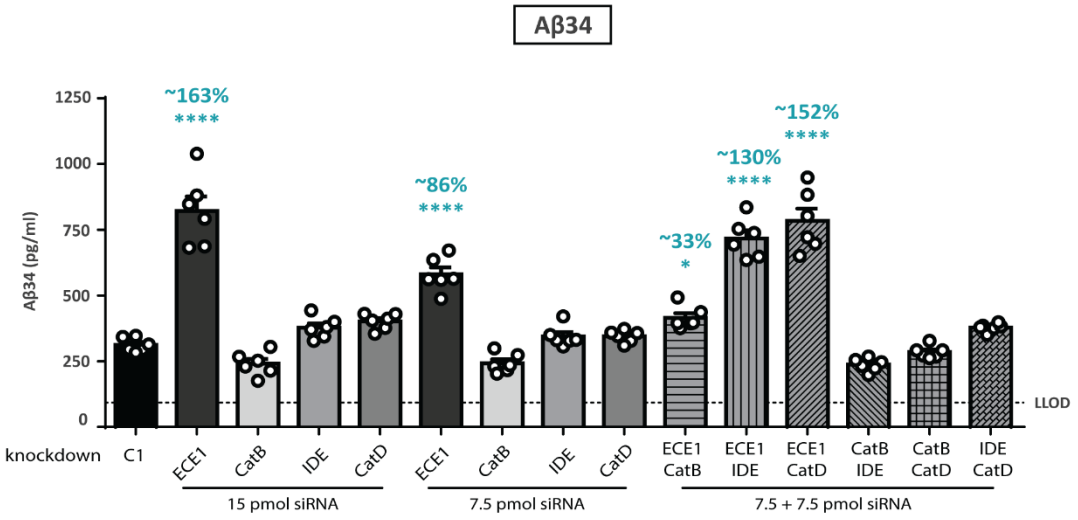
Aβ34
Aβ34 (pg/ml)
1250
1000
750
500
250
0
~163%
****
~86%
****
~33%
*
~130%
****
~152%
****
LLOD
knockdown
C1
ECE1
CatB
IDE
CatD
ECE1
CatB
IDE
CatD
ECE1 CatB
ECE1 IDE
ECE1 CatD
CatB IDE
CatB CatD
IDE CatD
15 pmol siRNA
7.5 pmol siRNA
7.5 + 7.5 pmol siRNA

b

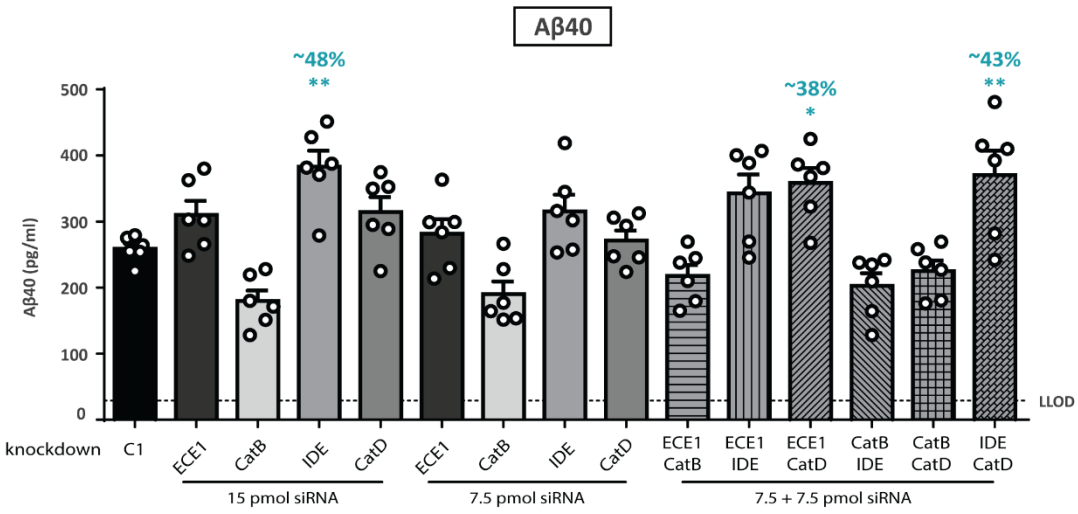
Aβ40
Aβ40 (pg/ml)
500
400
300
200
100
0
~48%
**
~38%
*
~43%
**
LLOD
knockdown
C1
ECE1
CatB
IDE
CatD
ECE1
CatB
IDE
CatD
ECE1 CatB
ECE1 IDE
ECE1 CatD
CatB IDE
CatB CatD
IDE CatD
15 pmol siRNA
7.5 pmol siRNA
7.5 + 7.5 pmol siRNA

c

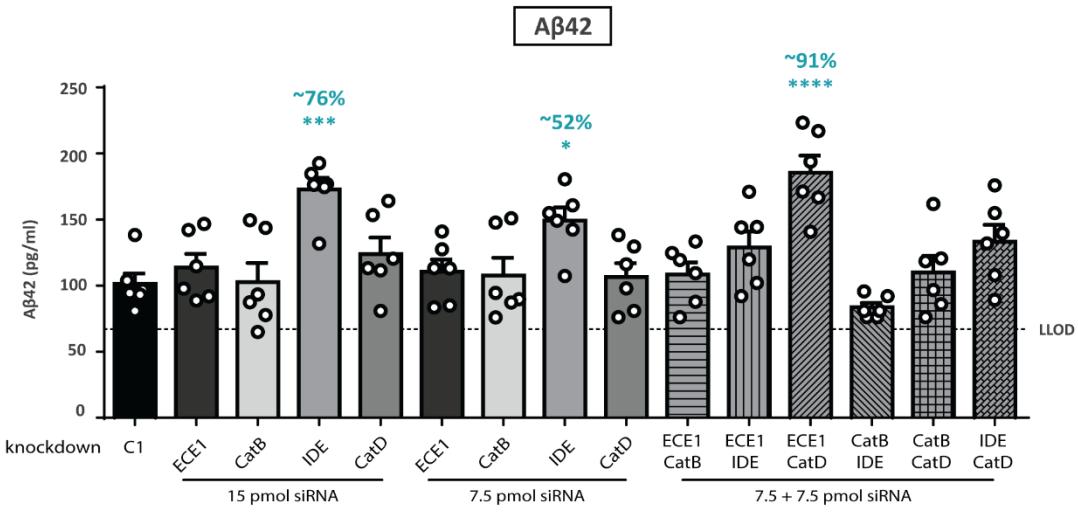
Aβ42
Aβ42 (pg/ml)
250
200
150
100
50
0
~76%
***
~52%
*
~91%
****
LLOD
knockdown
C1
ECE1
CatB
IDE
CatD
ECE1
CatB
IDE
CatD
ECE1 CatB
ECE1 IDE
ECE1 CatD
CatB IDE
CatB CatD
IDE CatD
15 pmol siRNA
7.5 pmol siRNA
7.5 + 7.5 pmol siRNA

`

Figure 12: ECE1 had the major impact on Aβ34 levels and dominated over other proteases

Aβ34, Aβ40 and Aβ42 levels were quantified by ELISA assays in SH-SY5Y-BACE1 cells. Data were collected from 6 independent experiments. Absolute Aβ34 (a), Aβ40 (c) and Aβ42 (e) levels when single protease was knocked down (controls) and when a pair of proteases was knocked down together. Percent changes in Aβ levels compared to the endogenous levels are indicated above each bar. Bars and error bars indicate mean ± s.e.m. Dunnett's post-hoc tests were performed for pairwise comparisons; selected comparisons are highlighted ****$p < 0.0001$, ***$p < 0.001$, **$p < 0.01$, *$p < 0.05$. (a) Aβ34, 1-WAY ANOVA, $F(14,75)=66.28$, $p < 0.0001$, (b) Aβ40, 1-WAY ANOVA, $F(14,75)=9.559$, $p < 0.0001$, (c) Aβ42, 1-WAY ANOVA, $F(14,75)=6.342$, $p < 0.0001$.

`

2.3.4. Pharmacological inhibition of ECE1 by a potent ECE1 inhibitor resulted in significantly elevated levels of Aβ34

To complement knockdown and overexpression experiments, we performed pharmacological inhibition of proteases by Phosphoramidon (PA) that targets MME (IC_{50} = $3.4x10^{-8}$ M), ECE1 (IC_{50} = $3.5x10^{-6}$ M) and ACE (IC_{50} = $7.8x10^{-5}$ M) (Kukkola et al., 1995). The cells were treated with different concentrations of PA, ranging from 10^{-11} to 10^{-5} M. Western blot analysis showed no difference in ECE1 protein levels (Figure 13a). Up to 10^{-5} M treatment, Aβ levels did not change. With 10^{-5} M treatment, increases in Aβ34 and Aβ40 levels were detected with no change in Aβ42 levels (Figure 13b). Compared to Aβ40, which increased ~26%, Aβ34 levels were elevated ~136%. These data suggest that PA treatment inhibits Aβ34 clearance to a greater extent and the proteases inhibited by PA could be involved in Aβ34 clearance.

Next, we chose a potent ECE1 inhibitor, CGS35066, that is over 100 folds more selective for ECE1 (IC_{50} = $2.2x10^{-8}$ M) compared to MME (IC_{50} = $2.3x10^{-6}$ M) (Trapani et al., 2000) and performed the same experiment. Western blot analysis showed no difference in ECE1 protein levels (Figure 13c) as PA treatment. No significant changes were observed in Aβ40 or Aβ42 levels at any concentration of the inhibitor tested (Figure 13d). Aβ34 levels started to significantly increase (~90%) at 10^{-6} M and reached ~224% increase at 10^{-5} M treatment (Figure 13d).

When two inhibitors compared, Aβ34 levels were affected at lower concentrations of CGS35066 treatment (10^{-6} M) compared to PA treatment (10^{-5} M). Furthermore, CGS35066 treatment led to a higher increase in Aβ34 levels (~224%) compared to PA treatment (~136%). Altogether the data suggest that Aβ34 is mainly degraded by ECE1 and ECE1 has a major role in Aβ34 clearance.

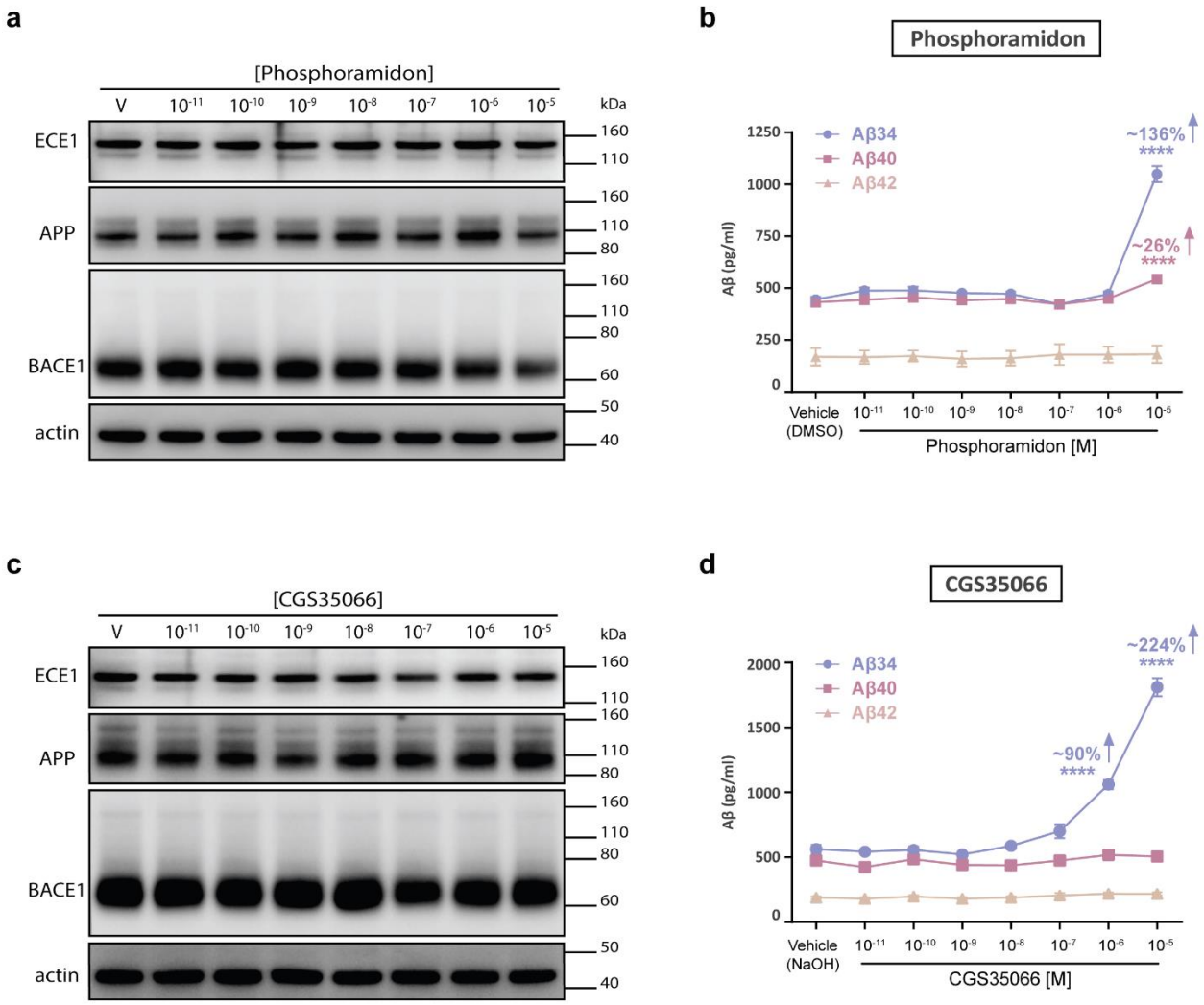

Figure 13: Pharmacological inhibition of proteases by Phosphoramidon (ECE1, MME and ACE) and by CGS35066 (ECE1 and MME) affected Aβ34 levels to a greater extent

Expression of ECE1, APP and BACE1 and Aβ levels were analyzed by Western blot and ELISA, respectively. Representative Western blots from 4 independent experiments where SH-SY5Y-BACE1 cells were treated with the protease inhibitor, either Phosphoramidon (a) or CGS35066 (c), at different concentrations ranging from 10^{-11} to 10^{-5} M. Quantification of absolute amounts of Aβ34, Aβ40, and Aβ42 after Phosphoramidon (b) or CGS35066 (d) treatment in cell media by ELISA. Percent changes in Aβ levels compared to the Vehicle condition are indicated. Bars and error bars indicate mean ± s.e.m. Dunnett's post-hoc tests were performed for pairwise comparisons; selected comparisons are highlighted ****$p < 0.0001$. (b) Aβ34, 1-WAY ANOVA, $F(7,24)=132.3$, $p < 0.0001$; Aβ40, 1-WAY ANOVA, $F(7,24)=13.23$, $p < 0.0001$; Aβ42, 1-WAY ANOVA, $F(7,24)=0.05029$, $p = 0.9998$, (d) Aβ34, 1-WAY ANOVA, $F(7,24)=128.0$, $p < 0.0001$; Aβ40, 1-WAY ANOVA, $F(7,24)=3.228$, $p = 0.0147$; Aβ42, 1-WAY ANOVA, $F(7,24)=1.570$, $p = 0.1924$.

`

2.4.Discussion

There is increasing evidence that Aβ clearance is as important as Aβ production to develop amyloid pathology. The focus of AD research has shifted towards an understanding of Aβ degradation, and the key players involved, i.e., ADEs. Many of the ADEs have been identified and characterized for their ability to degrade Aβ40 or Aβ42, either in *in vitro* or *in vivo* systems. However, there are conflicting results regarding their roles in AD and Aβ degradation. Since they were found decreased or increased in the brains of AD patients, it has remained unclear what their role in the degradation cascade is.

Here, we focused on Aβ34 as an important intermediate product in the degradation pathway in the context of the possibility that such proteases that can directly cleave Aβ40 and Aβ42 into non-toxic products might also be involved in Aβ34 degradation. We performed siRNA knockdowns of eight proteases in wild type and stably BACE1 overexpressing SH-SY5Y cells to compare their differential effects on Aβ34, Aβ40 and Aβ42. Here, the BACE1 overexpressing model served to mimic AD brain where higher amounts of BACE1 are found (Fukumoto et al., 2002, Holsinger et al., 2002, Li et al., 2004, Tyler et al., 2002, Yang et al., 2003) (Manuscript I). An increased enzymatic activity of BACE1 could boost Aβ34 production in such cells. Our previous studies showed that BACE1 produces Aβ34 in endo-lysosomal system; thus, we hypothesized that ECE1, Cat B and Cat D are good candidates for Aβ34 degradation. These proteases are active in endosomes and/or lysosomes (Eckman et al., 2001, Hsu et al., 2018, Westley and May, 1999) and have direct contact with the substrate, i.e., Aβ34. The possible roles of proteases in influencing Aβ34 levels would be either degradation of longer Aβ peptides into Aβ34 or degradation of Aβ34 itself. Upon protease knockdown, the former and the latter would yield either less or more Aβ34, respectively.

`

Comparing the effects of different proteases on Aβ34 peptides identified ECE1 as a major Aβ34 degrading enzyme in both BACE1 overexpressing and wild type cells with endogenous BACE1 levels. Elevated levels of Aβ34 were observed upon ECE1 knockdown likely because degradation of Aβ34 by ECE1 is impeded by ECE1 knockdown that preserves higher levels of Aβ34. To a lesser extent, MMP2 and MMP9 knockdowns had a similar effect on Aβ34 levels. However, we did not observe such effect in wild type cells that have low levels of Aβ34 compared to BACE1 overexpressing cells indicating that only ECE1 knockdown maintained Aβ34 levels above LLOD in wild type cells and allowed its quantification. Thus, we further examined effects of overexpression and pharmacological inhibition of ECE1.

Gradual ECE1 overexpression led to decreases in both Aβ34 and Aβ40 implying that both peptides may be recognized as substrates; however, Aβ34 levels responded already at a low amount of ECE1 expressed. This result suggests that Aβ34 is a preferred substrate for ECE1 proteolysis compared to Aβ40 and that in the presence of mixed Aβ pools consisting of Aβ34, Aβ40 and Aβ42, ECE1 primarily cleaves Aβ34. Pharmacological inhibition of ECE1 with two different protease inhibitors, namely PA and CGS35066 yielded increased levels of both Aβ34 and Aβ40 in the presence of PA. We detected a significant increase of Aβ34 levels only in the presence of CGS35066. Unlike PA that inhibits MME, ECE1 and ACE (Kukkola et al., 1995), CGS35066 inhibits ECE1 and MME and is >100-fold more potent against ECE1 (Trapani et al., 2000). Therefore, increase in Aβ40 levels upon PA treatment could also be explained by MME and/or ACE inhibition. On the other hand, ECE1 inhibition solely affected Aβ34 levels, further suggesting ECE1 as an Aβ34 degrading enzyme.

Unlike other proteases, Cat B knockdown led to a decrease in Aβ34 and Aβ40 levels. This could mean that Cat B is cleaving longer Aβ species into Aβ34 and/or Aβ40, and upon its

`

knockdown, this cleavage is disrupted so there is less Aβ34 and Aβ40. Another possible explanation could be that Cat B effects are more upstream cleaving APP and influences the production of Aβ species. Upon its knockdown, this pathway is blocked resulting in less Aβ34 and Aβ40.

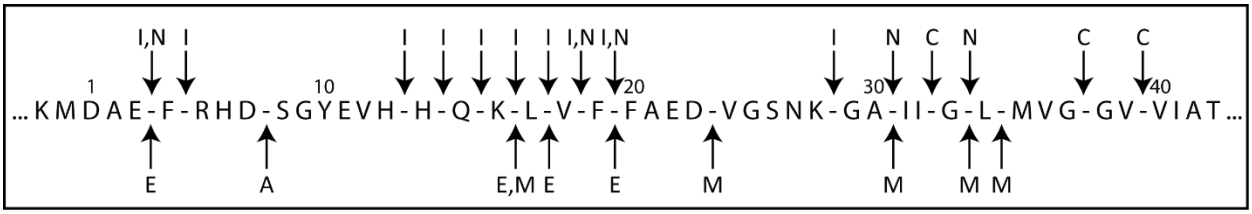

Figure 14: Cleavage sites of Aβ degrading proteases

Reported cleavage sites on Aβ40 or Aβ42 by different proteases. A = angiotensin converting enzyme, C = Cathepsins, E = endothelin converting enzyme, I = insulin degrading enzyme, M = matrix metalloproteinases, and N = neprilysin.

Specific cleavage sites within the Aβ sequence have been identified by mass spectrometry for most of these enzymes (Hampel et al., 2010, Macours et al., 2004, Yan et al., 2006) (Figure 14). As an example, MMP9 has more than five cleavage sites on Aβ42, including the site that generates Aβ34 (Yan et al., 2006). Although expected cleavage sites in Aβ40 and Aβ42 by ECE1 are clustered around Lys^{16} and Phe^{20}, a biochemical analysis to map Aβ34 cleavage sites of ECE1 and to identify possible other cleavage products, especially when monomers are compared with oligomers, will be important to improve our understanding of ECE1's role in Aβ degradation. Given that Aβ34 is suggested as a biomarker for prodromal AD and its levels are lower in body fluids compared to Aβ40 and Aβ42, the enzymes involved in Aβ34 metabolism as well as the cleavage products resulting from its degradation, such as Aβ17, could facilitate the development of novel approaches that lead to the discovery of new biomarkers in CSF and blood/plasma.

`

2.5.Materials and Methods

2.5.1. Plasmids and siRNAs

A human ECE1 construct (full length; pTT3; Addgene, plasmid #53361) was used for transient overexpression in SH-SY5Y cells. Mock control in pTT3 plasmid backbone was used. For creating stably BACE1 expressing SH-SY5Y cells, human full length BACE1 (isoform A) in the mammalian expression vector pCEP4, Hygro (Invitrogen) were used. For knockdown, siGENOME non-Targeting siRNA Pool #1 (D-001206-13-05), SMARTpool siGENOME ECE1 (M-005857), IDE (M-005899), Cat B (M-003649), Cat D (M-004266), MMP2 (M-005959), MMP9 (M-005970), ACE (M-005754), and MME (M-005112) were used.

2.5.2. Cell Culture

Wild-type human neuroblastoma (SH-SY5Y) cells (DSMZ No. ACC209; DSMZ, Braunschweig, Germany) and SH-SY5Y cells stably overexpressing BACE1 were grown in DMEM/F12 (10% fetal bovine serum (FBS), 2 mM L-glutamine, 1 mM sodium pyruvate) in a humidified incubator at 37°C 5% CO_2. Stable cell lines were selected with 250 µg/ml Hygromycin B (Milipore). For protease knockdown experiments, cells were seeded on 6-well plates (Fisher). 24 hours later, cells were treated with either control or protease targeting siRNAs (concentration of the siRNA indicated in the figures) by using RNAiMax according to the protocol provided by the manufacturer (Invitrogen). 72 hours after the treatment, cells were harvested. For ECE1 overexpression experiments, cells were seeded on 6-well plates (Fisher). 24 hours later, cells were transfected with FuGENE HD (Promega). 72 hours after the transfection, cells were harvested. For Phosphoramidon (PA, Sigma-Aldrich, R7386) experiment, cells were seeded on 6-well plates (Fisher). PA was dissolved in DMSO and compared to vehicle treatment (1:1000 = 0.1 %). 24 hours later, cells were treated with the inhibitor. 72 hours after the transfection, cells were

`

harvested. The same experimental setup was used for CGS35066 inhibitor (Biotechne, 2512) except that CGS35066 was dissolved in NaOH and NaOH used as vehicle treatment.

2.5.3. Sample Preparation

For all experiments performed, cells were harvested on ice. Conditioned media were centrifuged at 2000 rpm at 4°C for 10 minutes and the supernatants were used for Aβ34, Aβ40 and Aβ42 quantification by ELISA. Cells were washed with cold PBS and lysed with Whole Cell Extract Buffer (WCE) (25 mM HEPES (pH 7.7), 0.3 M NaCl, 1.5 mM $MgCl_2$, 0.2 mM ethylenediaminetetraacetic acid, 0.1% Triton-X-100, 0.5 mM dithiothreiol, 4 mM NaF, 0.1 mM Na_3VO_4, 1 mM PMSF, Complete Protease Inhibitor Coctail (Roche)) at 4°C for 60 mins. Cell lysates were centrifuged at 10000 rpm at 4°C for 15 minutes for the removal of nuclear material and the supernatants were used to detect protein levels by Western Blot.

2.5.4. Western Blot Analysis

Sample preparation was performed according to the protocol provided by Invitrogen. After LDS loading buffer and 2-Mercaptoethanol were added to the cell lysates, the samples were heated to 70°C for 10 mins for protein solubilization and denaturation. 4-12% Bis-Tris gradient gels (Invitrogen) were used for protein separation. Proteins were transferred to 0.45 μm nitrocellulose (Biorad) or polyvinylidene difluoride (PVDF) (Milipore) membranes at 400 mA and at 4°C for 2.5 hours. Proteins were detected with the antibodies listed below. The primary and secondary antibodies were used in phosphate buffered saline. Signals were recorded on ImageQuant LAS 600 (GE Healthcare Life Sciences).

The primary antibodies used for Western Blot analysis were the following: anti-ECE1 in 1:1000 dilution (ab71829), anti-IDE in 1:1000 dilution (ab32216), anti-Cat B in 25 μg/10 ml dilution (ab58802), anti-Cat D in 1:1000 dilution (ab6313), anti-MMP2 in 1:1000 dilution

`

(ab97779), anti-MMP9 in 1:1000 dilution (ab38898), and anti-ACE in 10 μg/10 ml dilution (ab270712) (all from Abcam), anti-ECE1 1:1000 dilution (Proteintech, 26088-1-AP), anti-BACE1 1:2000 dilution (monoclonal D10E5, Cell Signaling), anti-actin 1:5000 dilution (monoclonal mab1501, Millipore), anti-APP ectodomain 22C11 1:10,000 dilution (Millipore).

The secondary antibodies were the following: anti-mouse- and anti-rabbit-horseradish peroxidase 1:10,000 dilution (Promega).

ImageJ was used to quantify Western Blots and protein levels were normalized to actin.

2.5.5. Sandwich-based Enzyme-Linked Immunosorbent Assay (ELISA)

As capture antibodies, monoclonal anti-Aβ34 (226), anti-Aβ40 (G2-10) or anti-Aβ42 (G2-13) and as detection antibody, W02-biotin were used. The protocol stated in Manuscript I was performed for all ELISA measurements.

2.5.6. Statistical Analysis

For all experiments, different conditions were analyzed by one factor ANOVA (between subject design). Dunnet's or Tukey's post-hoc tests were performed for pairwise comparisons. GraphPad Prism 5 was used to run statistical analysis.

`

2.6.Authors Contributions

All authors mentioned in the manuscript have agreed for authorship, read and approved the manuscript. IU and GM designed research; IU and SCA designed and prepared the plasmids; IU performed research; IU and GM analyzed data; IU and GM wrote the paper.

`

2.7.Acknowledgements

This study was funded by Canadian Institute of Health Research (CIHR MOP-133411; CIHR/Baycrest CNA-163902); Australia National Health and Medical Research Council (NHMRC/Edith Cowan University); The Natural Sciences and Engineering Research Council of Canada (NSERC RGPIN-2015-04774) and The Canada Research Chairs Program (CRC-Multhaup-235976).

`

2.8.Supplementary Figures

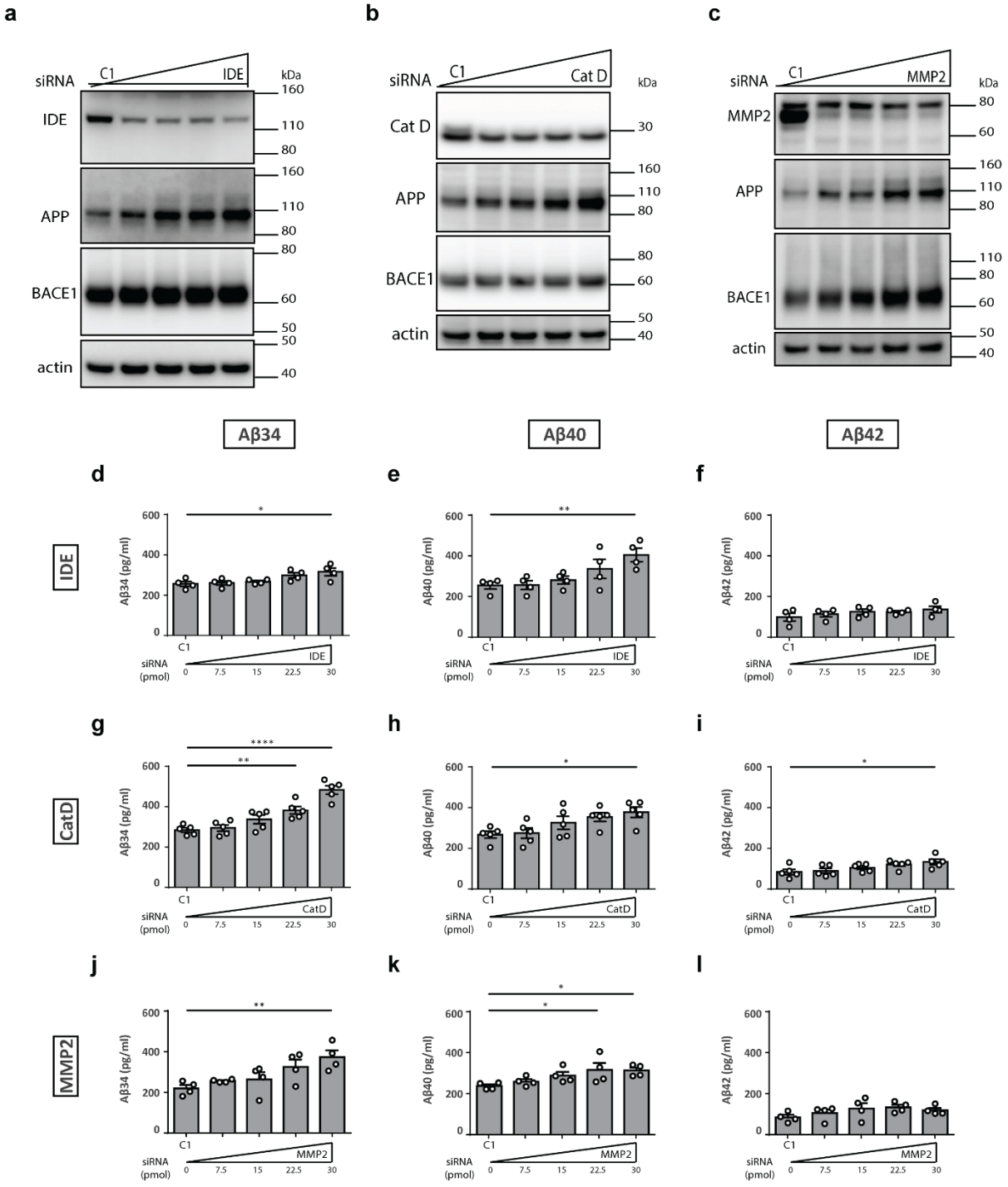

Supplementary Figure 4: Changes in Aβ levels upon IDE, Cat D and MMP2 knockdowns

Representative Western blots from 4 independent experiments for IDE overexpression (a), representative Western blots from 5 independent experiments for Cat D overexpression (b), and representative Western blots from 4 independent experiments for MMP2 overexpression (c) in SH-SY5Y-BACE1 cells. Absolute amounts of Aβ34 (d), Aβ40 (e), and Aβ42 (f) upon IDE knockdown, absolute amounts of Aβ34 (g), Aβ40

`

(h), and Aβ42 (i) upon Cat D knockdown, absolute amounts of Aβ34 (j), Aβ40 (k), and Aβ42 (l) upon MMP2 knockdown in cell media by ELISA. Bars and error bars indicate mean ± s.e.m. Dunnett's post-hoc tests were performed for pairwise comparisons; selected comparisons are highlighted ****$p < 0.0001$, **$p < 0.01$, *$p < 0.05$. (d) Aβ34, 1-WAY ANOVA, $F(4,15)=4.007$, $p = 0.0209$, (e) Aβ40, 1-WAY ANOVA, $F(4,15)=4.682$, $p = 0.0119$, (f) Aβ42, 1-WAY ANOVA, $F(4,15)=1.033$, $p = 0.4223$, (g) Aβ34, 1-WAY ANOVA, $F(4,20)=20.20$, $p < 0.0001$, (h) Aβ40, 1-WAY ANOVA, $F(4,20)=3.779$, $p = 0.0190$, (i) Aβ42, 1-WAY ANOVA, $F(4,20)=3.121$, $p = 0.0379$, (j) Aβ34, 1-WAY ANOVA, $F(4,15)=4.703$, $p = 0.0117$, (k) Aβ40, 1-WAY ANOVA, $F(4,15)=3.119$, $p = 0.0470$, (l) Aβ42, 1-WAY ANOVA, $F(4,15)=1.355$, $p = 0.2957$.

`

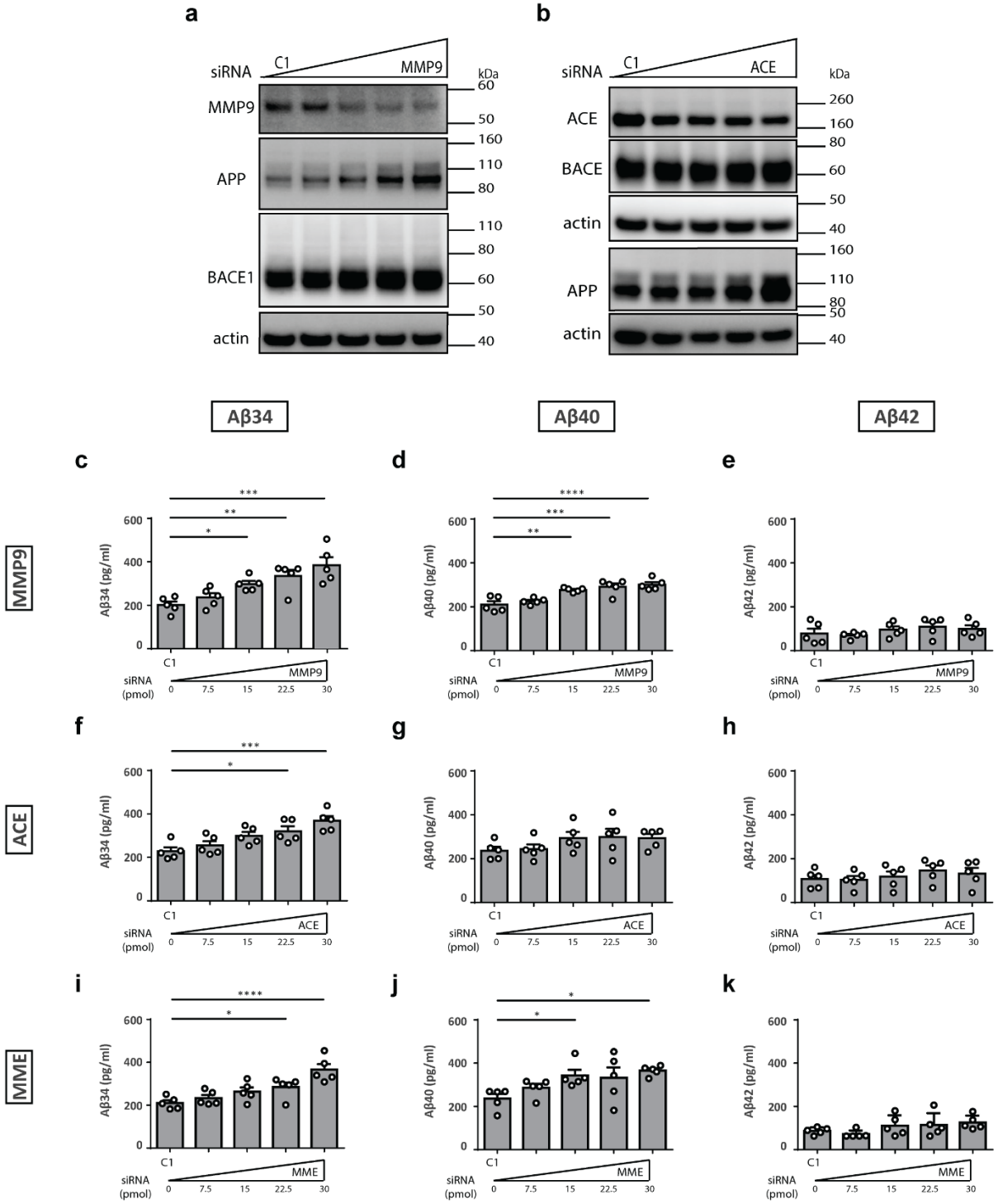

Supplementary Figure 5: Changes in Aβ levels upon MMP9, ACE and MME knockdowns

Representative Western blots from 5 independent experiments for MMP9 overexpression (a), and for ACE overexpression (b) in SH-SY5Y-BACE1 cells. Absolute amounts of Aβ34 (c), Aβ40 (d), and Aβ42 (e) upon MMP9 knockdown, absolute amounts of Aβ34 (f), Aβ40 (g), and Aβ42 (h) upon ACE knockdown, absolute amounts of Aβ34 (i), Aβ40 (j), and Aβ42 (k) upon MME knockdown in cell media by ELISA. Bars and

`

error bars indicate mean ± s.e.m. Dunnett's post-hoc tests were performed for pairwise comparisons; selected comparisons are highlighted ****$p < 0.0001$, ***$p < 0.001$, **$p < 0.01$, *$p < 0.05$. (c) Aβ34, 1-WAY ANOVA, $F(4,20)=8.625$, $p = 0.0003$, (d) Aβ40, 1-WAY ANOVA, $F(4,20)=12.72$, $p < 0.0001$, (e) Aβ42, 1-WAY ANOVA, $F(4,20)=0.9287$, $p = 0.4671$, (f) Aβ34, 1-WAY ANOVA, $F(4,20)=7.649$, $p = 0.0007$, (g) Aβ40, 1-WAY ANOVA, $F(4,20)=1.369$, $p = 0.2802$, (h) Aβ42, 1-WAY ANOVA, $F(4,20)=0.6469$, $p = 0.6355$, (i) Aβ34, 1-WAY ANOVA, $F(4,20)=9.297$, $p = 0.0002$, (j) Aβ40, 1-WAY ANOVA, $F(4,20)=3.362$, $p = 0.0293$, (k) Aβ42, 1-WAY ANOVA, $F(4,20)=1.752$, $p = 0.1783$.

`

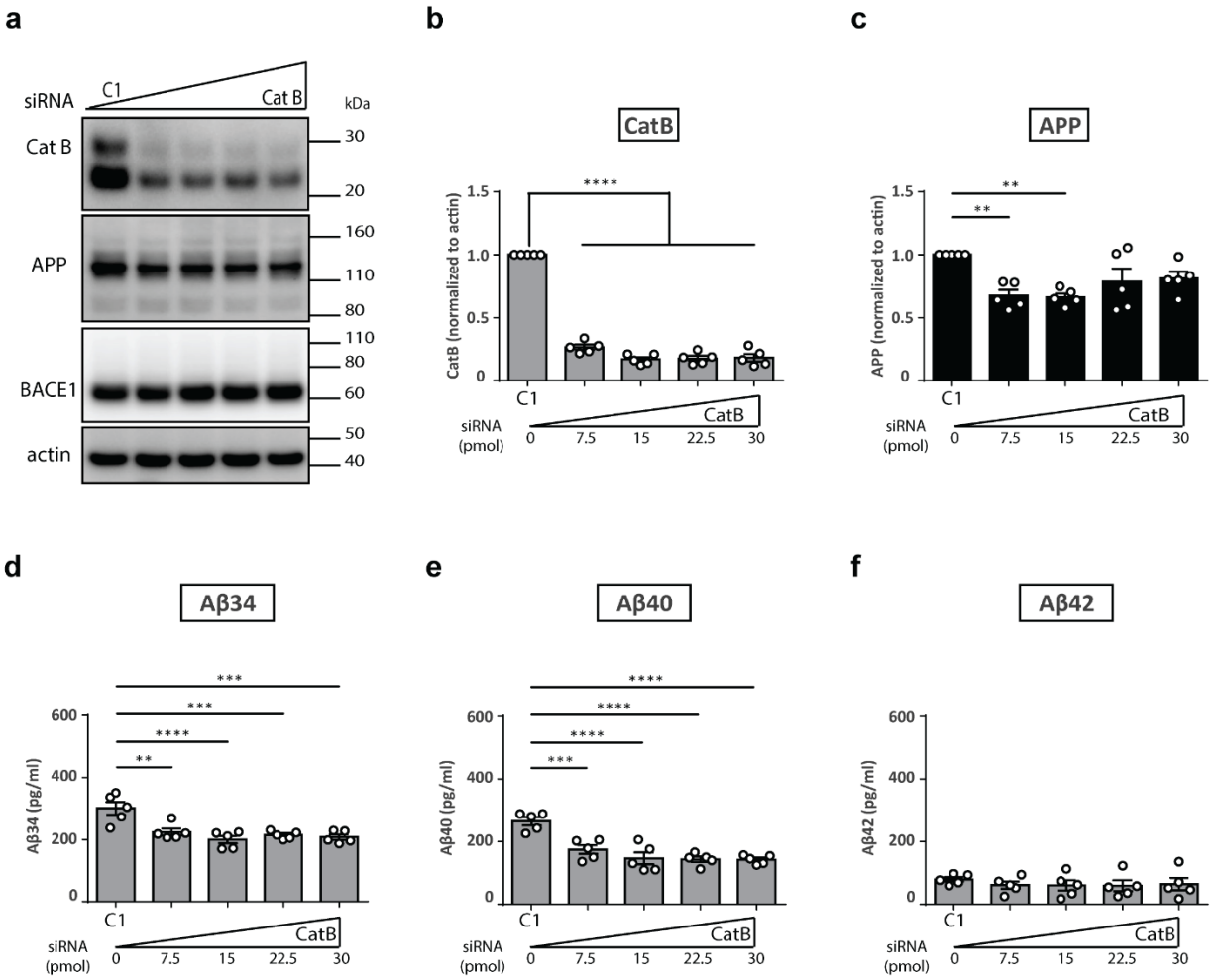

Supplementary Figure 6: Unlike other protease knockdowns, Aß levels decreased with Cat B knockdown

Expression of Cat B and APP and Aβ levels were analyzed by Western blot and ELISA, respectively. Representative Western blots from 5 independent experiments for Cat B knockdown titration in SH-SY5Y-BACE1 cells (a). Quantification of relative amounts of Cat B (b) and of APP (c), and absolute amounts of Aβ34 (d), Aβ40 (e), and Aβ42 (f) in cell media by ELISA. Bars and error bars indicate mean ± s.e.m. Dunnett's post-hoc tests were performed for pairwise comparisons; selected comparisons are highlighted ****$p < 0.0001$, ***$p < 0.001$, **$p < 0.01$. (b) Cat B, 1-WAY ANOVA, $F(4,20)=314.0$, $p < 0.0001$, (c) APP, 1-WAY ANOVA, $F(4,20)=5.550$, $p = 0.0036$, (d) Aβ34, 1-WAY ANOVA, $F(4,20)=10.27$, $p = 0.0001$, (e) Aβ40, 1-WAY ANOVA, $F(4,20)=16.30$, $p < 0.0001$, (f) Aβ42, 1-WAY ANOVA, $F(4,20)=0.3056$, $p = 0.8708$.

`

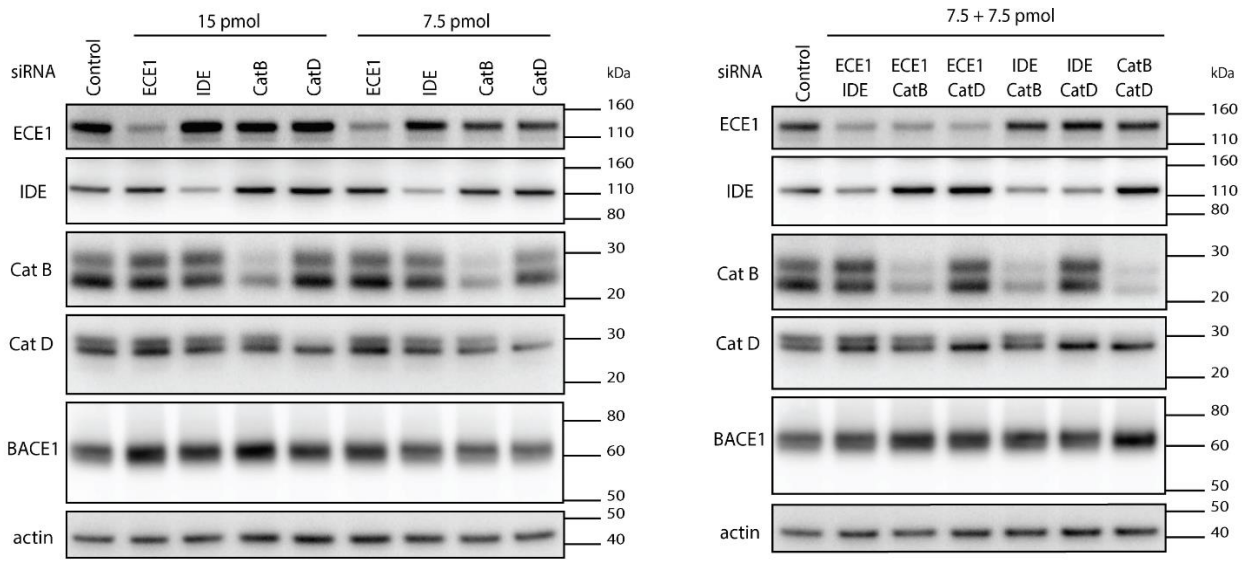

Supplementary Figure 7: Changes in protein levels of proteases with different knockdown conditions

Representative Western blots from 6 independent experiments for combinatorial knockdowns in SH-SY5Y-BACE1 cells.

`

Chapter III :

GENERAL DISCUSSION

`

In this thesis, we have explored the life cycle of Aβ34 by studying the proteases that have key roles in the production and degradation of the peptide at the molecular and the cellular level: BACE1, γ-secretase, ADEs, and the activity of such enzymes in the context of their environment.

In Manuscript I, we presented novel findings on BACE1's dual function, because these are the basis to find ways to modulate the balance between amyloidogenic (Aβ production) and amyloidolytic (Aβ clearance) activities. For example, we found that the substrate to enzyme ratio affect this balance. In this section, I will discuss how this balance or imbalance could explain failed BACE1 inhibitor clinical trials and how it could shed light on the discovery of new BACE1 modulators to target AD. Furthermore, we have presented results indicating that PS2 containing γ-secretase provides substrates for BACE1's amyloidolytic activity and processing of Aβ species into Aβ34 takes place in the endo-lysosomal system. I will discuss the current emphasis on attempts to inhibit or modulate PS1 and PS2 which are discussed in the AD field, and I will point out the clinical relevance of PS2 to Aβ degradation and AD progression based on my findings.

In Manuscript II, we presented results that are important to understand which proteases and how these proteases influence the Aβ34 metabolism. Strikingly, we identified ECE1 as the major enzyme involved in Aβ34 clearance. I will discuss the potential use of ECE1 and other ADEs for biomarker development or improvement and the importance of Aβ34 as an intermediate degradation product for an early AD diagnosis.

`

1. BACE1, γ-secretase and Aβ34

1.1.BACE1 in Clinical Trials and Open Questions

Aβ peptides are generated in the amyloidogenic pathway which starts with the cleavage of APP by BACE1. Since BACE1 is considered as the rate limiting step for Aβ production resulting in the formation of amyloid plaques, and since BACE1 knockout mice did not have major morphological or behavioral deficits except hypomyelination in peripheral nervous system (Cai et al., 2001, Hu et al., 2006), BACE1 inhibition has been investigated as AD treatment. So far, all BACE1 inhibitors were discontinued in clinical trials; although they reduce Aβ burden and plaque load, they fail to improve cognitive functioning and/or have severe side effects (Hampel et al., 2021, Kennedy et al., 2016, Kumar et al., 2018). Incomplete knowledge of BACE1's biology and physiological functions as well as its downstream pathways might be the reason for such failures.

BACE1 can cleave multiple substrates that have functions in neuronal migration, myelination, synaptic plasticity, axon guidance, and cell adhesion (Hampel et al., 2021). Complete inhibition of BACE1 blocks processing of many other substrates in addition to APP and leads to unwanted side-effects (Barão et al., 2016, McDade et al., 2021). Our work now adds the amyloidolytic activity of BACE1 to the picture. Previous clinical trials and pre-clinical research activities have not considered that inhibition of amyloidolytic activity of BACE1 (Aβ clearance) might be a major reason for failure. Mouse studies showed that there is no linear relationship between BACE1 levels and Aβ40 and Aβ42 production (Georgievska et al., 2015). BACE1 inhibition seems to increase some Aβ species in the CSF (Mattsson et al., 2012) while reduction of BACE1 activity did not necessarily lower Aβ levels or amyloid burden (Devi and Ohno, 2013). Such observations could not be explained until now without understanding the role of BACE1 in amyloid clearance.

`

The work from our laboratory shows that BACE1 acts as an ADE and degrades Aβ species, proven for Aβ40 and Aβ42, into non-amyloidogenic Aβ34, the process called amyloidolytic activity of BACE1 (Liebsch et al., 2019). Our current work (Manuscript I) shows that BACE1 inhibition leads to distinct results under enzyme or substrate surplus. When the substrate, APP, is in abundance, BACE1 inhibition lowers Aβ40 and Aβ42 levels. However, when the enzyme, BACE1, is in abundance, BACE1 inhibition elevates Aβ40 and Aβ42 levels. Conclusively, pharmacological inhibition of BACE1 acts first on amyloidolytic activity of BACE1 depending on the environment and the enzyme to substrate ratio. In Manuscript I, we show that in temporal cortex homogenates from AD patients, there are higher levels of BACE1 protein compared to healthy controls, which could point to a defense reaction based on the need for amyloidolytic activity in response to increased Aβ production. Thus, if these AD patients are treated with BACE1 inhibitors, a slowdown of clearance could cause an increase in toxic Aβ levels that might further accumulate and finally lead to worsening of symptoms.

Today, inconsistent results and futility of the BACE1 inhibitors suggest that BACE1 inhibition is more complex and goes beyond APP cleavage by BACE1. The possibility that inhibitors may preferentially inhibit amyloidogenic or amyloidolytic activity suggest that BACE1 inhibitors could now be tested for specifically targeting amyloidogenic activity of BACE1. An ideal BACE1 inhibitor without so-called “paradoxical” effects would lower Aβ production by inhibiting amyloidogenic cleavage of APP and at the same time would enhance Aβ clearance by boosting Aβ degradation of potentially aggregating and toxic Aβ species into non-aggregating Aβ34. Also, the concentration dependency of the inhibition might be crucial to modulate the Aβ40/ Aβ42 and Aβ34/Aβ42 ratio. Therefore, we suggest investigating concentration dependency and substrate specificity of BACE1 inhibitors.

`

1.2.Presenilin 1 and Presenilin 2 Mutations and Their Contributions to AD

Genetic mutations associated with FAD are found in either *APP* (chromosome 21), *PSEN1* (chromosome 14) or *PSEN2* (chromosome 1) (Levy-Lahad et al., 1995, Rogaev et al., 1995, Sherrington et al., 1995, St George-Hyslop et al., 1987, Tanzi et al., 1987). More than 300 mutations in *PSEN1* and about 90 mutations in *PSEN2* have been reported (https://www.alzforum.org/mutations/psen-1 and https://www.alzforum.org/mutations/psen-2). Beyond its involvement in Aβ production as the catalytic subunit of the γ-secretase complex, PS has additional functions such as regulation of calcium homeostasis, apoptosis and neural differentiation (Bonds et al., 2015, Lazarov and Marr, 2010, Leissring et al., 2001, Leissring et al., 2000, Wolozin et al., 1996).

Most of the mutations in *PSEN1* or *PSEN2* genes are heterozygous mutations that change Aβ metabolism in the brain and drive amyloidosis in FAD patients (Weggen and Beher, 2012). Studies conducted with transfected cells, transgenic mice and primary cells from FAD patients showed that almost all of these mutations increase the Aβ42/Aβ40 ratio; therefore, they were suggested to be gain-of-function mutations (Weggen and Beher, 2012). However, it has been reported that processing of other substrates of γ-secretase, e.g., Notch, is reduced in the same models, indicating that these mutations are loss-of-function (Baumeister et al., 1997, Song et al., 1999). APP cleavage by γ-secretase occurs in a stepwise manner producing Aβ peptides in two alternative pathways that converge at Aβ34: Aβ51 > 48 > 45 > 42 > 38 > 34 and Aβ49 > 46 > 43 > 40 > 37 > 34 (Olsson et al., 2014, Takami et al., 2009). It is possible that *PSEN1/2* mutations reduce the trimming of APP (carboxypeptidase-like activity) by reducing stability of the complex or by reducing the affinity of the enzyme for shorter Aβ species leading to accumulation of longer Aβ forms. Additionally, these mutations could favor the initial cleavage site and processing that

`

generates Aβ42 over the one generating Aβ40, both of which could explain the increase in Aβ42/Aβ40 ratio.

Mutations in both *PSEN1* and *PSEN2* (e.g., PSEN1-M146L, PSEN1-L166P, PSEN1-ΔExon9, PSEN2-N141I) have similar effects on the Aβ42/Aβ40 ratio (Weggen and Beher, 2012); however, as there are more *PSEN1* mutations reported and as the homozygous *PSEN1-null* mice is lethal (Donoviel et al., 1999), there has been a strong emphasis on PS1 in the AD field. Our work reveals that PS2 is equally important since PS2-γ-secretase is involved in Aβ clearance by providing substrates for BACE1's amyloidolytic activity that results in the production of Aβ34 (Manuscript I) (Figure 15). PS2 localization is restricted to endosomes and lysosomes and PS2 contributes to the intracellular Aβ pool. FAD-linked *PSEN2* mutations, such as PSEN2-N141I, increase the production of intracellular Aβ42 (Sannerud et al., 2016). In various transgenic AD mouse models, it has been reported that intraneuronal Aβ accumulation precedes extracellular amyloid plaque formation (Bayer and Wirths, 2010, Lee et al., 2022). It is possible that disrupted cellular homeostasis and lysosomal acidification in the disease state enhances PS2-γ-secretase processing of APP leading to more intracellular Aβ42 production which overwhelms amyloidolytic activity of BACE1 ultimately causing intracellular Aβ42 accumulation that spreads extracellularly.

`

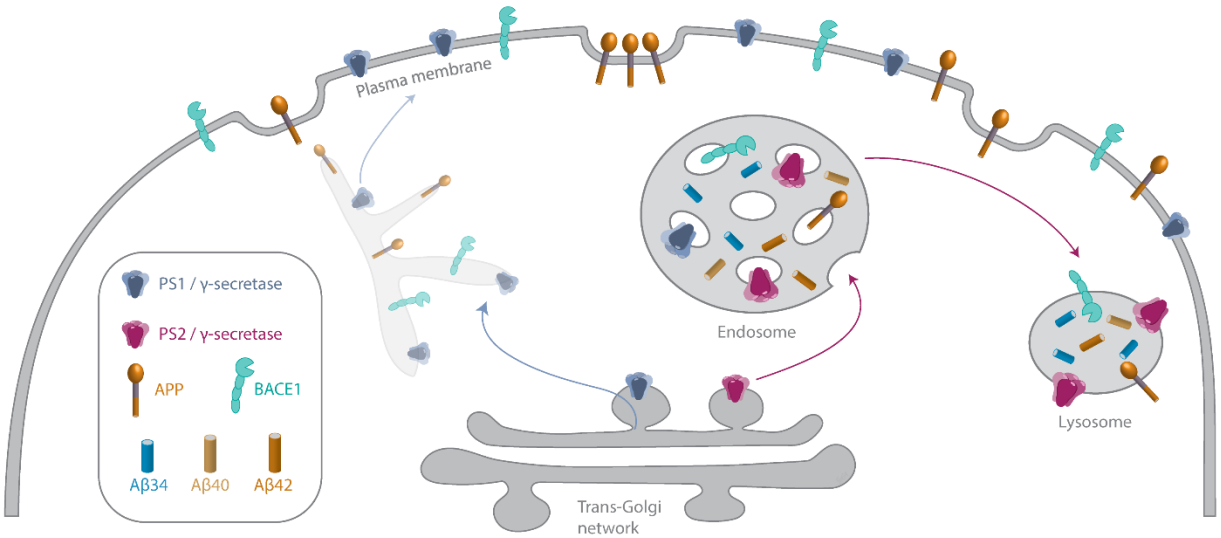

Figure 15: Cellular scheme for amyloidolytic activity of BACE1

APP, BACE1 and γ-secretase are produced in the trans-Golgi network and trafficked to different compartments in the cell guided by adaptor proteins. PS1-γ-secretase is more broadly distributed in the cell including plasma membrane whereas localization of PS2-γ-secretase is restricted to late endosomes and lysosomes. BACE1 has its highest activity in the endo-lysosomal system. Therefore, endosomes and lysosomes provide an acidic environment for APP processing by BACE1 and PS2-γ-secretase, which yield longer Aβ species that are further degraded there by BACE1 into Aβ34.

Over decades, γ-secretase has also been a target to treat AD. Numerous γ-secretase inhibitors (GSIs) and γ-secretase modulators (GSMs) were tested in clinical trials. GSMs evolved as a safer approach (Kukar and Golde, 2008). Unlike GSIs, GSMs do not interfere with the normal processivity of other γ-secretase substrates but interact with γ-secretase through allosteric binding site to APP-C99 to prevent Aβ deposition, lower the Aβ42:Aβ40 ratio and increase the processivity towards lower molecular weight Aβ species (Bursavich et al., 2016). However, due to limited potency, bioavailability, and central nervous system penetration, GSMs were abandoned (Eriksen et al., 2003, Green et al., 2009, Kumar et al., 2018). Such GSMs were not designed to specifically target PS1 or PS2. Consequently, a possible approach would be to design PS2 specific γ-secretase-targeting compounds that enhance trimming of APP into non-amyloidogenic Aβ species, such as Aβ34. Our work successfully aimed to dissect differential roles of PS1 and PS2 in Aβ metabolism

`

while it would be important as a next step to test various *PSEN* mutations in both *in vitro* and *in vivo* models to confirm the influence of PS2, in comparison to PS1, on earliest intracellular Aβ oligomerization. Overall, this work highlights the neglected role and importance of PS2 in Aβ life cycle, failure of which could lead to earliest biochemical changes in AD.

Targeting Aβ metabolism to prevent or slow down the progression of AD should include more than one target, e.g., both BACE1 and γ-secretase. Enhancing PS2-γ-secretase-mediated Aβ production that confines Aβ production in endosome/lysosomes and manipulating the dual role of BACE1 in a way to boost its amyloidolytic activity in endosome/lysosomes could increase Aβ clearance and could prevent both intracellular and extracellular Aβ accumulation. Clinical trials with Aβ-directed monoclonal antibodies that target Aβ oligomers and fibrils showed that repeated dosage is required to constantly remove Aβ aggregates (Sevigny et al., 2016). These antibodies target extracellular Aβ but not intracellular Aβ. One possibility is to block intracellular aggregation of Aβ by small molecules that can pass through plasma membrane and interact with Aβ. Overall, the treatments should also target intracellular Aβ accumulation to avoid further extracellular amyloid aggregations.

`

2. Aβ Clearance, ADEs, and Aβ34

Genetic studies and current biomarker research provide evidence that the imbalance between Aβ production and clearance plays a critical role in AD pathology and the accumulation of Aβ deposits in the brain begins decades before the clinical diagnosis of AD (Hanseeuw et al., 2019, Hardy and Higgins, 1992, Jack Jr et al., 2018, Jack Jr et al., 2019, Karran et al., 2011). Aβ clearance pathways include sequential cleavage of APP by γ-secretase, amyloidolytic cleavage of aggregation prone Aβ species by BACE1 and proteolytic degradation of Aβ species into Aβ fragments or non-aggregating Aβ forms by ADEs (Figure 16).

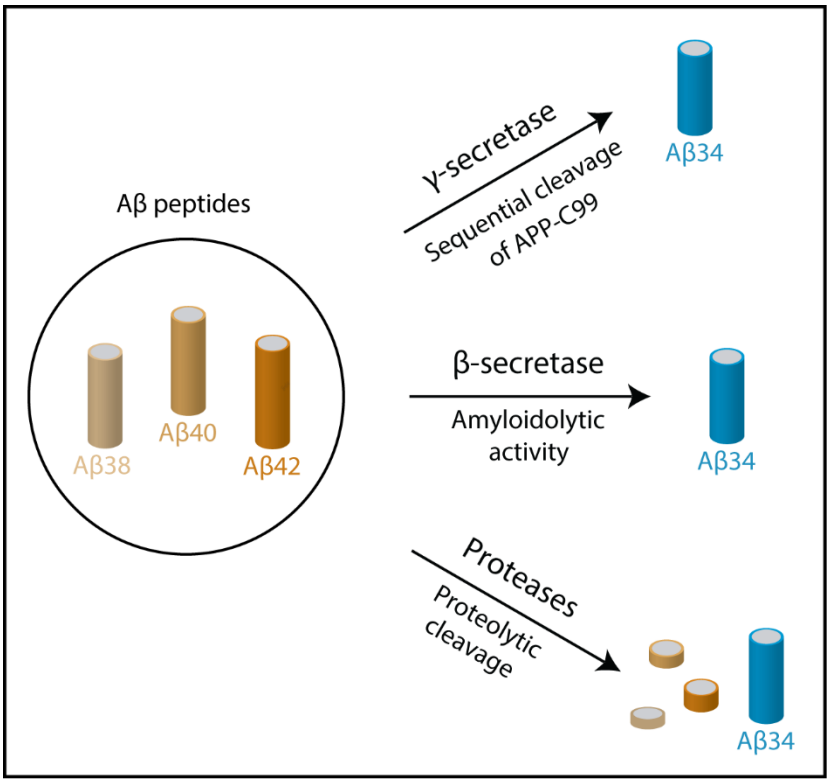

Figure 16: Aβ clearance pathways leading to generation of Aβ34

Aβ34 can be generated through several pathways including sequential cleavage of APP-C99 by γ-secretase, amyloidolytic cleavage of Aβ species by BACE1 and proteolytic degradation of Aβ species by several proteases.

`

Many studies have been conducted with cell lines, transgenic mouse models, post-mortem AD tissue and AD patients to unravel the roles of specific ADEs. Although some yielded promising results, for most of the ADEs, there is no consensus on how these proteases contribute to the disease state or how their protein and activity levels change with AD progression. Our study provides evidence that ECE1, which is the enzyme predominantly responsible for producing active Endothelin-1, also possesses a major role in Aβ34 degradation.

We showed that ECE1 is the major Aβ34 degrading enzyme with little or no effect on Aβ40 and Aβ42. Although the same result is obtained under both endogenous and BACE1 overexpression systems, cell lines do not fully recapitulate the disease state. Therefore, the next step is to dissect the roles of ECE1 in *in vivo* systems such as transgenic mouse models or human derived induced pluripotent stem cells. Revealing ECE1 cleavage sites on Aβ34 is as important as its effect on Aβ34 levels. Identification of the full spectrum of Aβ species that are generated as a result of Aβ34 degradation by ECE1 will improve the understanding of Aβ clearance pathways. Therefore, further studies will unravel cleavage sites on Aβ34 and cleavage products of Aβ34 degradation by ECE1.

Investigating the roles of ECE1 and cleavage products will aid the biomarker research and the development of novel tools used for early diagnosis of AD. Aβ34 has a potential to serve as an early biomarker for AD progression; however, its levels are lower in body fluids compared to other biomarkers of AD, such as Aβ40 and Aβ42. Treatment of body fluid samples with ECE1 inhibitors could impede rapid degradation of Aβ34 after sampling and increase its levels that is determined by immunoassays. Furthermore, Aβ34 is a meta-stable intermediate; therefore, if the cleavage products of Aβ34 are more stable, this study could pave the way to identify new biomarkers.

`

3. Concluding Remarks

Although the underlying cause of protein deposition in AD remains unclear, neurodegeneration is believed to be influenced by the dysregulation of protein metabolism, either/both through increased production or/and decreased clearance of Aβ peptides. Results of my projects provide novel explanations and descriptions to molecular pathways involving Aβ34, including the dual role of BACE1, and roles of PS2-γ-secretase, and ECE1.

The scientific evidence presented in this thesis supports that BACE1 is involved in both Aβ production that ultimately leads to formation of amyloid plaques and Aβ clearance that leads to conversion of toxic aggregation prone Aβ species into non-amyloidogenic Aβ34 and that imbalance between these two activities could be the explanation for the failure of BACE1 inhibitors in clinical trials. Our finding that PS2-γ-secretase in endo-lysosomal compartments provides substrates for amyloidolytic cleavage by BACE1 emphasizes a novel role for PS2 in Aβ clearance. Furthermore, our study identifies a novel role for ECE1 as the major Aβ34 degrading enzyme.

My thesis highlights the complex and highly dynamic nature of Aβ species in the brain and shows that manipulating this system towards enhanced clearance or manipulating intracellular Aβ levels is possible. Overall, revealing the life cycle of Aβ34 including the enzymes involved in AD will assist in the search for novel AD biomarkers, providing a better understanding of the molecular processes of AD pathogenesis, as well as facilitating the discovery of novel pathways and therapeutic targets.

`

REFERENCES

ACQUATI, F., ACCARINO, M., NUCCI, C., FUMAGALLI, P., JOVINE, L., OTTOLENGHI, S. & TARAMELLI, R. 2000. The gene encoding DRAP (BACE2), a glycosylated transmembrane protein of the aspartic protease family, maps to the down critical region. *FEBS letters,* 468**,** 59-64.

AHMAD, M., TAKINO, T., MIYAMORI, H., YOSHIZAKI, T., FURUKAWA, M. & SATO, H. 2006. Cleavage of amyloid-β precursor protein (APP) by membrane-type matrix metalloproteinases. *Journal of biochemistry,* 139**,** 517-526.

ALBERT, M. S., DEKOSKY, S. T., DICKSON, D., DUBOIS, B., FELDMAN, H. H., FOX, N. C., GAMST, A., HOLTZMAN, D. M., JAGUST, W. J. & PETERSEN, R. C. 2011. The diagnosis of mild cognitive impairment due to Alzheimer's disease: recommendations from the National Institute on Aging-Alzheimer's Association workgroups on diagnostic guidelines for Alzheimer's disease. *Alzheimer's & dementia,* 7**,** 270-279.

ALLINQUANT, B., HANTRAYE, P., MAILLEUX, P., MOYA, K., BOUILLOT, C. & PROCHIANTZ, A. 1995. Downregulation of amyloid precursor protein inhibits neurite outgrowth in vitro. *The Journal of cell biology,* 128**,** 919-927.

ALONSO, A. D. C., GRUNDKE-IQBAL, I. & IQBAL, K. 1996. Alzheimer's disease hyperphosphorylated tau sequesters normal tau into tangles of filaments and disassembles microtubules. *Nature medicine,* 2**,** 783-787.

ALONSO, A. D. C., ZAIDI, T., NOVAK, M., GRUNDKE-IQBAL, I. & IQBAL, K. 2001. Hyperphosphorylation induces self-assembly of τ into tangles of paired helical filaments/straight filaments. *Proceedings of the National Academy of Sciences,* 98**,** 6923-6928.

ALZHEIMER, A. 1907. Über eine eigenartige Erkrankung der Hirnrinde Allgemeine Zeitschrift fur Psychiatrie und Psychisch-gerichtliche Medizin. *Psychiatry (Edgmont),* 64**,** 146-148.

ALZHEIMER, A. 1911. Uber eigenartige Krankheitsfalle des spateren Alters. *Psychiatr Nervenkr Z Gesamte Neurol Psychiatr,* 4**,** 356-85.

ANDREW, R. J., FERNANDEZ, C. G., STANLEY, M., JIANG, H., NGUYEN, P., RICE, R. C., BUGGIA-PREVOT, V., DE ROSSI, P., VETRIVEL, K. S., LAMB, R., ARGEMI, A., ALLAERT, E. S., RATHBUN, E. M., KRAUSE, S. V., WAGNER, S. L., PARENT, A. T., HOLTZMAN, D. M. & THINAKARAN, G. 2017. Lack of BACE1 S-palmitoylation reduces amyloid burden and mitigates memory deficits in transgenic mouse models of Alzheimer's disease. *Proc Natl Acad Sci U S A,* 114**,** E9665-E9674.

ANDREW, R. J., KELLETT, K. A., THINAKARAN, G. & HOOPER, N. M. 2016. A Greek tragedy: the growing complexity of Alzheimer amyloid precursor protein proteolysis. *Journal of Biological Chemistry,* 291**,** 19235-19244.

ARNOLD, S. E., HYMAN, B. T., FLORY, J., DAMASIO, A. R. & VAN HOESEN, G. W. 1991. The topographical and neuroanatomical distribution of neurofibrillary tangles and neuritic plaques in the cerebral cortex of patients with Alzheimer's disease. *Cerebral cortex,* 1**,** 103-116.

AYDIN, F., TURKOGLU, V. & BAS, Z. 2021. Purification and characterization of angiotensin-converting enzyme (ACE) from sheep lung. *Molecular Biology Reports,* 48**,** 4191-4199.

BACKSTROM, J. R., LIM, G. P., CULLEN, M. J. & TÖKÉS, Z. A. 1996. Matrix metalloproteinase-9 (MMP-9) is synthesized in neurons of the human hippocampus and is capable of degrading the amyloid-β peptide (1–40). *Journal of Neuroscience,* 16**,** 7910-7919.

`

BALDACCI, F., VERGALLO, A., LISTA, S., MEGRET, L., BUN, R. S., ZETTENBERG, H., BLENNOW, K., LAMARI, F., GENTHON, R. & CAVEDO, E. 2018. O3-09-02: CORRELATION AND LONGITUDINAL DYNAMICS OF PLASMA NFL AND TAU CONCENTRATIONS IN AMYLOID-PET NEGATIVE INDIVIDUALS WITH SUBJECTIVE MEMORY COMPLAINTS. *Alzheimer's & Dementia,* 14**,** P1036-P1037.

BARÃO, S., MOECHARS, D., LICHTENTHALER, S. F. & DE STROOPER, B. 2016. BACE1 physiological functions may limit its use as therapeutic target for Alzheimer's disease. *Trends in neurosciences,* 39**,** 158-169.

BARTHÉLEMY, N. R., GABELLE, A., HIRTZ, C., FENAILLE, F., SERGEANT, N., SCHRAEN-MASCHKE, S., VIALARET, J., BUÉE, L., JUNOT, C. & BECHER, F. 2016. Differential mass spectrometry profiles of tau protein in the cerebrospinal fluid of patients with Alzheimer's disease, progressive supranuclear palsy, and dementia with lewy bodies. *Journal of Alzheimer's Disease,* 51**,** 1033-1043.

BARTHÉLEMY, N. R., HORIE, K., SATO, C. & BATEMAN, R. J. 2020a. Blood plasma phosphorylated-tau isoforms track CNS change in Alzheimer's disease. *Journal of Experimental Medicine,* 217.

BARTHÉLEMY, N. R., LI, Y., JOSEPH-MATHURIN, N., GORDON, B. A., HASSENSTAB, J., BENZINGER, T., BUCKLES, V., FAGAN, A. M., PERRIN, R. J. & GOATE, A. M. 2020b. A soluble phosphorylated tau signature links tau, amyloid and the evolution of stages of dominantly inherited Alzheimer's disease. *Nature medicine,* 26**,** 398-407.

BATEMAN, R. J., MUNSELL, L. Y., MORRIS, J. C., SWARM, R., YARASHESKI, K. E. & HOLTZMAN, D. M. 2006. Human amyloid-β synthesis and clearance rates as measured in cerebrospinal fluid in vivo. *Nature medicine,* 12**,** 856-861.

BATEMAN, R. J., XIONG, C., BENZINGER, T. L., FAGAN, A. M., GOATE, A., FOX, N. C., MARCUS, D. S., CAIRNS, N. J., XIE, X. & BLAZEY, T. M. 2012. Clinical and biomarker changes in dominantly inherited Alzheimer's disease. *N Engl J Med,* 367**,** 795-804.

BAUMEISTER, R., LEIMER, U., ZWECKBRONNER, I., JAKUBEK, C., GRÜNBERG, J. & HAASS, C. 1997. Human presenilin-1, but not familial Alzheimer's disease (FAD) mutants, facilitate Caenorhabditis elegans Notch signalling independently of proteolytic processing. *Genes and function,* 1**,** 149-159.

BAYER, T. A. & WIRTHS, O. 2010. Intracellular accumulation of amyloid-Beta-a predictor for synaptic dysfunction and neuron loss in Alzheimer's disease. *Frontiers in aging neuroscience***,** 8.

BECKER-PAULY, C. & PIETRZIK, C. U. 2017. The metalloprotease meprin β is an alternative β-secretase of APP. *Frontiers in molecular neuroscience,* 9**,** 159.

BEHER, D., WRIGLEY, J. D., OWENS, A. P. & SHEARMAN, M. S. 2002. Generation of C-terminally truncated amyloid-β peptides is dependent on γ-secretase activity. *Journal of neurochemistry,* 82**,** 563-575.

BEKRIS, L. M., YU, C.-E., BIRD, T. D. & TSUANG, D. W. 2010. Review Article: Genetics of Alzheimer Disease. *Journal of Geriatric Psychiatry and Neurology,* 23**,** 213-227.

BELLENGUEZ, C., KÜÇÜKALI, F., JANSEN, I. E., KLEINEIDAM, L., MORENO-GRAU, S., AMIN, N., NAJ, A. C., CAMPOS-MARTIN, R., GRENIER-BOLEY, B. & ANDRADE, V. 2022. New insights into the genetic etiology of Alzheimer's disease and related dementias. *Nature genetics,* 54**,** 412-436.

BERTRAM, L. & TANZI, R. E. 2004. Alzheimer's disease: one disorder, too many genes? *Human molecular genetics,* 13**,** R135-R141.

BIEN, J., JEFFERSON, T., CAUSEVIC, M., JUMPERTZ, T., MUNTER, L. M., MULTHAUP, G., WEGGEN, S., BECKER-PAULY, C. & PIETRZIK, C. 2012. O2-04-04: The metalloprotease meprin beta generates amino-terminally truncated beta-amyloid peptide species. *Alzheimer's & Dementia,* 8**,** P242-P242.

BIERER, L. M., HOF, P. R., PUROHIT, D. P., CARLIN, L., SCHMEIDLER, J., DAVIS, K. L. & PERL, D. P. 1995. Neocortical neurofibrillary tangles correlate with dementia severity in Alzheimer's disease. *Archives of neurology,* 52**,** 81-88.

`

BIRD, T. D., LAMPE, T. H., NEMENS, E. J., MINER, G. W., SUMI, S. & SCHELLENBERG, G. D. 1988. Familial Alzheimer's disease in American descendants of the Volga Germans: probable genetic founder effect. *Annals of Neurology: Official Journal of the American Neurological Association and the Child Neurology Society,* 23**,** 25-31.

BLENNOW, K., MATTSSON, N., SCHÖLL, M., HANSSON, O. & ZETTERBERG, H. 2015. Amyloid biomarkers in Alzheimer's disease. *Trends in pharmacological sciences,* 36**,** 297-309.

BLESSED, G., TOMLINSON, E. & ROTH, M. 1968. Cerebral plaque formation in old age. *Brit J Psychiat,* 114**,** 797-811.

BODENDORF, U., DANNER, S., FISCHER, F., STEFANI, M., STURCHLER-PIERRAT, C., WIEDERHOLD, K. H., STAUFENBIEL, M. & PAGANETTI, P. 2002. Expression of human β-secretase in the mouse brain increases the steady-state level of β-amyloid. *Journal of neurochemistry,* 80**,** 799-806.

BOLTE, S. & CORDELIÈRES, F. P. 2006. A guided tour into subcellular colocalization analysis in light microscopy. *Journal of microscopy,* 224**,** 213-232.

BONDS, J. A., KUTTNER-HIRSHLER, Y., BARTOLOTTI, N., TOBIN, M. K., PIZZI, M., MARR, R. & LAZAROV, O. 2015. Presenilin-1 dependent neurogenesis regulates hippocampal learning and memory. *PLoS One,* 10**,** e0131266.

BONIFACINO, J. S. & TRAUB, L. M. 2003. Signals for sorting of transmembrane proteins to endosomes and lysosomes. *Annu Rev Biochem,* 72**,** 395-447.

BORENSTEIN, A. R., COPENHAVER, C. I. & MORTIMER, J. A. 2006. Early-life risk factors for Alzheimer disease. *Alzheimer Disease & Associated Disorders,* 20**,** 63-72.

BRAAK, H. & BRAAK, E. 1991. Neuropathological stageing of Alzheimer-related changes. *Acta neuropathologica,* 82**,** 239-259.

BRION, J.-P., PASSAREIRO, H., NUNEZ, J. & FLAMENT-DURAND, J. 1985. Mise en évidence immunologique de la protéine tau au niveau des lésions de dégénérescence neurofibrillaire de la maladie d'Alzheimer. *Archives de biologie,* 96**,** 229-235.

BRIOZZO, P., MORISSET, M., CAPONY, F., ROUGEOT, C. & ROCHEFORT, H. 1988. In vitro degradation of extracellular matrix with M r 52,000 cathepsin D secreted by breast cancer cells. *Cancer research,* 48**,** 3688-3692.

BURSAVICH, M. G., HARRISON, B. A. & BLAIN, J.-F. 2016. Gamma secretase modulators: new Alzheimer's drugs on the horizon? *Journal of medicinal chemistry,* 59**,** 7389-7409.

CAI, H., WANG, Y., MCCARTHY, D., WEN, H., BORCHELT, D. R., PRICE, D. L. & WONG, P. C. 2001. BACE1 is the major β-secretase for generation of Aβ peptides by neurons. *Nature neuroscience,* 4**,** 233-234.

CAI, J., QI, X., KOCIOK, N., SKOSYRSKI, S., EMILIO, A., RUAN, Q., HAN, S., LIU, L., CHEN, Z. & BOWES RICKMAN, C. 2012. β-Secretase (BACE1) inhibition causes retinal pathology by vascular dysregulation and accumulation of age pigment. *EMBO molecular medicine,* 4**,** 980-991.

CAILLAVA, C., RANALDI, S., LAURITZEN, I., BAUER, C., FAREH, J., ABRAHAM, J.-D. & CHECLER, F. 2014. Study on Aβ34 biology and detection in transgenic mice brains. *Neurobiology of aging,* 35**,** 1570-1581.

CAMPION, D., DUMANCHIN, C., HANNEQUIN, D., DUBOIS, B., BELLIARD, S., PUEL, M., THOMAS-ANTERION, C., MICHON, A., MARTIN, C. & CHARBONNIER, F. 1999. Early-onset autosomal dominant Alzheimer disease: prevalence, genetic heterogeneity, and mutation spectrum. *The American Journal of Human Genetics,* 65**,** 664-670.

CATALDO, A. M. & NIXON, R. A. 1990. Enzymatically active lysosomal proteases are associated with amyloid deposits in Alzheimer brain. *Proceedings of the National Academy of Sciences,* 87**,** 3861-3865.

`

CHAI, Y. L., CHONG, J. R., WENG, J., HOWLETT, D., HALSEY, A., LEE, J. H., ATTEMS, J., AARSLAND, D., FRANCIS, P. T. & CHEN, C. P. 2019. Lysosomal cathepsin D is upregulated in Alzheimer's disease neocortex and may be a marker for neurofibrillary degeneration. *Brain pathology,* 29**,** 63-74.

CHEN, W.-J., GOLDSTEIN, J. L. & BROWN, M. S. 1990. NPXY, a sequence often found in cytoplasmic tails, is required for coated pit-mediated internalization of the low density lipoprotein receptor. *Journal of Biological Chemistry,* 265**,** 3116-3123.

CHIA, P. Z., TOH, W. H., SHARPLES, R., GASNEREAU, I., HILL, A. F. & GLEESON, P. A. 2013. Intracellular itinerary of internalised beta-secretase, BACE1, and its potential impact on beta-amyloid peptide biogenesis. *Traffic,* 14**,** 997-1013.

CHIOCCO, M. J., KULNANE, L. S., YOUNKIN, L., YOUNKIN, S., EVIN, G. & LAMB, B. T. 2004. Altered amyloid-β metabolism and deposition in genomic-based β-secretase transgenic mice. *Journal of Biological Chemistry,* 279**,** 52535-52542.

CHOW, V. W., MATTSON, M. P., WONG, P. C. & GLEICHMANN, M. 2010. An overview of APP processing enzymes and products. *Neuromolecular medicine,* 12**,** 1-12.

CHOY, R. W.-Y., CHENG, Z. & SCHEKMAN, R. 2012. Amyloid precursor protein (APP) traffics from the cell surface via endosomes for amyloid β (Aβ) production in the trans-Golgi network. *Proceedings of the National Academy of Sciences,* 109**,** E2077-E2082.

CICCOTOSTO, G. D., JAMES, S. A., ALTISSIMO, M., PATERSON, D., VOGT, S., LAI, B., DE JONGE, M. D., HOWARD, D. L., BUSH, A. I. & CAPPAI, R. 2014. Quantitation and localization of intracellular redox active metals by X-ray fluorescence microscopy in cortical neurons derived from APP and APLP2 knockout tissue. *Metallomics,* 6**,** 1894-1904.

CITRON, M., OLTERSDORF, T., HAASS, C., MCCONLOGUE, L., HUNG, A. Y., SEUBERT, P., VIGO-PELFREY, C., LIEBERBURG, I. & SELKOE, D. J. 1992. Mutation of the β-amyloid precursor protein in familial Alzheimer's disease increases β-protein production. *Nature,* 360**,** 672-674.

CLEARY, J. P., WALSH, D. M., HOFMEISTER, J. J., SHANKAR, G. M., KUSKOWSKI, M. A., SELKOE, D. J. & ASHE, K. H. 2005. Natural oligomers of the amyloid-β protein specifically disrupt cognitive function. *Nature neuroscience,* 8**,** 79-84.

COLE, S. L. & VASSAR, R. 2007. The Alzheimer's disease beta-secretase enzyme, BACE1. *Mol Neurodegener,* 2**,** 22.

COLOMBO, A., WANG, H., KUHN, P.-H., PAGE, R., KREMMER, E., DEMPSEY, P. J., CRAWFORD, H. C. & LICHTENTHALER, S. F. 2013. Constitutive α-and β-secretase cleavages of the amyloid precursor protein are partially coupled in neurons, but not in frequently used cell lines. *Neurobiology of disease,* 49**,** 137-147.

CONNELL, J., RODRIGUEZ-MARTIN, T., GIBB, G., KAHN, N., GRIERSON, A., HANGER, D., REVESZ, T., LANTOS, P., ANDERTON, B. & GALLO, J.-M. 2005. Quantitative analysis of tau isoform transcripts in sporadic tauopathies. *Molecular brain research,* 137**,** 104-109.

CORDER, E. H., SAUNDERS, A. M., STRITTMATTER, W. J., SCHMECHEL, D. E., GASKELL, P. C., SMALL, G., ROSES, A., HAINES, J. & PERICAK-VANCE, M. A. 1993. Gene dose of apolipoprotein E type 4 allele and the risk of Alzheimer's disease in late onset families. *Science,* 261**,** 921-923.

CRUTS, M. & VAN BROECKHOVEN, C. 1998. Presenilin mutations in Alzheimer's disease. *Human mutation,* 11**,** 183-190.

DA COSTA, I. B., DE LABIO, R. W., RASMUSSEN, L. T., VIANI, G. A., CHEN, E., VILLARES, J., TURECKI, G., SMITH, M. D. A. C. & PAYAO, S. L. 2017. Change in INSR, APBA2 and IDE gene expressions in brains of Alzheimer's disease patients. *Current Alzheimer Research,* 14**,** 760-765.

DAVIES, C. & MANN, D. 1993. Is the" preamyloid" of diffuse plaques in Alzheimer's disease really nonfibrillar? *The American journal of pathology,* 143**,** 1594.

DAWSON, G., SEABROOK, G., ZHENG, H., SMITH, D., GRAHAM, S., O'DOWD, G., BOWERY, B., BOYCE, S., TRUMBAUER, M. & CHEN, H. 1999. Age-related cognitive deficits, impaired long-term

potentiation and reduction in synaptic marker density in mice lacking the β-amyloid precursor protein. *Neuroscience,* 90**,** 1-13.
DE STROOPER, B. 2010. Proteases and proteolysis in Alzheimer disease: a multifactorial view on the disease process. *Physiological reviews,* 90**,** 465-494.
DE STROOPER, B., VASSAR, R. & GOLDE, T. 2010. The secretases: enzymes with therapeutic potential in Alzheimer disease. *Nature reviews neurology,* 6**,** 99-107.
DEANE, R., SAGARE, A. & ZLOKOVIC, B. 2008. The role of the cell surface LRP and soluble LRP in blood-brain barrier Aβ clearance in Alzheimer's disease. *Current pharmaceutical design,* 14**,** 1601-1605.
DELABY, C., ESTELLÉS, T., ZHU, N., ARRANZ, J., BARROETA, I., CARMONA-IRAGUI, M., ILLÁN-GALA, I., SANTOS-SANTOS, M. Á., ALTUNA, M. & SALA, I. 2022. The Aβ1–42/Aβ1–40 ratio in CSF is more strongly associated to tau markers and clinical progression than Aβ1–42 alone. *Alzheimer's research & therapy,* 14**,** 1-11.
DEVI, L. & OHNO, M. 2013. Mechanisms that lessen benefits of β-secretase reduction in a mouse model of Alzheimer's disease. *Translational Psychiatry,* 3**,** e284-e284.
DI FEDE, G., CATANIA, M., MORBIN, M., ROSSI, G., SUARDI, S., MAZZOLENI, G., MERLIN, M., GIOVAGNOLI, A. R., PRIONI, S. & ERBETTA, A. 2009. A recessive mutation in the APP gene with dominant-negative effect on amyloidogenesis. *Science,* 323**,** 1473-1477.
DICKSON, D. 1997a. Neuropathological diagnosis of Alzheimer's disease: a perspective from longitudinal clinicopathological studies. *Neurobiology of aging,* 18**,** S21-S26.
DICKSON, D. W. 1997b. The pathogenesis of senile plaques. *Journal of Neuropathology & Experimental Neurology,* 56**,** 321-339.
DOMINGUEZ, D., TOURNOY, J., HARTMANN, D., HUTH, T., CRYNS, K., DEFORCE, S., SERNEELS, L., CAMACHO, I. E., MARJAUX, E. & CRAESSAERTS, K. 2005. Phenotypic and biochemical analyses of BACE1-and BACE2-deficient mice. *Journal of Biological Chemistry,* 280**,** 30797-30806.
DONOVIEL, D. B., HADJANTONAKIS, A.-K., IKEDA, M., ZHENG, H., HYSLOP, P. S. G. & BERNSTEIN, A. 1999. Mice lacking both presenilin genes exhibitearlyembryonic patterningdefects. *Genes & development,* 13**,** 2801-2810.
DOREY, A., PERRET-LIAUDET, A., THOLANCE, Y., FOURIER, A. & QUADRIO, I. 2015. Cerebrospinal fluid Aβ40 improves the interpretation of Aβ42 concentration for diagnosing Alzheimer's disease. *Frontiers in Neurology,* 6**,** 247.
DUBOIS, B., FELDMAN, H. H., JACOVA, C., HAMPEL, H., MOLINUEVO, J. L., BLENNOW, K., DEKOSKY, S. T., GAUTHIER, S., SELKOE, D. & BATEMAN, R. 2014. Advancing research diagnostic criteria for Alzheimer's disease: the IWG-2 criteria. *The Lancet Neurology,* 13**,** 614-629.
DUCKWORTH, W. C., BENNETT, R. G. & HAMEL, F. G. 1998a. Insulin acts intracellularly on proteasomes through insulin-degrading enzyme. *Biochemical and Biophysical Research Communications,* 244**,** 390-394.
DUCKWORTH, W. C., BENNETT, R. G. & HAMEL, F. G. 1998b. Insulin degradation: progress and potential. *Endocrine reviews,* 19**,** 608-624.
DUKA, V., LEE, J.-H., CREDLE, J., WILLS, J., OAKS, A., SMOLINSKY, C., SHAH, K., MASH, D. C., MASLIAH, E. & SIDHU, A. 2013. Identification of the sites of tau hyperphosphorylation and activation of tau kinases in synucleinopathies and Alzheimer's diseases. *PloS one,* 8**,** e75025.
ECKMAN, E. A., ADAMS, S. K., TROENDLE, F. J., STODOLA, B. A., KAHN, M. A., FAUQ, A. H., XIAO, H. D., BERNSTEIN, K. E. & ECKMAN, C. B. 2006. Regulation of steady-state β-amyloid levels in the brain by neprilysin and endothelin-converting enzyme but not angiotensin-converting enzyme. *Journal of Biological Chemistry,* 281**,** 30471-30478.
ECKMAN, E. A. & ECKMAN, C. B. 2013. Aβ Degradation by Endothelin-Converting Enzymes. *Madame Curie Bioscience Database [Internet].* Landes Bioscience.

`

ECKMAN, E. A., REED, D. K. & ECKMAN, C. B. 2001. Degradation of the Alzheimer's amyloid β peptide by endothelin-converting enzyme. *Journal of Biological chemistry,* 276**,** 24540-24548.

ECKMAN, E. A., WATSON, M., MARLOW, L., SAMBAMURTI, K. & ECKMAN, C. B. 2003. Alzheimer's disease β-amyloid peptide is increased in mice deficient in endothelin-converting enzyme. *Journal of Biological Chemistry,* 278**,** 2081-2084.

EDBAUER, D., WINKLER, E., REGULA, J. T., PESOLD, B., STEINER, H. & HAASS, C. 2003. Reconstitution of γ-secretase activity. *Nature cell biology,* 5**,** 486-488.

EGAN, M. F., KOST, J., TARIOT, P. N., AISEN, P. S., CUMMINGS, J. L., VELLAS, B., SUR, C., MUKAI, Y., VOSS, T. & FURTEK, C. 2018. Randomized trial of verubecestat for mild-to-moderate Alzheimer's disease. *New England Journal of Medicine,* 378**,** 1691-1703.

ERIKSEN, J. L., SAGI, S. A., SMITH, T. E., WEGGEN, S., DAS, P., MCLENDON, D., OZOLS, V. V., JESSING, K. W., ZAVITZ, K. H. & KOO, E. H. 2003. NSAIDs and enantiomers of flurbiprofen target γ-secretase and lower Aβ42 in vivo. *The Journal of clinical investigation,* 112**,** 440-449.

ESBJÖRNER, E. K., CHAN, F., REES, E., ERDELYI, M., LUHESHI, L. M., BERTONCINI, C. W., KAMINSKI, C. F., DOBSON, C. M. & SCHIERLE, G. S. K. 2014. Direct observations of amyloid β self-assembly in live cells provide insights into differences in the kinetics of Aβ (1–40) and Aβ (1–42) aggregation. *Chemistry & biology,* 21**,** 732-742.

EWERS, M., CHENG, X., ZHONG, Z., NURAL, H. F., WALSH, C., MEINDL, T., TEIPEL, S. J., BUERGER, K., HE, P. & SHEN, Y. 2011. Increased CSF-BACE1 activity associated with decreased hippocampus volume in Alzheimer's disease. *Journal of Alzheimer's Disease,* 25**,** 373-381.

EWERS, M., ZHONG, Z., BÜRGER, K., WALLIN, A., BLENNOW, K., TEIPEL, S. J., SHEN, Y. & HAMPEL, H. 2008. Increased CSF-BACE 1 activity is associated with ApoE-ε4 genotype in subjects with mild cognitive impairment and Alzheimer's disease. *Brain,* 131**,** 1252-1258.

FAGAN, A. M., MINTUN, M. A., MACH, R. H., LEE, S. Y., DENCE, C. S., SHAH, A. R., LAROSSA, G. N., SPINNER, M. L., KLUNK, W. E. & MATHIS, C. A. 2006. Inverse relation between in vivo amyloid imaging load and cerebrospinal fluid Aβ42 in humans. *Annals of neurology,* 59**,** 512-519.

FAGAN, A. M., SHAW, L. M., XIONG, C., VANDERSTICHELE, H., MINTUN, M. A., TROJANOWSKI, J. Q., COART, E., MORRIS, J. C. & HOLTZMAN, D. M. 2011. Comparison of analytical platforms for cerebrospinal fluid measures of β-amyloid 1-42, total tau, and p-tau181 for identifying Alzheimer disease amyloid plaque pathology. *Archives of neurology,* 68**,** 1137-1144.

FAHNOE, D. C., KNAPP, J., JOHNSON, G. D. & AHN, K. 2000. Inhibitor potencies and substrate preference for endothelin-converting enzyme-1 are dramatically affected by pH. *Journal of cardiovascular pharmacology,* 36**,** S22-5.

FALKEVALL, A., ALIKHANI, N., BHUSHAN, S., PAVLOV, P. F., BUSCH, K., JOHNSON, K. A., ENEQVIST, T., TJERNBERG, L., ANKARCRONA, M. & GLASER, E. 2006. Degradation of the Amyloid β-Protein by the Novel Mitochondrial Peptidasome, PreP*♦. *Journal of Biological Chemistry,* 281**,** 29096-29104.

FARRER, L. A., SHERBATICH, T., KERYANOV, S. A., KOROVAITSEVA, G. I., ROGAEVA, E. A., PETRUK, S., PREMKUMAR, S., MOLIAKA, Y., SONG, Y. Q. & PEI, Y. 2000. Association between angiotensin-converting enzyme and Alzheimer disease. *Archives of Neurology,* 57**,** 210-214.

FARRIS, W., MANSOURIAN, S., CHANG, Y., LINDSLEY, L., ECKMAN, E. A., FROSCH, M. P., ECKMAN, C. B., TANZI, R. E., SELKOE, D. J. & GUÉNETTE, S. 2003. Insulin-degrading enzyme regulates the levels of insulin, amyloid β-protein, and the β-amyloid precursor protein intracellular domain in vivo. *Proceedings of the National Academy of Sciences,* 100**,** 4162-4167.

FARRIS, W., MANSOURIAN, S., LEISSRING, M. A., ECKMAN, E. A., BERTRAM, L., ECKMAN, C. B., TANZI, R. E. & SELKOE, D. J. 2004. Partial loss-of-function mutations in insulin-degrading enzyme that induce diabetes also impair degradation of amyloid β-protein. *The American journal of pathology,* 164**,** 1425-1434.

`

FINCKH, U., ALBERICI, A., ANTONIAZZI, M., BENUSSI, L., FEDI, V., GIANNINI, C., GAL, A., NITSCH, R. & BINETTI, G. 2000. Variable expression of familial Alzheimer disease associated with presenilin 2 mutation M239I. *Neurology,* 54**,** 2006-2008.

FLUHRER, R., MULTHAUP, G., SCHLICKSUPP, A., OKOCHI, M., TAKEDA, M., LAMMICH, S., WILLEM, M., WESTMEYER, G., BODE, W. & WALTER, J. 2003. Identification of a β-secretase activity, which truncates amyloid β-peptide after its presenilin-dependent generation. *Journal of Biological Chemistry,* 278**,** 5531-5538.

FORMAN, M., KLEIJN, H. J., DOCKENDORF, M., PALCZA, J., TSENG, J., CANALES, C., EGAN, M., KENNEDY, M., LATERZA, O. & MA, L. 2013. O1–06–05: The novel BACE inhibitor MK-8931 dramatically lowers CSF beta-amyloid in patients with mild-to-moderate Alzheimer's disease. *Alzheimer's & Dementia,* 9**,** P139-P139.

FORMAN, M., PALCZA, J., TSENG, J., LEEMPOELS, J., RAMAEL, S., HAN, D., JHEE, S., ERESHEFSKY, L., TANEN, M. & LATERZA, O. 2012. P4-196: The novel BACE inhibitor MK-8931 dramatically lowers cerebrospinal fluid Aβ peptides in healthy subjects following single-and multiple-dose administration. *Alzheimer's & Dementia,* 8**,** P704-P704.

FUKAMI, S., WATANABE, K., IWATA, N., HARAOKA, J., LU, B., GERARD, N. P., GERARD, C., FRASER, P., WESTAWAY, D. & GEORGE-HYSLOP, P. S. 2002. Aβ-degrading endopeptidase, neprilysin, in mouse brain: synaptic and axonal localization inversely correlating with Aβ pathology. *Neuroscience research,* 43**,** 39-56.

FUKUMOTO, H., CHEUNG, B. S., HYMAN, B. T. & IRIZARRY, M. C. 2002. β-Secretase protein and activity are increased in the neocortex in Alzheimer disease. *Archives of neurology,* 59**,** 1381-1389.

GALLWITZ, L., SCHMIDT, L., MARQUES, A. R., THOLEY, A., CASSIDY, L., ULKU, I., MULTHAUP, G., DI SPIEZIO, A. & SAFTIG, P. 2022. Cathepsin D: Analysis of its potential role as an amyloid beta degrading protease. *Neurobiology of Disease***,** 105919.

GEORGIEVSKA, B., GUSTAVSSON, S., LUNDKVIST, J., NEELISSEN, J., EKETJÄLL, S., RAMBERG, V., BUETERS, T., AGERMAN, K., JURÉUS, A. & SVENSSON, S. 2015. Revisiting the peripheral sink hypothesis: inhibiting BACE 1 activity in the periphery does not alter β-amyloid levels in the CNS. *Journal of neurochemistry,* 132**,** 477-486.

GIRARD, S. D., JACQUET, M., BARANGER, K., MIGLIORATI, M., ESCOFFIER, G., BERNARD, A., KHRESTCHATISKY, M., FÉRON, F., RIVERA, S. & ROMAN, F. S. 2014. Onset of hippocampus-dependent memory impairments in 5XFAD transgenic mouse model of Alzheimer's disease. *Hippocampus,* 24**,** 762-772.

GLENNER, G. G. & WONG, C. W. 1984. Alzheimer's disease: initial report of the purification and characterization of a novel cerebrovascular amyloid protein. *Biochemical and biophysical research communications,* 120**,** 885-890.

GOATE, A., CHARTIER-HARLIN, M.-C., MULLAN, M., BROWN, J., CRAWFORD, F., FIDANI, L., GIUFFRA, L., HAYNES, A., IRVING, N. & JAMES, L. 1991. Segregation of a missense mutation in the amyloid precursor protein gene with familial Alzheimer's disease. *Nature,* 349**,** 704-706.

GÓMEZ-ISLA, T., HOLLISTER, R., WEST, H., MUI, S., GROWDON, J. H., PETERSEN, R. C., PARISI, J. E. & HYMAN, B. T. 1997. Neuronal loss correlates with but exceeds neurofibrillary tangles in Alzheimer's disease. *Annals of Neurology: Official Journal of the American Neurological Association and the Child Neurology Society,* 41**,** 17-24.

GOURAS, G. K., XU, H., JOVANOVIC, J. N., BUXBAUM, J. D., WANG, R., GREENGARD, P., RELKIN, N. R. & GANDY, S. 1998. Generation and regulation of β-amyloid peptide variants by neurons. *Journal of neurochemistry,* 71**,** 1920-1925.

GRAEBER, M., KÖSEL, S., EGENSPERGER, R., BANATI, R., MÜLLER, U., BISE, K., HOFF, P., MÖLLER, H., FUJISAWA, K. & MEHRAEIN, P. 1997. Rediscovery of the case described by Alois Alzheimer in 1911: historical, histological and molecular genetic analysis. *Neurogenetics,* 1**,** 73-80.

`

GREEN, R. C., SCHNEIDER, L. S., AMATO, D. A., BEELEN, A. P., WILCOCK, G., SWABB, E. A., ZAVITZ, K. H. & GROUP, T. P. S. 2009. Effect of tarenflurbil on cognitive decline and activities of daily living in patients with mild Alzheimer disease: a randomized controlled trial. *Jama,* 302**,** 2557-2564.

GRIMM, M. O., METT, J., STAHLMANN, C. P., HAUPENTHAL, V. J., ZIMMER, V. C. & HARTMANN, T. 2013. Neprilysin and Aβ clearance: impact of the APP intracellular domain in NEP regulation and implications in Alzheimer's disease. *Frontiers in aging neuroscience,* 5**,** 98.

GRIMMER, T., RIEMENSCHNEIDER, M., FÖRSTL, H., HENRIKSEN, G., KLUNK, W. E., MATHIS, C. A., SHIGA, T., WESTER, H.-J., KURZ, A. & DRZEZGA, A. 2009. Beta amyloid in Alzheimer's disease: increased deposition in brain is reflected in reduced concentration in cerebrospinal fluid. *Biological psychiatry,* 65**,** 927-934.

GRUNDKE-IQBAL, I., IQBAL, K., QUINLAN, M., TUNG, Y.-C., ZAIDI, M. S. & WISNIEWSKI, H. M. 1986a. Microtubule-associated protein tau. A component of Alzheimer paired helical filaments. *Journal of Biological Chemistry,* 261**,** 6084-6089.

GRUNDKE-IQBAL, I., IQBAL, K., TUNG, Y.-C., QUINLAN, M., WISNIEWSKI, H. M. & BINDER, L. I. 1986b. Abnormal phosphorylation of the microtubule-associated protein tau (tau) in Alzheimer cytoskeletal pathology. *Proceedings of the National Academy of Sciences,* 83**,** 4913-4917.

HAASS, C., KAETHER, C., THINAKARAN, G. & SISODIA, S. 2012. Trafficking and proteolytic processing of APP. *Cold Spring Harbor perspectives in medicine,* 2**,** a006270.

HAASS, C. & SELKOE, D. J. 1993. Cellular processing of beta-amyloid precursor protein and the genesis of amyloid beta-peptide. *Cell,* 75**,** 1039-1042.

HAMPEL, H., LISTA, S., TEIPEL, S. J., GARACI, F., NISTICO, R., BLENNOW, K., ZETTERBERG, H., BERTRAM, L., DUYCKAERTS, C. & BAKARDJIAN, H. 2014. Perspective on future role of biological markers in clinical therapy trials of Alzheimer's disease: a long-range point of view beyond 2020. *Biochemical pharmacology,* 88**,** 426-449.

HAMPEL, H., O'BRYANT, S. E., MOLINUEVO, J. L., ZETTERBERG, H., MASTERS, C. L., LISTA, S., KIDDLE, S. J., BATRLA, R. & BLENNOW, K. 2018. Blood-based biomarkers for Alzheimer disease: mapping the road to the clinic. *Nature Reviews Neurology,* 14**,** 639-652.

HAMPEL, H., SHEN, Y., WALSH, D. M., AISEN, P., SHAW, L. M., ZETTERBERG, H., TROJANOWSKI, J. Q. & BLENNOW, K. 2010. Biological markers of amyloid β-related mechanisms in Alzheimer's disease. *Experimental neurology,* 223**,** 334-346.

HAMPEL, H., VASSAR, R., DE STROOPER, B., HARDY, J., WILLEM, M., SINGH, N., ZHOU, J., YAN, R., VANMECHELEN, E. & DE VOS, A. 2021. The β-secretase BACE1 in Alzheimer's disease. *Biological psychiatry,* 89**,** 745-756.

HANIU, M., DENIS, P., YOUNG, Y., MENDIAZ, E. A., FULLER, J., HUI, J. O., BENNETT, B. D., KAHN, S., ROSS, S. & BURGESS, T. 2000. Characterization of Alzheimer's β-secretase protein BACE: a pepsin family member with unusual properties. *Journal of Biological Chemistry,* 275**,** 21099-21106.

HANSEEUW, B. J., BETENSKY, R. A., JACOBS, H. I., SCHULTZ, A. P., SEPULCRE, J., BECKER, J. A., COSIO, D. M. O., FARRELL, M., QUIROZ, Y. T. & MORMINO, E. C. 2019. Association of amyloid and tau with cognition in preclinical Alzheimer disease: a longitudinal study. *JAMA neurology,* 76**,** 915-924.

HANSSON, O. 2021. Biomarkers for neurodegenerative diseases. *Nature medicine,* 27**,** 954-963.

HANSSON, O., EDELMAYER, R. M., BOXER, A. L., CARRILLO, M. C., MIELKE, M. M., RABINOVICI, G. D., SALLOWAY, S., SPERLING, R., ZETTERBERG, H. & TEUNISSEN, C. E. 2022. The Alzheimer's Association appropriate use recommendations for blood biomarkers in Alzheimer's disease. *Alzheimer's & Dementia*.

HANSSON, O., LEHMANN, S., OTTO, M., ZETTERBERG, H. & LEWCZUK, P. 2019. Advantages and disadvantages of the use of the CSF Amyloid β (Aβ) 42/40 ratio in the diagnosis of Alzheimer's Disease. *Alzheimer's research & therapy,* 11**,** 1-15.

`

HARDY, J. & ALLSOP, D. 1991. Amyloid deposition as the central event in the aetiology of Alzheimer's disease. *Trends in pharmacological sciences,* 12**,** 383-388.

HARDY, J. A. & HIGGINS, G. A. 1992. Alzheimer's disease: the amyloid cascade hypothesis. *Science,* 256**,** 184-185.

HAROUTUNIAN, V., DAVIES, P., VIANNA, C., BUXBAUM, J. & PUROHIT, D. 2007. Tau protein abnormalities associated with the progression of alzheimer disease type dementia. *Neurobiology of aging,* 28**,** 1-7.

HARRISON, S. M., HARPER, A. J., HAWKINS, J., DUDDY, G., GRAU, E., PUGH, P. L., WINTER, P. H., SHILLIAM, C. S., HUGHES, Z. A. & DAWSON, L. A. 2003. BACE1 (β-secretase) transgenic and knockout mice: identification of neurochemical deficits and behavioral changes. *Molecular and Cellular Neuroscience,* 24**,** 646-655.

HEMMING, M. L., ELIAS, J. E., GYGI, S. P. & SELKOE, D. J. 2009. Identification of β-secretase (BACE1) substrates using quantitative proteomics. *PloS one,* 4**,** e8477.

HEMMING, M. L., SELKOE, D. J. & FARRIS, W. 2007. Effects of prolonged angiotensin-converting enzyme inhibitor treatment on amyloid β-protein metabolism in mouse models of Alzheimer disease. *Neurobiology of disease,* 26**,** 273-281.

HÉRARD, A.-S., BESRET, L., DUBOIS, A., DAUGUET, J., DELZESCAUX, T., HANTRAYE, P., BONVENTO, G. & MOYA, K. 2006. siRNA targeted against amyloid precursor protein impairs synaptic activity in vivo. *Neurobiology of aging,* 27**,** 1740-1750.

HERNANDEZ-GUILLAMON, M., MAWHIRT, S., BLAIS, S., MONTANER, J., NEUBERT, T. A., ROSTAGNO, A. & GHISO, J. 2015. Sequential amyloid-β degradation by the matrix metalloproteases MMP-2 and MMP-9. *Journal of Biological Chemistry,* 290**,** 15078-15091.

HIGASHI, S. & MIYAZAKI, K. 2003. Novel processing of β-amyloid precursor protein catalyzed by membrane type 1 matrix metalloproteinase releases a fragment lacking the inhibitor domain against gelatinase A. *Biochemistry,* 42**,** 6514-6526.

HOLSINGER, R. D., MCLEAN, C. A., BEYREUTHER, K., MASTERS, C. L. & EVIN, G. 2002. Increased expression of the amyloid precursor β-secretase in Alzheimer's disease. *Annals of neurology: Official journal of the American neurological association and the child neurology society,* 51**,** 783-786.

HOLTZMAN, D. M., MORRIS, J. C. & GOATE, A. M. 2011. Alzheimer's disease: the challenge of the second century. *Science translational medicine,* 3**,** 77sr1-77sr1.

HOOK, V. Y., KINDY, M. & HOOK, G. 2008. Inhibitors of cathepsin B improve memory and reduce β-amyloid in transgenic Alzheimer disease mice expressing the wild-type, but not the Swedish mutant, β-secretase site of the amyloid precursor protein. *Journal of Biological Chemistry,* 283**,** 7745-7753.

HOOK, V. Y., KINDY, M., REINHECKEL, T., PETERS, C. & HOOK, G. 2009. Genetic cathepsin B deficiency reduces β-amyloid in transgenic mice expressing human wild-type amyloid precursor protein. *Biochemical and biophysical research communications,* 386**,** 284-288.

HORSTMANN, S., BUDIG, L., GARDNER, H., KOZIOL, J., DEUSCHLE, M., SCHILLING, C. & WAGNER, S. 2010. Matrix metalloproteinases in peripheral blood and cerebrospinal fluid in patients with Alzheimer's disease. *International psychogeriatrics,* 22**,** 966-972.

HSU, A., PODVIN, S. & HOOK, V. 2018. Lysosomal cathepsin protease gene expression profiles in the human brain during normal development. *Journal of molecular neuroscience,* 65**,** 420-431.

HU, J., IGARASHI, A., KAMATA, M. & NAKAGAWA, H. 2001. Angiotensin-converting enzyme degrades Alzheimer amyloid β-peptide (Aβ); retards Aβ aggregation, deposition, fibril formation; and inhibits cytotoxicity. *Journal of Biological Chemistry,* 276**,** 47863-47868.

`

HU, J., MIYATAKE, F., AIZU, Y., NAKAGAWA, H., NAKAMURA, S., TAMAOKA, A., TAKAHASH, R., URAKAMI, K. & SHOJI, M. 1999. Angiotensin-converting enzyme genotype is associated with Alzheimer disease in the Japanese population. *Neuroscience letters,* 277**,** 65-67.

HU, X., CRICK, S. L., BU, G., FRIEDEN, C., PAPPU, R. V. & LEE, J.-M. 2009. Amyloid seeds formed by cellular uptake, concentration, and aggregation of the amyloid-beta peptide. *Proceedings of the National Academy of Sciences,* 106**,** 20324-20329.

HU, X., HICKS, C. W., HE, W., WONG, P., MACKLIN, W. B., TRAPP, B. D. & YAN, R. 2006. Bace1 modulates myelination in the central and peripheral nervous system. *Nature neuroscience,* 9**,** 1520-1525.

HULSTAERT, F., BLENNOW, K., IVANOIU, A., SCHOONDERWALDT, H., RIEMENSCHNEIDER, M., DE DEYN, P., BANCHER, C., CRAS, P., WILTFANG, J. & MEHTA, P. 1999. Improved discrimination of AD patients using β-amyloid (1-42) and tau levels in CSF. *Neurology,* 52**,** 1555-1555.

HUSE, J. T., PIJAK, D. S., LESLIE, G. J., LEE, V. M.-Y. & DOMS, R. W. 2000. Maturation and endosomal targeting of β-site amyloid precursor protein-cleaving enzyme: the Alzheimer's disease β-secretase. *Journal of Biological Chemistry,* 275**,** 33729-33737.

HUSSAIN, I., POWELL, D., HOWLETT, D. R., TEW, D. G., MEEK, T. D., CHAPMAN, C., GLOGER, I. S., MURPHY, K. E., SOUTHAN, C. D. & RYAN, D. M. 1999. Identification of a novel aspartic protease (Asp 2) as β-secretase. *Molecular and Cellular Neuroscience,* 14**,** 419-427.

HYMAN, B. T., VAN HOESEN, G. W., DAMASIO, A. R. & BARNES, C. L. 1984. Alzheimer's disease: cell-specific pathology isolates the hippocampal formation. *Science,* 225**,** 1168-1170.

ILIFF, J. J., WANG, M., LIAO, Y., PLOGG, B. A., PENG, W., GUNDERSEN, G. A., BENVENISTE, H., VATES, G. E., DEANE, R. & GOLDMAN, S. A. 2012. A paravascular pathway facilitates CSF flow through the brain parenchyma and the clearance of interstitial solutes, including amyloid β. *Science translational medicine,* 4**,** 147ra111-147ra111.

ITAGAKI, S., MCGEER, P., AKIYAMA, H., ZHU, S. & SELKOE, D. 1989. Relationship of microglia and astrocytes to amyloid deposits of Alzheimer disease. *Journal of neuroimmunology,* 24**,** 173-182.

IWATA, N., TAKAKI, Y., FUKAMI, S., TSUBUKI, S. & SAIDO, T. C. 2002. Region-specific reduction of Aβ-degrading endopeptidase, neprilysin, in mouse hippocampus upon aging. *Journal of neuroscience research,* 70**,** 493-500.

IWATA, N., TSUBUKI, S., TAKAKI, Y., SHIROTANI, K., LU, B., GERARD, N. P., GERARD, C., HAMA, E., LEE, H.-J. & SAIDO, T. C. 2001. Metabolic regulation of brain Aβ by neprilysin. *Science,* 292**,** 1550-1552.

IWATA, N., TSUBUKI, S., TAKAKI, Y., WATANABE, K., SEKIGUCHI, M., HOSOKI, E., KAWASHIMA-MORISHIMA, M., LEE, H.-J., HAMA, E. & SEKINE-AIZAWA, Y. 2000. Identification of the major Aβ1–42-degrading catabolic pathway in brain parenchyma: suppression leads to biochemical and pathological deposition. *Nature medicine,* 6**,** 143-150.

IWATSUBO, T., ODAKA, A., SUZUKI, N., MIZUSAWA, H., NUKINA, N. & IHARA, Y. 1994. Visualization of Aβ42 (43) and Aβ40 in senile plaques with end-specific Aβ monoclonals: evidence that an initially deposited species is Aβ42 (43). *Neuron,* 13**,** 45-53.

JACK JR, C. R., BENNETT, D. A., BLENNOW, K., CARRILLO, M. C., DUNN, B., HAEBERLEIN, S. B., HOLTZMAN, D. M., JAGUST, W., JESSEN, F. & KARLAWISH, J. 2018. NIA-AA research framework: toward a biological definition of Alzheimer's disease. *Alzheimer's & Dementia,* 14**,** 535-562.

JACK JR, C. R., KNOPMAN, D. S., JAGUST, W. J., SHAW, L. M., AISEN, P. S., WEINER, M. W., PETERSEN, R. C. & TROJANOWSKI, J. Q. 2010. Hypothetical model of dynamic biomarkers of the Alzheimer's pathological cascade. *The Lancet Neurology,* 9**,** 119-128.

JACK JR, C. R., WISTE, H. J., BOTHA, H., WEIGAND, S. D., THERNEAU, T. M., KNOPMAN, D. S., GRAFF-RADFORD, J., JONES, D. T., FERMAN, T. J. & BOEVE, B. F. 2019. The bivariate distribution of amyloid-β and tau: relationship with established neurocognitive clinical syndromes. *Brain,* 142**,** 3230-3242.

`

JAGUST, W. J., LANDAU, S., SHAW, L., TROJANOWSKI, J., KOEPPE, R., REIMAN, E., FOSTER, N., PETERSEN, R., WEINER, M. & PRICE, J. 2009. Relationships between biomarkers in aging and dementia. *Neurology,* 73**,** 1193-1199.

JANELIDZE, S., STOMRUD, E., PALMQVIST, S., ZETTERBERG, H., VAN WESTEN, D., JEROMIN, A., SONG, L., HANLON, D., TAN HEHIR, C. A. & BAKER, D. 2016a. Plasma β-amyloid in Alzheimer's disease and vascular disease. *Scientific reports,* 6**,** 1-11.

JANELIDZE, S., TEUNISSEN, C. E., ZETTERBERG, H., ALLUÉ, J. A., SARASA, L., EICHENLAUB, U., BITTNER, T., OVOD, V., VERBERK, I. M. & TOBA, K. 2021. Head-to-head comparison of 8 plasma amyloid-β 42/40 assays in Alzheimer disease. *JAMA neurology,* 78**,** 1375-1382.

JANELIDZE, S., ZETTERBERG, H., MATTSSON, N., PALMQVIST, S., VANDERSTICHELE, H., LINDBERG, O., VAN WESTEN, D., STOMRUD, E., MINTHON, L. & BLENNOW, K. 2016b. CSF Aβ42/Aβ40 and Aβ42/Aβ38 ratios: better diagnostic markers of Alzheimer disease. *Annals of clinical and translational neurology,* 3**,** 154-165.

JEFFERSON, T., ČAUŠEVIĆ, M., AUF DEM KELLER, U., SCHILLING, O., ISBERT, S., GEYER, R., MAIER, W., TSCHICKARDT, S., JUMPERTZ, T. & WEGGEN, S. 2011. Metalloprotease meprin β generates nontoxic N-terminal amyloid precursor protein fragments in vivo. *Journal of Biological Chemistry,* 286**,** 27741-27750.

JELLINGER, K. 1998. The neuropathological diagnosis of Alzheimer disease. *Ageing and Dementia***,** 97-118.

JOHNSON, G. D., STEVENSON, T. & AHN, K. 1999. Hydrolysis of peptide hormones by endothelin-converting enzyme-1: a comparison with neprilysin. *Journal of Biological Chemistry,* 274**,** 4053-4058.

JOHNSON, L. L., PAVLOVSKY, A. G., JOHNSON, A. R., JANOWICZ, J. A., MAN, C.-F., ORTWINE, D. F., PURCHASE, C. F., WHITE, A. D. & HUPE, D. J. 2000. A rationalization of the acidic pH dependence for stromelysin-1 (matrix metalloproteinase-3) catalysis and inhibition. *Journal of Biological Chemistry,* 275**,** 11026-11033.

JONSSON, T., ATWAL, J. K., STEINBERG, S., SNAEDAL, J., JONSSON, P. V., BJORNSSON, S., STEFANSSON, H., SULEM, P., GUDBJARTSSON, D. & MALONEY, J. 2012. A mutation in APP protects against Alzheimer's disease and age-related cognitive decline. *Nature,* 488**,** 96-99.

KAESER, S. A., HÄSLER, L. M., LAMBERT, M., BERGMANN, C., BOTTELBERGS, A., THEUNIS, C., MERCKEN, M. & JUCKER, M. 2022. CSF p-tau increase in response to Aβ-type and Danish-type cerebral amyloidosis and in the absence of neurofibrillary tangles. *Acta neuropathologica,* 143**,** 287-290.

KAKUDA, N., FUNAMOTO, S., YAGISHITA, S., TAKAMI, M., OSAWA, S., DOHMAE, N. & IHARA, Y. 2006. Equimolar production of amyloid β-protein and amyloid precursor protein intracellular domain from β-carboxyl-terminal fragment by γ-secretase. *Journal of Biological Chemistry,* 281**,** 14776-14786.

KANDALEPAS, P. C., SADLEIR, K. R., EIMER, W. A., ZHAO, J., NICHOLSON, D. A. & VASSAR, R. 2013. The Alzheimer's β-secretase BACE1 localizes to normal presynaptic terminals and to dystrophic presynaptic terminals surrounding amyloid plaques. *Acta neuropathologica,* 126**,** 329-352.

KANG, E. L., BISCARO, B., PIAZZA, F. & TESCO, G. 2012. BACE1 protein endocytosis and trafficking are differentially regulated by ubiquitination at lysine 501 and the Di-leucine motif in the carboxyl terminus. *Journal of Biological Chemistry,* 287**,** 42867-42880.

KANG, J., LEMAIRE, H.-G., UNTERBECK, A., SALBAUM, J. M., MASTERS, C. L., GRZESCHIK, K.-H., MULTHAUP, G., BEYREUTHER, K. & MÜLLER-HILL, B. 1987. The precursor of Alzheimer's disease amyloid A4 protein resembles a cell-surface receptor. *Nature,* 325**,** 733-736.

KARRAN, E., MERCKEN, M. & STROOPER, B. D. 2011. The amyloid cascade hypothesis for Alzheimer's disease: an appraisal for the development of therapeutics. *Nature reviews Drug discovery,* 10**,** 698-712.

`

KATZMAN, R. 1976. The prevalence and malignancy of Alzheimer disease: a major killer. *Archives of neurology,* 33**,** 217-218.

KAYED, R., HEAD, E., THOMPSON, J. L., MCINTIRE, T. M., MILTON, S. C., COTMAN, C. W. & GLABE, C. G. 2003. Common structure of soluble amyloid oligomers implies common mechanism of pathogenesis. *Science,* 300**,** 486-489.

KENNEDY, M. E., STAMFORD, A. W., CHEN, X., COX, K., CUMMING, J. N., DOCKENDORF, M. F., EGAN, M., ERESHEFSKY, L., HODGSON, R. A. & HYDE, L. A. 2016. The BACE1 inhibitor verubecestat (MK-8931) reduces CNS β-amyloid in animal models and in Alzheimer's disease patients. *Science translational medicine,* 8**,** 363ra150-363ra150.

KESHAVAN, A., PANNEE, J., KARIKARI, T. K., RODRIGUEZ, J. L., ASHTON, N. J., NICHOLAS, J. M., CASH, D. M., COATH, W., LANE, C. A. & PARKER, T. D. 2021. Population-based blood screening for preclinical Alzheimer's disease in a British birth cohort at age 70. *Brain,* 144**,** 434-449.

KIDD, M. 1963. Paired helical filaments in electron microscopy of Alzheimer's disease. *Nature,* 197**,** 192-193.

KIM, J.-W., JUNG, S.-Y., KIM, Y., HEO, H., HONG, C.-H., SEO, S.-W., CHOI, S.-H., SON, S.-J., LEE, S. & CHANG, J. 2021. Identification of cathepsin D as a plasma biomarker for Alzheimer's disease. *Cells,* 10**,** 138.

KIM, T.-W., WU, K., XU, J.-L., MCAULIFFE, G., TANZI, R. E., WASCO, W. & BLACK, I. B. 1995. Selective localization of amyloid precursor-like protein 1 in the cerebral cortex postsynaptic density. *Molecular brain research,* 32**,** 36-44.

KIMBERLY, W. T., LAVOIE, M. J., OSTASZEWSKI, B. L., YE, W., WOLFE, M. S. & SELKOE, D. J. 2003. γ-Secretase is a membrane protein complex comprised of presenilin, nicastrin, aph-1, and pen-2. *Proceedings of the National Academy of Sciences,* 100**,** 6382-6387.

KINDY, M. S., YU, J., ZHU, H., EL-AMOURI, S. S., HOOK, V. & HOOK, G. R. 2012. Deletion of the cathepsin B gene improves memory deficits in a transgenic Alzheimer's disease mouse model expressing AβPP containing the wild-type β-secretase site sequence. *Journal of Alzheimer's Disease,* 29**,** 827-840.

KINOSHITA, A., FUKUMOTO, H., SHAH, T., WHELAN, C. M., IRIZARRY, M. C. & HYMAN, B. T. 2003. Demonstration by FRET of BACE interaction with the amyloid precursor protein at the cell surface and in early endosomes. *J Cell Sci,* 116**,** 3339-46.

KIRABALI, T., RIGOTTI, S., SICCOLI, A., LIEBSCH, F., SHOBO, A., HOCK, C., NITSCH, R. M., MULTHAUP, G. & KULIC, L. 2019. The amyloid-β degradation intermediate Aβ34 is pericyte-associated and reduced in brain capillaries of patients with Alzheimer's disease. *Acta neuropathologica communications,* 7**,** 1-14.

KNOWLES, R. B., WYART, C., BULDYREV, S. V., CRUZ, L., URBANC, B., HASSELMO, M. E., STANLEY, H. E. & HYMAN, B. T. 1999. Plaque-induced neurite abnormalities: implications for disruption of neural networks in Alzheimer's disease. *Proceedings of the National Academy of Sciences,* 96**,** 5274-5279.

KOO, E. H., SISODIA, S. S., ARCHER, D. R., MARTIN, L. J., WEIDEMANN, A., BEYREUTHER, K., FISCHER, P., MASTERS, C. L. & PRICE, D. L. 1990. Precursor of amyloid protein in Alzheimer disease undergoes fast anterograde axonal transport. *Proceedings of the National Academy of Sciences,* 87**,** 1561-1565.

KORTH, P., BOHLE, R. M., CORVOL, P. & PINET, F. 1999. Cellular distribution of endothelin-converting enzyme-1 in human tissues. *Journal of Histochemistry & Cytochemistry,* 47**,** 447-461.

KUKAR, T. & GOLDE, T. E. 2008. Possible mechanisms of action of NSAIDs and related compounds that modulate γ-secretase cleavage. *Current topics in medicinal chemistry,* 8**,** 47-53.

KUKKOLA, P. J., SAVAGE, P., SAKANE, Y., BERRY, J. C., BILCI, N. A., GHAI, R. D. & JENG, A. Y. 1995. Differential structure-activity relationships of phosphoramidon analogues for inhibition of three

metalloproteases: endothelin-converting enzyme, neutral endopeptidase, and angiotensin-converting enzyme. *Journal of cardiovascular pharmacology,* 26**,** S65-8.

KULIC, L., MCAFOOSE, J., WELT, T., TACKENBERG, C., SPÄNI, C., WIRTH, F., FINDER, V., KONIETZKO, U., GIESE, M. & ECKERT, A. 2012. Early accumulation of intracellular fibrillar oligomers and late congophilic amyloid angiopathy in mice expressing the Osaka intra-Aβ APP mutation. *Translational psychiatry,* 2**,** e183-e183.

KUMAR, D., GANESHPURKAR, A., KUMAR, D., MODI, G., GUPTA, S. K. & SINGH, S. K. 2018. Secretase inhibitors for the treatment of Alzheimer's disease: long road ahead. *European Journal of Medicinal Chemistry,* 148**,** 436-452.

KURUPPU, S. & SMITH, A. I. 2012. Endothelin Converting Enzyme-1 phosphorylation and trafficking. *FEBS letters,* 586**,** 2212-2217.

LAI, M.-T., CHEN, E., CROUTHAMEL, M.-C., DIMUZIO-MOWER, J., XU, M., HUANG, Q., PRICE, E., REGISTER, R. B., SHI, X.-P. & DONOVIEL, D. B. 2003. Presenilin-1 and presenilin-2 exhibit distinct yet overlapping γ-secretase activities. *Journal of Biological Chemistry,* 278**,** 22475-22481.

LAMBERT, M. P., BARLOW, A., CHROMY, B. A., EDWARDS, C., FREED, R., LIOSATOS, M., MORGAN, T., ROZOVSKY, I., TROMMER, B. & VIOLA, K. L. 1998. Diffusible, nonfibrillar ligands derived from Aβ1–42 are potent central nervous system neurotoxins. *Proceedings of the National Academy of Sciences,* 95**,** 6448-6453.

LANDRY, C., SANTAGATA, P., BAWAB, W., FOURNIÉ-ZALUSKI, M. C., ROQUES, B. P., VINAY, P. & CRINE, P. 1993. Characterization of neutral endopeptidase 24.11 in dog glomeruli. *Biochemical Journal,* 291**,** 773-779.

LAZAROV, O. & MARR, R. A. 2010. Neurogenesis and Alzheimer's disease: at the crossroads. *Experimental neurology,* 223**,** 267-281.

LEE, E. B., SKOVRONSKY, D. M., ABTAHIAN, F., DOMS, R. W. & LEE, V. M.-Y. 2003. Secretion and intracellular generation of truncated Aβ in β-site amyloid-β precursor protein-cleaving enzyme expressing human neurons. *Journal of Biological Chemistry,* 278**,** 4458-4466.

LEE, E. B., ZHANG, B., LIU, K., GREENBAUM, E. A., DOMS, R. W., TROJANOWSKI, J. Q. & LEE, V. M.-Y. 2005. BACE overexpression alters the subcellular processing of APP and inhibits Aβ deposition in vivo. *The Journal of cell biology,* 168**,** 291-302.

LEE, J.-H., YANG, D.-S., GOULBOURNE, C. N., IM, E., STAVRIDES, P., PENSALFINI, A., CHAN, H., BOUCHET-MARQUIS, C., BLEIWAS, C. & BERG, M. J. 2022. Faulty autolysosome acidification in Alzheimer's disease mouse models induces autophagic build-up of Aβ in neurons, yielding senile plaques. *Nature Neuroscience***,** 1-14.

LEE, V. M., GOEDERT, M. & TROJANOWSKI, J. Q. 2001. Neurodegenarative tauopathies. *Annual review of neuroscience,* 24**,** 1121.

LEISSRING, M. A., LAFERLA, F. M., CALLAMARAS, N. & PARKER, I. 2001. Subcellular mechanisms of presenilin-mediated enhancement of calcium signaling. *Neurobiology of disease,* 8**,** 469-478.

LEISSRING, M. A., REINSTATLER, L., SAHARA, T., SEVLEVER, D., ROMAN, R., JI, Z., LI, L., LU, Q., SÄFTIG, P. & LEVITES, Y. 2009. O4-03-07: Cathepsin D knockout mice harbor large and highly selective increases in cerebral Aß42 and tau: Implications for Alzheimer's disease pathogenesis. *Alzheimer's & Dementia,* 5**,** P155-P156.

LEISSRING, M. A., YAMASAKI, T. R., WASCO, W., BUXBAUM, J. D., PARKER, I. & LAFERLA, F. M. 2000. Calsenilin reverses presenilin-mediated enhancement of calcium signaling. *Proceedings of the National Academy of Sciences,* 97**,** 8590-8593.

LEUZY, A., CHIOTIS, K., HASSELBALCH, S. G., RINNE, J. O., DE MENDONÇA, A., OTTO, M., LLEO, A., CASTELO-BRANCO, M., SANTANA, I. & JOHANSSON, J. 2016. Pittsburgh compound B imaging and cerebrospinal fluid amyloid-β in a multicentre European memory clinic study. *Brain,* 139**,** 2540-2553.

`

LEVY-LAHAD, E., WASCO, W., POORKAJ, P., ROMANO, D. M., OSHIMA, J., PETTINGELL, W. H., YU, C.-E., JONDRO, P. D., SCHMIDT, S. D. & WANG, K. 1995. Candidate gene for the chromosome 1 familial Alzheimer's disease locus. *Science,* 269**,** 973-977.

LEWCZUK, P., MATZEN, A., BLENNOW, K., PARNETTI, L., MOLINUEVO, J. L., EUSEBI, P., KORNHUBER, J., MORRIS, J. C. & FAGAN, A. M. 2017. Cerebrospinal fluid Aβ 42/40 corresponds better than Aβ 42 to amyloid PET in Alzheimer's Disease. *Journal of Alzheimer's Disease,* 55**,** 813-822.

LI, R., LINDHOLM, K., YANG, L.-B., YUE, X., CITRON, M., YAN, R., BEACH, T., SUE, L., SABBAGH, M. & CAI, H. 2004. Amyloid β peptide load is correlated with increased β-secretase activity in sporadic Alzheimer's disease patients. *Proceedings of the National Academy of Sciences,* 101**,** 3632-3637.

LICHTENTHALER, S. F., MULTHAUP, G., MASTERS, C. L. & BEYREUTHER, K. 1999. A novel substrate for analyzing Alzheimer's disease γ-secretase. *FEBS letters,* 453**,** 288-292.

LIEBSCH, F., KULIC, L., TEUNISSEN, C., SHOBO, A., ULKU, I., ENGELSCHALT, V., HANCOCK, M. A., VAN DER FLIER, W. M., KUNACH, P., ROSA-NETO, P., SCHELTENS, P., POIRIER, J., SAFTIG, P., BATEMAN, R., BREITNER, J., HOCK, C. & MULTHAUP, G. 2019. Aβ34 is a BACE1-derived degradation intermediate associated with amyloid clearance and Alzheimer's disease progression. *Nature communications,* 10**,** 1-15.

LINEBAUGH, B. E., SAMENI, M., DAY, N. A., SLOANE, B. F. & KEPPLER, D. 1999. Exocytosis of active cathepsin B: enzyme activity at pH 7.0, inhibition and molecular mass. *European journal of biochemistry,* 264**,** 100-109.

LISTA, S., FALTRACO, F. & HAMPEL, H. 2013a. Biological and methodical challenges of blood-based proteomics in the field of neurological research. *Progress in neurobiology,* 101**,** 18-34.

LISTA, S., FALTRACO, F., PRVULOVIC, D. & HAMPEL, H. 2013b. Blood and plasma-based proteomic biomarker research in Alzheimer's disease. *Progress in neurobiology,* 101**,** 1-17.

LORENZL, S., ALBERS, D. S., RELKIN, N., NGYUEN, T., HILGENBERG, S. L., CHIRICHIGNO, J., CUDKOWICZ, M. E. & BEAL, M. F. 2003. Increased plasma levels of matrix metalloproteinase-9 in patients with Alzheimer's disease. *Neurochemistry international,* 43**,** 191-196.

LORENZL, S., BÜERGER, K., HAMPEL, H. & BEAL, M. F. 2008. Profiles of matrix metalloproteinases and their inhibitors in plasma of patients with dementia. *International psychogeriatrics,* 20**,** 67-76.

LUO, Y., BOLON, B., KAHN, S., BENNETT, B. D., BABU-KHAN, S., DENIS, P., FAN, W., KHA, H., ZHANG, J. & GONG, Y. 2001. Mice deficient in BACE1, the Alzheimer's β-secretase, have normal phenotype and abolished β-amyloid generation. *Nature neuroscience,* 4**,** 231-232.

MACOURS, N., POELS, J., HENS, K., FRANCIS, C. & HUYBRECHTS, R. 2004. Structure, evolutionary conservation, and functions of angiotensin-and endothelin-converting enzymes. *International review of cytology,* 239**,** 47.

MAIA, L. F., KAESER, S. A., REICHWALD, J., HRUSCHA, M., MARTUS, P., STAUFENBIEL, M. & JUCKER, M. 2013. Changes in amyloid-β and Tau in the cerebrospinal fluid of transgenic mice overexpressing amyloid precursor protein. *Science translational medicine,* 5**,** 194re2-194re2.

MASTERS, C. L., MULTHAUP, G., SIMMS, G., POTTGIESSER, J., MARTINS, R. & BEYREUTHER, K. 1985. Neuronal origin of a cerebral amyloid: neurofibrillary tangles of Alzheimer's disease contain the same protein as the amyloid of plaque cores and blood vessels. *The EMBO journal,* 4**,** 2757-2763.

MATTSSON, N., RAJENDRAN, L., ZETTERBERG, H., GUSTAVSSON, M., ANDREASSON, U., OLSSON, M., BRINKMALM, G., LUNDKVIST, J., JACOBSON, L. H. & PERROT, L. 2012. BACE1 inhibition induces a specific cerebrospinal fluid β-amyloid pattern that identifies drug effects in the central nervous system. *PloS one,* 7**,** e31084.

MAURER, K., VOLK, S. & GERBALDO, H. 1997. Auguste D and Alzheimer's disease. *The lancet,* 349**,** 1546-1549.

`

MAWUENYEGA, K. G., SIGURDSON, W., OVOD, V., MUNSELL, L., KASTEN, T., MORRIS, J. C., YARASHESKI, K. E. & BATEMAN, R. J. 2010. Decreased clearance of CNS β-amyloid in Alzheimer's disease. *Science,* 330**,** 1774-1774.

MAY, P. C., DEAN, R. A., LOWE, S. L., MARTENYI, F., SHEEHAN, S. M., BOGGS, L. N., MONK, S. A., MATHES, B. M., MERGOTT, D. J. & WATSON, B. M. 2011. Robust central reduction of amyloid-β in humans with an orally available, non-peptidic β-secretase inhibitor. *Journal of Neuroscience,* 31**,** 16507-16516.

MAY, P. C., WILLIS, B. A., LOWE, S. L., DEAN, R. A., MONK, S. A., COCKE, P. J., AUDIA, J. E., BOGGS, L. N., BORDERS, A. R. & BRIER, R. A. 2015. The potent BACE1 inhibitor LY2886721 elicits robust central Aβ pharmacodynamic responses in mice, dogs, and humans. *Journal of Neuroscience,* 35**,** 1199-1210.

MAYNARD, C. J., CAPPAI, R., VOLITAKIS, I., CHERNY, R. A., WHITE, A. R., BEYREUTHER, K., MASTERS, C. L., BUSH, A. I. & LI, Q.-X. 2002. Overexpression of Alzheimer's disease amyloid-β opposes the age-dependent elevations of brain copper and iron. *Journal of Biological Chemistry,* 277**,** 44670-44676.

MCDADE, E., VOYTYUK, I., AISEN, P., BATEMAN, R. J., CARRILLO, M. C., DE STROOPER, B., HAASS, C., REIMAN, E. M., SPERLING, R. & TARIOT, P. N. 2021. The case for low-level BACE1 inhibition for the prevention of Alzheimer disease. *Nature Reviews Neurology,* 17**,** 703-714.

MCKHANN, G. M., KNOPMAN, D. S., CHERTKOW, H., HYMAN, B. T., JACK JR, C. R., KAWAS, C. H., KLUNK, W. E., KOROSHETZ, W. J., MANLY, J. J. & MAYEUX, R. 2011. The diagnosis of dementia due to Alzheimer's disease: Recommendations from the National Institute on Aging-Alzheimer's Association workgroups on diagnostic guidelines for Alzheimer's disease. *Alzheimer's & dementia,* 7**,** 263-269.

MECKLER, X. & CHECLER, F. 2016. Presenilin 1 and presenilin 2 target γ-secretase complexes to distinct cellular compartments. *Journal of Biological Chemistry,* 291**,** 12821-12837.

MOLINUEVO, J. L., AYTON, S., BATRLA, R., BEDNAR, M. M., BITTNER, T., CUMMINGS, J., FAGAN, A. M., HAMPEL, H., MIELKE, M. M. & MIKULSKIS, A. 2018. Current state of Alzheimer's fluid biomarkers. *Acta neuropathologica,* 136**,** 821-853.

MÖLLER, H.-J. & GRAEBER, M. B. 1998. The case described by Alois Alzheimer in 1911. *European archives of psychiatry and clinical neuroscience,* 248**,** 111-122.

MORENA, F., ARGENTATI, C., TROTTA, R., CRISPOLTONI, L., STABILE, A., PISTILLI, A., DI BALDASSARRE, A., CALAFIORE, R., MONTANUCCI, P. & BASTA, G. 2017. A comparison of lysosomal enzymes expression levels in peripheral blood of mild-and severe-Alzheimer's disease and MCI patients: Implications for regenerative medicine approaches. *International Journal of Molecular Sciences,* 18**,** 1806.

MOTTER, N., VIGO-PELFREY, C., KHOLODENKO, D., BARBOUR, R., JOHNSON-WOOD, K., GALASKO, D., CHANG, L., MILLER, B., CLARK, C. & GREEN, R. 1995. Reduction of β-amyloid peptide42 in the cerebrospinal fluid of patients with Alzheimer's disease. *Annals of Neurology: Official Journal of the American Neurological Association and the Child Neurology Society,* 38**,** 643-648.

MROCZKO, B., GROBLEWSKA, M., ZBOCH, M., KULCZYŃSKA, A., KOPER, O. M., SZMITKOWSKI, M., KORNHUBER, J. & LEWCZUK, P. 2014. Concentrations of matrix metalloproteinases and their tissue inhibitors in the cerebrospinal fluid of patients with Alzheimer's disease. *Journal of Alzheimer's Disease,* 40**,** 351-357.

MUELLER-STEINER, S., ZHOU, Y., ARAI, H., ROBERSON, E. D., SUN, B., CHEN, J., WANG, X., YU, G., ESPOSITO, L. & MUCKE, L. 2006. Antiamyloidogenic and neuroprotective functions of cathepsin B: implications for Alzheimer's disease. *Neuron,* 51**,** 703-714.

`

MULLAN, M., CRAWFORD, F., AXELMAN, K., HOULDEN, H., LILIUS, L., WINBLAD, B. & LANNFELT, L. 1992. A pathogenic mutation for probable Alzheimer's disease in the APP gene at the N–terminus of β–amyloid. *Nature genetics,* 1**,** 345-347.

MÜLLER, U., CRISTINA, N., LI, Z.-W., WOLFER, D. P., LIPP, H.-P., RÜLICKE, T., BRANDNER, S., AGUZZI, A. & WEISSMANN, C. 1994. Behavioral and anatomical deficits in mice homozygous for a modified β-amyloid precursor protein gene. *Cell,* 79**,** 755-765.

NACMIAS, B., BAGNOLI, S., TEDDE, A., CELLINI, E., BESSI, V., GUARNIERI, B., ORTENSI, L., PIACENTINI, S., BRACCO, L. & SORBI, S. 2007. Angiotensin converting enzyme insertion/deletion polymorphism in sporadic and familial Alzheimer's disease and longevity. *Archives of gerontology and geriatrics,* 45**,** 201-206.

NAKAMURA, A., KANEKO, N., VILLEMAGNE, V. L., KATO, T., DOECKE, J., DORÉ, V., FOWLER, C., LI, Q.-X., MARTINS, R. & ROWE, C. 2018. High performance plasma amyloid-β biomarkers for Alzheimer's disease. *Nature,* 554**,** 249-254.

NALIVAEVA, N. N., BELYAEV, N. D., KERRIDGE, C. & TURNER, A. J. 2014. Amyloid-clearing proteins and their epigenetic regulation as a therapeutic target in Alzheimer's disease. *Frontiers in aging neuroscience,* 6**,** 235.

NEUMANN, U., RUEEGER, H., MACHAUER, R., VEENSTRA, S. J., LUEOEND, R. M., TINTELNOT-BLOMLEY, M., LAUE, G., BELTZ, K., VOGG, B. & SCHMID, P. 2015. A novel BACE inhibitor NB-360 shows a superior pharmacological profile and robust reduction of amyloid-β and neuroinflammation in APP transgenic mice. *Molecular neurodegeneration,* 10**,** 1-15.

NISHITOMI, K., SAKAGUCHI, G., HORIKOSHI, Y., GRAY, A. J., MAEDA, M., HIRATA-FUKAE, C., BECKER, A. G., HOSONO, M., SAKAGUCHI, I. & MINAMI, S. S. 2006. BACE1 inhibition reduces endogenous Abeta and alters APP processing in wild-type mice 2. *Journal of neurochemistry,* 99**,** 1555-1563.

O'BRIEN, R. J. & WONG, P. C. 2011. Amyloid precursor protein processing and Alzheimer's disease. *Annual review of neuroscience,* 34**,** 185-204.

OLSSON, B., LAUTNER, R., ANDREASSON, U., ÖHRFELT, A., PORTELIUS, E., BJERKE, M., HÖLTTÄ, M., ROSÉN, C., OLSSON, C. & STROBEL, G. 2016. CSF and blood biomarkers for the diagnosis of Alzheimer's disease: a systematic review and meta-analysis. *The Lancet Neurology,* 15**,** 673-684.

OLSSON, F., SCHMIDT, S., ALTHOFF, V., MUNTER, L. M., JIN, S., ROSQVIST, S., LENDAHL, U., MULTHAUP, G. & LUNDKVIST, J. 2014. Characterization of intermediate steps in amyloid beta (Aβ) production under near-native conditions. *Journal of Biological Chemistry,* 289**,** 1540-1550.

PACHECO-QUINTO, J. & ECKMAN, E. A. 2013. Endothelin-converting enzymes degrade intracellular β-amyloid produced within the endosomal/lysosomal pathway and autophagosomes. *Journal of Biological Chemistry,* 288**,** 5606-5615.

PALMQVIST, S., JANELIDZE, S., QUIROZ, Y. T., ZETTERBERG, H., LOPERA, F., STOMRUD, E., SU, Y., CHEN, Y., SERRANO, G. E. & LEUZY, A. 2020. Discriminative accuracy of plasma phospho-tau217 for Alzheimer disease vs other neurodegenerative disorders. *Jama,* 324**,** 772-781.

PANNEE, J., PORTELIUS, E., MINTHON, L., GOBOM, J., ANDREASSON, U., ZETTERBERG, H., HANSSON, O. & BLENNOW, K. 2016. Reference measurement procedure for CSF amyloid beta (Aβ) 1–42 and the CSF Aβ1–42/Aβ1–40 ratio–a cross-validation study against amyloid PET. *Journal of neurochemistry,* 139**,** 651-658.

PARDOSSI-PIQUARD, R., PETIT, A., KAWARAI, T., SUNYACH, C., DA COSTA, C. A., VINCENT, B., RING, S., D'ADAMIO, L., SHEN, J. & MÜLLER, U. 2005. Presenilin-dependent transcriptional control of the Aβ-degrading enzyme neprilysin by intracellular domains of βAPP and APLP. *Neuron,* 46**,** 541-554.

PASCHKOWSKY, S., HAMZÉ, M., OESTEREICH, F. & MUNTER, L. M. 2016. Alternative processing of the amyloid precursor protein family by rhomboid protease RHBDL4. *Journal of Biological Chemistry,* 291**,** 21903-21912.

`

PATTERSON, B. W., ELBERT, D. L., MAWUENYEGA, K. G., KASTEN, T., OVOD, V., MA, S., XIONG, C., CHOTT, R., YARASHESKI, K. & SIGURDSON, W. 2015. Age and amyloid effects on human central nervous system amyloid-beta kinetics. *Annals of neurology,* 78**,** 439-453.

PEACOCK, M. L., WARREN, J. T., ROSES, A. D. & FINK, J. K. 1993. Novel polymorphism in the A4 region of the amyloid precursor protein gene in a patient without Alzheimer's disease. *Neurology,* 43**,** 1254-1254.

PEREZ, R. G., ZHENG, H., VAN DER PLOEG, L. H. & KOO, E. H. 1997. The β-amyloid precursor protein of Alzheimer's disease enhances neuron viability and modulates neuronal polarity. *Journal of Neuroscience,* 17**,** 9407-9414.

PETERS, F., SALIHOGLU, H., RODRIGUES, E., HERZOG, E., BLUME, T., FILSER, S., DOROSTKAR, M., SHIMSHEK, D. R., BROSE, N. & NEUMANN, U. 2018. BACE1 inhibition more effectively suppresses initiation than progression of β-amyloid pathology. *Acta neuropathologica,* 135**,** 695-710.

PHINNEY, A., CALHOUN, M., WOLFER, D., LIPP, H.-P., ZHENG, H. & JUCKER, M. 1999. No hippocampal neuron or synaptic bouton loss in learning-impaired aged β-amyloid precursor protein-null mice. *Neuroscience,* 90**,** 1207-1216.

PHINNEY, A. L., HORNE, P., YANG, J., JANUS, C., BERGERON, C. & WESTAWAY, D. 2003. Mouse models of Alzheimer's disease: the long and filamentous road. *Neurological research,* 25**,** 590-600.

PIKE, C. J., CUMMINGS, B. J. & COTMAN, C. W. 1995. Early association of reactive astrocytes with senile plaques in Alzheimer's disease. *Experimental neurology,* 132**,** 172-179.

PORTELIUS, E., GUSTAVSSON, M. K., ZETTERBERG, H., ANDREASSON, U. & BLENNOW, K. 2012. Evaluation of the performance of novel Aβ isoforms as theragnostic markers in Alzheimer's disease: from the cell to the patient. *Neurodegenerative Diseases,* 10**,** 138-140.

PRABHU, Y., BURGOS, P. V., SCHINDLER, C., FARIAS, G. G., MAGADAN, J. G. & BONIFACINO, J. S. 2012. Adaptor protein 2-mediated endocytosis of the beta-secretase BACE1 is dispensable for amyloid precursor protein processing. *Mol Biol Cell,* 23**,** 2339-51.

PUZZO, D., PRIVITERA, L., LEZNIK, E., FA, M., STANISZEWSKI, A., PALMERI, A. & ARANCIO, O. 2008. Picomolar amyloid-β positively modulates synaptic plasticity and memory in hippocampus. *Journal of Neuroscience,* 28**,** 14537-14545.

QIU, W. Q., YE, Z., KHOLODENKO, D., SEUBERT, P. & SELKOE, D. J. 1997. Degradation of amyloid β-protein by a metalloprotease secreted by microglia and other neural and non-neural cells. *Journal of Biological Chemistry,* 272**,** 6641-6646.

QUARTEY, M. O., NYARKO, J. N., MALEY, J. M., BARNES, J. R., BOLANOS, M. A., HEISTAD, R. M., KNUDSEN, K. J., PENNINGTON, P. R., BUTTIGIEG, J. & DE CARVALHO, C. E. 2021. The Aβ (1–38) peptide is a negative regulator of the Aβ (1–42) peptide implicated in Alzheimer disease progression. *Scientific reports,* 11**,** 1-17.

RASMUSSEN, M. K., MESTRE, H. & NEDERGAARD, M. 2018. The glymphatic pathway in neurological disorders. *The Lancet Neurology,* 17**,** 1016-1024.

RING, S., WEYER, S. W., KILIAN, S. B., WALDRON, E., PIETRZIK, C. U., FILIPPOV, M. A., HERMS, J., BUCHHOLZ, C., ECKMAN, C. B. & KORTE, M. 2007. The secreted β-amyloid precursor protein ectodomain APPsα is sufficient to rescue the anatomical, behavioral, and electrophysiological abnormalities of APP-deficient mice. *Journal of Neuroscience,* 27**,** 7817-7826.

RIVERO-SANTANA, A., FERREIRA, D., PERESTELO-PEREZ, L., WESTMAN, E., WAHLUND, L.-O., SARRIA, A. & SERRANO-AGUILAR, P. 2017. Cerebrospinal fluid biomarkers for the differential diagnosis between Alzheimer's disease and frontotemporal lobar degeneration: systematic review, HSROC analysis, and confounding factors. *Journal of Alzheimer's Disease,* 55**,** 625-644.

ROBERDS, S. L., ANDERSON, J., BASI, G., BIENKOWSKI, M. J., BRANSTETTER, D. G., CHEN, K. S., FREEDMAN, S., FRIGON, N. L., GAMES, D. & HU, K. 2001. BACE knockout mice are healthy

despite lacking the primary β-secretase activity in brain: implications for Alzheimer's disease therapeutics. *Human molecular genetics,* 10**,** 1317-1324.

ROCKENSTEIN, E., MANTE, M., ALFORD, M., ADAME, A., CREWS, L., HASHIMOTO, M., ESPOSITO, L., MUCKE, L. & MASLIAH, E. 2005. High β-secretase activity elicits neurodegeneration in transgenic mice despite reductions in amyloid-β levels: implications for the treatment of Alzheimer disease. *Journal of Biological Chemistry,* 280**,** 32957-32967.

RODRIGUES, D. I., GUTIERRES, J., PLIASSOVA, A., OLIVEIRA, C. R., CUNHA, R. A. & AGOSTINHO, P. 2014. Synaptic and sub-synaptic localization of amyloid-β protein precursor in the rat hippocampus. *Journal of Alzheimer's Disease,* 40**,** 981-992.

ROGAEV, E., SHERRINGTON, R., ROGAEVA, E., LEVESQUE, G., IKEDA, M., LIANG, Y., CHI, H., LIN, C., HOLMAN, K. & TSUDA, T. 1995. Familial Alzheimer's disease in kindreds with missense mutations in a gene on chromosome 1 related to the Alzheimer's disease type 3 gene. *Nature,* 376**,** 775-778.

ROZEMULLER, J., EIKELENBOOM, P., STAM, F., BEYREUTHER, K. & MASTERS, C. 1989. A4 protein in Alzheimer's disease: primary and secondary cellular events in extracellular amyloid deposition. *Journal of Neuropathology & Experimental Neurology,* 48**,** 674-691.

SADLEIR, K. R., KANDALEPAS, P. C., BUGGIA-PRÉVOT, V., NICHOLSON, D. A., THINAKARAN, G. & VASSAR, R. 2016. Presynaptic dystrophic neurites surrounding amyloid plaques are sites of microtubule disruption, BACE1 elevation, and increased Aβ generation in Alzheimer's disease. *Acta neuropathologica,* 132**,** 235-256.

SAGARE, A., DEANE, R., BELL, R. D., JOHNSON, B., HAMM, K., PENDU, R., MARKY, A., LENTING, P. J., WU, Z. & ZARCONE, T. 2007. Clearance of amyloid-β by circulating lipoprotein receptors. *Nature medicine,* 13**,** 1029-1031.

SAIDO, T. & LEISSRING, M. A. 2012. Proteolytic degradation of amyloid β-protein. *Cold Spring Harbor perspectives in medicine,* 2**,** a006379.

SAITO, T., TAKAKI, Y., IWATA, N., TROJANOWSKI, J. & SAIDO, T. C. 2003. Alzheimer's disease, neuropeptides, neuropeptidase, and amyloid-β peptide metabolism. *Science of Aging Knowledge Environment,* 2003**,** pe1-pe1.

SAMIMI, N., SHARMA, G., KIMURA, T., MATSUBARA, T., HUO, A., CHIBA, K., SAITO, Y., MURAYAMA, S., AKATSU, H. & HASHIZUME, Y. 2021. Distinct phosphorylation profiles of tau in brains of patients with different tauopathies. *Neurobiology of Aging,* 108**,** 72-79.

SANNERUD, R., DECLERCK, I., PERIC, A., RAEMAEKERS, T., MENENDEZ, G., ZHOU, L., VEERLE, B., COEN, K., MUNCK, S., DE STROOPER, B., SCHIAVO, G. & ANNAERT, W. 2011. ADP ribosylation factor 6 (ARF6) controls amyloid precursor protein (APP) processing by mediating the endosomal sorting of BACE1. *Proc Natl Acad Sci U S A,* 108**,** E559-68.

SANNERUD, R., ESSELENS, C., EJSMONT, P., MATTERA, R., ROCHIN, L., THARKESHWAR, A. K., DE BAETS, G., DE WEVER, V., HABETS, R. & BAERT, V. 2016. Restricted location of PSEN2/γ-secretase determines substrate specificity and generates an intracellular Aβ pool. *Cell,* 166**,** 193-208.

SARIC, A., BRÜGGE, L. Z., MÜLLER-POMPALLA, D., RYSIOK, T., OUSSON, S., PERMANNE, B., QUATTROPANI, A., BUSCH, M., BEHER, D. & HUSSAIN, I. 2013. Development and characterization of a novel membrane assay for full-length BACE-1 at pH 6.0. *Journal of biomolecular screening,* 18**,** 277-285.

SATO, C., TAKAGI, S., TOMITA, T. & IWATSUBO, T. 2008. The C-terminal PAL motif and transmembrane domain 9 of presenilin 1 are involved in the formation of the catalytic pore of the γ-secretase. *Journal of Neuroscience,* 28**,** 6264-6271.

SAUNDERS, A. M., STRITTMATTER, W. J., SCHMECHEL, D., GEORGE-HYSLOP, P. S., PERICAK-VANCE, M. A., JOO, S., ROSI, B., GUSELLA, J., CRAPPER-MACLACHLAN, D. & ALBERTS, M. 1993. Association of

apolipoprotein E allele ϵ4 with late-onset familial and sporadic Alzheimer's disease. *Neurology,* 43**,** 1467-1467.

SCHOENFELD, H. A., WEST, T., VERGHESE, P. B., HOLUBASCH, M., SHENOY, N., KAGAN, D., BUONO, C., ZHOU, W., DECRISTOFARO, M. & DOUVILLE, J. 2017. The effect of angiotensin receptor neprilysin inhibitor, sacubitril/valsartan, on central nervous system amyloid-β concentrations and clearance in the cynomolgus monkey. *Toxicology and applied pharmacology,* 323**,** 53-65.

SCHOLZ, D., CHERNYSHOVA, Y., ÜCKERT, A. K. & LEIST, M. 2018. Reduced Aβ secretion by human neurons under conditions of strongly increased BACE activity. *Journal of neurochemistry,* 147**,** 256-274.

SCHWEIZER, A., VALDENAIRE, O., NELBOCK, P., DEUSCHILE, U., DUMAS MILNE EDWARDS, J.-B., STUMPF, J. G. & LOFFLER, B.-M. 1997. Human endothelin-converting enzyme (ECE-1): three isoforms with distinct subcellular localizations. *Biochemical Journal,* 328**,** 871-877.

SEABROOK, G., SMITH, D., BOWERY, B., EASTER, A., REYNOLDS, T., FITZJOHN, S., MORTON, R., ZHENG, H., DAWSON, G. & SIRINATHSINGHJI, D. 1999. Mechanisms contributing to the deficits in hippocampal synaptic plasticity in mice lacking amyloid precursor protein. *Neuropharmacology,* 38**,** 349-359.

SEEBURGER, J. L., HOLDER, D. J., COMBRINCK, M., JOACHIM, C., LATERZA, O., TANEN, M., DALLOB, A., CHAPPELL, D., SNYDER, K. & FLYNN, M. 2015. Cerebrospinal fluid biomarkers distinguish postmortem-confirmed Alzheimer's disease from other dementias and healthy controls in the OPTIMA cohort. *Journal of Alzheimer's Disease,* 44**,** 525-539.

SELKOE, D. J. & HARDY, J. 2016. The amyloid hypothesis of Alzheimer's disease at 25 years. *EMBO molecular medicine,* 8**,** 595-608.

SERRANO-POZO, A., FROSCH, M. P., MASLIAH, E. & HYMAN, B. T. 2011. Neuropathological alterations in Alzheimer disease. *Cold Spring Harbor perspectives in medicine,* 1**,** a006189.

SEVIGNY, J., CHIAO, P., BUSSIÈRE, T., WEINREB, P. H., WILLIAMS, L., MAIER, M., DUNSTAN, R., SALLOWAY, S., CHEN, T. & LING, Y. 2016. The antibody aducanumab reduces Aβ plaques in Alzheimer's disease. *Nature,* 537**,** 50-56.

SHAW, L. M., VANDERSTICHELE, H., KNAPIK-CZAJKA, M., CLARK, C. M., AISEN, P. S., PETERSEN, R. C., BLENNOW, K., SOARES, H., SIMON, A. & LEWCZUK, P. 2009. Cerebrospinal fluid biomarker signature in Alzheimer's disease neuroimaging initiative subjects. *Annals of neurology,* 65**,** 403-413.

SHERRINGTON, R., ROGAEV, E., LIANG, Y. A., ROGAEVA, E., LEVESQUE, G., IKEDA, M., CHI, H., LIN, C., LI, G. & HOLMAN, K. 1995. Cloning of a gene bearing missense mutations in early-onset familial Alzheimer's disease. *Nature,* 375**,** 754-760.

SHI, X.-P., TUGUSHEVA, K., BRUCE, J. E., LUCKA, A., WU, G.-X., CHEN-DODSON, E., PRICE, E., LI, Y., XU, M. & HUANG, Q. 2003. β-Secretase cleavage at amino acid residue 34 in the amyloid β peptide is dependent upon γ-secretase activity. *Journal of Biological Chemistry,* 278**,** 21286-21294.

SHIMIZU, H., TOSAKI, A., KANEKO, K., HISANO, T., SAKURAI, T. & NUKINA, N. 2008. Crystal structure of an active form of BACE1, an enzyme responsible for amyloid β protein production. *Molecular and cellular biology,* 28**,** 3663-3671.

SHIROTANI, K., EDBAUER, D., KOSTKA, M., STEINER, H. & HAASS, C. 2004. Immature nicastrin stabilizes APH-1 independent of PEN-2 and presenilin: identification of nicastrin mutants that selectively interact with APH-1. *Journal of neurochemistry,* 89**,** 1520-1527.

SINHA, S., ANDERSON, J. P., BARBOUR, R., BASI, G. S., CACCAVELLO, R., DAVIS, D., DOAN, M., DOVEY, H. F., FRIGON, N. & HONG, J. 1999. Purification and cloning of amyloid precursor protein β-secretase from human brain. *Nature,* 402**,** 537-540.

`

SKOVRONSKY, D. M., LEE, V. M.-Y. & TROJANOWSKI, J. Q. 2006. Neurodegenerative diseases: new concepts of pathogenesis and their therapeutic implications. *Annu. Rev. Pathol. Mech. Dis.,* 1**,** 151-170.

SLUNT, H. H., THINAKARAN, G., VON KOCH, C., LO, A., TANZI, R. E. & SISODIA, S. S. 1994. Expression of a ubiquitous, cross-reactive homologue of the mouse beta-amyloid precursor protein (APP). *Journal of Biological Chemistry,* 269**,** 2637-2644.

SONG, W., NADEAU, P., YUAN, M., YANG, X., SHEN, J. & YANKNER, B. A. 1999. Proteolytic release and nuclear translocation of Notch-1 are induced by presenilin-1 and impaired by pathogenic presenilin-1 mutations. *Proceedings of the National Academy of Sciences,* 96**,** 6959-6963.

ST GEORGE-HYSLOP, P. H., TANZI, R. E., POLINSKY, R. J., HAINES, J. L., NEE, L., WATKINS, P. C., MYERS, R. H., FELDMAN, R. G., POLLEN, D. & DRACHMAN, D. 1987. The genetic defect causing familial Alzheimer's disease maps on chromosome 21. *Science,* 235**,** 885-890.

STACK, M. S. & GRAY, R. D. 1990. The effect of pH, temperature, and D2O on the activity of porcine synovial collagenase and gelatinase. *Archives of biochemistry and biophysics,* 281**,** 257-263.

STROZYK, D., BLENNOW, K., WHITE, L. & LAUNER, L. 2003. CSF Aβ 42 levels correlate with amyloid-neuropathology in a population-based autopsy study. *Neurology,* 60**,** 652-656.

SUDOH, S., FROSCH, M. P. & WOLF, B. A. 2002. Differential effects of proteases involved in intracellular degradation of amyloid β-protein between detergent-soluble and-insoluble pools in CHO-695 cells. *Biochemistry,* 41**,** 1091-1099.

SUIRE, C. N., ABDUL-HAY, S. O., SAHARA, T., KANG, D., BRIZUELA, M. K., SAFTIG, P., DICKSON, D. W., ROSENBERRY, T. L. & LEISSRING, M. A. 2020. Cathepsin D regulates cerebral Aβ42/40 ratios via differential degradation of Aβ42 and Aβ40. *Alzheimer's research & therapy,* 12**,** 1-13.

SUIRE, C. N. & LEISSRING, M. A. 2021. Cathepsin D: a candidate link between amyloid β-protein and tauopathy in Alzheimer disease. *Journal of experimental neurology,* 2**,** 10.

SUN, Y., RONG, X., LU, W., PENG, Y., LI, J., XU, S., WANG, L. & WANG, X. 2015. Translational study of Alzheimer's disease (AD) biomarkers from brain tissues in AβPP/PS1 mice and serum of AD patients. *Journal of Alzheimer's Disease,* 45**,** 269-282.

SUNDELÖF, J., SUNDSTRÖM, J., HANSSON, O., ERIKSDOTTER-JÖNHAGEN, M., GIEDRAITIS, V., LARSSON, A., DEGERMAN-GUNNARSSON, M., INGELSSON, M., MINTHON, L. & BLENNOW, K. 2010. Higher cathepsin B levels in plasma in Alzheimer's disease compared to healthy controls. *Journal of Alzheimer's Disease,* 22**,** 1223-1230.

TAKAMI, M., NAGASHIMA, Y., SANO, Y., ISHIHARA, S., MORISHIMA-KAWASHIMA, M., FUNAMOTO, S. & IHARA, Y. 2009. γ-Secretase: successive tripeptide and tetrapeptide release from the transmembrane domain of β-carboxyl terminal fragment. *Journal of Neuroscience,* 29**,** 13042-13052.

TAKASUGI, N., TOMITA, T., HAYASHI, I., TSURUOKA, M., NIIMURA, M., TAKAHASHI, Y., THINAKARAN, G. & IWATSUBO, T. 2003. The role of presenilin cofactors in the γ-secretase complex. *Nature,* 422**,** 438-441.

TANZI, R. E., GUSELLA, J. F., WATKINS, P. C., BRUNS, G. A., ST GEORGE-HYSLOP, P., VAN KEUREN, M. L., PATTERSON, D., PAGAN, S., KURNIT, D. M. & NEVE, R. L. 1987. Amyloid β protein gene: cDNA, mRNA distribution, and genetic linkage near the Alzheimer locus. *Science,* 235**,** 880-884.

TAPIOLA, T., ALAFUZOFF, I., HERUKKA, S.-K., PARKKINEN, L., HARTIKAINEN, P., SOININEN, H. & PIRTTILÄ, T. 2009. Cerebrospinal fluid β-amyloid 42 and tau proteins as biomarkers of Alzheimer-type pathologic changes in the brain. *Archives of neurology,* 66**,** 382-389.

TERNI, B. & FERRER, I. 2015. Abnormal expression and distribution of MMP2 at initial stages of Alzheimer's disease-related pathology. *Journal of Alzheimer's Disease,* 46**,** 461-469.

THAL, D. R., CAPETILLO-ZARATE, E., DEL TREDICI, K. & BRAAK, H. 2006. The development of amyloid β protein deposits in the aged brain. *Science of aging knowledge environment,* 2006**,** re1-re1.

`

THERRIAULT, J., PASCOAL, T. A., SAVARD, M., MATHOTAARACHCHI, S., BENEDET, A. L., CHAMOUN, M., TISSOT, C., LUSSIER, F. Z., RAHMOUNI, N. & STEVENSON, J. 2022. Intrinsic connectivity of the human brain provides scaffold for tau aggregation in clinical variants of Alzheimer's disease. *Science Translational Medicine,* 14**,** eabc8693.

THIJSSEN, E. H., LA JOIE, R., STROM, A., FONSECA, C., IACCARINO, L., WOLF, A., SPINA, S., ALLEN, I. E., COBIGO, Y. & HEUER, H. 2021. Plasma phosphorylated tau 217 and phosphorylated tau 181 as biomarkers in Alzheimer's disease and frontotemporal lobar degeneration: a retrospective diagnostic performance study. *The Lancet Neurology,* 20**,** 739-752.

TOH, W. H., CHIA, P. Z. C., HOSSAIN, M. I. & GLEESON, P. A. 2018. GGA1 regulates signal-dependent sorting of BACE1 to recycling endosomes, which moderates Aβ production. *Molecular biology of the cell,* 29**,** 191-208.

TRAPANI, A. J., BEIL, M. E., BRUSEO, C. W., DE LOMBAERT, S. & JENG, A. Y. 2000. Pharmacological properties of CGS 35066, a potent and selective endothelin-converting enzyme inhibitor, in conscious rats. *Journal of Cardiovascular Pharmacology,* 36**,** S40-3.

TSAN, M.-F. & JIANG, M.-S. 1985. Membrane endopeptidases of human neutrophil. *Inflammation,* 9**,** 113-126.

TURNER, A. J. & MURPHY, L. J. 1996. Molecular pharmacology of endothelin converting enzymes. *Biochemical pharmacology,* 51**,** 91-102.

TYLER, S. J., DAWBARN, D., WILCOCK, G. K. & ALLEN, S. J. 2002. α-and β-secretase: profound changes in Alzheimer's disease. *Biochemical and biophysical research communications,* 299**,** 373-376.

VALDENAIRE, O., LEPAILLEUR-ENOUF, D., EGIDY, G., THOUARD, A., BARRET, A., VRANCKX, R., TOUGARD, C. & MICHEL, J. B. 1999. A fourth isoform of endothelin-converting enzyme (ECE-1) is generated from an additional promoter: Molecular cloning and characterization. *European Journal of Biochemistry,* 264**,** 341-349.

VANDERMEEREN, M., GERAERTS, M., PYPE, S., DILLEN, L., VAN HOVE, C. & MERCKEN, M. 2001. The functional γ-secretase inhibitor prevents production of amyloid β 1–34 in human and murine cell lines. *Neuroscience letters,* 315**,** 145-148.

VASSAR, R., BENNETT, B. D., BABU-KHAN, S., KAHN, S., MENDIAZ, E. A., DENIS, P., TEPLOW, D. B., ROSS, S., AMARANTE, P. & LOELOFF, R. 1999. β-Secretase cleavage of Alzheimer's amyloid precursor protein by the transmembrane aspartic protease BACE. *science,* 286**,** 735-741.

VASSAR, R., KOVACS, D. M., YAN, R. & WONG, P. C. 2009. The β-secretase enzyme BACE in health and Alzheimer's disease: regulation, cell biology, function, and therapeutic potential. *Journal of neuroscience,* 29**,** 12787-12794.

VEHMAS, A. K., KAWAS, C. H., STEWART, W. F. & TRONCOSO, J. C. 2003. Immune reactive cells in senile plaques and cognitive decline in Alzheimer's disease. *Neurobiology of aging,* 24**,** 321-331.

VEKRELLIS, K., CHESNEAU, V., YE, Z., MANSOURIAN, S., ROSNER, M. & SELKOE, D. J. 2000. Insulin degrading enzyme (IDE): implications for the degradation and neurotoxicity of the amyloid β-protein. *Neurobiology of Aging***,** 115.

VERBERK, I. M., SLOT, R. E., VERFAILLIE, S. C., HEIJST, H., PRINS, N. D., VAN BERCKEL, B. N., SCHELTENS, P., TEUNISSEN, C. E. & VAN DER FLIER, W. M. 2018. Plasma amyloid as prescreener for the earliest A lzheimer pathological changes. *Annals of neurology,* 84**,** 648-658.

VETRIVEL, K. S., BARMAN, A., CHEN, Y., NGUYEN, P. D., WAGNER, S. L., PRABHAKAR, R. & THINAKARAN, G. 2011. Loss of cleavage at β'-site contributes to apparent increase in β-amyloid peptide (Aβ) secretion by β-secretase (BACE1)-glycosylphosphatidylinositol (GPI) processing of amyloid precursor protein. *Journal of Biological Chemistry,* 286**,** 26166-26177.

WALTER, J., KAETHER, C., STEINER, H. & HAASS, C. 2001. The cell biology of Alzheimer's disease: uncovering the secrets of secretases. *Current opinion in neurobiology,* 11**,** 585-590.

`

WANG, C., SUN, B., ZHOU, Y., GRUBB, A. & GAN, L. 2012. Cathepsin B degrades amyloid-β in mice expressing wild-type human amyloid precursor protein. *Journal of Biological Chemistry,* 287**,** 39834-39841.

WANG, Y.-J., ZHOU, H.-D. & ZHOU, X.-F. 2006. Clearance of amyloid-beta in Alzheimer's disease: progress, problems and perspectives. *Drug discovery today,* 11**,** 931-938.

WASCO, W., BUPP, K., MAGENDANTZ, M., GUSELLA, J. F., TANZI, R. E. & SOLOMON, F. 1992. Identification of a mouse brain cDNA that encodes a protein related to the Alzheimer disease-associated amyloid beta protein precursor. *Proceedings of the National Academy of Sciences,* 89**,** 10758-10762.

WEBER, M., WU, T., MEILANDT, W. J., DOMINGUEZ, S. L., SOLANOY, H. O., MALONEY, J. A., NGU, H., BACA, M., KUNG, C. & LIMA, L. 2017. BACE1 across species: a comparison of the in vivo consequences of BACE1 deletion in mice and rats. *Scientific reports,* 7**,** 1-17.

WEGGEN, S. & BEHER, D. 2012. Molecular consequences of amyloid precursor protein and presenilin mutations causing autosomal-dominant Alzheimer's disease. *Alzheimer's research & therapy,* 4**,** 1-14.

WEIDEMANN, A., EGGERT, S., REINHARD, F. B., VOGEL, M., PALIGA, K., BAIER, G., MASTERS, C. L., BEYREUTHER, K. & EVIN, G. 2002. A novel ϵ-cleavage within the transmembrane domain of the Alzheimer amyloid precursor protein demonstrates homology with Notch processing. *Biochemistry,* 41**,** 2825-2835.

WESTLEY, B. & MAY, F. 1999. Prognostic value of cathepsin D in breast cancer. *British journal of cancer,* 79**,** 189.

WILDSMITH, K. R., HOLLEY, M., SAVAGE, J. C., SKERRETT, R. & LANDRETH, G. E. 2013. Evidence for impaired amyloid β clearance in Alzheimer's disease. *Alzheimer's research & therapy,* 5**,** 1-6.

WILLEM, M., TAHIROVIC, S., BUSCHE, M. A., OVSEPIAN, S. V., CHAFAI, M., KOOTAR, S., HORNBURG, D., EVANS, L. D., MOORE, S. & DARIA, A. 2015. η-Secretase processing of APP inhibits neuronal activity in the hippocampus. *Nature,* 526**,** 443-447.

WOLFE, M. S., XIA, W., OSTASZEWSKI, B. L., DIEHL, T. S., KIMBERLY, W. T. & SELKOE, D. J. 1999. Two transmembrane aspartates in presenilin-1 required for presenilin endoproteolysis and γ-secretase activity. *Nature,* 398**,** 513-517.

WOLOZIN, B., IWASAKI, K., VITO, P., GANJEI, J. K., LACANÀ, E., SUNDERLAND, T., ZHAO, B., KUSIAK, J. W., WASCO, W. & D'ADAMIO, L. 1996. Participation of presenilin 2 in apoptosis: enhanced basal activity conferred by an Alzheimer mutation. *Science,* 274**,** 1710-1713.

WU, G., SANKARANARAYANAN, S., WONG, J., TUGUSHEVA, K., MICHENER, M. S., SHI, X., COOK, J. J., SIMON, A. J. & SAVAGE, M. J. 2012. Characterization of plasma β-secretase (BACE1) activity and soluble amyloid precursor proteins as potential biomarkers for Alzheimer's disease. *Journal of neuroscience research,* 90**,** 2247-2258.

XU, D., EMOTO, N., GIAID, A., SLAUGHTER, C., KAW, S., DEWIT, D. & YANAGISAWA, M. 1994. ECE-1: a membrane-bound metalloprotease that catalyzes the proteolytic activation of big endothelin-1. *Cell,* 78**,** 473-485.

YAN, P., HU, X., SONG, H., YIN, K., BATEMAN, R. J., CIRRITO, J. R., XIAO, Q., HSU, F. F., TURK, J. W. & XU, J. 2006. Matrix metalloproteinase-9 degrades amyloid-β fibrils in vitro and compact plaques in situ. *Journal of Biological Chemistry,* 281**,** 24566-24574.

YAN, R., BIENKOWSKI, M. J., SHUCK, M. E., MIAO, H., TORY, M. C., PAULEY, A. M., BRASHLER, J. R., STRATMAN, N. C., MATHEWS, W. R. & BUHL, A. E. 1999. Membrane-anchored aspartyl protease with Alzheimer's disease β-secretase activity. *Nature,* 402**,** 533-537.

YAN, R. & VASSAR, R. 2014. Targeting the β secretase BACE1 for Alzheimer's disease therapy. *The Lancet Neurology,* 13**,** 319-329.

YANG, L.-B., LINDHOLM, K., YAN, R., CITRON, M., XIA, W., YANG, X.-L., BEACH, T., SUE, L., WONG, P. & PRICE, D. 2003. Elevated β-secretase expression and enzymatic activity detected in sporadic Alzheimer disease. *Nature medicine,* 9**,** 3-4.

YASOJIMA, K., AKIYAMA, H., MCGEER, E. G. & MCGEER, P. L. 2001a. Reduced neprilysin in high plaque areas of Alzheimer brain: a possible relationship to deficient degradation of β-amyloid peptide. *Neuroscience letters,* 297**,** 97-100.

YASOJIMA, K., MCGEER, E. & MCGEER, P. 2001b. Relationship between beta amyloid peptide generating molecules and neprilysin in Alzheimer disease and normal brain. *Brain research,* 919**,** 115-121.

YASUHARA, O., KAWAMATA, T., AIMI, Y., MCGEER, E. G. & MCGEER, P. L. 1994. Two types of dystrophic neurites in senile plaques of Alzheimer disease and elderly non-demented cases. *Neuroscience letters,* 171**,** 73-76.

YIN, K.-J., CIRRITO, J. R., YAN, P., HU, X., XIAO, Q., PAN, X., BATEMAN, R., SONG, H., HSU, F.-F. & TURK, J. 2006. Matrix metalloproteinases expressed by astrocytes mediate extracellular amyloid-β peptide catabolism. *Journal of Neuroscience,* 26**,** 10939-10948.

YOUNG-PEARSE, T. L., CHEN, A. C., CHANG, R., MARQUEZ, C. & SELKOE, D. J. 2008. Secreted APP regulates the function of full-length APP in neurite outgrowth through interaction with integrin beta1. *Neural development,* 3**,** 1-14.

ZETTERBERG, H., ANDREASSON, U., HANSSON, O., WU, G., SANKARANARAYANAN, S., ANDERSSON, M. E., BUCHHAVE, P., LONDOS, E., UMEK, R. M. & MINTHON, L. 2008. Elevated cerebrospinal fluid BACE1 activity in incipient Alzheimer disease. *Archives of neurology,* 65**,** 1102-1107.

ZHANG, H., LIU, D., HUANG, H., ZHAO, Y. & ZHOU, H. 2018. Characteristics of insulin-degrading enzyme in alzheimer's disease: a meta-analysis. *Current Alzheimer Research,* 15**,** 610-617.

ZHANG, X., LI, Y., XU, H. & ZHANG, Y.-W. 2014. The γ-secretase complex: from structure to function. *Frontiers in cellular neuroscience,* 8**,** 427.

ZHANG, Z., SONG, M., LIU, X., SU KANG, S., DUONG, D. M., SEYFRIED, N. T., CAO, X., CHENG, L., SUN, Y. E. & PING YU, S. 2015. Delta-secretase cleaves amyloid precursor protein and regulates the pathogenesis in Alzheimer's disease. *Nature communications,* 6**,** 1-16.

ZHAO, G., MAO, G., TAN, J., DONG, Y., CUI, M.-Z., KIM, S.-H. & XU, X. 2004. Identification of a New Presenilin-dependent ζ-Cleavage Site within the Transmembrane Domain of Amyloid Precursor Protein*♦. *Journal of Biological Chemistry,* 279**,** 50647-50650.

ZHAO, J., FU, Y., YASVOINA, M., SHAO, P., HITT, B., O'CONNOR, T., LOGAN, S., MAUS, E., CITRON, M. & BERRY, R. 2007. β-Site amyloid precursor protein cleaving enzyme 1 levels become elevated in neurons around amyloid plaques: implications for Alzheimer's disease pathogenesis. *Journal of Neuroscience,* 27**,** 3639-3649.

ZHAO, J., LI, L. & LEISSRING, M. A. 2009. Insulin-degrading enzyme is exported via an unconventional protein secretion pathway. *Molecular neurodegeneration,* 4**,** 1-5.

ZHAO, L. N., LONG, H., MU, Y. & CHEW, L. Y. 2012. The toxicity of amyloid β oligomers. *International journal of molecular sciences,* 13**,** 7303-7327.

ZHENG, H., JIANG, M., TRUMBAUER, M. E., SIRINATHSINGHJI, D. J., HOPKINS, R., SMITH, D. W., HEAVENS, R. P., DAWSON, G. R., BOYCE, S. & CONNER, M. W. 1995. β-Amyloid precursor protein-deficient mice show reactive gliosis and decreased locomotor activity. *Cell,* 81**,** 525-531.

ZHONG, Z., EWERS, M., TEIPEL, S., BÜRGER, K., WALLIN, A., BLENNOW, K., HE, P., MCALLISTER, C., HAMPEL, H. & SHEN, Y. 2007. Levels of β-secretase (BACE1) in cerebrospinal fluid as a predictor of risk in mild cognitive impairment. *Archives of general psychiatry,* 64**,** 718-726.

ZHOU, B., LU, J. G., SIDDU, A., WERNIG, M. & SÜDHOF, T. C. 2022. Synaptogenic effect of APP-Swedish mutation in familial Alzheimer's disease. *Science Translational Medicine,* 14**,** eabn9380.

ZOU, K., YAMAGUCHI, H., AKATSU, H., SAKAMOTO, T., KO, M., MIZOGUCHI, K., GONG, J.-S., YU, W., YAMAMOTO, T. & KOSAKA, K. 2007. Angiotensin-converting enzyme converts amyloid β-protein

1–42 (Aβ1–42) to Aβ1–40, and its inhibition enhances brain Aβ deposition. *Journal of Neuroscience,* 27**,** 8628-8635.

`

ABBREVIATIONS

AD	Alzheimer disease
ACE	Angiotensin converting enzyme
ADEs	Amyloid-β-degrading enzymes
AICD	Amyloid precursor protein intracellular domain
AP-1	Adaptor protein 1
APLP	Amyloid precursor-like proteins
APP	Amyloid precursor protein
APP-C99	99-amino acid long C-terminus of amyloid precursor protein
Aβ	Amyloid-β
Aβ42	42-amino acid long amyloid-β peptide
BACE1	β-secretase / β-site amyloid precursor protein-cleaving enzyme 1
BCA	Bicinchoninic acid
BSA	Bovine serum albumin
C57BL/6	C57 black 6
Cat B	Cathepsin B
Cat D	Cathepsin D
CNS	Central nervous system
CO_2	Carbon dioxide
CSF	Cerebrospinal fluid
CTF	C-terminus of amyloid precursor protein
DAPI	4',6-Diamidino-2-Phenylindole, Dihydrochloride
DMEM	Dulbecco's Modified Eagle Medium
DMEM/F12	Dulbecco's Modified Eagle Medium and Ham's F-12
DMSO	Dimethyl sulfoxide
ECE1	Endothelin converting enzyme 1
EDTA	Ethylenediaminetetraacetic acid
EEA1	Early-endosome associated protein 1
ELISA	Enzyme-linked immunosorbent assay
ER	Endoplasmic reticulum
FAD	Familial Alzheimer disease
FBS	Fetal bovine serum
H_2SO_4	Sulfuric acid
hAPP	Human amyloid precursor protein

`

HEK293T	Human embryonic kidney cells
HEPES	4-(2-hydroxyethyl)-1-piperazineethanesulfonic acid
HRP	Horseradish peroxidase
ICC	Immunocytochemistry
IDE	Insulin degrading enzyme
LAMP1	Lysosome-associated membrane protein 1
LLOD	Lower limit of detection
MALDI-MS	Matrix-assisted laser desorption/ionization mass spectrometry
MALDI-TOF	Matrix-assisted laser desorption/ionization time-of-flight mass spectrometry
MCI	Mild cognitive impairment
$MgCl_2$	Magnesium chloride
MK-8931	Verubecestat
MMP2	Matrix metalloproteinase 2
MMP9	Matrix metalloproteinase 9
MSD	Meso Scale Discovery
Na_2HPO_4	Disodium phosphate
Na_3VO_4	Sodium orthovanadate
NaCl	Sodium chloride
NaF	Sodium fluoride
NaH_2PO_4	Monosodium phosphate
NBB	The Netherlands Brain Bank
NEP/MME	Neprilysin
NFT	Neurofibrillary tangles
NP-40	Nonyl phenoxypolyethoxylethanol
Opti-MEM	Improved Minimal Essential Medium
PBS	Phosphate buffered saline
PBS-T	hosphate-buffered saline solution with Tween-20
PCR	Polymerase chain reaction
PEG	Polyethylene glycol
PET	Positron emission tomography
PMSF	Phenyl-methylsulfonyl fluoride
PS	Presenilin
PSEN	Presenilin gene
p-tau	Phosphorylated tubulin-associated unit
PVDF	Polyvinylidene difluoride
RIP	Regulated intramembrane proteolysis
RNA	Ribonucleic acid
sAPP	Soluble amyloid precursor protein fragment
SH-SY5Y	Human neuroblastoma cell line
SILK	Stable isotope labeling kinetics

`

siRNA	Small-interfering ribonucleic acid
tau	Tubulin-associated unit
TGN	Trans-Golgi network
Tris-HCl	Tris hydrochloride
t-tau	Total tubulin-associated unit
WCE	Whole cell extract buffer

`

APPENDIX

`

APPENDIX A

The following article is reprinted with permission from:

Filip Liebsch, Luka Kulic, Charlotte Teunissen, Adeola Shobo, Irem Ulku, Vivienne Engelschalt, Mark A. Hancock, Wiesje M. van der Flier, Peter Kunach, Pedro Rosa-Neto, Philip Scheltens, Judes Poirier, Paul Saftig, Randall J. Bateman, John Breitner, Christoph Hock & Gerhard Multhaup

Aβ34 is a BACE1-derived degradation intermediate associated with amyloid clearance and Alzheimer's disease progression

Nat Commun., 10, 2240 (2019). https://doi.org/10.1038/s41467-019-10152-w

nature COMMUNICATIONS

ARTICLE

https://doi.org/10.1038/s41467-019-10152-w OPEN

Aβ34 is a BACE1-derived degradation intermediate associated with amyloid clearance and Alzheimer's disease progression

Filip Liebsch[1], Luka Kulic[2], Charlotte Teunissen[3], Adeola Shobo[1], Irem Ulku[1], Vivienne Engelschalt[4], Mark A. Hancock[5], Wiesje M. van der Flier[6], Peter Kunach[7], Pedro Rosa-Neto[7], Philip Scheltens[6], Judes Poirier[8], Paul Saftig[9], Randall J. Bateman[10], John Breitner[8], Christoph Hock[2,11] & Gerhard Multhaup[1]

The beta-site APP cleaving enzyme 1 (BACE1) is known primarily for its initial cleavage of the amyloid precursor protein (APP), which ultimately leads to the generation of Aβ peptides. Here, we provide evidence that altered BACE1 levels and activity impact the degradation of Aβ40 and Aβ42 into a common Aβ34 intermediate. Using human cerebrospinal fluid (CSF) samples from the Amsterdam Dementia Cohort, we show that Aβ34 is elevated in individuals with mild cognitive impairment who later progressed to dementia. Furthermore, Aβ34 levels correlate with the overall Aβ clearance rates in amyloid positive individuals. Using CSF samples from the PREVENT-AD cohort (cognitively normal individuals at risk for Alzheimer's disease), we further demonstrate that the Aβ34/Aβ42 ratio, representing Aβ degradation and cortical deposition, associates with pre-clinical markers of neurodegeneration. We propose that Aβ34 represents a marker of amyloid clearance and may be helpful for the characterization of Aβ turnover in clinical samples.

[1] Department of Pharmacology and Therapeutics and Integrated Program in Neuroscience, McGill University, Montreal, QC H3G 1Y6, Canada. [2] Institute for Regenerative Medicine, University of Zurich, CH-8952 Schlieren, Switzerland. [3] Department of Clinical Chemistry, Amsterdam Neuroscience, Amsterdam UMC, Vrije Universiteit Amsterdam, 1081HZ Amsterdam, The Netherlands. [4] Institut für Chemie und Biochemie, Freie Universität Berlin, 14195 Berlin, Germany. [5] SPR-MS Facility, McGill University, Montreal, QC H3G 1Y6, Canada. [6] Alzheimer Center Amsterdam, Department of Neurology, Amsterdam Neuroscience, Amsterdam UMC, Vrije Universiteit Amsterdam, Amsterdam 1081HZ, The Netherlands. [7] Translational Neuroimaging Laboratory, The McGill University Research Centre for Studies in Aging, Alzheimer's Disease Research Unit, Douglas Research Institute, McGill University, Montreal H4H 1R3 QC, Canada. [8] Department of Psychiatry, McGill University, Montreal, QC H4H 1R3, Canada. [9] Biochemisches Institut, Christian-Albrechts-Universität-Kiel, 24118 Kiel, Germany. [10] Department of Neurology, Washington University in St. Louis, St. Louis, MO 63110, USA. [11] Neurimmune, CH-8952 Schlieren, Switzerland. Correspondence and requests for materials should be addressed to G.M. (email: gerhard.multhaup@mcgill.ca)

The pathogenesis of Alzheimer's disease (AD) is characterized by amyloid-β (Aβ) plaque formation in the brain[1,2]. Sequential cleavage of the amyloid precursor protein (APP) by β-secretase (BACE1) and the γ-secretase complex results in the generation of Aβ species of varying lengths, e.g., Aβ38, Aβ40, and Aβ42[3,4,5,6]. More neurotoxic than Aβ38 or Aβ40, the Aβ42 peptide is prone to form oligomers (i.e., precursor to larger fibrils), which are thought to contribute to plaque formation and cognitive decline[7].

To block the first step of amyloid production, the pharmaceutical industry has focused on inhibitors of BACE1 as a therapeutic strategy for AD. However, BACE1 inhibitors have failed in clinical trials due to side effects, possible toxicity, or the absence of beneficial cognitive outcomes[8]. The lack of success may also relate to the timing of administration, since treatments in the symptomatic stage might be too late.

BACE1 levels are elevated in the neocortex of AD patients[9–11]. Perhaps as a pathological response to fibrillar Aβ, the accumulation of BACE1 in the vicinity of amyloid plaques can enhance local Aβ generation[12–16]. However, excess BACE1 activity can also lead to (i) alternative APP processing at the β'-site, generating metabolically labile Aβ11-X peptides[17], or (ii) Aβ degradation, by catalyzing the C-terminal truncation of Aβ40 and Aβ42 into non-amyloidogenic Aβ34[18–21]. In human and canine in vivo studies, cerebrospinal fluid (CSF) levels of Aβ34 decline with pharmacological BACE1 inhibition, most likely due to an interruption of the BACE1-mediated degradation of Aβ40 and Aβ42[22,23]. However, the amyloidolytic roles of BACE1 in Aβ metabolism are currently not well defined, either in health (i.e., physiological homeostasis) or disease (i.e., AD pathogenesis).

The pathological cascade of sporadic AD appears to be triggered by impaired Aβ degradation and clearance[24]. Aβ clearance from the brain can occur by several mechanisms including interstitial fluid drainage, cellular uptake, and passive elimination[25,26]. Enzymatic degradation generates specific patterns of soluble Aβ peptides in the CSF[27], as mediated by Aβ-degrading enzymes (ADEs), which include metalloprotease family members such as endothelin-converting enzyme (ECE), insulin-degrading enzyme (IDE), and neprilysin (NEP)[28]. Results obtained with ^{18}O-labeling mass spectrometry demonstrated that the Aβ peptide pattern in CSF is not generated by proteolytic activities in CSF itself—except in the acute phase of a bacterial meningitis[29]—but Aβ fragments are likely generated prior to entering the CSF.

The normal clearance rate for Aβ40 or Aβ42 in human CSF is estimated to be ~8% per hour[30], but clearance is impaired by approximately 30% in AD patients[24]. Aβ stable isotope labeling kinetics (SILK) studies found that production and clearance of soluble Aβ isoforms are similar for Aβ38 and Aβ40, but Aβ42 turnover is altered with increasing age and amyloidosis[31].

Since we have previously shown that Aβ34 is a common intermediate in the enzymatic processing of two distinct Aβ degradation pathways[6], the present study examines the levels and metabolism of Aβ34 in the brains of BACE1-deficient mice, in brain and CSF of rats treated with a BACE1-specific inhibitor, a cultured human neuronal cell line (SH-SY5Y), and CSF samples from individuals at various clinical stages of AD. To accomplish this, we utilize a custom, ultra-sensitive Meso Scale Discovery (MSD) electrochemiluminescence assay, using a monoclonal neo-epitope antibody that binds specifically to the C-terminus of Aβ34 with nanomolar affinity. Our results show that cerebral BACE1 levels are limiting for Aβ34 generation in vivo. Specifically, in well-characterized clinical groups, CSF levels of Aβ34 are notably elevated in individuals with mild cognitive impairment (MCI) who later progressed to AD dementia. Compared with the classical Aβ40/Aβ42 ratio (i.e., marker of amyloid deposition in clinical practice), the Aβ34/Aβ42 ratio improves our ability to distinguish between individuals with MCI who later converted to AD from those who did not. Among cognitively normal individuals at risk for AD, an elevated CSF-Aβ34/Aβ42 ratio is detected together with current biomarkers of pre-clinical AD, such as elevated CSF levels of total-tau (t-tau) and phosphorylated (P_{181})-tau. Furthermore, the overall Aβ clearance rates positively correlate with CSF-Aβ34 levels in amyloid-positive (Aβ+) individuals.

While the interesting Aβ34 biology of this article directly impacts the design of future studies looking at Aβ turnover and clinical studies involving BACE inhibitors, we anticipate that combining markers of amyloid clearance (Aβ34 measurements) and deposition (well-established Aβ42 measurements in CSF) may provide a more complete biomarker panel to assess AD samples (i.e., early-stage biochemical changes vs. late-stage plaque/tangle pathology). Future studies are needed to validate whether an increased CSF-Aβ34/Aβ42 ratio may provide an opportunity for earlier intervention strategies.

Results

Cerebral Aβ34 is decreased in BACE1-deficient mice. Given that BACE1 can directly cleave longer Aβ species between Leu34 and Met35 in vitro[19,20] (Supplementary Fig. 1), we hypothesized that Aβ degradation would be affected by altered BACE1 expression levels in vivo. To test this, we analyzed endogenous cerebral BACE1, APP, and Aβ levels from BACE1−/− and BACE1+/− mice, as well as their wild-type (BACE1+/+) littermates (Fig. 1a–g). In agreement with previously published results[32,33], BACE1 protein levels in the brain of BACE1+/− mice were approximately half that of wild-type mice, as analyzed by western blot (Fig. 1a, b). Furthermore, BACE1−/− mice had significantly elevated levels of cerebral APP and/or soluble APP (sAPP) compared with their BACE1+/− and wild-type littermates, whereas there was no significant difference between BACE1+/− and wild-type animals (Fig. 1a, c). Notably, the former is possibly due to increased levels of full-length APP[34].

We next measured endogenous levels of Aβ34, Aβ38, Aβ40, and Aβ42 peptides in the brains of these same mice using a custom 4-plex MSD multiplexing assay (Supplementary Methods, Supplementary Figs. 2, 3). In agreement with previous findings in mice and rats[32,35,36], Aβ38, Aβ40, and Aβ42 were significantly decreased in BACE1−/− mouse brains, whereas their levels did not differ significantly between BACE1+/− and wild-type littermates (Fig. 1e–g). As expected for a fragment generated by BACE1 activity, cerebral Aβ34 levels were decreased in BACE1−/− mice compared with BACE1+/− (Fig. 1d). Notably, Aβ34 levels were also significantly lower in BACE1+/− mice compared with wild-type littermates. Apparently, the cerebral amyloidogenic processing of endogenous APP by BACE1 is not impaired by a 50% decreased enzyme availability, as it is indistinguishable in heterozygous knockouts and wild-type littermates (Fig. 1e–g). Furthermore, the Aβ34/Aβ38, Aβ34/Aβ40, and Aβ34/Aβ42 ratios revealed a step-wise decrease with decreasing BACE1 levels (Fig. 1h–j). These findings support the concept that cerebral BACE1 levels are limiting for its amyloidolytic activity in vivo relying on conversion of the longer Aβ species to Aβ34, whereas BACE1 levels are not limiting for APP cleavage resulting in Aβ38, Aβ40, and Aβ42.

BACE1 inhibition lowers rat CSF and brain Aβ34 levels. To independently assess whether the above findings hold true for the pharmacological intervention with BACE1 activity, wild-type rats were treated with the BACE1-specific inhibitor MK-8931[37]. The inhibitor had no effect on cerebral APP and/or sAPP levels

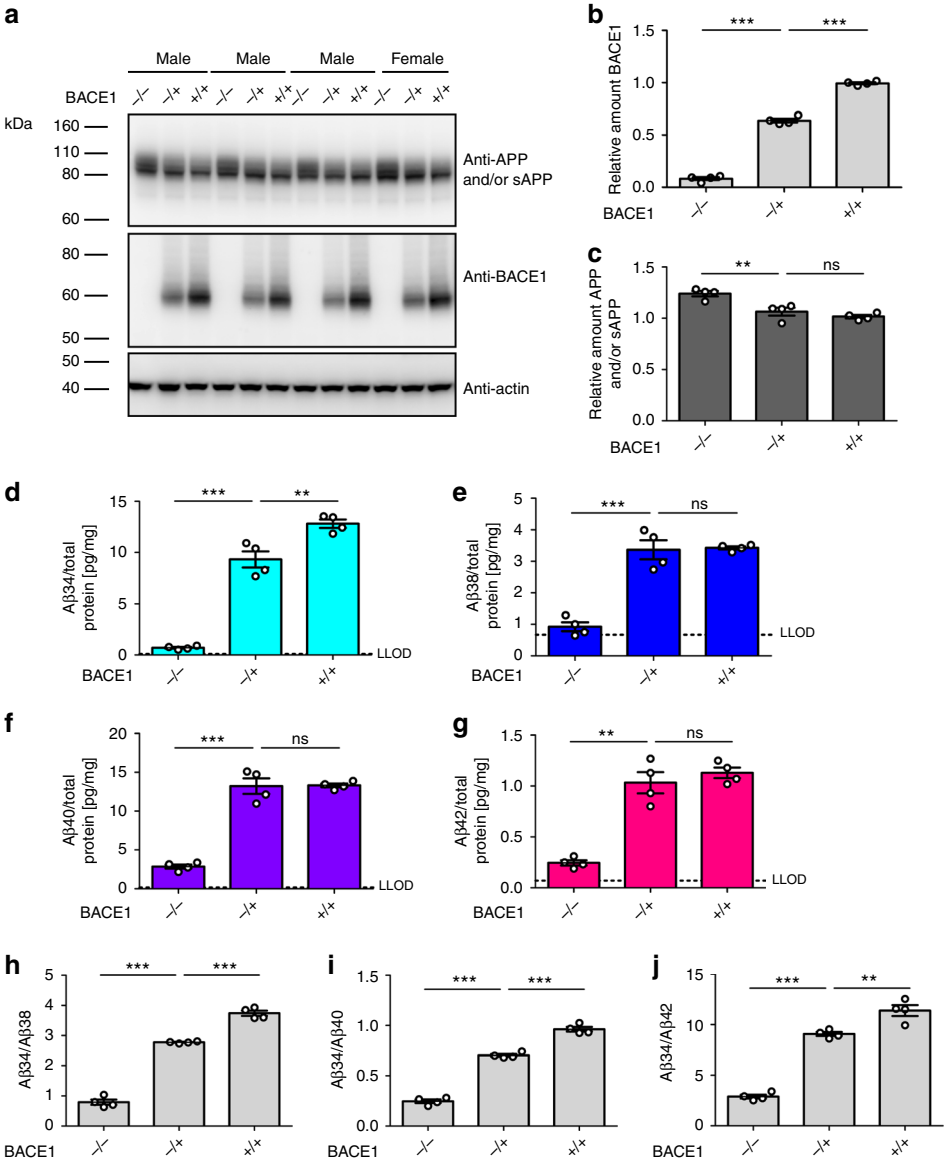

Fig. 1 Endogenous BACE1 generates Aβ34 in the murine brain. Endogenous levels of murine APP and/or sAPP, BACE1, and Aβ in BACE1−/−, BACE1+/−, and wild-type littermates (+/+). $N = 4$ animals per group. Western blot of endogenous APP and/or sAPP and BACE1 expression in male and female mice (**a**) and corresponding quantification of relative protein amounts of BACE1 (**b**) and APP and/or sAPP (**c**). Quantification (pg/mg total protein) of absolute amounts of Aβ34 (**d**), Aβ38 (**e**), Aβ40 (**f**), and Aβ42 (**g**) as determined by custom 4-plex MSD multiplexing assays. Ratios of Aβ34/Aβ38 (**h**), Aβ34/Aβ40 (**i**), and Aβ34/Aβ42 (**j**) are displayed. Statistics: **b** one-way ANOVA, $F(2, 9) = 1021$, $p < 0.0001$, **c** one-way ANOVA, $F(2, 9) = 17.28$, $p < 0.001$, **d** one-way ANOVA, $F(2, 9) = 145.7$, $p < 0.0001$, **e** one-way ANOVA, $F(2, 9) = 53.68$, $p < 0.0001$, **f** one-way ANOVA, $F(2, 9) = 95.65$, $p < 0.0001$, **g** one-way ANOVA, $F(2, 9) = 49.70$, $p < 0.0001$, **h** one-way ANOVA, $F(2, 9) = 425.2$, $p < 0.0001$, **i** one-way ANOVA, $F(2, 9) = 378.0$, $p < 0.0001$, **j** one-way ANOVA, $F(2, 9) = 157.6$, $p < 0.0001$. Bars and error bars indicate mean ± s.e.m. Tukey's post-hoc tests were performed for pairwise comparisons; selected comparisons are highlighted ***$p < 0.001$, **$p < 0.01$, ns = nonsignificant $p > 0.05$. For each target, the MSD software computes the lower limit of detection (LLOD) as 2.5 standard deviations above the blank

(Fig. 2a, b). Cerebral Aβ34 levels were significantly decreased in rats treated with concentrations of 1 and 20 mg/kg (Fig. 2c). In contrast, cerebral Aβ40 and Aβ42 levels were only decreased in the 20 mg/kg but not the 1 mg/kg cohort (Fig. 2d, e). Consequently, the ratios Aβ34/Aβ40 and Aβ34/Aβ42 were significantly decreased at 1 and 20 mg/kg (Fig. 2f, g). In agreement with our findings in BACE1+/− mice, these results indicate that cerebral Aβ34 levels are more sensitive to changes in BACE1 activity than the longer Aβ species.

We next measured CSF levels of Aβ34, Aβ38, Aβ40, and Aβ42. CSF-Aβ34 was significantly decreased in the cohorts treated with 1 and 20 mg/kg (Fig. 2h), however, there was no change for Aβ38, Aβ40, and Aβ42 (Fig. 2i–k). Furthermore, the ratios Aβ34/Aβ38, Aβ34/Aβ40, and Aβ34/Aβ42 in CSF were significantly decreased in the animals treated with 1 and 20 mg/kg (Fig. 2l–n). Overall, the results of these experiments demonstrate that the pharmacological inhibition of BACE1 differentially affects the amyloidogenic and the amyloidolytic activities of the enzyme in vivo. Importantly, the latter seems more sensitive than the former to the amount (Fig. 1) and activity (Fig. 2) of BACE1.

Aβ34 is an Aβ degradation intermediate. Previous studies showed that APP and BACE1 expression can change the quantity

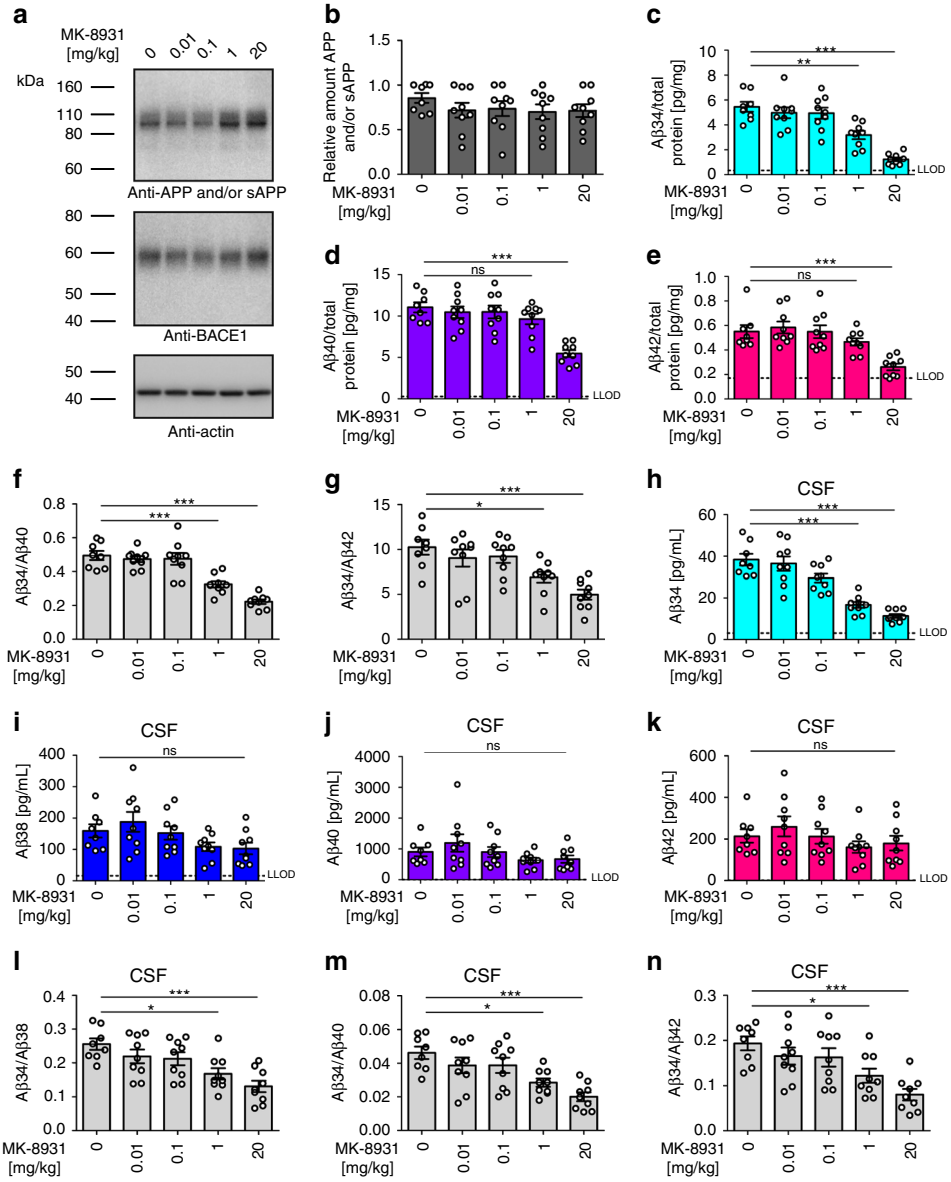

Fig. 2 Pharmacological inhibition of Aβ34 generation in rats. Endogenous levels of APP and/or sAPP, BACE1, and Aβ in rats 1 h after intravenous injection of the indicated concentrations (mg/kg) of the BACE1-specific inhibitor (MK-8931) $n = 9$ animals per group or vehicle $n = 8$ animals. Western blot of endogenous APP and/or sAPP and BACE1 expression (**a**) and corresponding quantification of relative protein amounts of APP and/or sAPP (**b**). Quantification (pg/mg total protein) of absolute amounts of Aβ34 (**c**), Aβ40 (**d**), and Aβ42 (**e**) as determined by custom MSD multiplexing assays. Ratios of Aβ34/Aβ40 (**f**) and Aβ34/Aβ2 (**g**) are displayed. Quantification of CSF levels of Aβ34 (**h**), Aβ38 (**i**), Aβ40 (**j**), and Aβ42 (**k**), as well as display of the ratios Aβ34/Aβ38 (**l**), Aβ34/Aβ40 (**m**), and Aβ34/Aβ42 (**n**). Statistics: **b** one-way ANOVA, $F(4, 39) = 0.63$, $p > 0.05$, **c** one-way ANOVA, $F(4, 39) = 22.40$, $p < 0.0001$, **d** one-way ANOVA, $F(4, 39) = 12.81$, $p < 0.0001$, **e** one-way ANOVA, $F(4, 39) = 9.38$, $p < 0.0001$, **f** one-way ANOVA, $F(4, 39) = 25.93$, $p < 0.0001$, **g** one-way ANOVA, $F(4, 39) = 8.02$, $p < 0.0001$, **h** one-way ANOVA, $F(4, 39) = 26.55$, $p < 0.0001$, **i** one-way ANOVA, $F(4, 39) = 2.69$, $p < 0.05$, **j** one-way ANOVA, $F(4, 39) = 1.71$, $p > 0.05$, **k** one-way ANOVA, $F(4, 39) = 1.09$, $p > 0.05$, **l** one-way ANOVA, $F(4, 39) = 6.87$, $p < 0.001$, **m** one-way ANOVA, $F(4, 39) = 7.36$, $p < 0.001$, **n** one-way ANOVA, $F(4, 39) = 6.74$, $p < 0.001$. Bars and error bars indicate mean ± s.e.m. Tukey's post-hoc tests were performed for pairwise comparisons; selected comparisons are highlighted $^{***}p < 0.001$, $^{**}p < 0.01$, $^{*}p < 0.05$, ns = nonsignificant $p > 0.05$

of Aβ produced[33,38]. Therefore, we tested whether Aβ34 levels would be affected by a surplus of either substrate or enzyme in a human neuronal cell type. Using human neuroblastoma (SH-SY5Y) cells stably overexpressing APP or BACE1 (Fig. 3a), we measured secreted levels of Aβ34, Aβ38, Aβ40, and Aβ42 in the supernatants using the ultra-sensitive 4-plex assay, whereas sAPPβ and $sAPP_{total}$ were detected by western blot (Fig. 3a–h). Overexpression of APP mildly increased Aβ34 levels (not statistically different from empty plasmid (Mock)-transfected cells, $p = 0.06$) and significantly elevated sAPPβ, $sAPP_{total}$, Aβ38, Aβ40, and Aβ42, as compared with Mock-transfected cells (Fig. 3b–h). Conversely, in BACE1-overexpressing cells, Aβ34 levels were significantly elevated approximately threefold compared with APP-overexpressing conditions, whereas Aβ38, Aβ40, and Aβ42 levels showed only a mild trend toward elevation compared with the control (Fig. 3e–h). Furthermore, more APP was shed from either of these cell lines (Fig. 3c, d). Note that the apparent molecular weights of endogenous APP and sAPPs are slightly higher than those from APP695-transfected cells (Fig. 3a, b), which is likely due to the fact that undifferentiated SH-SY5Y cells express not only APP695 but also splice variants with KPI- and OX-2 domains[39,40]. Overall, we conclude that a surplus of either

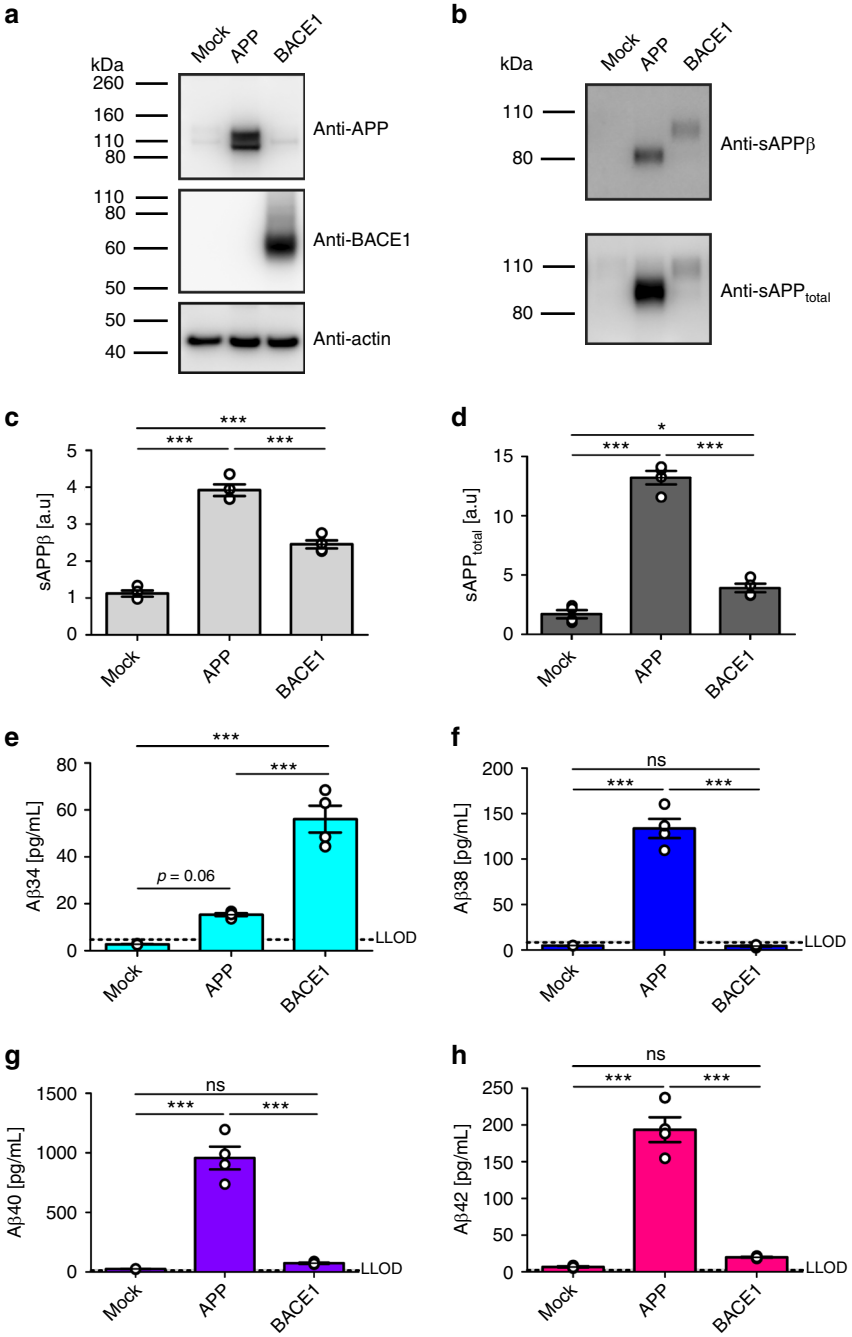

Fig. 3 Surplus of APP or BACE1 differentially affect APP processing. Using SH-SY5Y cells stably expressing APP695 or BACE1, cleavage of APP was analyzed by western blot and ultra-sensitive MSD assay. Representative western blots for the examination of APP, BACE1, sAPPβ, and $sAPP_{total}$ (**a**, **b**), and the corresponding quantification for the relative amounts of sAPPβ (**c**) and $sAPP_{total}$ (**d**). MSD multiplexing to quantify the absolute amounts of Aβ34 (**e**), Aβ38 (**f**), Aβ40 (**g**), and Aβ42 (**h**). Data were collected from four independent experiments. Bars and error bars indicate mean ± s.e.m. **c–h** Data were analyzed with one-way ANOVAs and Tukey's post-hoc tests were performed for pairwise comparisons; selected comparisons are highlighted ***$p < 0.001$, *$p < 0.05$, ns = nonsignificant $p > 0.05$. **c** sAPPβ, $F(2, 9) = 131.2$, $p < 0.0001$, **d** $sAPP_{total}$, $F(2, 9) = 190.3$, $p < 0.0001$, **e** Aβ34, $F(2, 9) = 70.04$, $p < 0.0001$, **f** Aβ38, $F(2, 9) = 149.0$, $p < 0.0001$, **g** Aβ40, $F(2, 9) = 89.96$, $p < 0.0001$, **h** Aβ42, $F(2, 9) = 113.6$, $p < 0.0001$

substrate or enzyme affects APP processing differentially in the human neuronal cell line, resulting in (i) increased Aβ38, Aβ40, and Aβ42 release from APP-overexpressing cells, or (ii) an enhanced degradation of all longer Aβ forms into Aβ34 in BACE1-overexpressing cells.

To investigate whether BACE1 inhibition differentially affects the Aβ profiles, SH-SY5Y cells overexpressing APP or BACE1 were treated with MK-8931[37] at approximately 20-fold of its published IC_{50} (i.e., [MK-8931] = 100 nM, Fig. 4, Supplementary Fig. 4). Conditioned medium from APP-overexpressing SH-SY5Y cells showed significantly decreased levels of sAPPβ, Aβ34, Aβ38, Aβ40, and Aβ42 in the presence of MK-8931 (Fig. 4a–d, Supplementary Fig. 4a–c). Furthermore, a dose-inhibition curve for MK-8931 was performed and sAPPβ (western blot), Aβ34 (MSD 1-plex), and Aβ40 (MSD 1-plex) were measured (Supplementary Fig. 4d–f). In APP-overexpressing SH-SY5Y cells, MK-8931 dose-dependently decreased sAPPβ (pIC_{50} = 10.7 ± 0.3 (s.e.m.)), Aβ34 (pIC_{50} = 14.1 ± 0.6), and Aβ40 levels

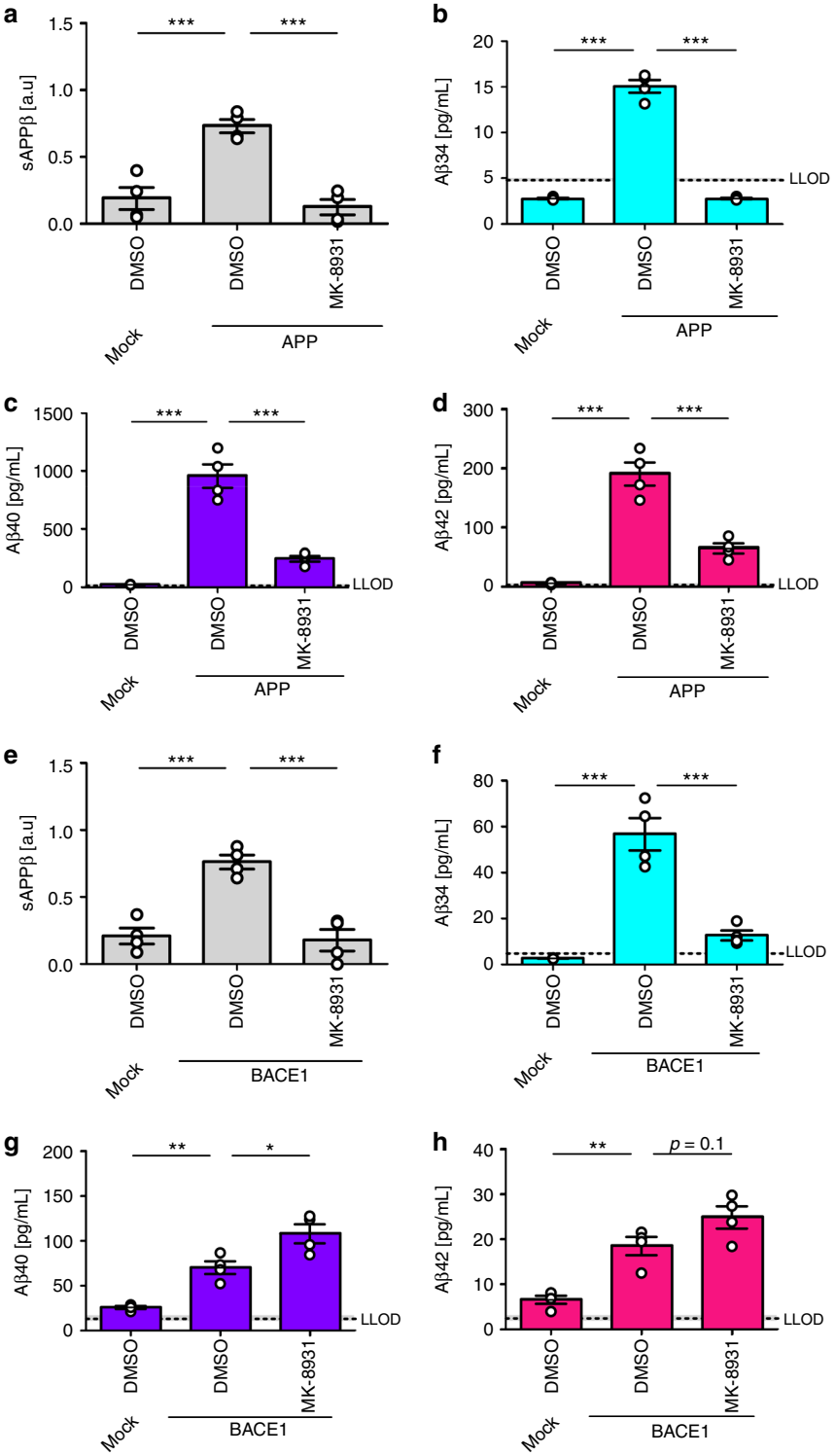

Fig. 4 Surplus of APP or BACE1 affect BACE1 inhibition. Cleavage of APP was analyzed by western blot and ultra-sensitive MSD assays. Absolute or relative amounts of products were quantified from SH-SY5Y cells stably expressing APP695 (**a**–**d**) or BACE1 (**e**–**h**). Quantification of relative amounts of sAPPβ (**a**, **e**), and absolute amounts of Aβ34 (**b**, **f**), Aβ40 (**c**, **g**), and Aβ42 (**d**, **h**). Data were collected from four independent experiments. Bars and error bars indicate mean ± s.e.m. Tukey's post-hoc tests were performed for pairwise comparisons; selected comparisons are highlighted ***$p < 0.001$, **$p < 0.01$, *$p < 0.05$. **a** sAPPβ, one-way ANOVA, $F(2, 9) = 26.6$, $p < 0.001$, **b** Aβ34, one-way ANOVA, $F(2, 9) = 296.1$, $p < 0.0001$, **c** Aβ40, one-way ANOVA, $F(2, 9) = 65.9$, $p < 0.0001$, **d** Aβ42, one-way ANOVA, $F(2,9) = 59.4$, $p < 0.0001$, **e** sAPPβ, one-way ANOVA, $F(2, 9) = 25.4$, $p < 0.001$, **f** Aβ34, one-way ANOVA, $F(2,9) = 45.3$, $p < 0.0001$, **g** Aβ40, one-wayANOVA, $F(2, 9) = 30.8$, $p < 0.0001$, **h** Aβ42, one-way ANOVA, $F(2, 9) = 23.3$, $p < 0.001$

($pIC_{50} = 11.3 \pm 0.7$) (Supplementary Fig. 4d–f). In contrast, in conditioned medium from BACE1-overexpressing SH-SY5Y cells, only the levels of sAPPβ and Aβ34 were significantly decreased in the presence of the inhibitor (Fig. 4e, f, Supplementary Fig. 4g, h), whereas Aβ38 and Aβ40 were significantly increased and Aβ42 levels showed a trend for being elevated, $p = 0.1$ (Supplementary Fig. 4i, Fig. 4g, h). In BACE1-overexpressing SH-SY5Y cells, MK-8931 only dose-dependently decreased sAPPβ ($pIC_{50} = 8.3 \pm 0.3$) and Aβ34 levels ($pIC_{50} = 7.3 \pm 0.2$) (Supplementary Fig. 4j, l). Interestingly, Aβ40 levels were decreased at high inhibitor concentrations (p[MK-8931] > −6), elevated at intermediate concentrations (−10 < p[MK-8931] < −6) and unchanged at low concentrations (−10 > p[MK-8931]) (Supplementary Fig. 4k). Ultimately, these results show that the response to pharmacological BACE1 inhibition depends on the relative abundances of BACE1 and its substrate APP. Notably, inhibition with insufficient amounts of compound at high levels of BACE1 could result in undesired elevated Aβ40 and Aβ42 levels. However, BACE1 inhibitor doses used in vivo can effectively reduce the levels of longer Aβ species[37].

ADEs include the metalloproteases, a large group of proteases that likely cleave Aβ peptide substrates[28]. In general, ADE-derived fragments are short, soluble, and not prone to aggregate. To investigate how Aβ34, Aβ38, Aβ40, and Aβ42 degradation is affected by metalloproteases, we treated APP- or BACE1-overexpressing SH-SY5Y cells with the metalloprotease inhibitor phosphoramidon (PA). Supernatants were analyzed using the 4-plex MSD assay as before (Fig. 5). In APP-overexpressing cells, PA treatment significantly elevated the levels of all Aβ species measured (Fig. 5a–d). In the presence of PA, however, Aβ34 was increased approximately ninefold, whereas the levels of Aβ38, Aβ40, and Aβ42 were only about two to threefold higher (Fig. 5a–d). In agreement with previously published data[21], these findings imply that Aβ34 is more sensitive to metalloprotease-mediated degradation compared with the longer species tested. In BACE1-overexpressing cells, Aβ34 levels were increased by about 2.5-fold in the presence of PA, whereas Aβ38, Aβ40, and Aβ42 levels were not significantly changed (Fig. 5a–d). Together, these results suggest that Aβ34 is a stable Aβ degradation intermediate of the amyloid degradation cascade. Thus, we propose that in the presence of surplus APP substrate, Aβ38, Aβ40, and Aβ42 are degraded by both metalloproteases and the BACE1-mediated Aβ34 pathway (Fig. 5e). Conversely, in the presence of surplus BACE1 enzyme, longer forms of Aβ are predominantly degraded by BACE1, yielding Aβ34 as a metastable cleavage product (Fig. 5e).

CSF-Aβ34 levels are associated with AD progression. To explore the associations between Aβ34 and putative changes in BACE1 expression observed in AD[9–11], we analyzed Aβ34 in 98 human CSF samples from the Amsterdam Dementia Cohort. Samples were collected from 22 people with subjective cognitive complaints (SC), 17 with MCI that remained stable, 27 with MCI that later progressed to AD dementia (i.e., MCI converters), and 32 AD patients. Using our MSD assay, we found significantly elevated Aβ34 levels in the CSF of MCI converters when compared with SC or MCI stable (Fig. 6a). Furthermore, the levels in MCI converters showed a trend for being elevated compared with AD patients (the greater variability is likely due to a larger heterogeneity in this group). CSF-Aβ34 levels from all groups did not associate with age, the genetic risk allele *APOE ε4*, or gender (Supplementary Fig. 5a–c). As expected, there was a decrease in Aβ42 in AD patients and MCI converters compared with the SC and MCI stable group (Fig. 6b). These changes are likely due to the sequestration of Aβ42 into amyloid plaques and indicate that MCI converters and AD patients are typically Aβ+[41]. The Aβ34/Aβ42 ratio is significantly elevated in the MCI converter and AD groups compared with the other groups (Fig. 6c).

To assess whether CSF-Aβ34 could provide important information during the early stages of AD, we tested whether Aβ34 could discriminate between MCI converters vs. non-converters from the Amsterdam Dementia Cohort. Receiver operating characteristic (ROC) curves of the CSF analytes were used to determine the accuracy of distinction between the MCI converters (i.e., prodromal AD) vs. stable patients. The area under the curve (AUC) for Aβ34 alone was slightly smaller than for Aβ42 (Fig. 6d). Interestingly, the Aβ34/Aβ42 ratio (AUC = 0.91) significantly improved the diagnostic accuracy compared with the classical Aβ40/Aβ42 ratio (AUC = 0.82) (Fig. 6e). An optimal cut-off analysis[42] yielded the best cut-off for an Aβ34/Aβ42 ratio >0.245, where sensitivity was 81.48% and specificity 82.35% (Supplementary Fig. 5d). The improved diagnostic accuracy of the Aβ34/Aβ42 ratio seemed specific for the distinction between MCI converters and stables. Similar AUCs ranging from 0.93 to 0.98 were obtained for Aβ42, Aβ40/Aβ42, and Aβ34/Aβ42 for the distinction between the SC and MCI converters or the SC and AD populations respectively (Supplementary Fig. 5e, f). For the distinction between MCI converters and stable patients, p-tau and t-tau yielded AUCs of 0.93 and 0.94, respectively (Fig. 6f). To assess how Aβ34/Aβ42 compares with the core AD biomarkers[43], we calculated the ratio between the MCI converter and MCI stable groups (Fig. 6g). Aβ34/Aβ42 ranked third after the core markers, i.e., total- and phosphorylated-tau but before Aβ40/Aβ42 and Aβ42 (Fig. 6g). Overall, these results suggest that using Aβ34, an indicator for Aβ degradation in combination with Aβ42, a core biomarker for Aβ deposition, can improve the accuracy of prediction compared with Aβ40/Aβ42 regarding MCI patients who will convert to dementia vs. non-converters. The Aβ34/Aβ42 ratio could complement but not supplant existing biomarkers, such as CSF levels of total- and phosphorylated-tau. This finding suggests that, at certain stages of Aβ34 elevation in the CSF, the combination of this marker with reduced Aβ42 may indicate a failure in the clearance pathway associated with AD progression.

To test whether changes in the Aβ34/Aβ42 ratio are already detectable in earlier, pre-symptomatic AD, likely even before signs of neuronal injury become evident, we analyzed another 94 human CSF samples from cognitively normal, at-risk individuals from the PREVENT-AD cohort[44]. Individuals enrolled in this study have no diagnosable cognitive dysfunction and are in good general health, but they have a family history of a parent or multiple siblings affected with AD dementia[45–47]. At enrollment, these individuals were on average 10.2 years younger than the age of dementia onset for their earliest-affected relative. Consistent with our earlier Amsterdam Dementia Cohort findings, CSF-Aβ34 levels in the PREVENT-AD samples were not associated with age, *APOE ε4*, or gender (Supplementary Fig. 6a–c). We then tested whether an increased Aβ34/Aβ42 ratio (optimal cut-off Aβ34/Aβ42 > 0.245; Fig. 6e) could also be observed in cognitively normal individuals from the PREVENT-AD cohort. We identified 17 out of 94 individuals (18.09%) with Aβ34/Aβ42 ratios that were above our estimated cut-off.

According to current views, the asymptomatic phase of AD is characterized by a sequential appearance of abnormalities, starting with increased cortical Aβ deposition (stage 1), leading to additional signs of neurodegeneration (stage 2; no abnormalities are seen in stage 0)[48]. Figure 7a depicts the Aβ42 and t-tau distribution of the PREVENT-AD samples from individuals at different stages of pre-symptomatic AD, with most individuals remaining in the stage 0 group. The horizontal and vertical dotted lines and shaded areas represent Aβ42[41] and t-tau cut-off values[49,50] and their inter-assay variances[51] (Fig. 7a). The biomarker assessments (validated CSF-Aβ42 cut-off values

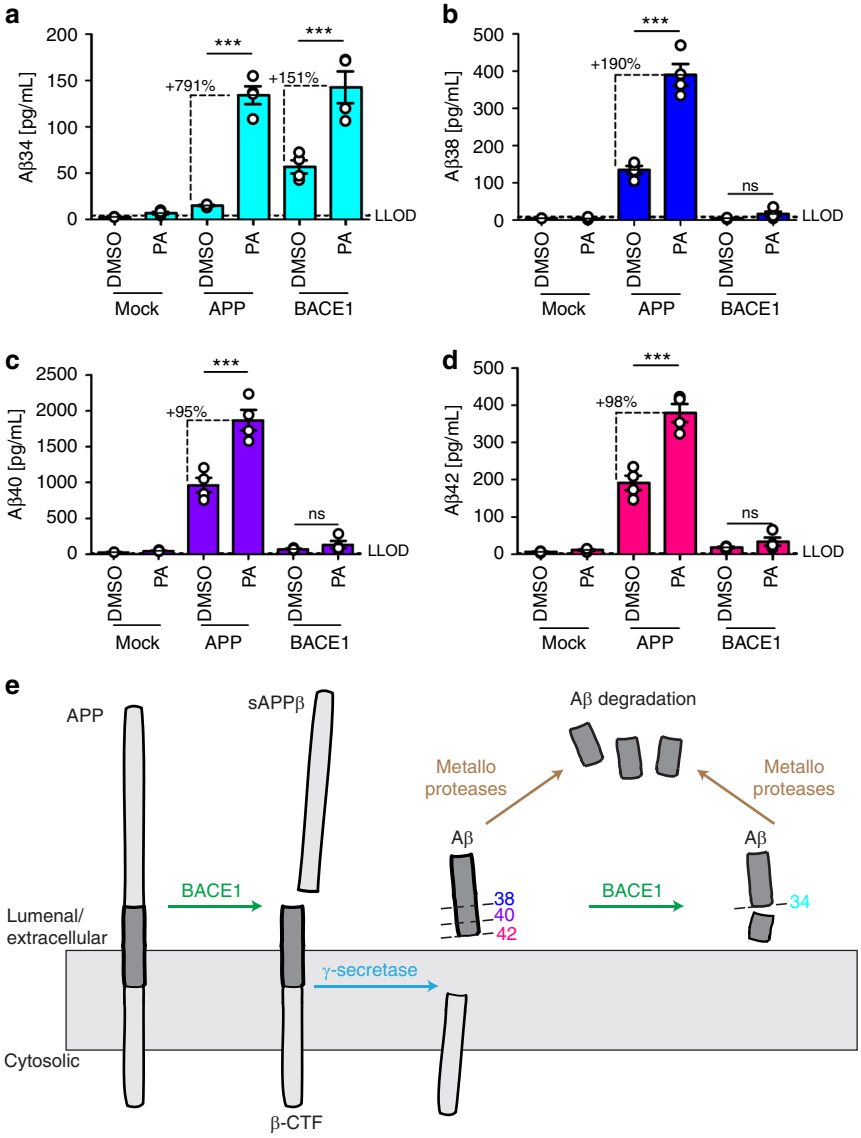

Fig. 5 Aβ34 degradation by PA-sensitive metalloproteases. Using SH-SY5Y cells stably expressing APP695 or BACE1, MSD multiplexing to quantify the absolute amounts of Aβ34 (**a**), Aβ38 (**b**), Aβ40 (**c**), and Aβ42 (**d**) was performed. Data were collected from four independent experiments. Bars and error bars indicate mean ± s.e.m. Data were analyzed with two-way ANOVAs and significant interactions were followed up with simple main effects @treatment. ***$p < 0.001$, ns = nonsignificant $p > 0.05$. **a** Aβ34, interaction $F(2, 18) = 23.93$, $p < 0.0001$, simple main effects @Mock $F(1, 18) = 0.12$, $p > 0.05$, @APP $F(1, 18) = 97.02$, $p < 0.0001$, @BACE1 $F(1, 18) = 50.41$, $p < 0.0001$, **b** Aβ38, interaction $F(2, 18) = 63.26$, $p < 0.0001$, simple main effects @Mock $F(1, 18) = 0.002$, $p > 0.05$, @APP $F(1, 18) = 197.54$, $p < 0.0001$, @BACE1 $F(1, 18) = 0.39$, $p > 0.05$, **c** Aβ40, interaction $F(2, 18) = 25.54$, $p < 0.0001$, simple main effects @Mock $F(1, 18) = 0.03$, $p > 0.05$, @APP $F(1, 18) = 73.97$, $p < 0.0001$, @BACE1 $F(1, 18) = 0.34$, $p > 0.05$, **d** Aβ42, interaction $F(2, 18) = 29.08$, $p < 0.0001$, simple main effects @Mock $F(1, 18) = 0.07$, $p > 0.05$, @APP $F(1, 18) = 97.47$, $p < 0.0001$, @BACE1 $F(1, 18) = 0.67$, $p > 0.05$. Schematic model (**e**) describes the proposed APP and Aβ processing pathways involving BACE1 and metalloproteases

including the inter-assay variances[41,51]) indicated that 15 PREVENT-AD participants are likely candidates having preclinical AD at stages 1 and 2 (Fig. 7a). Out of these, 11 presented with Aβ34/Aβ42 ratios above our cut-off (11/15 = 73.33%) (Fig. 7a). In addition, 6 out of 73 (8.22%) individuals at stage 0 also showed an elevated Aβ34/Aβ42 ratio. Individuals with elevated Aβ34/Aβ42 were not significantly older (Fig. 7b), but they exhibited significantly increased Cardiovascular Risk Factors, Aging, and Incidence of Dementia scores (CAIDE; Fig. 7c), and significantly increased CSF levels of total- and phosphorylated-tau (t-tau, p-tau; Fig. 7d, e).

CSF-Aβ34 correlates with Aβ clearance in Aβ+ individuals. In MCI and sporadic AD brain tissue, the levels and enzymatic activity of BACE1 are increased[9–11] and localized to the surroundings of amyloid deposits[12–15]. Above, we presented evidence that Aβ34 (an amyloidolytic product of BACE1) is associated with BACE1-mediated Aβ clearance and is elevated in MCI converters, who show evidence of amyloid plaques (based on their CSF-Aβ42 levels[41]). Thus, we analyzed the CSF concentrations of Aβ34, Aβ38, Aβ40, and Aβ42 in Aβ+ and amyloid-negative (Aβ–) individuals (10 individuals per group; Fig. 8), whose Aβ turnover was previously assessed by SILK^{TM} [31]. SILK^{TM} data of these 20 individuals were previously reported[31] and we correlated our results with the published data. The fractional turnover rate (FTR) or true fractional clearance rate[31], which is associated with the irreversible loss of Aβ38, Aβ40, and Aβ42[52], showed a significant positive correlation with the

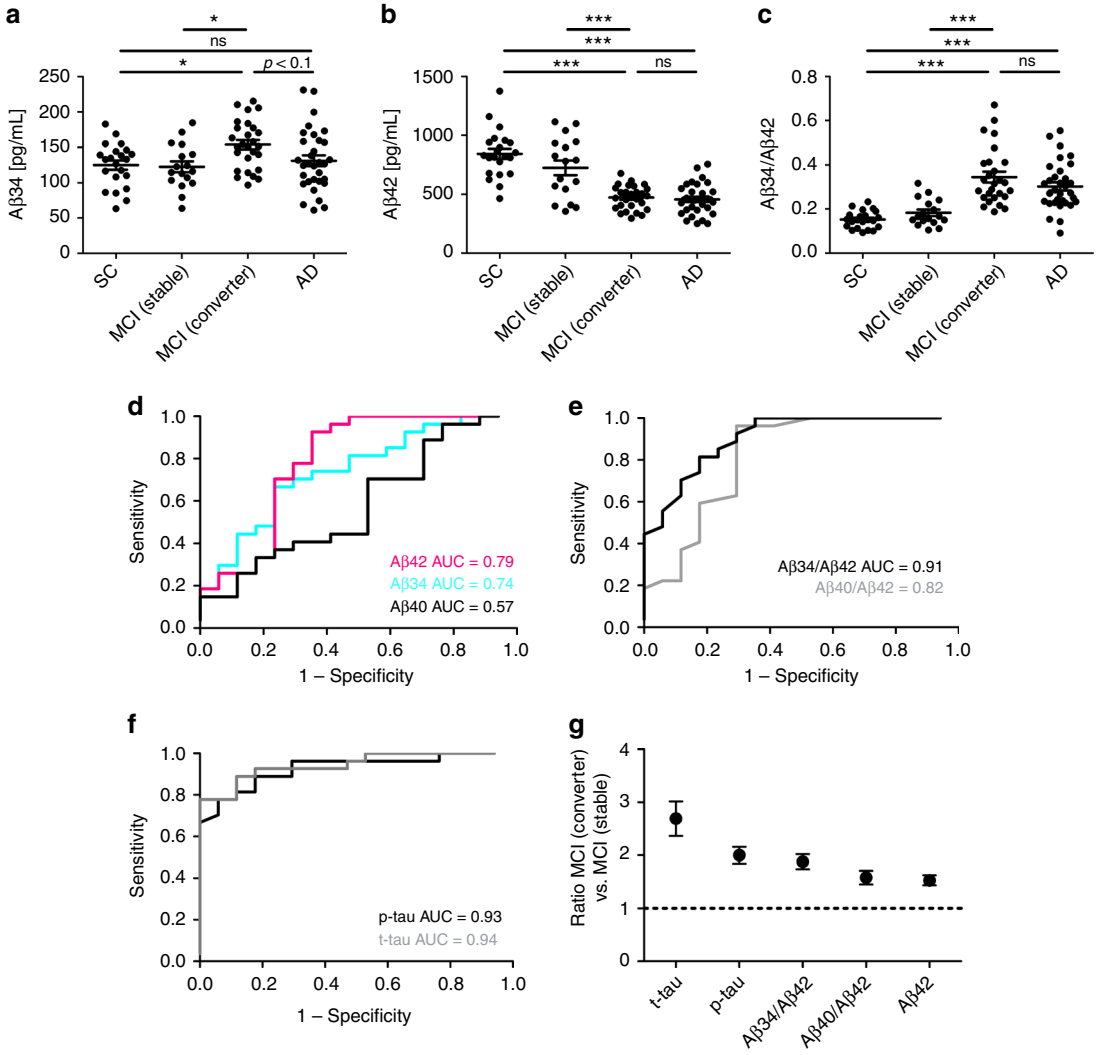

Fig. 6 Aβ34 and core biomarkers in the Amsterdam Dementia Cohort. **a**–**c** Analyses of Aβ34 and Aβ42 in human CSF samples. $n = 22$ subjective complaints (SC), $n = 17$ MCI (stable), $n = 27$ MCI (converter), $n = 32$ Alzheimer's disease (AD). Horizontal lines indicate mean ± s.e.m. The data were analyzed with one-way ANOVAs and Tukey's post-hoc tests (***$p < 0.001$, *$p < 0.05$, ns $p > 0.05$). **a** Aβ34, one-way ANOVA $F(3, 94) = 3.71$, $p < 0.05$, **b** Aβ42, one-way ANOVA $F(3, 94) = 30.91$, $p < 0.0001$, **c** Aβ 34/Aβ42, one-way ANOVA $F(3, 94) = 21.71$, $p < 0.0001$. **d** Receiver operating characteristic (ROC) curves were computed on CSF levels of Aβ34, Aβ40, and Aβ42 in samples from the Amsterdam Dementia Cohort $n = 17$ MCI (stable), $n = 27$ MCI (converter). **e** ROC curves on Aβ40/Aβ42 and Aβ34/Aβ42 ratios from MCI (stable) and MCI (converter)). ROCs were compared using DeLong test: Aβ40/Aβ42 vs. Aβ34/Aβ42 ($p = 0.0298$). **f** ROC curves on p-tau and t-tau from MCI (stable) and MCI (converter)). **g** Comparison of the performance of various molecules measured in CSF, which is based on average MCI (converter) to MCI (stable) ratios in the Amsterdam Dementia Cohort. The MCI (converter) to MCI (stable) ratio of Aβ42 was inverted for better comparison with the other ratios

CSF-Aβ34 concentrations only in Aβ+ individuals (Fig. 8a–c). Moreover, the CSF concentrations of Aβ38, Aβ40, and Aβ42 showed no significant correlation with Aβ38, Aβ40, or Aβ42 FTRs in our dataset (Fig. 8d–l). Interestingly, the ratio Aβ34/Aβ42 correlated with all three FTRs in Aβ– individuals, whereas the other ratios showed no correlation (Supplementary Fig. 7a–i). Overall, the correlation between Aβ34 and the clearance of the longer Aβ species is consistent with our results from rodent brains and SH-SY5Y cells, suggesting that elevated BACE1 levels in Aβ+ individuals might shift Aβ38, Aβ40, and Aβ42 into the Aβ34 degradation pathway. In conclusion, Aβ34 might serve as a surrogate marker for the overall clearance of Aβ38, Aβ40, and Aβ42 in Aβ+ and the ratio Aβ34/Aβ42 for the overall clearance in Aβ– individuals.

Discussion

In the AD field, research has traditionally focused on the conversion of APP into Aβ42 peptides leading to pathological amyloid plaque deposition in the brain and cognitive decline during the clinical progression of the disease. In recent years, however, emerging literature now identifies amyloid clearance as an important paradigm to better understand amyloid imbalances in sporadic AD patients.

BACE1 is thought to play a major role in the pathogenesis of AD and several inhibitors have been evaluated in clinical trials for their potential to slow or halt the production of neurotoxic Aβ peptides[8]. In order to attenuate disease progression in individuals with existing amyloid plaques, Aβ production would need to be inhibited by at least 95% since deposition is expected to be fast in

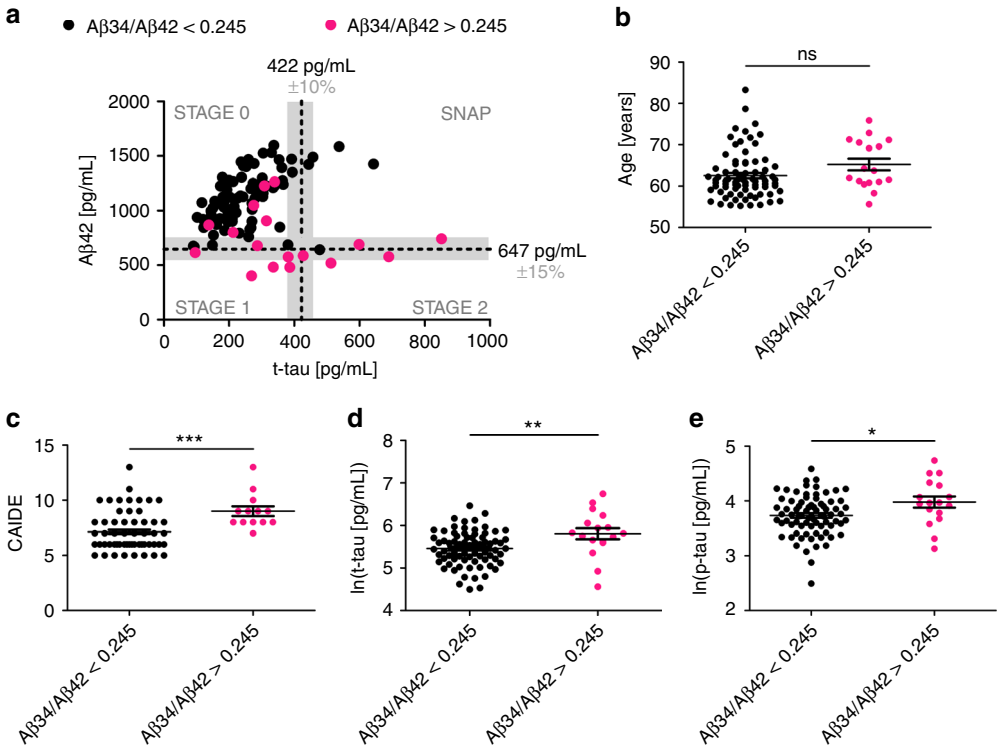

Fig. 7 Aβ34, Aβ42, t-tau, and p-tau in PREVENT-AD. **a**–**e** PREVENT-AD Study: analysis of Aβ34, Aβ42, t-tau, and p-tau in CSF samples from cognitively normal individuals at risk for Alzheimer's disease ($n = 94$). **a** Individuals can be separated into stages of pre-symptomatic AD, based on CSF biomarker assessment (t-tau cut-off > 422 pg/mL[49,50], Aβ42 cut-off ≤ 647 pg/mL[41], the gray shaded area indicates common inter-assay variances of the used cut-off values[41,51]). STAGE 0: t-tau and Aβ42 normal; STAGE1: t-tau normal and Aβ42 ≤ 647 pg/mL; STAGE 2: t-tau > 422 pg/mL, and Aβ42 ≤ 647 pg/mL; Suspected-non-AD pathology (SNAP): t-tau > 422 pg/mL and Aβ42 normal. Individuals with Aβ34/Aβ42 ratio above the optimal cut-off calculated in this study (Aβ34/Aβ42 > 0.245) are highlighted in magenta. **b**–**e** Comparison of age, Mann–Whitney $U = 461.5$, $p = 0.0586$ (**b**); Cardiovascular Risk Factors, Aging, and Incidence of Dementia (CAIDE), Mann–Whitney $U = 184.5$, $p = 0.0004$ (**c**); t-tau, unpaired t-test $t(92) = 3.027$, $p = 0.0032$ (**d**); and P_{181}-tau (p-tau), unpaired *t*-test $t(92) = 2.453$, $p = 0.0168$ (**e**); between individuals with Aβ34/Aβ42 ratios above and below optimal cut-off (***$p < 0.001$, **$p < 0.01$, *$p < 0.05$, ns $p > 0.05$). Horizontal lines indicate mean ± s.e.m.

Aβ+ individuals, even at lowered rates of newly produced Aβ[53,54]. Recently, current treatment approaches have been challenged based upon reports of disappointing results and adverse effects from BACE inhibitor trials (press release, 25 October 2018, Is there a role for BACE inhibition in Alzheimer's treatment?, Clinical Trials on Alzheimer's Disease (CTAD) conference).

BACE1 levels are increased in the AD brain[9–11], and this could potentially result in increased Aβ production. However, a ~50% reduction in cerebral BACE1 (as reported in BACE1+/− mice and rats) does not alter Aβ38, Aβ40, and Aβ42 levels, suggesting that half the usual amount of BACE1 is sufficient to fully process endogenous APP[32,33,35,36]. Furthermore, increased enzyme levels do not lead to an increased amyloid load in the brains of mice overexpressing human BACE1[55].

We found that cerebral Aβ34 levels were decreased by about 30% in BACE1+/− mice and by about 40% in wild-type rats, 1 h after intravenous injection of 1 mg/kg MK-8931 (with longer Aβ species unaltered). In the CSF of these MK-8931-treated rats, Aβ34 was the only Aβ species that was significantly decreased in the 1 and 20 mg/kg groups. However, since we administered the inhibitor intravenously, the greatest reduction in Aβ was likely achieved much earlier than in the original study, where rats received the compound orally and Aβ40 was significantly reduced in CSF and cortex at 1 and 3 h[37]. Due to the different routes of administration, our data cannot be directly compared with this study[37]. In contrast to the initial APP cleavage, BACE1 is a limiting factor for the amyloidolytic cleavage of longer Aβ species into Aβ34. Furthermore, our data imply that cerebral BACE1 possesses Aβ-degrading properties in vivo, as consistent with an earlier hypothesis based on in vitro studies[19–21]. The dichotomy between the amyloidogenic and amyloidolytic roles of BACE1 becomes more evident in experimental systems with elevated BACE1 levels. In the present study, for example, we found that an excess of APP favors amyloidogenic Aβ peptide production, but an excess of BACE1 results in increased Aβ degradation to Aβ34. Our characterization of the BACE1-mediated Aβ34 pathway is consistent with previous findings that cerebral BACE1 is not limiting for Aβ production[32,33,35,36], observations that until now had remained unexplained due to our lack of understanding of amyloidolytic BACE1 activity.

As BACE1-derived Aβ34 can be further degraded by PA-sensitive metalloproteases[21], it may be classified as a metastable intermediate in the degradation cascade of amyloidogenic peptides. The current findings show that this process is regulated by BACE1 expression such that when BACE1 may become limiting (i.e., when APP is overexpressed), amyloidogenic Aβ peptides are enzymatically degraded by both metalloproteases and BACE1. However, when BACE1 is present in sufficient or excess amounts (i.e., when overexpressed), the Aβ34 pathway is favored. As BACE1 is strongly expressed in neurons, particularly at sites of Aβ production in the brain[14,15], longer Aβ peptides may be favorably converted into non-toxic Aβ34 at these sites. It is likely that Aβ34 might have a specific biological function and anti-apoptotic actions of this fragment on cultured human cells have been described[21], however, a more thorough characterization is needed in order to determine its physiological role.

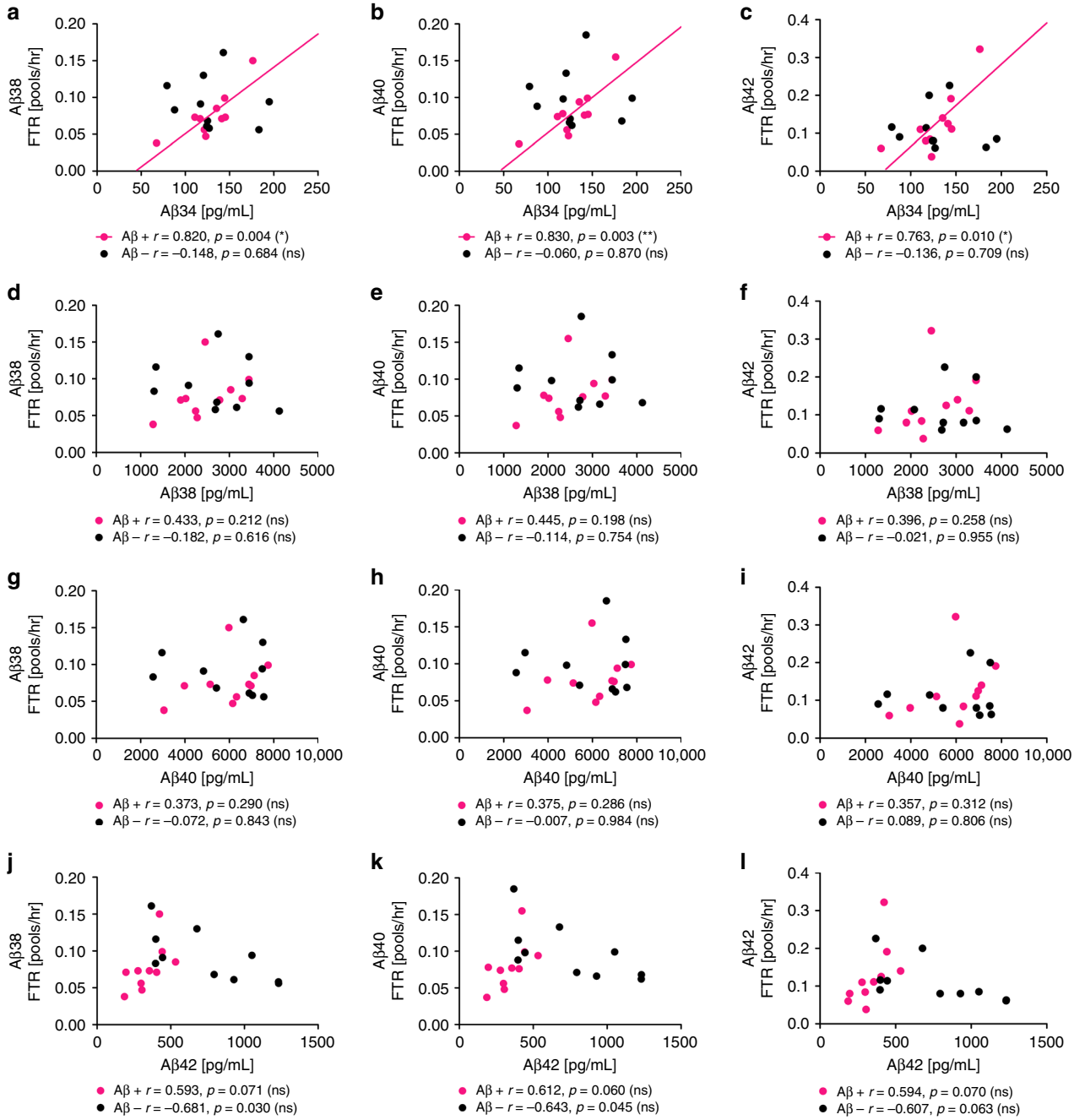

Fig. 8 Association between CSF-Aβ34 and Aβ clearance rates. Analysis of Aβ34, Aβ38, Aβ40, and Aβ42 in human CSF with ultra-sensitive assays (Meso Scale Discovery (MSD)). Aβ38, Aβ40, and Aβ42 clearance (fractional turnover rate, FTR) was previously measured using stable isotope labeling kinetic (SILK)[31]. Samples were from $n = 10$ Aβ+ and $n = 10$ Aβ- individuals. Scatterplots of CSF-Aβ34 (**a**–**c**), Aβ38 (**d**–**f**), Aβ40 (**g**–**i**), or Aβ42 (**j**–**l**) with Aβ38 FTR (**a**, **d**, **g**, **j**), Aβ40 FTR (**b**, **e**, **h**, **k**), or Aβ42 FTR (**c**, **f**, **i**, **l**). Pearson correlation coefficients (r) were computed to assess the relationship between the variables. The Bonferroni adjusted p-values are: $^{**}p < 0.003$, $^{*}p < 0.016$, ns = nonsignificant $p > 0.0125$

Site-specific mutations in APP were found in rare cases of familial early-onset AD (FEOAD) and processing at the β-cleavage site of APP could be causally linked to increased and decreased risk of AD. For example, β-cleavage of APP carrying the Swedish mutation (KM670/671NL) is increased and causes FEOAD[56]. In contrast, the Icelandic mutation (A673T) protects against AD[57], primarily by reducing the β-cleavage of APP, as well as modulating Aβ aggregation[58]. In light of our findings, it is plausible that the Icelandic mutation results in reduced Aβ generation, whereas BACE1-mediated Aβ degradation still occurs. Although inhibition of BACE1-mediated cleavage of APP remains an attractive therapeutic approach in AD, it appears that reducing BACE1-mediated generation of pathogenic Aβ peptides alone will not be sufficient to stop plaque growth[53,54]. Furthermore, BACE1 inhibition is likely to affect amyloidolytic cleavage of longer Aβ species into smaller, non-amyloidogenic Aβ34. For this reason, we tested for clearance effects in human CSF and, notably, we found elevated baseline levels of Aβ34 in MCI patients who later progressed to AD. Aβ34 can be detected in human plasma samples[59], therefore, it would be interesting to test whether its levels in CSF and plasma correlate or whether MCI converters show elevated amounts of plasma-Aβ34. By combining

an indicator for Aβ degradation (i.e., Aβ34) and a biomarker for Aβ deposition (i.e., Aβ42), we found that the Aβ34/Aβ42 ratio significantly improved the diagnostic accuracy to distinguish between prodromal AD and stable MCI compared with the classical Aβ40/Aβ42 ratio. However, elevated CSF levels of p-tau and t-tau showed the best distinction between the two MCI groups. An elevated Aβ34/Aβ42 ratio in the prodromal stage of AD could indicate that, at early stages of Aβ plaque formation (i.e., decreased CSF-Aβ42 levels[41]), the increased levels and amyloidolytic activity of BACE1 elicit a defense reaction (i.e., increased generation of Aβ34 to facilitate amyloid clearance). Although BACE1 levels are elevated around fibrillar Aβ[12–15], the fibrillar conformation is resistant to BACE1 cleavage because of its unique structure[60] (under the condition of their co-presence in a cellular compartment with a low pH). Aβ42 fibrils are stabilized by hydrophobic clusters in such a way that they do not grant BACE1 access to the Aβ34 cleavage site[60]. Furthermore, since only Aβ42 turnover (and not Aβ38 or Aβ40) is altered when amyloidosis has started[31], the surplus of Aβ34 could be mainly derived from Aβ42 since its conformation is different from Aβ38 and Aβ40. We speculate that intracellular Aβ42 can adopt a conformation that is favorable for fibril formation, which makes it especially susceptible to BACE1-mediated degradation at the Aβ34 cleavage site.

We hypothesized that the Aβ34/Aβ42 ratio might be potentially useful to monitor pre-symptomatic AD, as changes in the classical biomarkers of AD pathogenesis can already be observed before cognitive symptoms appear[48]. In human samples from the PREVENT-AD cohort (i.e., at-risk individuals without current cognitive impairment), we found that the Aβ34/Aβ42 ratio was elevated, especially in individuals whose biomarker assessment classified them in stages 1 and 2 (signs of cortical Aβ deposition). Overall, few individuals in PREVENT-AD showed reduced CSF-Aβ42 ($\leq$ 647 pg/mL[41]). In families with autosomal-dominant AD, reduced CSF-Aβ42 and increased tau in asymptomatic mutation carriers were already detected 10–20 years before the estimated age of onset[61]. At present, members of the PREVENT-AD cohort tend to be several years younger compared with the onset of dementia in their affected relative(s) and, in contrast to mutation carriers, they probably vary substantially in their degree of progression of pre-symptomatic AD. Interestingly, we identified individuals in stage 0 with an elevated Aβ34/Aβ42 ratio. However, our data are cross-sectional and should not be interpreted as representing change over chronological ageing. Therefore, it will be crucial to follow the longitudinal trajectory of Aβ34 in these individuals, in combination with classical CSF measures, since we expect that these biomarker changes are closely related to aging, as previously seen in cognitively normal middle-aged volunteers[62].

Consistent with the concept of amyloid clearance and deposition mechanisms indicating failed clearance in pre-symptomatic stages of AD, we find that the Aβ34 levels in CSF correlate with the overall clearance rates of Aβ38, Aβ40, and Aβ42 in Aβ+ but not Aβ− individuals. In contrast, the CSF Aβ34/Aβ42 ratios correlate with the overall clearance rates of Aβ38, Aβ40, and Aβ42 in Aβ− but not Aβ+ individuals. Since inter-individual variances in Aβ clearance rates are affected by various factors including age, genetics, or pathological processes[24,31,52,63], it is rather unlikely that the levels of an individual protein, such as BACE1, could determine the overall Aβ clearance from the brain. However, our findings suggest that under pathological conditions, elevated BACE1 levels in the brain direct a large proportion of Aβ38, Aβ40, and Aβ42 into BACE1-mediated Aβ clearance via the Aβ34 degradation pathway. Given this, Aβ34 might be used as a marker for the overall clearance of these peptides in Aβ+ individuals. We speculate that under non-pathological conditions, a special relationship exists between Aβ34 and Aβ42, which might explain the correlation of their ratio with the overall Aβ clearance. Once Aβ42 gets deposited in plaques, the correlation with clearance is lost, likely due to an altered Aβ42 degradation. Under these circumstances, Aβ34 alone becomes the predictor of clearance rates.

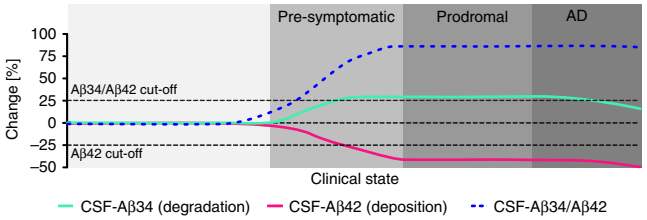

Fig. 9 Conceptual model of early changes in AD. Before a clinical diagnosis of Alzheimer's disease (AD), decades of Aβ peptide deposition lead to plaque formation in pre-symptomatic and prodromal stages of the disease. Incorporating Aβ34 (marker of enzymatic Aβ degradation) with measures of Aβ42 (marker for cerebral Aβ deposition) could complement current biomarker assessments and provide additional information about Aβ turnover

In summary, our results show that, in vivo, BACE1 is limiting for the degradation of longer Aβ peptides into the intermediate Aβ34. The levels of this amyloidolytic fragment are elevated in the CSF of prodromal AD patients (i.e., MCI that progresses to AD). Thus, incorporating Aβ34 as a marker of amyloid clearance with a marker of amyloid deposition (i.e., Aβ42) might complement current CSF measures, especially in clinical intervention trials that aim at a modulation of APP processing (Fig. 9). Ultimately, the present study proposes that enzymatic processes affecting Aβ metabolism are altered in early phases of AD and, accordingly, Aβ34 can be used to monitor Aβ turnover at earlier stages of this devastating disease.

Methods

Synthetic Aβ peptides. Synthetic peptides Aβ34, Aβ35, Aβ38, Aβ40, and Aβ42 (PSL, Germany) dissolved in formic acid and vacuum dried in a speed-vac (Thermo) were resuspended (2 mg/mL) in 1% Milli-Q/ammonia water, ultrasonicated (10 min 4 °C), diluted to 1 mg/mL with Milli-Q and ultrasonicated again. Peptide concentrations ($\varepsilon = 1490$ M/cm), integrity, and molecular weight were confirmed by absorption measurements at 280 nm (Synergy H1, BioTek Instruments Inc. plate reader), Coomassie dye stains after performing denaturing polyacrylamide gel electrophoresis (SDS-PAGE), and matrix-assisted laser desorption ionization mass spectrometry (Bruker UltrafleXtreme MALDI-TOF/TOF system in standard reflector-positive mode; samples mixed 1:1 with α-cyanocinnamic acid matrix and applied to ground steel targets using dried-droplet method).

BACE1-mediated Aβ degradation in vitro. BACE1 from Fc purification[64] 10 µg/mL (a kind gift from Johan Lundkvist, AstraZeneca) was incubated with synthetic Aβ35, Aβ40, or Aβ42 at 50 µg/mL for 10 min at 37° C in 20 mM (sodium acetate/HCl, pH4.5), directly mixed 1:1 with α-cyanocinnamic acid matrix, and applied to ground steel targets using dried-droplet method.

MSD assay. Using the ELISA Conversion Kit from MSD (USA), an electrochemiluminescence-based assay was developed (neo-epitope specific Aβ34 and the sulfo-tagged 6E10 (binds to the N-terminus of human Aβ) or the sulfo-tagged 4G8 for rodent samples (binds to the mid domain of Aβ)). High-bind or custom-printed 4-plex plates (using our mab34, 4G8 (Biolegend) for pan-Aβ assay, G2-10 for 1-plex Aβ40 assay, and MSD's validated mouse monoclonal anti-Aβ38, anti-Aβ40, as well as anti-Aβ42 antibodies, see MSD Aβ peptide V-PLEX) were blocked (MSD 5% Blocker A in PBS) for 1 h at 22 °C and washed three times with PBS-Tween (PBS-T) for 1 min at 22 °C, loaded with SULFO-TAG™ 6E10 or 4G8 detection antibody (diluted to 1× in MSD Diluent 100) and sample or peptide calibrator (in MSD Diluent 35 or cell culture medium), and incubated for 16 h at 4 °C with shaking at 600 rpm. After three washing steps with PBS-T for 1 min at 22 °C, 150 µL 2× MSD read buffer was added per well. All plates were read using an MSD QuickPlex SQ 120 Imager and data analyzed using MSD Workbench® software. Standard curves were fitted using a non-linear four-parameter logistic fit

with $1/y^2$ weighting. The equation is:

$$y = b_2 + \frac{b_1 - b_2}{1 + \left(\frac{x}{b_3}\right)^{b_4}} \quad (1)$$

y = signal, x = concentration, b_2 = estimated response at infinite concentration, b_1 = estimated response at Zero concentration, b_3 = mid-range concentration, b_4 = slope factor.

In the WORKBENCH® software, lower limit of detection (LLOD) was determined as the analyte concentration equivalent to the signal that is 2.5× standard deviations (SD) above the back-fit signal of the blank. Assay performance (inter-plate, intra-plate coefficient of variation (CV), LLOD, and upper limit of detection (ULOD)) were assessed using peptide calibrators in MSD diluent 35 (Supplementary Fig. 1e). Spike-and-recovery and linearity-of-dilution assessments for human CSF samples (compared with calibrators in MSD diluent 35) are given in Supplementary Table 1.

Western blot analysis. Lithium dodecyl sulfate loading buffer (Invitrogen) with 2-Mercaptoethanol (final concentration 5% (*v*/*v*)) was added to samples and the mix was heated to 70 °C for 10 min. Proteins were separated on 4–12% bis/tris gradient gels. Novex® Sharp Pre-Stained Protein Standard (Invitrogen) was used. Peptides/proteins were transferred onto polyvinylidene fluoride membranes (Millipore) by tank blotting (Bio-Rad) at 4 °C. The primary antibodies, anti-actin C4 dilution 1:4000 (Millipore, Catalog #MAB1501), anti-APP ectodomain 22C11 dilution 1:10,000 (Millipore, Catalog #MAB348), anti-BACE1 D10E5 dilution 1:2000 (Cell Signaling, Catalog #mAb5606), anti-sAPPβ dilution 1:2000 (IBL, Catalog #JP18957), and secondary antibodies dilutions 1:10,000 (horseradish peroxidase-conjugated anti-mouse, anti-rabbit, Promega, Catalog #W4021 and # W4011), were used. Most important full-size western blots are displayed in Supplementary Fig. 8. Signals were recorded on ImageQuant LAS 500 or Amersham Imager 600 (GE Healthcare Life Sciences).

Mouse brain lysates. We complied with all relevant ethical regulations for animal testing and research. Brains were obtained from BACE1−/− and BACE1+/− mice, as well as their wild-type littermates[65] in accordance with the guidelines of the Institutional Animal Care and Use Committee at the University of Kiel. Frozen mouse brains were thawed on ice, weighed and homogenized in 100 mM Tris-HCl, 150 mM NaCl, 2× complete protease inhibitor cocktail (Roche) using gentleMACS™ M Tubes/Dissociator at 4 °C (Miltenyi Biotech). Triton X-100 was added for a final concentration of 1% and brain homogenates were lysed for 1 h at 4 °C. Lysates were centrifuged at 10,621 × *g* in a microfuge (Eppendorf) at 4 °C for 15 min to remove nuclear fraction. Samples were diluted in the appropriate buffers for protein determination using bicinchoninic acid assay (BCA assay, Pierce) and MSD assays.

Pharmacological treatment of rats. We complied with all relevant ethical regulations for animal testing and research. Experiments were approved by the McGill Animal Care Ethics Committee. Six to 8 weeks old male Sprague–Dawley rats were housed at the Douglas Mental Health University Institute animal facility and treatments were performed in accordance with the guidelines of the Canadian Council on Animal Care. Rats were intravenously injected with indicated concentrations of MK-8931 (Selleckchem) or vehicle (20% Cyclodextrin) and samples were collected after 1 h of treatment. CSF was collected with the aid of a stereotaxic instrument to appropriately position the head of the rat and samples stored at −80 °C. Brain tissue samples were harvested and immediately preserved on dry ice, later stored at −80 °C. Rat brain lysates were prepared in the same way as mouse brain lysates.

Plasmids, mutagenesis. Human full-length BACE1 (isoform A) and human full-length APP (isoform APP695, with an N-terminal Myc tag and a C-terminal FLAG tag), in the mammalian expression vector pCEP4, Hygro (Invitrogen) were used for expression. All constructs were verified by DNA sequencing.

Cell culture and transfection. Human neuroblastoma (SH-SY5Y) cells (DSMZ No.: ACC 209; DSMZ, Braunschweig/ Germany) were cultured in 50% Dulbecco's modified Eagle's medium, 50% Hams-F12, 10% fetal bovine serum, 2 mM L-glutamine, 0.5 mM sodium pyruvate, 1× MEM non-essential amino-acid solution in a humidified incubator at 37 °C with 5% CO_2. Cells were routinely tested for mycoplasma contamination. SH-SY5Y cells were transfected using TransFectin™ according to the manufacturer's instructions (Bio-Rad) and stable clones were selected using 250 µg/mL Hygromycin B. For experiments, culturing medium without Hygromycin B was used and conditioned for 16 h. Protease inhibitors, were dissolved in Dimethyl sulfoxide (DMSO) at a 1000× concentration and compared with vehicle treatment (DMSO 1:1000). Cells were harvested on ice. Cell culture supernatants were collected, centrifuged for 10 min at 450 × *g* in a microcentrifuge at 4 °C and used for further analysis. Cells were washed once on ice with ice-cold PBS^{++} and lysed in 20 mM Tris-HCl, pH 7.5, 150 mM NaCl, 20 mM 3-[(3-cholamidopropyl) dimethyl-ammonio]-1-propanesulfonate (CHAPS), 2× Complete protease inhibitor (Roche), for 60 min at 4 °C. Cell lysates were centrifuged for 15 min at 10,621 × *g* in a microcentrifuge at 4 °C to remove nuclear fraction.

CSF samples. We complied with all relevant ethical regulations for work with human participants. The studies were performed in accordance with The Code of Ethics of the World Medical Association (Declaration of Helsinki). The studies were approved by the regional ethics committees. Written informed consent was received from participants prior to inclusion in the studies.

CSF samples for initial assay development were received from the Clinic at the Division of Psychiatry, Zurich. CSF samples from individuals with SILK data[31] were obtained from the Department of Neurology, Washington University in St. Louis. CSF samples from individuals with different clinical diagnoses were received from the Amsterdam Dementia Cohort and the time interval between CSF collection and assessment of cognition was <24 h[66]. CSF samples from cognitively normal individuals at risk for AD (PREVENT-AD study) were received from the Douglas Mental Health University Institute and the time interval between CSF collection and assessment of cognition was on average 5.6 ± 3.9 (SD) months[44]. The experimentalist was blinded from diagnosis until completion of measurements. Diagnoses of probable AD[67] or MCI[68], were made by consensus of a multidisciplinary team according to diagnostic criteria. For the Amsterdam Dementia Cohort, patients who presented with cognitive complaints but were considered as normal after thorough investigation (i.e., criteria for MCI, dementia or any psychiatric or neurological results not fulfilled) were defined as patients with subjective cognitive complaints (SC). Subjects were followed annually and MCI to AD conversion (or MCI that remained stable) was defined based on conversion to AD within 3 years after the CSF collection, and stable as no conversion occurred within 3 years. Lumbar punctures after an overnight fast were performed using the Sprotte 24-gauge atraumatic needle. Samples were aliquoted into propylene cryotubes and stored at −80 °C. Procedures from the BIOMARK-APD consortium of the EU Joint Program in Neurodegenerative Disease were used for sample preparation and measurements[69]. A summary of samples included in the study is given in Supplementary Table 2. CSF t-tau, p-tau, and Aβ42 were measured using INNOTEST ELISA; Fujirebio (formerly Innogenetics).

Statistical analysis. The statistical evaluation was carried out by GraphPad Prism, SPSS, MedCalc Version 18.2.1, and the indicated statistical tests and algorithms (analysis of variance (ANOVA), *t*-test, Pearson correlation, Mann–Whitney *U*-tests, Spearman correlations, De Long statistics to compare ROC curves[70]). The optimal cut-off (point on the ROC curve with the minimum distance (d) to sensitivity = 1 and specificity = 1)[42] was determined using Pythagoras' theorem:

$$d = \sqrt{(1 - \text{sensitivity})^2 + (1 - \text{specificity})^2} \quad (2)$$

Individual data points, mean and s.e.m. are displayed in the figures. Data were tested for normality, using violation of the Shapiro–Wilk test at $p < 0.01$ as the criterion. Data sets not meeting the normality assumption were analyzed using non-parametric tests (as indicated in the figure legends).

Reporting summary. Further information on research design is available in the Nature Research Reporting Summary linked to this article.

Data availability

Data used in the preparation of this article were obtained from the Pre-symptomatic Evaluation of Novel or Experimental Treatments for Alzheimer's Disease (PREVENT-AD) program (http://www.prevent-alzheimer.ca) data release 2.0 (30 November 2015, Update: 07 June 2016). Other relevant data are available directly from the authors.

Received: 1 May 2018 Accepted: 17 April 2019
Published online: 20 May 2019

References

1. Hardy, J. & Selkoe, D. J. The amyloid hypothesis of Alzheimer's disease: progress and problems on the road to therapeutics. *Science* **297**, 353–356 (2002).
2. Walsh, D. M. & Selkoe, D. J. Oligomers on the brain: the emerging role of soluble protein aggregates in neurodegeneration. *Protein Pept. Lett.* **11**, 213–228 (2004).
3. Wilquet, V. & De Strooper, B. Amyloid-beta precursor protein processing in neurodegeneration. *Curr. Opin. Neurobiol.* **14**, 582–588 (2004).
4. Thinakaran, G. & Koo, E. H. Amyloid precursor protein trafficking, processing, and function. *J. Biol. Chem.* **283**, 29615–29619 (2008).
5. Takami, M. et al. gamma-Secretase: successive tripeptide and tetrapeptide release from the transmembrane domain of beta-carboxyl terminal fragment. *J. Neurosci.* **29**, 13042–13052 (2009).

6. Olsson, F. et al. Characterization of intermediate steps in amyloid beta (Abeta) production under near-native conditions. *J. Biol. Chem.* **289**, 1540–1550 (2014).
7. Glabe, C. G. & Kayed, R. Common structure and toxic function of amyloid oligomers implies a common mechanism of pathogenesis. *Neurology* **66**, S74–S78 (2006).
8. Mullard, A. BACE inhibitor bust in Alzheimer trial. *Nat. Rev. Drug Disco.* **16**, 155 (2017).
9. Fukumoto, H., Cheung, B. S., Hyman, B. T. & Irizarry, M. C. Beta-secretase protein and activity are increased in the neocortex in Alzheimer disease. *Arch. Neurol.* **59**, 1381–1389 (2002).
10. Holsinger, R. M., McLean, C. A., Beyreuther, K., Masters, C. L. & Evin, G. Increased expression of the amyloid precursor beta-secretase in Alzheimer's disease. *Ann. Neurol.* **51**, 783–786 (2002).
11. Yang, L. B. et al. Elevated beta-secretase expression and enzymatic activity detected in sporadic Alzheimer disease. *Nat. Med.* **9**, 3–4 (2003).
12. Sadleir, K. R., Eimer, W. A., Kaufman, R. J., Osten, P. & Vassar, R. Genetic inhibition of phosphorylation of the translation initiation factor eIF2alpha does not block Abeta-dependent elevation of BACE1 and APP levels or reduce amyloid pathology in a mouse model of Alzheimer's disease. *PLoS ONE* **9**, e101643 (2014).
13. Sadleir, K. R. et al. Presynaptic dystrophic neurites surrounding amyloid plaques are sites of microtubule disruption, BACE1 elevation, and increased Abeta generation in Alzheimer's disease. *Acta Neuropathol.* **132**, 235–256 (2016).
14. Zhao, J. et al. Beta-site amyloid precursor protein cleaving enzyme 1 levels become elevated in neurons around amyloid plaques: implications for Alzheimer's disease pathogenesis. *J. Neurosci.* **27**, 3639–3649 (2007).
15. Kandalepas, P. C. et al. The Alzheimer's beta-secretase BACE1 localizes to normal presynaptic terminals and to dystrophic presynaptic terminals surrounding amyloid plaques. *Acta Neuropathol.* **126**, 329–352 (2013).
16. Zhang, X. M. et al. Beta-secretase-1 elevation in transgenic mouse models of Alzheimer's disease is associated with synaptic/axonal pathology and amyloidogenesis: implications for neuritic plaque development. *Eur. J. Neurosci.* **30**, 2271–2283 (2009).
17. Kimura, A., Hata, S. & Suzuki, T. Alternative selection of beta-site APP-cleaving enzyme 1 (BACE1) cleavage sites in amyloid beta-protein precursor (APP) harboring protective and pathogenic mutations within the Abeta sequence. *J. Biol. Chem.* **291**, 24041–24053 (2016).
18. Hernandez-Guillamon, M. et al. Sequential amyloid-beta degradation by the matrix metalloproteases MMP-2 and MMP-9. *J. Biol. Chem.* **290**, 15078–15091 (2015).
19. Fluhrer, R. et al. Identification of a beta-secretase activity, which truncates amyloid beta-peptide after its presenilin-dependent generation. *J. Biol. Chem.* **278**, 5531–5538 (2003).
20. Shi, X. P. et al. Beta-secretase cleavage at amino acid residue 34 in the amyloid beta peptide is dependent upon gamma-secretase activity. *J. Biol. Chem.* **278**, 21286–21294 (2003).
21. Caillava, C. et al. Study on Abeta34 biology and detection in transgenic mice brains. *Neurobiol. Aging* **35**, 1570–1581 (2014).
22. Portelius, E. et al. beta-site amyloid precursor protein-cleaving enzyme 1 (BACE1) inhibitor treatment induces Abeta5-X peptides through alternative amyloid precursor protein cleavage. *Alzheimer's Res. Ther.* **6**, 75 (2014).
23. Mattsson, N. et al. BACE1 inhibition induces a specific cerebrospinal fluid beta-amyloid pattern that identifies drug effects in the central nervous system. *PLoS ONE* **7**, e31084 (2012).
24. Mawuenyega, K. G. et al. Decreased clearance of CNS beta-amyloid in Alzheimer's disease. *Science* **330**, 1774 (2010).
25. Iliff, J. J. et al. A paravascular pathway facilitates CSF flow through the brain parenchyma and the clearance of interstitial solutes, including amyloid beta. *Sci. Transl. Med.* **4**, 147ra111 (2012).
26. Deane, R., Sagare, A. & Zlokovic, B. V. The role of the cell surface LRP and soluble LRP in blood-brain barrier Abeta clearance in Alzheimer's disease. *Curr. Pharm. Des.* **14**, 1601–1605 (2008).
27. Lewczuk, P. et al. The amyloid-beta (Abeta) peptide pattern in cerebrospinal fluid in Alzheimer's disease: evidence of a novel carboxyterminally elongated Abeta peptide. *Rapid Commun. Mass Spectrom.* **17**, 1291–1296 (2003).
28. Saido, T. & Leissring, M. A. Proteolytic degradation of amyloid beta-protein. *Cold Spring Harb. Perspect. Med.* **2**, a006379 (2012).
29. Portelius, E. et al. Ex vivo (18)O-labeling mass spectrometry identifies a peripheral amyloid beta clearance pathway. *Mol. Neurodegener.* **12**, 18 (2017).
30. Bateman, R. J. et al. Human amyloid-beta synthesis and clearance rates as measured in cerebrospinal fluid in vivo. *Nat. Med.* **12**, 856–861 (2006).
31. Patterson, B. W. et al. Age and amyloid effects on human central nervous system amyloid-beta kinetics. *Ann. Neurol.* **78**, 439–453 (2015).
32. Weber, M. et al. BACE1 across species: a comparison of the in vivo consequences of BACE1 deletion in mice and rats. *Sci. Rep.* **7**, 44249 (2017).
33. Rabe, S. et al. The Swedish APP mutation alters the effect of genetically reduced BACE1 expression on the APP processing. *J. Neurochem.* **119**, 231–239 (2011).
34. Sala Frigerio, C. et al. Beta-secretase cleavage is not required for generation of the intracellular C-terminal domain of the amyloid precursor family of proteins. *FEBS J.* **277**, 1503–1518 (2010).
35. Nishitomi, K. et al. BACE1 inhibition reduces endogenous Abeta and alters APP processing in wild-type mice. *J. Neurochem.* **99**, 1555–1563 (2006).
36. Georgievska, B. et al. Revisiting the peripheral sink hypothesis: inhibiting BACE1 activity in the periphery does not alter beta-amyloid levels in the CNS. *J. Neurochem.* **132**, 477–486 (2015).
37. Kennedy, M. E. et al. The BACE1 inhibitor verubecestat (MK-8931) reduces CNS beta-amyloid in animal models and in Alzheimer's disease patients. *Sci. Transl. Med* **8**, 363ra150 (2016).
38. Sadleir, K. R., Eimer, W. A., Cole, S. L. & Vassar, R. Abeta reduction in BACE1 heterozygous null 5XFAD mice is associated with transgenic APP level. *Mol. Neurodegener.* **10**, 1 (2015).
39. Konig, G., Masters, C. L. & Beyreuther, K. Retinoic acid induced differentiated neuroblastoma cells show increased expression of the beta A4 amyloid gene of Alzheimer's disease and an altered splicing pattern. *FEBS Lett.* **269**, 305–310 (1990).
40. Belyaev, N. D. et al. The transcriptionally active amyloid precursor protein (APP) intracellular domain is preferentially produced from the 695 isoform of APP in a {beta}-secretase-dependent pathway. *J. Biol. Chem.* **285**, 41443–41454 (2010).
41. Palmqvist, S. et al. Accuracy of brain amyloid detection in clinical practice using cerebrospinal fluid beta-amyloid 42: a cross-validation study against amyloid positron emission tomography. *JAMA Neurol.* **71**, 1282–1289 (2014).
42. Indrayan, A. *Medical Biostatistics* 3rd edn, (CRC Press, Boca Raton, FL, 2013).
43. Olsson, B. et al. CSF and blood biomarkers for the diagnosis of Alzheimer's disease: a systematic review and meta-analysis. *Lancet Neurol.* **15**, 673–684 (2016).
44. Breitner, J. C. S., Poirier, J., Etienne, P. E. & Leoutsakos J.M. Rationale and Structure for a New Center for Studies on Prevention of Alzheimer's Disease (StoP-AD). *J. Prev. Alzheimer's Dis.* **3**, 236–242 (2016).
45. van Duijn, C. M. et al. Familial aggregation of Alzheimer's disease and related disorders: a collaborative re-analysis of case-control studies. *Int J. Epidemiol.* **20**(Suppl 2), S13–S20 (1991).
46. Cupples, L. A. et al. Estimating risk curves for first-degree relatives of patients with Alzheimer's disease: the REVEAL study. *Genet. Med.* **6**, 192–196 (2004).
47. Fratiglioni, L., Ahlbom, A., Viitanen, M. & Winblad, B. Risk factors for late-onset Alzheimer's disease: a population-based, case-control study. *Ann. Neurol.* **33**, 258–266 (1993).
48. Jack, C. R. Jr. et al. An operational approach to National Institute on Aging-Alzheimer's Association criteria for preclinical Alzheimer disease. *Ann. Neurol.* **71**, 765–775 (2012).
49. Le Bastard, N. et al. Comparison of two analytical platforms for the clinical qualification of Alzheimer's disease biomarkers in pathologically-confirmed dementia. *J. Alzheimer's Dis.* **33**, 117–131 (2013).
50. Struyfs, H., Molinuevo, J. L., Martin, J. J., De Deyn, P. P. & Engelborghs, S. Validation of the AD-CSF-index in autopsy-confirmed Alzheimer's disease patients and healthy controls. *J. Alzheimer's Dis.* **41**, 903–909 (2014).
51. Mattsson, N. et al. CSF biomarker variability in the Alzheimer's Association quality control program. *Alzheimer's Dement. J. Alzheimer's Assoc.* **9**, 251–261 (2013).
52. Elbert, D. L., Patterson, B. W. & Bateman, R. J. Analysis of a compartmental model of amyloid beta production, irreversible loss and exchange in humans. *Math. Biosci.* **261**, 48–61 (2015).
53. Wolfe, M. S. *The Molecular and Cellular Basis of Neurodegenerative Diseases: Underlying Mechanisms*. (Elsevier Science & Technology Books, Amsterdam, The Netherlands, 2018).
54. Roberts, B. R. et al. Biochemically-defined pools of amyloid-beta in sporadic Alzheimer's disease: correlation with amyloid PET. *Brain* **140**, 1486–1498 (2017).
55. Lee, E. B. et al. BACE overexpression alters the subcellular processing of APP and inhibits Abeta deposition in vivo. *J. Cell Biol.* **168**, 291–302 (2005).
56. Haass, C. et al. The Swedish mutation causes early-onset Alzheimer's disease by beta-secretase cleavage within the secretory pathway. *Nat. Med.* **1**, 1291–1296 (1995).
57. Jonsson, T. et al. A mutation in APP protects against Alzheimer's disease and age-related cognitive decline. *Nature* **488**, 96–99 (2012).
58. Benilova, I. et al. The Alzheimer disease protective mutation A2T modulates kinetic and thermodynamic properties of amyloid-beta (Abeta) aggregation. *J. Biol. Chem.* **289**, 30977–30989 (2014).
59. Pannee, J. et al. The amyloid-beta degradation pattern in plasma--a possible tool for clinical trials in Alzheimer's disease. *Neurosci. Lett.* **573**, 7–12 (2014).
60. Gremer, L. et al. Fibril structure of amyloid-beta(1-42) by cryo-electron microscopy. *Science* **358**, 116–119 (2017).
61. Fagan, A. M. et al. Longitudinal change in CSF biomarkers in autosomal-dominant Alzheimer's disease. *Sci. Transl. Med.* **6**, 226ra230 (2014).

62. Sutphen, C. L. et al. Longitudinal cerebrospinal fluid biomarker changes in preclinical Alzheimer disease during middle age. *JAMA Neurol.* **72**, 1029–1042 (2015).
63. Potter, R. et al. Increased in vivo amyloid-beta42 production, exchange, and loss in presenilin mutation carriers. *Sci. Transl. Med.* **5**, 189ra177 (2013).
64. Bridges, K. G. et al. A novel approach to identifying beta-secretase inhibitors: bis-statine peptide mimetics discovered using structure and spot synthesis. *Peptides* **27**, 1877–1885 (2006).
65. Dominguez, D. et al. Phenotypic and biochemical analyses of BACE1- and BACE2-deficient mice. *J. Biol. Chem.* **280**, 30797–30806 (2005).
66. van der Flier, W. M. et al. Optimizing patient care and research: the Amsterdam Dementia Cohort. *J. Alzheimer's Dis.* **41**, 313–327 (2014).
67. McKhann, G. et al. Clinical diagnosis of Alzheimer's disease: report of the NINCDS-ADRDA Work Group under the auspices of Department of Health and Human Services Task Force on Alzheimer's Disease. *Neurology* **34**, 939–944 (1984).
68. Petersen, R. C. et al. Mild cognitive impairment: clinical characterization and outcome. *Arch. Neurol.* **56**, 303–308 (1999).
69. Del Campo, M. et al. Facilitating the validation of novel protein biomarkers for dementia: an optimal workflow for the development of sandwich immunoassays. *Front Neurol.* **6**, 202 (2015).
70. DeLong, E. R., DeLong, D. M. & Clarke-Pearson, D. L. Comparing the areas under two or more correlated receiver operating characteristic curves: a nonparametric approach. *Biometrics* **44**, 837–845 (1988).

Acknowledgements

Thanks to Robert Umek and Martin Boissonneault (Meso Scale Discovery) for their help and support with the electrochemiluminescence assay development, to Konrad Beyreuther and Chris Weise for discussions, as well as Peter Kang and Arthuro Aliaga for technical support with the rat experiments. We thank Johan Lundkvist for providing us with Fc-BACE1 and discussions. We thank the PREVENT-AD group (public-private partnership using funds provided by McGill University, the Fonds de Recherche du Québec – Santé (FRQ-S), an unrestricted research grant from Pfizer Canada, the Levesque Foundation, the Douglas Hospital Research Centre and Foundation, the Government of Canada, and the Canada Fund for Innovation). The Founding Director of the program is John C. S. Breitner, MD, MPH, Douglas Hospital Research Centre and Faculty of Medicine, McGill University, Montréal, QC, Canada. Program Co-Directors include Associate Directors Judes Poirier, PhD, and Pierre Etienne, MD, and Deputy Director Pedro Rosa-Neto, MD, PhD, all at the same institutions. For up-to-date information, see http://www.preventalzheimer.ca. Thanks to Brain@McGill, the Velux Stiftung, the Natural Sciences and Engineering Research Council of Canada, the Canadian Consortium on Neurodegeneration in Aging, and the Canadian Institute of Health Research (MOP-133411) for support awarded to G.M, C.H., L.K., or F.L. Thanks to the Studienstiftung des Deutschen Volkes, and the Groupe de Recherche Axé sur la Structure des Protéines (GRASP, McGill University) for Ph.D. fellowships awarded to F.L., and the DFG (SFB877-TPA3) for funding awarded to P.S. G.M. holds both a Canada Research Chair in Molecular Pharmacology and a Canada Foundation for Innovation (CFI) grant. The McGill SPR-MS Facility thanks the CFI for infrastructure support.

Author contributions

F.L. designed and performed experiments, analyzed data, prepared the figures, and wrote the manuscript. L.K., A.S., I.U., M.A.H., V.E, and P.K. designed and performed experiments, analyzed data, and helped writing the manuscript. C.T., W.M.v.d.F., P. R.-N., Ph. S., J.P., P.S., R.J.B, J.B., and C.H. designed experiments, analyzed data, and helped writing the manuscript. G.M. conceived the study, designed experiments, analyzed data, and wrote the manuscript. All authors have approved the final version of the manuscript.

Additional information

Supplementary Information accompanies this paper at https://doi.org/10.1038/s41467-019-10152-w.

Competing interests: The authors declare no competing interests.

Reprints and permission information is available online at http://npg.nature.com/reprintsandpermissions/

Journal peer review information: *Nature Communications* thanks Dominic Walsh and other anonymous reviewer(s) for their contribution to the peer review of this work.

Publisher's note: Springer Nature remains neutral with regard to jurisdictional claims in published maps and institutional affiliations.

APPENDIX B

The following article is reprinted with permission from:

Lisa Gallwitz, Alessandro Di Spiezio, Lina Schmidt, André R. A. Marques, Florian Bleibaum, Andreas Tholey, Liam Cassidy, Irem Ulku, Gerhard Multhaup and Paul Saftig

Cathepsin D: Analysis of Its Potential Role as an Amyloid Beta Degrading Protease

Neurobiol Dis., 175, 105919 (2022). https://doi.org/10.1016/j.nbd.2022.105919

Neurobiology of Disease 175 (2022) 105919

Contents lists available at ScienceDirect

Neurobiology of Disease

journal homepage: www.elsevier.com/locate/ynbdi

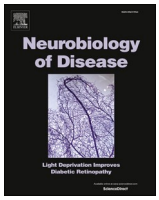

Cathepsin D: Analysis of its potential role as an amyloid beta degrading protease

Lisa Gallwitz [a], Lina Schmidt [a], André R.A. Marques [b], Andreas Tholey [c], Liam Cassidy [c], Irem Ulku [d], Gerhard Multhaup [d], Alessandro Di Spiezio [a,1], Paul Saftig [a,*,1]

[a] Institute of Biochemistry, Christian-Albrechts-University Kiel, 24118 Kiel, Germany
[b] iNOVA4Health, NOVA Medical School, Universidade NOVA de Lisboa, 1150-082 Lisbon, Portugal
[c] Systematic Proteomics and Bioanalytics – Institute for Experimental Medicine, Christian-Albrechts-University Kiel, 24105 Kiel, Germany
[d] Department of Pharmacology and Therapeutics, Faculty of Medicine and Health Sciences McGill University, Montreal, Canada

ARTICLE INFO

Keywords:
Cathepsin-D
Lysosome
Neuronal ceroid lipofuscinosis 10
Proteolysis
Amyloid beta
Amyloid precursor protein
Alzheimer's disease

ABSTRACT

Proteolysis catalyzed by the major lysosomal aspartyl protease cathepsin-D (CTSD) appears to be of pivotal importance for proteostasis within the central nervous system and in neurodegeneration. Neuronal Ceroid Lipofuscinosis (NCL) type 10 is caused by a lack of CTSD leading to a defective autophagic flow and pathological accumulation of proteins. We previously demonstrated a therapeutic-relevant clearance of protein aggregates after dosing a NCL10 mouse model with recombinant human pro-cathepsin-D (proCTSD). Similar results could be achieved in cells and mice accumulating α-synuclein. Prompted by these positive effects and our *in vitro* findings showing that cathepsin-D can cleave the Alzheimer's Disease (AD)-causing amyloid beta peptides (Aβ), we envisaged that such a treatment with proCTSD could similarly be effective in clearance of potentially toxic Aβ species.

We demonstrated that CTSD is able to cleave human $A\beta^{1-42}$ by using liquid chromatography-mass spectrometry. Intracerebral dosing of proCTSD in a NCL10 (CTSD knockout) mouse model revealed uptake and processing of CTSD to its mature and active form. However, the re-addition of CTSD did not obviously affect intracellular APP processing or the generation of soluble APP and Aβ-species. ProCTSD treated HEK cells in comparison with untreated cells were found to contain comparable levels of soluble and membrane bound APP and Aβ-species. Also, the early intracranial application (P1 and P20) of proCTSD in the 5xFAD mouse model did not change Aβ pathology, plaque number and plaque composition and neuroinflammation, however we observed an increased level of $A\beta^{1-42}$ in the CSF.

Our data confirm proteolytic cleavage of human $A\beta^{1-42}$ by CTSD but exclude a prominent role of CTSD in APP processing and Aβ degradation in our *in vitro* and *in vivo* models.

1. Introduction

Lysosomes are of pivotal importance for macromolecule and protein degradation (Saftig and Klumperman, 2009). Endocytosis, phagocytosis or autophagy deliver the substrates to lysosomal proteases. Cathepsins are the major lysosomal proteases. After synthesis in the endoplasmic reticulum as inactive pro-forms they transit to lysosomes where they are proteolytically processed to mature fully active forms (Katunuma, 2010). Cathepsins have been implicated in a wide range of cellular functions including bulk protein degradation, antigen processing and presentation, proprotein processing, degradation of matrix constituents and initiation of apoptotic processes.

The aspartyl protease cathepsin-D (CTSD) is ubiquitously expressed and plays a pivotal role in the central nervous system. This is reflected by a loss of cathepsin-D in mice and men leading to a severe congenital neurodegenerative disease classified as Neuronal Ceroid Lipofuscinosis type 10 (NCL10). Undegraded protein aggregates in neurons lead to cell death associated with premature death in patients and in a NCL10 mouse model (Saftig et al., 1995; Koike et al., 2000; Steinfeld et al., 2006). In contrast, cathepsin-B or cathepsin-L deficiency in mice does

* Corresponding author at: Biochemical Institute, Christian-Albrechts-University Kiel, Olshausenstr. 40, D-24098 Kiel, Germany.
E-mail address: psaftig@biochem.uni-kiel.de (P. Saftig).
[1] Equal senior authorship.

https://doi.org/10.1016/j.nbd.2022.105919
Received 2 August 2022; Received in revised form 30 October 2022; Accepted 3 November 2022
Available online 5 November 2022

not lead to such severe phenotypic changes indicating a redundant function of some cathepsins. However, mouse models harbouring a combined loss of cathepsin-B and -L share a comparable drastic phenotype as found in cathepsin-D knockout mice (Felbor et al., 2002; Di Spiezio et al., 2021). The predominant role of cathepsin-D is already indicated by the observation that it can constitute as much as 10% of the soluble lysosomal protein in rat liver. Cathepsin-D's concentration inside liver was estimated to reach 0.7 mM (Dean and Barrett, 1976). In early studies based on the inhibitor pepstatin it was estimated that cathepsin-D contributes to about 10–50% of lysosomal protein degradation (Dean, 1975).

Interestingly, the application of pro-CTSD in a NCL10 preclinical mouse model could accelerate lysosomal protein degradation. It led to clearance of the pathologically relevant protein aggregates and reduced gliosis and neurodegeneration (Di Spiezio et al., 2021; Marques et al., 2020). This type of protease replacement strategy also increased the life span of these mice (Marques et al., 2020). This strategy was used to provide additional protease activity to foster the proteolytic capacity of lysosomes. In an independent study intraocular administration of CTSD effectively restored the disrupted autophagy-lysosomal pathway and reduced the retinal degeneration by promoting the survival of photoreceptors and rod bipolar cells (Liu et al., 2022). The beneficial effect of adding recombinant human CTSD to disease models was also illustrated by recent findings in α-synucleinopathy models where application of pro-CTSD to cells and mice with enhanced synuclein pathology increased α-synuclein degradation (Prieto Huarcaya et al., 2022).

CSTD has also been implicated in the pathogenesis of Alzheimer's Disease (AD). Late onset AD had been linked with a variation in the gene encoding for CSTD (Davidson et al., 2006) which is also associated with an increase of $A\beta^{1-42}$ and tau in cerebrospinal fluid (Papassotiropoulos et al., 2002; Riemenschneider et al., 2006). It is of note that early studies already identified a degrading activity of cathepsin-D towards tau (Kenessey et al., 1997) and Aβ (Hamazaki, 1996; McDermott and Gibson, 1996). In a more recent study, cathepsin-D turned out to be one of the principal intracellular Aβ-degrading proteases that can influence Aβ42/40 ratios *via* differential degradation of $A\beta^{1-42}$ *vs.* $A\beta^{1-40}$ (Suire et al., 2020). An upregulation of CTSD as a possible adaptive response in AD neocortex was also described (Chai et al., 2019). Recently, lysosome activity has also been linked to the intraneuronal build-up of Aβ which later leads to neuronal cell death and extracellular Aβ-deposits (Lee et al., 2022).

The major hypothesis tested here was that an initiation of lysosomal proteolysis by endoproteolysis through CTSD could contribute to increased overall lysosomal proteolysis and autophagic flux after application of proCTSD and endogenous processing of the pro-form into the active form in lysosomes. Cathepsin-D application should reduce both the intracellular and extracellular levels of the neurotoxic and aggregation prone amyloid peptides. Using cell-based assays and studies in a preclinical NCL mouse model and the 5xFAD mouse model we observed efficient uptake of proCTSD which raised intra-lysosomal activity and expression of the mature active form of the protease. In the different experimental systems, however, a significant impact of the therapeutic enzyme on APP processing, Aβ levels, plaque formation and neuroinflammation was not observed. This finding suggests that a CTSD-based enzyme therapy may be inappropriate to modulate the Aβ-caused pathology in AD.

2. Results

2.1. Recombinant human pro-cathepsin-D (rhproCTSD) is self-activated in vitro and cleaves amyloid beta 1–42

A recombinantly expressed form of human pro-cathepsin-D (rhproCTSD) dosed to mouse models of neuronal ceroid lipofuscinosis (Marques et al., 2020) and α-synucleinopathy (Prieto Huarcaya et al., 2022) revealed its therapeutic value to remove protein aggregates including α-synuclein. The expression and activity of CTSD in connection with lysosomal proteolysis have been linked to the pathogenesis of AD and the processing and removal of amyloid peptides (Di Domenico et al., 2016). We were first interested to investigate wheather our rhproCTSD could also cleave $A\beta^{1-42}$ *in vitro*. The pro-form of CTSD does not display a considerable proteolytic activity which makes it attractive as a drug for *in vivo* dosing where it remains inactive in the interstitial fluid but is activated after endocytic uptake in cells and delivery to lysosomes. For the use *in vitro*, we supported self-activation of rhproCTSD by incubating it for at least 30 min at a lysosome-like pH of 4.5. Under this condition the enzyme was fully active (Fig. 1A) and was detected as a mature 30 kDa CTSD form by immunoblot analysis (Fig. 1B). When such a pre-activated fraction of 2 μg rhproCTSD was co-incubated for 15, 30 and 60 min with 100 μM $A\beta^{1-42}$ peptides and analyzed by liquid chromatography-mass spectrometry (LC-MS) specific cleavage fragments were observed. While the educts in our experiment contained <2% of pre-cleaved peptides, according to the summed peptide spectral matches (Supplementary Fig. S1), a number of hydrolysis products were observed after 15 min (Fig. 1C, D, Supplementary Fig. S1). In particular, hydrolysis C-terminal to Phe19, leading to two peptides with masses of 2314.50 Da (average mass) and 2217.61 Da, representing the N- and the C-terminal cleavage product, respectively, could be detected and confirmed by MS/MS experiments (Supplementary Fig. S1). The C-terminal fragment was additionally proteolyzed C-terminal to Leu34 after 15 min. In addition, further processing products of the N-terminal (cleavage C-terminal to Leu17) and the C-terminal fragment (loss of the N-terminal Phe20) were observed. The later, two products were further increased in abundance at longer incubation times. In a control, the $A\beta^{1-42}$ peptide/ rhproCTSD was additionally incubated with pepstatin A, an aspartyl protease inhibitor. Here, no cleavage products could be observed; the increased fraction of the oxidized peptide (Met35) compared to the educt is common for Met-containing peptides at elevated incubation times. In summary, rhproCTSD is able to rapidly degrade the $A\beta^{1-42}$ peptide under the chosen acidic *in vitro* conditions.

2.2. Intracranial dosing of rhproCTSD in an NCL10 model did not affect the expression of mouse Aβ-species

Having provided an *in vitro* proof of principle that rhproCTSD is able to proteolytically process $A\beta^{1-42}$ we tested if also an *in vivo* application of the pro-enzyme has an impact on APP amyloid peptide metabolism. Using the previously mentioned model of NCL10 ($CTSD^{-/-}$ knockout (KO) mice) (Koike et al., 2000) we intracranially dosed 0.1 mg rhproCTSD at postnatal day 1 and 20 (Fig. 2A). Cathepsin-D was taken up by neurons (MAP-2-positive cells) and microglia (Iba 1-positive cells) as demonstrated by fluorescence microscopy (Fig. 2B) and detection of the mature active form of cathepsin-D by immunoblot analysis (Fig. 2C). The therapeutic effect of rhproCTSD became evident since treated mice did not lose weight caused by the disease progression, compared to PBS injected mice (Supplementary Fig. S2A). Biochemical analysis of the brain lysates revealed that cathepsin-D deficiency did not alter the expression levels of the full-length form of the murine amyloid precursor protein (APP) as well as the level of the C-terminal APP fragments C99 and C83, respectively (Fig. 2C, D). Dosing the CTSD KO mice with rhproCTSD did also not change levels of APP and APP-C99. There was a ~ 40% decrease of APP-C83 levels after treatment indicating that this fragment could be subject to lysosomal CTSD degradation (Fig. 2D(ii)). Importantly, the soluble APP fragments showed a tendency towards decreased levels of sAPPα and sAPPβ in homogenates of CTSD KO brains (Fig. E). However, treatment did only mildly but not significantly increase these levels (Fig. 2F). By immunoblot, endogenous Aβ could not be detected in the membrane bound and soluble fractions of the brain homogenates (Fig. 2C, E). ELISA and MSD measurements of soluble (diethylamine, DEA), insoluble (formic acid, FA) and RIPA (complete cell lysis) fractions of $A\beta^{1-40}$ and $A\beta^{1-42}$ did not reveal a clear trend towards an anti-amyloid effect of the rhproCTSD application (Fig. 2G,

Supplementary Fig. S2 B). In summary, after intracranial dosing of rhproCTSD in the CTSD KO mice the enzyme was endocytosed by neurons and microglia and matured to the active form. However, this treatment did not obviously affect the processing of APP or the generation of soluble APP and Aβ fragments.

2.3. RhproCTSD application to human APP overexpressing cells

Although the CTSD KO (NCL10) mouse model is suitable to follow up the therapeutic effect of rhproCTSD dosage (Marques et al., 2020) the levels of APP and Aβ are very low and despite of a neurodegenerative phenotype and lysosomal dysfunction these mice do not develop typical AD pathologies (Koike et al., 2000). To investigate whether cathepsin-D would alter APP and Aβ metabolism we used HEK293 cells expressing the human wildtype APP or the swedish mutant of APP (APPswe) (Mullan et al., 1992). These cells as well as wildtype HEK293 cells were incubated for 48 h with 20 μg/ml rhproCTSD with or without Pepstatin A (PepA) (Fig. 3A). Cathepsin-D was taken up and processed to the proteolytically active forms (Fig. 3B). HEK cell lysates (Fig. 3B) and supernatants (Fig. 3D) were analyzed by immunoblot to quantify APP fragments (Fig. 3C,E). No changes in cell lysates of flAPP, APP-C83 and APP-C99 were noted (Fig. 3C). Interestingly, pepstatin A inhibition caused statistically significant upregulated levels of $A\beta^{1-42}$ (Fig. 3C(vi)). In the supernatant of the cultured cells (where the rhproCTSD was not self-activated; Supplementary Fig. S3) no effect on the levels of soluble APP fragments sAPPα and sAPPβ (Fig. 3E(i) and (ii)), as well no obvious change in levels of amyloid fragments ($A\beta^{1-37}$, $A\beta^{1-40}$ and $A\beta^{1-42}$, Fig. 3E (iii)-(v)) was observed.

2.4. Analysis of rhproCTSD uptake and Aβ clearance in an Alzheimer mouse model

The cell-based data suggest that application of rhproCTSD did not influence APP-dependent proteolysis. However, to exclude that this is limited to a specific cellular system and experimental set up with the chosen incubation times we decided to study the effect of the intracranially dosed therapeutic enzyme in a well-established AD mouse model. We have chosen the 5xFAD mice that express human APP mutations (Swedish (K670N/M671L), Florida (I716V), and London (V717I)) and presenilin transgenes (M146L and L286V). These mice are well suited to study AD-related pathology such as amyloid plaque formation, gliosis and Aβ-accumulation starting in two-month-old mice (Oakley et al., 2006). We took profit from our experiences with the dosing study in the NCL10 model where the therapeutic enzyme was intracranially delivered at postnatal day P1 and P20 and could be detected in brain lysates for >31 days (Marques et al., 2020). We hypothesized that such an early delivery of rhproCTSD would interfere with the early production of Aβ and the processing of APP in the 5xFAD mouse model. To adapt the previously established protocol to the 5xFAD mice we first analyzed mice at 2 and 3 months of age for soluble APP fragments and Aβ. Immunoblot analysis revealed that two-month old brains contained considerable levels of hsAPPα and minute levels of Aβ. Aβ species were clearly detectable by immunoblot in three-month-old brain lysates (Supplementary Fig. S4 A). Subsequently, we intracerebrally dosed the 5xFAD mice at P1 and P20 with rhproCTSD. Mice were sacrificed and their brains were analyzed at one, two or three months of age (Supplementary Fig. S4 B). The dosed enzyme was readily detectable as the mature and active form of CTSD in brain lysates of one-month-old mice (Fig. 4A). Sets of one-month-old (Fig. 4 A,B), two-month-old (Supplementary Fig. S4 C,D) and three-month-old (Fig. 4C,D) wild-type and 5xFAD mice either injected with PBS or with rhproCTSD were biochemically analyzed for soluble proteins (DEA fraction), membrane-bound proteins (RIPA fraction) and insoluble proteins (formic acid fraction). At one month of age (Fig. 4A) the rhproCTSD-dosed 5xFAD brain samples showed no obvious changes in the levels of sAPPα, sAPPβ and soluble Aβ (Fig. 4B(i)-(iii)) compared to the PBS-dosed 5xFAD. Also, in the RIPA fractions the levels of full-length APP, APP-CTFs C99 and C83 as well as the intracellular levels of Aβ (Fig. 4B(iv)-(vi)) did not change after treatment. Whereas mature CTSD was present in the cell lysates, this did not cause a change in the number of lysosomes as indicated by an unchanged level of the lysosomal membrane protein LAMP-1 (Fig. 4B(vii)). At two months of age (Supplementary Fig. S4 C, D) the immunoblot analysis confirmed the data from the one-month old cohort of mice. Here we quantified the amounts of $A\beta^{1-40}$ and $A\beta^{1-42}$ in wild-type and 5xFAD DEA, RIPA and FA fractions by ELISA and observed a trend towards upregulated $A\beta^{1-40}$ and $A\beta^{1-42}$ levels of the 5xFAD mice treated with rhpro-CTSD in all of the investigated fractions (Supplementary Fig. S4 E). At three months of age (Fig. 4C,D) we observed a slight but statistically significant decrease of APP-CTF83 (Fig. 4D(iv)) and LAMP-1 (Fig. 4D(vii)) after dosing. However, all other APP fragments including the Aβ peptide did not change. The lack of an effect on Aβ-species was also confirmed in ELISA studies revealing an increase in Aβ in the one and three-month-old 5xFAD mice as compared to wild-type mice (Fig. 4E). However, rhproCTSD dosing did not change these levels in neither sample fraction. Additionally, we compared the amounts of $A\beta^{1-34}$, $A\beta^{1-38}$, $A\beta^{1-40}$, $A\beta^{1-42}$ of 3-months-old wild-type and 5xFAD mice via 4-plex MSD assays (Liebsch et al., 2019) (Supplementary Fig. S4 F) but failed to detect changes after treatment. It is of note that when cerobrospinal fluid (CSF) was investigated in one-month-old mice rhproCTSD treatment even increased the levels of $A\beta^{1-42}$ (Fig. 4 F). To analyze the stability of the applied recombinant CTSD in mice we compared samples from one, two and three months old wild-type and 5xFAD mice injected either with PBS or rhpro-CTSD by immunoblot and an CTSD activity assays (Supplementary Fig. S4 G-I). We found an increased CTSD activity and expression in the one month old 5xFAD mice treated with rhpro-CTSD. The expression of the mature form of CTSD was still increased in two months old mice. It is of note that there was no increased CTSD activity measurable at two and three-month-old mice. Taken together, we did not find evidence for an obvious effect of CTSD treatment on Aβ levels as well on soluble and intracellular APP fragments.

2.5. Plaque morphology, number and neuroinflammation after intracranial rhproCTSD dosing in the 5xFAD mouse model

Despite the fact that our biochemical analysis did not reveal alterations in the expression levels of Aβ peptides we studied plaque formation, number and morphology after intracerebrally dosing the rhproCTSD. Using staining for Aβ and LAMP-1, as an indicator for the presence of lysosomes we observed in both PBS- and rhproCTSD-treated three-month-old brain cortices the formation of plaques which were surrounded by LAMP-1-positive cells (Fig. 5A). Calculation of the number of these structures in cortices and hippocampus did not reveal differences when PBS-injected and rhproCTSD-dosed mice were compared (Fig. 5B, Supplementary Fig. S5 A). Since the used E610 antibody also detects soluble Aβ fragments we also applied AmyloGlo staining (Schmued et al., 2012) to selectively stain amyloid plaques (Fig. 5C). The number of plaques and the plaque size in cortices and hippocampus was not affected after rhproCTSD dosing in the 5xFAD model (Fig. 5D, Supplementary S5 B). To not exclude earlier signs associated with the neurodegenerative process in the 5xFAD model we were interested if the treatment would affect neuroinflammation exerted by microglia and astroglia cells. Both, the degree of microgliosis (Fig. 5 E, F) and astrogliosis (Fig. 5 G, H; Supplementary Fig. S5 D) as judged by immunostaining and a ramification analysis (Fig. 5F, Supplementary Fig. S5 C) with Iba1 and GFAP did not change in the brains of three-month-old 5xFAD mice after having received rhproCTSD. These data clearly show that treatment with rhproCTSD did not affect the development of neuroinflammation which corresponds with a lack of an effect of the therapeutic enzyme on the levels of Aβ species.

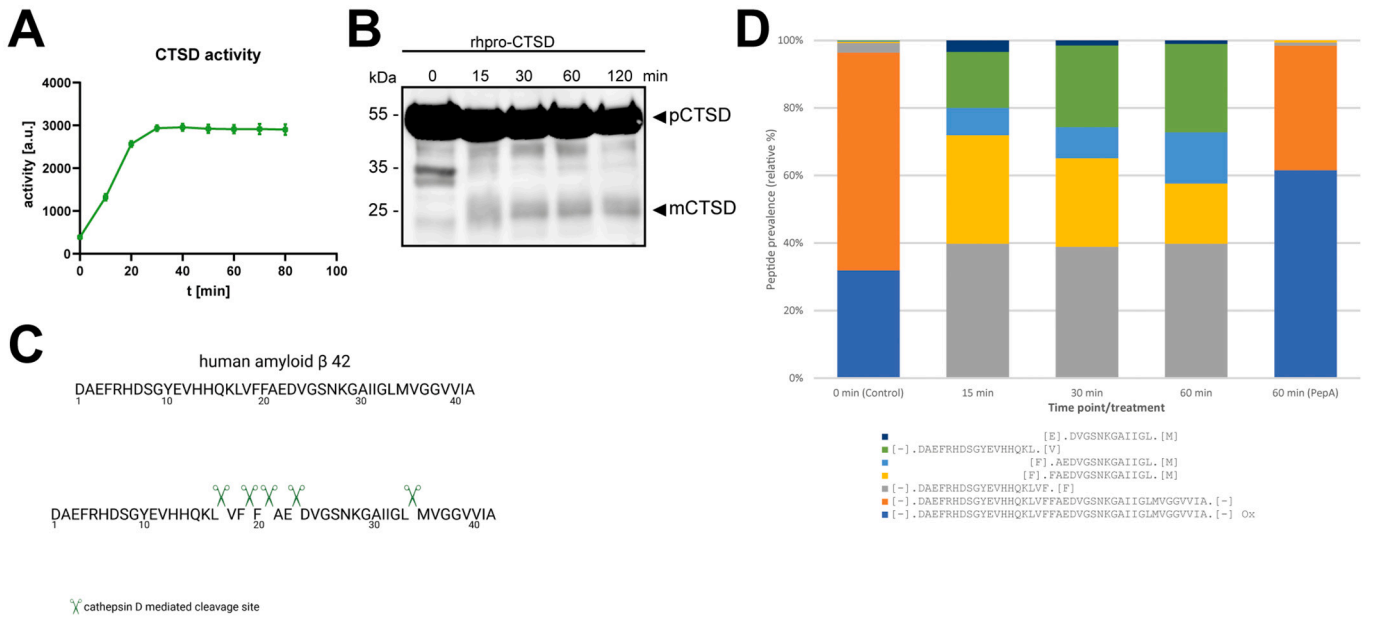

Fig. 1. *In vitro* digestion of Amyloid beta by recombinant human cathepsin-D. A The graph shows the measured CTSD-activity of self-activated rhproCTSD over time at pH 4.5. By cleaving a quenched CTSD-substrate the fluorescence intensity can be measured after excitation at 360 nm. B Western Blot of pre-incubated rh-pro-CTSD in processing buffer (0.1 M Tris-HCl, 3 mM EDTA, 5 mM Cysteine pH 4.5) shows activation of proCTSD (pCTSD) into mature CTSD (mCTSD). C Determined cleavage sites by rhCTSD within human aβ1–42. D Most abundant peptides identified following enzymatic digestion of aβ1–42 after 0 min (Control), 15 min, 30 min, or 60 min), or protease treatment plus the addition of pepstatin A (PepA, 60 min. incubation). Peptides detected with >9 peptide spectral matches (PSM) are shown, peptide prevalence was plotted as a percentage of the total PSM counts for each time point/treatment.

3. Discussion

The *endo*-lysosomal system has long been regarded as one of the most important intracellular factors affecting the molecular pathogenesis in AD. It has been realized that autophagic/lysosomal dysfunction and deficient lysosomal proteolysis contribute to the development of AD (Nixon, 2017). This assumption is supported by a boosted lysosomal proteolysis seen in an AD-mouse model after removal of cystatin B, an endogenous inhibitor of lysosomal cysteine proteases which led to an improvement of the Aβ levels, amyloid depositions and cognitive deficits (Yang et al., 2011). It is of note that different cystatins act in different ways, *i.e.* cystatin B is localized within the lumen of lysosomes (Yang et al., 2011) inhibiting cysteine proteases (*e.g.* cathepsin B,L,S,H), while cystatin C is found in the cytosol under oxidative stress conditions, protecting the cells from cathepsin leakage into cytosol (Watanabe et al., 2014).

Another study showed accelerated Aβ deposition after pepstatin A treatment, an aspartic protease inhibitor (Yamada et al., 1996). Furthermore, recent observation highlighted that dysfunctional autophagosomes are the basis of intracellular fibrillar Aβ accumulation (Lee et al., 2022).

CTSD has raised attention as a therapeutic target in AD (Di Domenico et al., 2016) through a considerable number of studies. The importance of CTSD as a principle lysosomal protease for lysosomal proteolysis in neurons is illustrated by the severe neurodegeneration associated with a lack of the protease in human, mice and sheep (Saftig et al., 1995; Steinfeld et al., 2006; Tyynela et al., 2000). The lack of CTSD leads to the congenital variant NCL10 of neuronal ceroid lipofuscinosis, severe lysosomal storage diseases (LSD) with accumulation of protein aggregates, blindness and neuronal death (Jalanko and Braulke, 2009). Prompted by the successful application of a "protease replacement therapy" in the NCL10 model leading to an improvement of neuropathology and lifespan extension (Marques et al., 2020) and clinically approved approaches to treat LSDs even with severe neurological manifestations (Schulz et al., 2018) we studied the efficacy of such a novel potentially therapeutic approach in cellular and animal models of AD. This was encouraged also by exogenously applied rhproCTSD that led to a decrease of pathological α-synuclein conformers *in vivo* and a restoration of *endo*-lysosome and autophagy function (Prieto Huarcaya et al., 2022). In AD, the pathological hallmarks are accumulations of Aβ and tau proteins and reduced clearance of both through the autophagy-lysosomal system has been suggested (Nixon and Yang, 2011). Therefore, we have chosen an approach to foster lysosomal proteolysis by supplying additional cathepsin-D in cell-based and *in vivo* models of AD with an increased expression of APP and accumulation of Aβ. This was especially relevant since studies implicated CTSD in the processing of APP forms (Ladror et al., 1994), in degradation of tau (Kenessey et al., 1997) and Aβ (Suire et al., 2020), respectively. *In vitro* the principle ability of the pre-activated CTSD to cleave in a time-dependent fashion $A\beta^{1-42}$ could be confirmed. CTSD endopeptidase cleavage prefers hydrophobic residues at P1 (Sun et al., 2013) and such residues are present within the Aβ sequence at positions Phe4, Leu17, Phe19, Phe20, and Leu34. Our LC-MS analysis of the *in vitro* digestion verifies these positions except from Phe4. Additionally, a CTSD-mediated cleavage site is shown for Glu22. In the NCL10 model pathological accumulation of proteins and a defect in autophagic flux could be reversed (Marques et al., 2020; Liu et al., 2022) after intracerebral and intravitreal dosing of rhproCTSD. However, the successful delivery of CTSD to lysosomes in different cell types of the CNS did not apparently affect APP processing, stability of APP CTFs and the level of Aβ. This is also in accordance with early studies that failed to show a direct role of CTSD in neuronal APP processing (Saftig et al., 1996). *In cellula* experiments studying cells with an overexpression of wildtype and the Swedish mutant of APP revealed that also in this set up, despite successful uptake and maturation of exogenously added CTSD, no significant impact of the protease in APP processing and the generation of soluble APP fragments including Aβ could be observed. Most importantly, we also intracerebrally applied pro-CTSD very early to one of the best described AD mouse models, the 5xFAD mice. Careful analysis of the brains of these mice after one, two and three months of age did not reveal a therapeutic effect in terms of a reduction of Aβ species, reduced plaque burden and neuroinflammation. Despite that, we focused on the early stages of pathology in these mice it

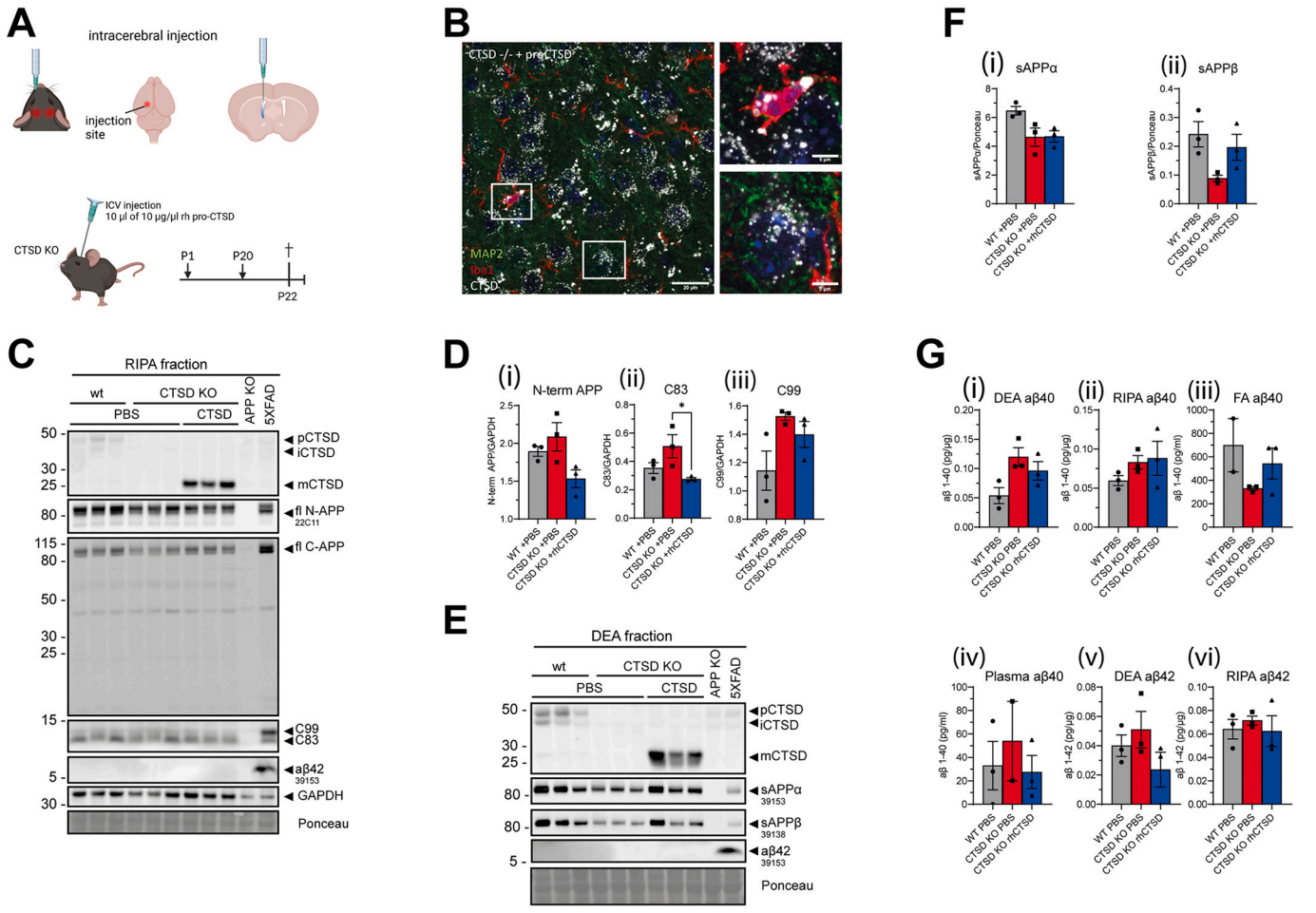

Fig. 2. Intracranial injection with rhproCTSD of CTSD-deficient mice has no evident effect on APP processing. A Scheme of intracranial injection area and time schedule for CTSD KO mice. B Immunohistochemistry of the cortex of P23 CTSD-deficient mice injected with 0,1 mg rhproCTSD shows the neuronal marker MAP2, the microglia marker Iba1 and CTSD. Nuclei are stained with DAPI Scale bar: 20 µm, insert: 5 µm. C Immunoblot of RIPA samples from brains of P23 WT mice treated with PBS and CTSD-deficient mice injected with either PBS or 0,1 mg rhproCSTD. Antibodies directed against epitopes of cathepsin-D, APP and aβ1–42 were used. Brains from APP KO and 5xFAD served as an antibody control ($n = 3$). D Quantifications of full-length APP and C-terminal fragments C83 and C99. GAPDH was used as loading control. E Immunoblot of DEA samples from brains of P23 WT mice injected with PBS and CTSD-deficient mice injected with either PBS or rhproCTSD along with control samples from brains of APP KO and 5xFAD mice. Antibodies directed against epitopes of cathepsin-D, APP and $a\beta^{1-42}$ were used. F Quantification of soluble APP fragments, normalized to Ponceau S staining (n = 3). G ELISA analysis of RIPA, DEA, FA brain samples and plasma from P23 WT mice injected with PBS and CTSD-deficient mice with PBS or 0,1 mg rhproCTSD (n = 3). Data represent mean ± SEM. Statistical analysis was performed by using one-way ANOVA with a Tukey's multiple comparison test. ** $p < 0.01$, * $p < 0.05$.

is conceivable that the dramatic and continuous production of Aβ in these AD mouse model (Manji et al., 2019) would have masked a possible therapeutic effect of CTSD. However, our analyses of the NCL10 mouse model as well as in the HEK cell system where also no effect of CTSD was observed argue against this assumption. Of note, CTSD application raised the level of $A\beta^{1-42}$ in the CSF of 5xFAD mice. It was suggested that CTSD may have a BACE1-like activity on APP especially when the Swedish version of APP is expressed (Hook et al., 2008) This could indicate that an increase of CTSD activity leads to a preference towards full length APP compared to Aβ. It is also conceivable that CTSD increases CSF $A\beta^{1-42}$ levels in an indirect way by accelerating the maturation of other lysosomal enzymes such as the cysteine protease CTSB. Similar to CTSD and BACE1, also CTSB as a cysteine hydrolase may act as with a BACE1-like activity (Hook et al., 2005).

3.1. Limitation of the study and perspectives

Our selected approach with the 5xFAD model was to accelerate lysosomal proteolysis by dosing rhproCTSD as early as possible to lower Aβ levels as soon as they might appear. However, despite a relative long half-life of the dosed enzyme (Marques et al., 2020) in mouse brain we were unable to detect significant activity of the enzyme at two and three months of age. A regular dosing protocol for longer periods may be suited to judge "therapeutic" effects at later stages. It should, however be noted that the progressive nature of the Aβ pathology observed in the 5xFAD mice may counteract any expected positive effect of the treatment at later time points.

Despite that, we have disproven our initial hypothesis that an exogenous delivery of the principle lysosomal protease CTSD assists in the amyloid degrading pathway, the lack of a therapeutic effect also raises important questions for future research. How important are lysosomal proteases for APP and Aβ metabolism? Does one require an application of a mixture of lysosomal proteases both active as *endo-* or exopeptidase to allow sufficient breakdown and disappearance of Aβ species? Our recent study where an application of cathepsin B and L for the removal of protein aggregates in neurodegeneration was investigated (Di Spiezio et al., 2021) suggested a hierarchical process of activities of both cysteine and aspartyl proteinases. In summary, lysosomal protease supplementation may be a useful approach to remove unwanted protein accumulation by improving lysosomal proteolytic

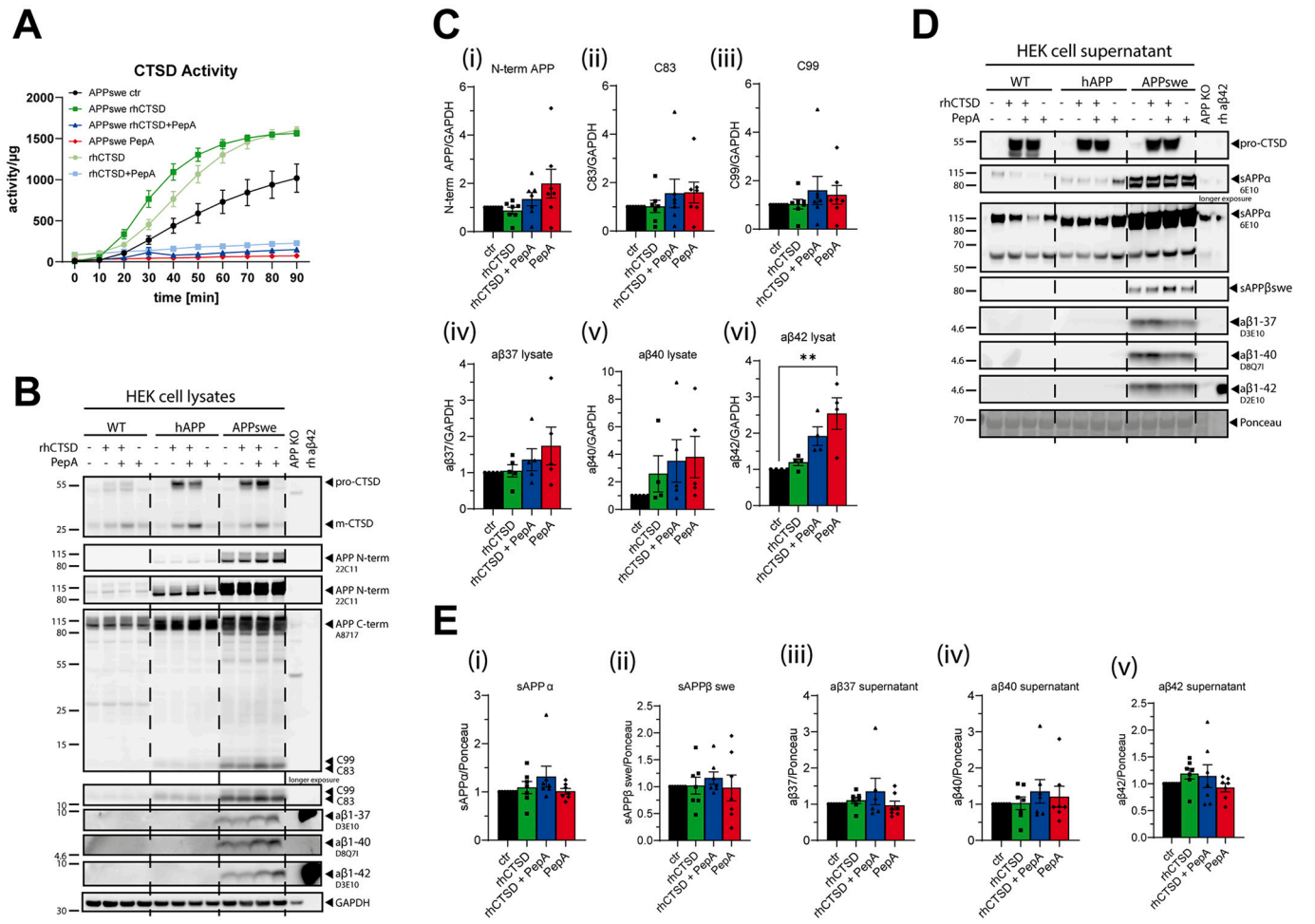

Fig. 3. Inhibition of Cathepsin-D increases cellular amyloid β 42 in HEK APPswe cells. A Cathepsin-D activity assayed with an artificial fluorescent substrate in HEK WT, hAPP and APPswe cell lysates over a time period of 90 min. B Immunoblot of cell lysates of HEK WT, hAPP and APPswe cells treated with 20 µg/ml rhproCTSD with or without 10 µg/ml pepstatin A (PepA). APP KO mouse brain lysates and human aβ1–42 protein served as antibody controls. Antibodies directed against cathepsin-D, various epitopes of APP and aβ species were used. C Quantifications of N- and C-terminal APP and amyloid β fragments of cell lysates from (B). GAPDH served as loading control ($n = 4$–7). D Immunoblot of supernatant of cells shown in (B). Antibodies detecting, CTSD, soluble APPα and APPβ and various aβ species were used. Ponceau S staining was used to verify equal loading amounts. E Quantifications of samples from (D) ($n = 6$–7). Ponceau S staining served as loading control. Data represent mean ± SEM. Statistical analysis was performed by using one-way ANOVA with a Tukey's multiple comparison test. ** $p < 0.01$, * $p < 0.05$.

degradation. However, in the case of Aβ degradation most likely more than one lysosomal protease has to act in concert.

4. Material and methods

4.1. Cell lines and treatment

Human Embryonic Kidney (HEK) WT and overexpressing human Amyloid Precursor Protein (HEK hAPP) and Swedish mutated APP (HEK APPswe) cells were cultured in Dulbecco's modified Eagle Medium (DMEM) containing 4.5 g/L of D-Glucose and L-glutamine (Thermo Fisher Scientific) and were supplemented with 10% (*v*/v) fetal bovine serum (FBS) and 1% Penicillin/Streptomycin (Pen/Strep). HEK hAPP and HEK APPswe cells were additionally treated with 200 µg/ml Geneticin (G418, Invivogen). Cells were cultivated at 37 °C/ 5% CO2. Cells were plated into 6 cm-dishes one day before any assay was implemented. For the treatment with recombinant proCTSD (rhproCTSD) cells were carefully washed three times with PBS and 20 µg/ml and/or 10 µg/ml Pepstatin A (PepA) was added to DMEM containing 1% FBS and 1% Pen/Strep for 48 h.

4.2. Mouse models and intracranial injection

In agreement with the German animal welfare law all animal handling and care were performed according to the guidelines of the Christian- Albrechts-University of Kiel. The Ministry of Energy, Agriculture, the Environment and Rural Areas Schleswig-Holstein approved animal experiments under the reference number V242–40536/2016 (81–6/16). All mice were housed in individually ventilated cage (IVC) under a 12 h light/12 h dark cycle with free access to food (pellets by Sniff Spezialdiäten, V1534) and water. Mice cages were maintained in a room with a temperature between 19 and 22 °C and humidity of 45–60%.

CTSD-deficient mice (NCL10 model) were obtained from heterozygotes matings and genotyped as previously described (Saftig et al. 1995). 5xFAD mice (AD model, expressing human APP and PSEN1 transgenes with a total of five AD-linked mutations: Swedish (K670N/M671L), Florida (I716V), and London (V717I) mutations in APP, and the M146L and L286V mutations in PSEN1) were generated with a C57BL/6 N background and genotyped for its transgenic mutations in PSEN1.

Intracranial injections with 10 µl of 10 µg/µl recombinant procathepsin D (purified as described in (Marques et al., 2020)) were performed at P1 and P20 for both CTSD-deficient and 5xFAD mice as

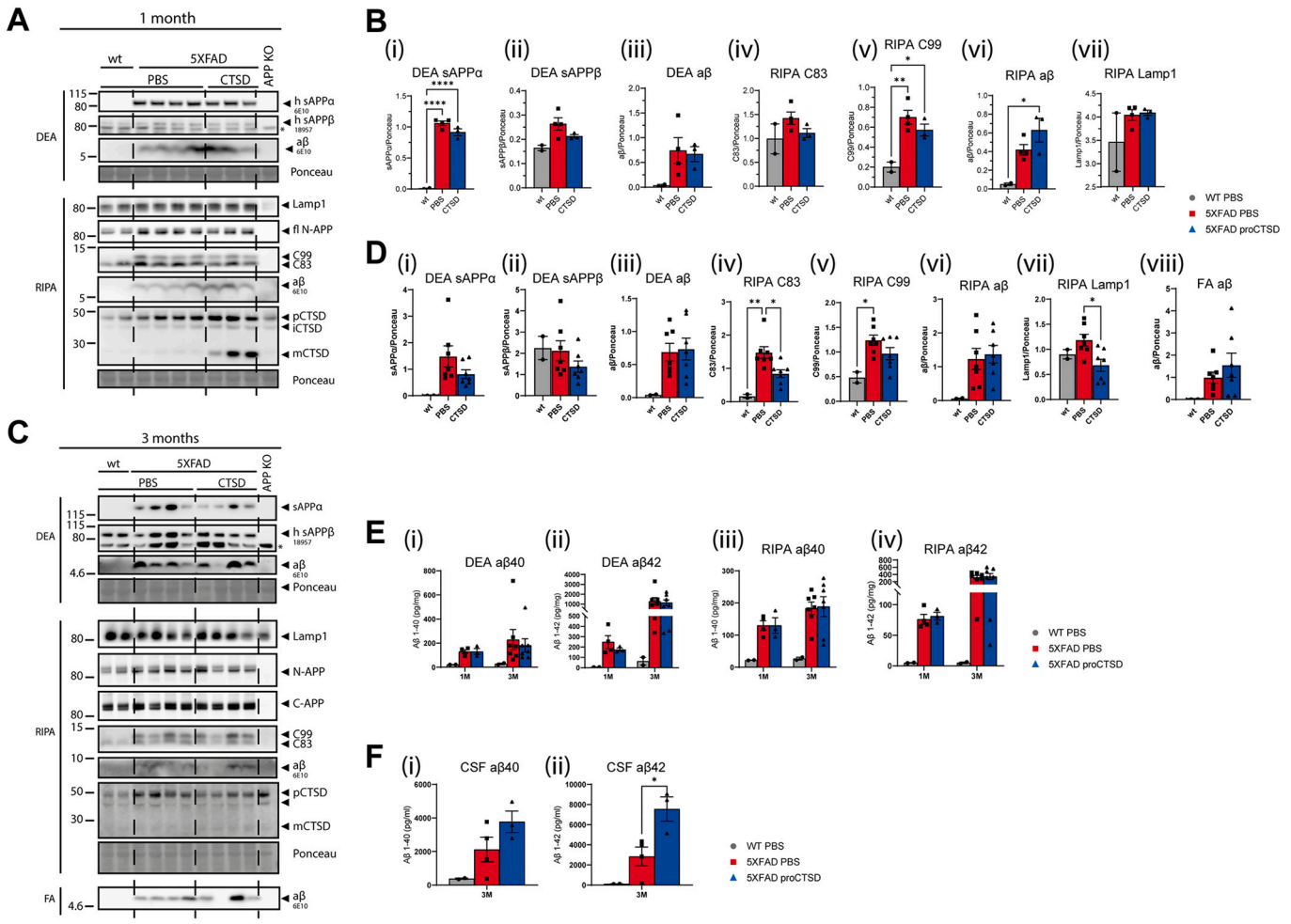

Fig. 4. Intracranial injection with rhproCTSD of 5xFAD mice has no beneficial effect on preventing aβ load within the mouse brain. A Immunoblot of soluble and membrane bound protein fractions from brain hemispheres of one-month-old female WT and 5xFAD mice intracranially injected with either PBS or 0,1 mg rhproCTSD at P1 and P20. Antibodies detecting CTSD, Lamp-1, various APP species and aβ were used. Brain lysate of an APP KO mice was used as antibody control for APP antibodies. Ponceau S staining served as loading control. B Quantitative analysis of one-month-old female 5xFAD shown in (A) ($n = 2$–4). C Representative immunoblot of DEA, RIPA an FA fractions from brain hemispheres of three-month-old female WT and 5xFAD mice intracranially injected with either PBS or 0,1 mg rhproCTSD at P1 and P20. Antibodies directed against epitopes of CTSD, Lamp1, various APP species and aβ were used. APP KO brain lysate was used as an antibody control for APP antibodies. Ponceau S staining verified equal loading amounts. D Quantitative analysis of three-month-old female 5xFAD shown in (C) (WT: $n = 7$, 5xFAD: n = 7). E ELISA analysis of samples used in (A) and (C). (one month: WT: n = 2, 5xFAD: n = 3–4; three months: WT: n = 2, 5xFAD: n = 7). F ELISA analysis of CSF (cerebrospinal fluid) collected from one-month-old 5xFAD injected with either PBS or 100 µg rhproCTSD (n = 2–4). Data represent mean ± SEM. Statistical analysis was performed by using one-way ANOVA with a Tukey's multiple comparison test. **** $p < 0{,}001$, *** $p < 0{,}005$, ** $p < 0.01$, * $p < 0.05$.

previously described (Marques et al., 2020). Briefly, mice were anaesthetized using isoflurane (2% in oxygenized air). The PBS or proCTSD was injected in the cauda putamen with a microsyringe (30 G) using a spacing devise with an injection depth of 1.15 mm over a period of 3 min. Injections in pups P1 were done in the right hemisphere, while P20 injections were done in the left hemisphere. For transcardially perfusion with 0.1 M phosphate buffer CTSD-deficient mice were anaesthetized by intraperitoneal injection of 10 mg/ml Ketamine (Bremer Pharma GmbH, 26,706) and 6 mg/ml Rompun® (Bayer, KPOCCNU) in 0.9% (*w/v*) NaCl solution and at P22 (Fig. 2A) and 5xFAD after one, two or three months (Supplement Fig. S4 B). Brains were collected, the right hemisphere fixed with 4% PFA (paraformaldehyde) for immunohistochemistry and the left hemisphere was snap-frozen in liquid nitrogen for biochemical analysis.

4.3. Western blot analysis

Cells were washed three times in ice cold PBS and lysed in RIPA buffer (50 mM Tris-Cl, 150 mM NaCl, 1% NP-40, 0.05% sodium deoxycholate, 0.01% SDS, pH 7.5), supplemented with 1× (Roche, 11836145001) on ice for 1 h. Lysates were cleared by centrifugation at 13.000 rpm for 10 min at 4 °C. Brain lysates were generated by DEA extraction for soluble proteins followed by RIPA extraction for membrane and cytosolic proteins and FA extraction for insoluble proteins. Tissue was first homogenized with porcelain beads (PeqLab) in DEA buffer (50 mM NaCl, 0,2% diethylamine, pH 10) with 1× complete Protease Inhibitor Cocktail with a Precellys® 24 homogenizer (Bertin) at 6500 g for 30 s at 4 °C. The supernatant was cleared by ultracentrifugation at 130.000 *g* for 1 h at 4 °C. The supernatant contains soluble proteins while the resulting pellet was further resuspended in RIPA buffer (20 Mm Tris-HCl [pH 7,5], 150 mM NaCl, 1 mM Na_2EDTA, 1% NP-40, 1% sodium deoxycholate, 2,5 mM sodium pyrophosphate) and dissolved with Precellys at 6500 g for 30 s at 4 °C. After centrifugation at 5000 *g* for 10 min at 4 °C the supernatant was ultracentrifuged again at 130.000 rpm for 1 h at 4 °C. The supernatant contains the membrane bound proteins. The first pellet from the RIPA lysate contains insoluble proteins which gets resuspended in 70% formic acid (FA fraction) and again ultracentrifuged at 130.000 rpm for 1 h at 4 °C. The resulting

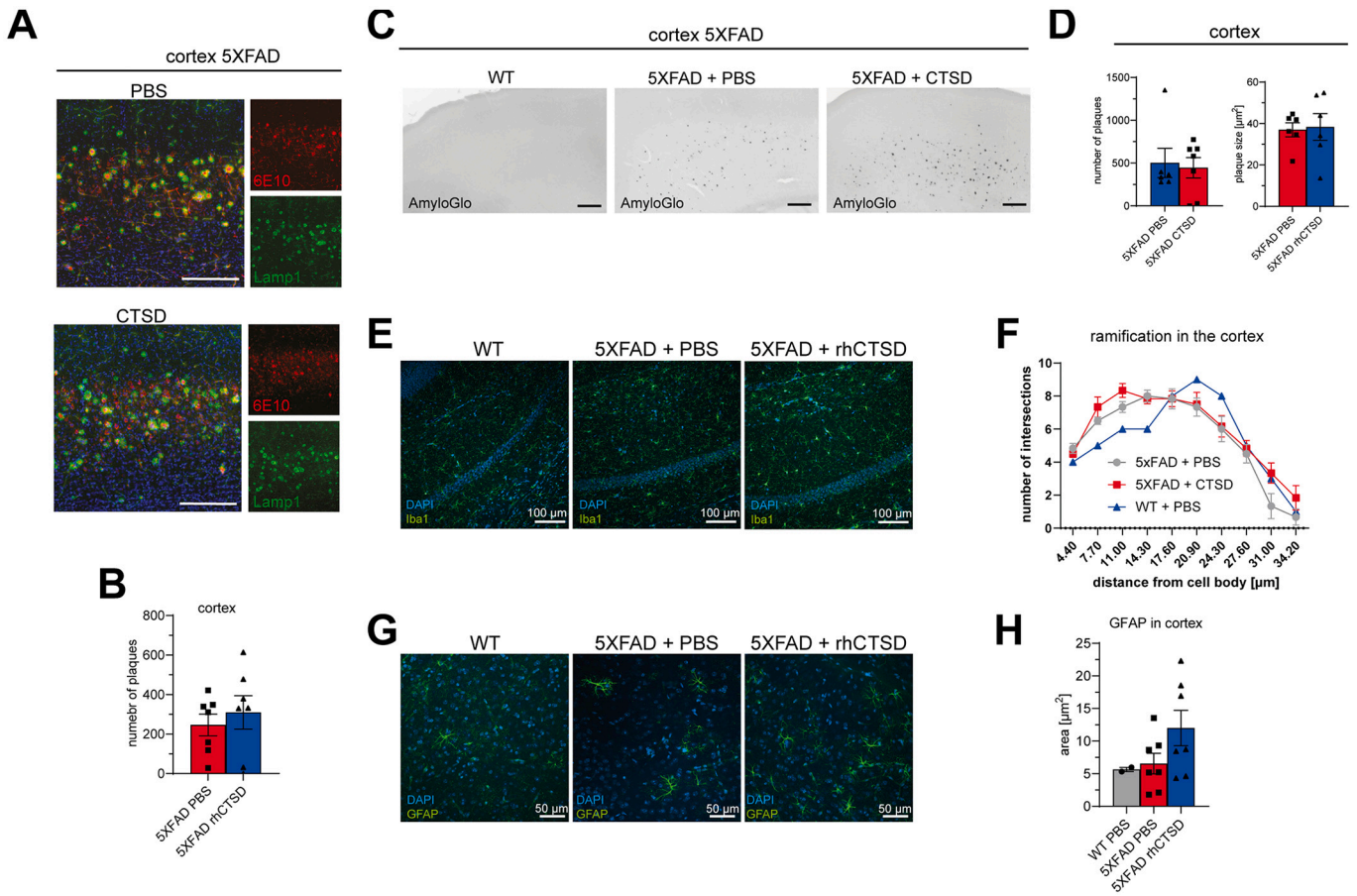

Fig. 5. Intracranial injection with rhproCTSD of 5xFAD mice does not lead to advantages on clearing aβ and does not prevent inflammation in 5xFAD brain. A Immunostainings from stained with DAPI (blue), anti-aβ (red, 6E10, Biolegend) and Lamp-1 (green, 1D4B, DSHB). Scale bar: 500 µm. B Counted aβ plaques in cortex of three-month-old female 5xFAD mice double injected with either PBS or 0,1 mg rhCTSD (n = 7). C Staining of aβ plaques with Amylo-Glo RTD Amyloid Plaque Stain Reagent (Biosensis) from cortex of three-month-old female 5xFAD mice double injected with either PBS or 0,1 mg rhproCTSD. Scale bar: 200 µm. D Number and size (μm^2) of aβ plaques from cortex (n = 7). E Immunostainings of microglia (Iba1, GeneTex, green) of the hippocampus of three-month-old female 5xFAD mice double injected with either PBS or 0,1 mg rhproCTSD. Nuclei are stained with DAPI (blue, Sigma-Aldrich). Scale bar: 100 µm. F Ramification analysis of microglia (Iba1-positive) in the cortex of three-month-old female 5xFAD mice double injected with either PBS or 0,1 mg rhproCTSD (n = 7). G Immunostainings of astrocytes (GFAP, Sigma-Aldrich, green) from the cortex of three-month-old female 5xFAD mice double injected with either PBS or 0,1 mg rhproCTSD. Nuclei are stained with DAPI (blue). Scale bar: 50 µm. H Analysis of the GFAP-positive area (μm^2) in the cortex of three-month-old female 5xFAD mice double injected with either PBS or 0,1 mg rhproCTSD (n = 7). Data represent mean ± SEM. (For interpretation of the references to colour in this figure legend, the reader is referred to the web version of this article.)

supernatant contains insoluble proteins. Protein concentration was determined using the BCA assay (Thermo Fisher Scientific) and denatured with 5× Laemmli (60 mM Tris-Cl pH 6.8, 2% SDS, 10% glycerol, 5% β-mercaptoethanol, 0.01% bromophenol blue) for 5 min at 95 °C. Equal amounts of denatured lysates were separated by electrophoresis on 4–12% NuPage gradient gels (Thermo Fisher Scientific, NP0336BOX) continuously running at 80 V. Then, proteins were transferred to a nitrocellulose membrane (Whatman, GE Healthcare, 10426994) using wet blotting. The membranes were blocked for 30 min with 5% dry milk in TBS-T (20 mM Tris/HCl pH 7.0, 150 mM NaCl, 0.1% (*v*/v) Tween® 20). The following primary antibodies were used: 1:1000 rat anti-Lamp1 (1D4B, Developmental Studies Hybridoma Bank, Iowa City, IA, USA), 1:1000 mouse anti-Lamp1 (H4A3, DSHB), 1:500 goat anti-CTSD (AF1014, R&D Systems), 1:2000 mouse anti-tubulin (E7, DSHB), 1:2000 rabbit anti-GAPDH (sc-25778, Santa Cruz Biotechnology), 1:1000 rabbit anti-APP (A8717, Sigma), 1:1000 mouse anti-APP (22C11, Thermo Fisher Scientific), 1:1000 mouse anti-β-Amyloid (6E10, Biolegend), 1:1000 rabbit anti-β-Amyloid (18058, Biolegend), 1:1000 rabbit anti-sAPPβ-WT (18957, IBL), 1:2000 mouse anti-sAPPβ-swe (6A1, IBL), β-Amyloid Antibody Sampler Kit (85314T, Cell Signaling). Afterwards, blots were washed with TBS-T for 30 min and incubated for 1 h at RT with 1:10.000 secondary antibodies coupled to horseradish-peroxidase (HRP) (goat anti-rabbit HRP, rabbit anti-goat HRP, goat anti-mouse HRP, goat anti-rat HRP) in blocking solution. Horseradish peroxidase activity was detected by ImageQuant™ LAS 680 (GE Healthcare) after incubation with Amersham ECL Advanced Western Blotting Detection kit (GE Healthcare, RPN2135).

4.4. Immunostainings

Mouse brains were fixed in 4% PFA for 4 h to be subsequently washed in phosphate buffer (PB) at 4 °C overnight, immersed in 30% sucrose in PB, and stored at 4 °C. Sections (35 µm) were cut sagittal with a Leica SM 2000R sliding microtome (Leica Microsystems) with dry-ice cooling and stored in PB containing 0.02% (*w*/*v*) sodium azide. Floating slides were washed three times with PB, blocked and permeabilized 0.5% Triton X-100, 4% normal goat serum (Gibco) and incubated overnight with rabbit 1:750 anti-Iba1 (GTX100042, GeneTex), mouse anti-GFAP (G3893, Sigma), 1:500 rabbit anti-CTSD (kindly provided by Prof. Andrej Hasilik, Münster), 1:750 rat anti-Lamp1 (1D4B, DSHB) and 1:300 mouse anti-β-Amyloid (6E10, Biolegend) antibodies in blocking solution. After three washing steps with 0.25% Triton X-100 in PB,

sections were incubated with 1:750 Alexa Fluor-conjugated secondary antibodies (A21208 donkey anti-rat 488, A21202 donkey anti-mouse 488, A21203 donkey anti-rabbit 594, A21203 donkey anti-mouse 594, A78947 donkey anti-rat 647, A31573 donkey anti-rabbit 647, A21447 donkey anti-goat 647, Thermo Fisher Scientific) for 3 h at room temperature, washed again 3 times in washing buffer, and finally coverslipped in Mowiol/DABCO. For AmyloGlo staining the brain sections were dried at 55 °C on a gelatin-coated slide, transferred into a 70% ethanol solution for 5 min, washed in water and then incubated for 10 min with the AmyloGlo staining solution. Slides were briefly rinsed with 0,9% saline solution and coverslipped in Mowiol/DABCO. Imaging was performed on the Zeiss laser scanning microscope 980 with Airyscan 2 (Zeiss) or the Keyence fluorescence microscope BZ-X 800 (Keyence).

4.5. ELISA

To quantify mouse and human amyloid β 1–40 and 1–42 from CTSD-deficient and 5xFAD mice the DEA, RIPA and FA factions were analyzed after total protein determination by using the ELISA Kits from IBL (27718, 27719, 27720, 27721, IBL). To also determine amyloid β in the CSF, the mice were anaesthetized and the CSF was collected from the cisterna magna compartment using a glass capillary. The CSF was snap-frozen in liquid nitrogen until usage for ELISA. The assay was performed according to the supplier's manual.

4.6. MSD assay

An electrochemiluminescence-based assay was developed (neo-epitope specific Aβ34 and the sulfo-tagged 6E10 (binds to the N-terminus of human Aβ) or the sulfo-tagged 4G8 for rodent samples (binds to the mid domain of Aβ)) using the ELISA Conversion Kit from MSD (USA). High-bind or custom-printed 4-plex plates (using our mab34, 4G8 (Biolegend) for pan-Aβ assay, G2–10 for 1-plex Aβ40 assay, and MSD's validated mouse monoclonal anti-Aβ38, anti-Aβ40, as well as anti-Aβ42 antibodies, see MSD Aβ peptide V-PLEX) were blocked (MSD 5% Blocker A in PBS) for 1 h at 22 °C and washed three times with PBS-Tween (PBS-T) for 1 min at 22 °C, loaded with SULFO-TAG TM 6E10 or 4G8 detection antibody (diluted to 1× in MSD Diluent 100) and sample or peptide calibrator (in MSD Diluent 35 or cell culture medium), and incubated for 16 h at 4 °C with shaking at 600 rpm. After three washing steps with PBS-T for 1 min at 22 °C, 150 µl 2× MSD read buffer was added per well. All plates were read using an MSD QuickPlex SQ 120 Imager and data analyzed using MSD Workbench® software. Standard curves were fitted using a non-linear four-parameter logistic fit.

4.7. Purification of recombinant human pro-cathepsin D

HEK 293-EBNA cells stable expressing pCEP-Pu containing pro-CTSD were grown in purification medium (DMEM, 2.5% FBS and 1% Pen/Strep for one week. Cell culture supernatant was collected, filtrated and concentrated *via* an Amicon system and an ultrafiltration disk with a 10 kDa cutoff (Millipore, PLGC07610). Recombinant protein was purified *via* its N-terminal His-Tag using a His-Trap 1 ml column (GE Healthcare, 29–0510-21) on an Aekta Purifier System (GE Healthcare) and eluted with 250 mM imidazole (Roth, X998.4) in PBS, pH 7.4. The protein was further purified via size exclusion chromatography on a Superdex 75 column (GE Healthcare, GE17–5174–1). Monomeric rhCTSD was concentrated using a Vivaspin 20 tube with 10 kDa cutoff (Sartorious, VS2002). The purified protein was stored at -20 °C.

4.8. Cathepsin activity assay

To measure Cathepsin D activity in cells, lysates were prepared in RIPA buffer without protease inhibitors to keep protease activity. Activity buffer (50 mM sodium acetate (pH 5.5), 0.1 M NaCl, 1 mM EDTA, and 0.2% Triton X-100) containing 10 µM of CTSD substrate (P-145, Enzo Life Sciences) together with tested sample and pre-activated rhproCTSD as control was incubated at 37 °C and the fluorescence was measured over a time of 90 min using a Synergy™ HT Multi-Detection microplate reader (exc: 360 nm; em: 440 nm, band pass 40).

4.9. Liquid chromatography-mass spectrometry (LC-MS)

To analyze the ability of our purified cathepsin D to cleave human recombinant amyloid β 42, pro-cathepsin D was pre-activated in 50 mM sodium acetate and 50 mM NaCl at pH 4.5 for 2 h at 37 °C and afterwards incubated with 100 µM of human amyloid β 42 (151–002, Enzo) with or without Pepstatin A at 37 °C. Samples were collected after 0, 15, 30 and 60 min and directly frozen at -20 °C and analyzed *via* LC-MS. Aliquots of the samples were diluted 1:100 in LC loading buffer (3% acetonitrile (ACN) and 0.1% trifluoroacetic acid in water), and transferred to glass autosampler vials. LC-MS analysis was performed on a Dionex U3000 nanoRSLC UHPLC (Thermofisher, Dreieich, Germany) equipped with an Acclaim PepMap100 column (2 µm particle size, 75 µm × 500 mm) and µ-precolumn (300 µm × 5 mm) coupled online to a Q Exactive HF mass spectrometer (Thermofisher, Bremen, Germany). The eluents used were; eluent A: 0.05% formic acid (FA), eluent B: 80% ACN + 0.05% FA. The separation was performed over a programmed 40-min run. Chromatographic conditions were: 4% B for 3 min followed by a linear gradient from 4% to 50% B over 10 min, a 2-min increase to 90% B, and 10 min at 90% B. Following this, an inter-run equilibration of the column was achieved by 15 min at 4% B. A constant flow rate of 300 nl/min was used and 1 µl of sample was injected per run. Acquisition of data was performed on the Orbitrap Q Exactive HF mass spectrometer utilizing HCD fragmentation at a normalized collision energy of 27. A full scan MS acquisition was performed (resolution 60,000) with subsequent data dependent MS/MS (resolution 15,000) of the top 10 most intense ions; dynamic exclusion was enabled (2 s duration).

Database searches were performed in Proteome Discoverer (Ver. 2.2.0.388) using the SequestHT search algorithm and combined database that included the Aβ1–42 peptide, cathepsin D, and the cRAP list of commonly occurring laboratory contaminants. Small database search criteria were employed in which a fixed PSM was used and only peptides assigned as high confidence (Maximum delta Cn:0.5).

4.10. Statistical analysis and data analysis

Data are shown as mean ± S.E.M. For statistical analysis one-way ANOVA was employed using GraphPad Prism 5 (Graph Pad Software, Inc., San Diego, USA): * $P < 0.05$; ** $P < 0.01$; *** $P < 0.001$; **** $P < 0.0001$.

The ramification analysis was done using the Sholl Analysis plugin in ImageJ (Fiji) with following setting: start radius: 4.4 µm, step size: 3.3 µm, end radius: 34,9 µm. For each brain sample two slides were analyzed in the hippocampal region (CA1, CA3 and dentate gyrus) and cortex.

Supplementary data to this article can be found online at https://doi.org/10.1016/j.nbd.2022.105919.

Funding

This work was supported in part by the Deutsche Forschungsgemeinschaft (SFB877, A3 and Z2) and the Canadian Institutes of Health Research – CIHR (to GM).

CRediT authorship contribution statement

Lisa Gallwitz: Conceptualization, Methodology, Investigation, Validation, Visualization. **Lina Schmidt:** Methodology, Investigation. **André R.A. Marques:** Methodology, Investigation. **Andreas Tholey:** Investigation, Formal analysis. **Liam Cassidy:** Investigation, Validation. **Irem Ulku:** Investigation, Validation. **Gerhard Multhaup:** Conceptualization, Supervision, Writing – original draft, Writing – review &

editing. **Alessandro Di Spiezio:** Conceptualization, Supervision, Writing – original draft, Writing – review & editing. **Paul Saftig:** Conceptualization, Supervision, Writing – original draft, Writing – review & editing.

Data availability

Data will be made available on request.

Acknowledgments

We would like to thank Marlies Rusch for her crucial technical support and François Cossais for the support with the Keyence microscope. We are also thankful for Ulrike Müller, Heidelberg University for providing APP-deficient murine brains for control experiments. Illustrations were created with BioRender.com

References

Chai, Y.L., Chong, J.R., Weng, J., Howlett, D., Halsey, A., Lee, J.H., et al., 2019. Lysosomal cathepsin D is upregulated in Alzheimer's disease neocortex and may be a marker for neurofibrillary degeneration. Brain Pathol. 29 (1), 63–74.

Davidson, Y., Gibbons, L., Pritchard, A., Hardicre, J., Wren, J., Tian, J., et al., 2006. Genetic associations between cathepsin D exon 2 C–>T polymorphism and Alzheimer's disease, and pathological correlations with genotype. J. Neurol. Neurosurg. Psychiatry 77 (4), 515–517.

Dean, R.T., 1975. Direct evidence of importance of lysosomes in degradation of intracellular proteins. Nature 257 (5525), 414–416.

Dean, R.T., Barrett, A.J., 1976. Lysosomes. Essays Biochem. 12, 1–40.

Di Domenico, F., Tramutola, A., Perluigi, M., 2016. Cathepsin D as a therapeutic target in Alzheimer's disease. Expert Opin. Ther. Targets 20 (12), 1393–1395.

Di Spiezio, A., Marques, A.R.A., Schmidt, L., Thiessen, N., Gallwitz, L., Fogh, J., et al., 2021. Analysis of cathepsin B and cathepsin L treatment to clear toxic lysosomal protein aggregates in neuronal ceroid lipofuscinosis. Biochim. Biophys. Acta Mol. basis Dis. 1867 (10), 166205.

Felbor, U., Kessler, B., Mothes, W., Goebel, H.H., Ploegh, H.L., Bronson, R.T., et al., 2002. Neuronal loss and brain atrophy in mice lacking cathepsins B and L. Proc. Natl. Acad. Sci. U. S. A. 99 (12), 7883–7888.

Hamazaki, H., 1996. Cathepsin D is involved in the clearance of Alzheimer's beta-amyloid protein. FEBS Lett. 396 (2–3), 139–142.

Hook, V., Toneff, T., Bogyo, M., Greenbaum, D., Medzihradszky, K.F., Neveu, J., et al., 2005. Inhibition of cathepsin B reduces beta-amyloid production in regulated secretory vesicles of neuronal chromaffin cells: evidence for cathepsin B as a candidate beta-secretase of Alzheimer's disease. Biol. Chem. 386 (9), 931–940.

Hook, V., Schechter, I., Demuth, H.U., Hook, G., 2008. Alternative pathways for production of beta-amyloid peptides of Alzheimer's disease. Biol. Chem. 389 (8), 993–1006.

Jalanko, A., Braulke, T., 2009. Neuronal ceroid lipofuscinoses. Biochim. Biophys. Acta 1793 (4), 697–709.

Katunuma, N., 2010. Posttranslational processing and modification of cathepsins and cystatins. Journal of Signal Transduction 2010, 375345.

Kenessey, A., Nacharaju, P., Ko, L.W., Yen, S.H., 1997. Degradation of tau by lysosomal enzyme cathepsin D: implication for Alzheimer neurofibrillary degeneration. J. Neurochem. 69 (5), 2026–2038.

Koike, M., Nakanishi, H., Saftig, P., Ezaki, J., Isahara, K., Ohsawa, Y., et al., 2000. Cathepsin D deficiency induces lysosomal storage with ceroid lipofuscin in mouse CNS neurons. J. Neurosci. 20 (18), 6898–6906.

Ladror, U.S., Snyder, S.W., Wang, G.T., Holzman, T.F., Krafft, G.A., 1994. Cleavage at the amino and carboxyl termini of Alzheimer's amyloid-beta by cathepsin D. J. Biol. Chem. 269 (28), 18422–18428.

Lee, J.H., Yang, D.S., Goulbourne, C.N., Im, E., Stavrides, P., Pensalfini, A., et al., 2022. Faulty autolysosome acidification in Alzheimer's disease mouse models induces autophagic build-up of Abeta in neurons, yielding senile plaques. Nat. Neurosci. 25 (6), 688–701.

Liebsch, F., Kulic, L., Teunissen, C., Shobo, A., Ulku, I., Engelschalt, V., et al., 2019. Abeta34 is a BACE1-derived degradation intermediate associated with amyloid clearance and Alzheimer's disease progression. Nat. Commun. 10 (1), 2240.

Liu, J., Bassal, M., Schlichting, S., Braren, I., Di Spiezio, A., Saftig, P., et al., 2022. Intravitreal gene therapy restores the autophagy-lysosomal pathway and attenuates retinal degeneration in cathepsin D-deficient mice. Neurobiol. Dis. 164, 105628.

Manji, Z., Rojas, A., Wang, W., Dingledine, R., Varvel, N.H., Ganesh, T., 2019. 5xFAD mice display sex-dependent inflammatory gene induction during the prodromal stage of Alzheimer's disease. J. Alzheimers Dis. 70 (4), 1259–1274.

Marques, A.R.A., Di Spiezio, A., Thiessen, N., Schmidt, L., Grotzinger, J., Lullmann-Rauch, R., et al., 2020. Enzyme replacement therapy with recombinant pro-CTSD (cathepsin D) corrects defective proteolysis and autophagy in neuronal ceroid lipofuscinosis. Autophagy 16 (5), 811–825.

McDermott, J.R., Gibson, A.M., 1996. Degradation of Alzheimer's beta-amyloid protein by human cathepsin D. Neuroreport 7 (13), 2163–2166.

Mullan, M., Crawford, F., Axelman, K., Houlden, H., Lilius, L., Winblad, B., et al., 1992. A pathogenic mutation for probable Alzheimer's disease in the APP gene at the N-terminus of beta-amyloid. Nat. Genet. 1 (5), 345–347.

Nixon, R.A., 2017. Amyloid precursor protein and endosomal-lysosomal dysfunction in Alzheimer's disease: inseparable partners in a multifactorial disease. FASEB Journal 31 (7), 2729–2743.

Nixon, R.A., Yang, D.S., 2011. Autophagy failure in Alzheimer's disease—locating the primary defect. Neurobiol. Dis. 43 (1), 38–45.

Oakley, H., Cole, S.L., Logan, S., Maus, E., Shao, P., Craft, J., et al., 2006. Intraneuronal beta-amyloid aggregates, neurodegeneration, and neuron loss in transgenic mice with five familial Alzheimer's disease mutations: potential factors in amyloid plaque formation. J. Neurosci. 26 (40), 10129–10140.

Papassotiropoulos, A., Lewis, H.D., Bagli, M., Jessen, F., Ptok, U., Schulte, A., et al., 2002. Cerebrospinal fluid levels of beta-amyloid(42) in patients with Alzheimer's disease are related to the exon 2 polymorphism of the cathepsin D gene. Neuroreport 13 (10), 1291–1294.

Prieto Huarcaya, S., Drobny, A., Marques, A.R.A., Di Spiezio, A., Dobert, J.P., Balta, D., et al., 2022. Recombinant pro-CTSD (cathepsin D) enhances SNCA/alpha-Synuclein degradation in alpha-Synucleinopathy models. Autophagy 18 (5), 1127–1151.

Riemenschneider, M., Blennow, K., Wagenpfeil, S., Andreasen, N., Prince, J.A., Laws, S. M., et al., 2006. The cathepsin D rs17571 polymorphism: effects on CSF tau concentrations in Alzheimer disease. Hum. Mutat. 27 (6), 532–537.

Saftig, P., Klumperman, J., 2009. Lysosome biogenesis and lysosomal membrane proteins: trafficking meets function. Nat. Rev. Mol. Cell Biol. 10 (9), 623–635.

Saftig, P., Hetman, M., Schmahl, W., Weber, K., Heine, L., Mossmann, H., et al., 1995. Mice deficient for the lysosomal proteinase cathepsin D exhibit progressive atrophy of the intestinal mucosa and profound destruction of lymphoid cells. EMBO J. 14 (15), 3599–3608.

Saftig, P., Peters, C., von Figura, K., Craessaerts, K., Van Leuven, F., De Strooper, B., 1996. Amyloidogenic processing of human amyloid precursor protein in hippocampal neurons devoid of cathepsin D. J. Biol. Chem. 271 (44), 27241–27244.

Schmued, L., Raymick, J., Tolleson, W., Sarkar, S., Zhang, Y.H., Bell-Cohn, A., 2012. Introducing Amylo-Glo, a novel fluorescent amyloid specific histochemical tracer especially suited for multiple labeling and large scale quantification studies. J. Neurosci. Methods 209 (1), 120–126.

Schulz, A., Ajayi, T., Specchio, N., de Los, Reyes E., Gissen, P., Ballon, D., et al., 2018. Study of intraventricular Cerliponase alfa for CLN2 disease. N. Engl. J. Med. 378 (20), 1898–1907.

Steinfeld, R., Reinhardt, K., Schreiber, K., Hillebrand, M., Kraetzner, R., Bruck, W., et al., 2006. Cathepsin D deficiency is associated with a human neurodegenerative disorder. Am. J. Hum. Genet. 78 (6), 988–998.

Suire, C.N., Abdul-Hay, S.O., Sahara, T., Kang, D., Brizuela, M.K., Saftig, P., et al., 2020. Cathepsin D regulates cerebral Abeta42/40 ratios via differential degradation of Abeta42 and Abeta40. Alzheimers Res. Ther. 12 (1), 80.

Sun, H., Lou, X., Shan, Q., Zhang, J., Zhu, X., Zhang, J., et al., 2013. Proteolytic characteristics of cathepsin D related to the recognition and cleavage of its target proteins. PLoS One 8 (6), e65733.

Tyynela, J., Sohar, I., Sleat, D.E., Gin, R.M., Donnelly, R.J., Baumann, M., et al., 2000. A mutation in the ovine cathepsin D gene causes a congenital lysosomal storage disease with profound neurodegeneration. EMBO J. 19 (12), 2786–2792.

Watanabe, S., Hayakawa, T., Wakasugi, K., Yamanaka, K., 2014. Cystatin C protects neuronal cells against mutant copper-zinc superoxide dismutase-mediated toxicity. Cell Death Dis. 5, e1497.

Yamada, T., Liepnieks, J., Benson, M.D., Kluve-Beckerman, B., 1996. Accelerated amyloid deposition in mice treated with the aspartic protease inhibitor, pepstatin. J. Immunol. 157 (2), 901–907.

Yang, D.S., Stavrides, P., Mohan, P.S., Kaushik, S., Kumar, A., Ohno, M., et al., 2011. Reversal of autophagy dysfunction in the TgCRND8 mouse model of Alzheimer's disease ameliorates amyloid pathologies and memory deficits. Brain 134 (Pt 1), 258–277.